Wheat Inflorescence Architecture

Julian Greenwood

July 2017

A thesis submitted for the degree of Doctor of Philosophy at the Australian National University

Statement of authorship

The research carried out in this thesis was conducted at the Commonwealth Scientific and Industrial Research Organisation (CSIRO) department of Agriculture & Food between March 2014 and July 2017 with support from the Australian National University (ANU). I declare that this submission is my own work, and to the best of my knowledge contains no material previously published or written by another person nor material which has been accepted for the award of any degree or diploma of a university or other institution of higher learning except where due acknowledgement has been made.

Julian R. Greenwood

Acknowledgements

Thank you to Kerrie Ramm and Scott Boden who taught me the bulk of my basic laboratory skills. Without your support in the lab none of what follows would have been possible. You are both fantastic scientists and generally just good people.

I would also like to thank Jose Barrero, Frank Gubler, Brett Ford, Sandra Stops, Tanya Phongkham, Trijntje Hughes, Jessica Hyles, Saul Newman and Ming Luo for all your general support, conversation and smiling faces in the lab. Special thanks to Jean Finnegan for your support, enthusiasm and sour dough starter. Thank you to John Evans who always made me feel relaxed. Thanks to Carl Davies for your excellent photography.

My research supervisors at CSIRO, Steve Swain and Ben Trevaskis possess a wealth of knowledge that I drew on frequently. I have learnt so much from them both. Despite you both having very busy schedules, you would always take the time to discuss things with me and see how I was doing. I was lucky to have you as supervisors and CSIRO is lucky to have you also.

The best thing about staying in your home town to do a PhD is that you have your family close by. Thank you all for being there for me. We don't get to choose our families so it's a blessing that you are all such lovely people.

Timo, I have never had another brother but I am certain they do not come better than you. You are the best thing that Mum and Dad have given me, though I did not yet exist when you were born. I hope my appreciation for you goes without saying because I don't, and cannot thank you enough.

To my parents who brought me into this world. You have provided me with everything I could ever need and more. Without you, I can assuredly say, I would not exist nor would I have been able to do so many of the things I love.

My biggest thanks go to my beautiful partner, Katia. She is without a doubt the most loving and caring person I have ever met. She has taken the brunt of my PhD induced stress and procrastination over the past couple of years, but with her support and upbeat attitude I have been able to achieve so much. I promise I will support you in kind.

Thank you to the ANU and CSIRO for providing me with the means to live during my PhD. Thank you to the CSIRO for providing me with research funding. ANU and CSIRO are both fantastic research institutions filled with terrific scientists. I hope we will cross paths again in the future.

Publications and presentations

Publications

Equal first author, currently under review at Plant Cell: Dixon, L; Greenwood J. *et al.* **TEOSINTE BRANCHED1 is a key regulator of inflorescence architecture and development in bread wheat.**

First author, article accepted April 2017: Greenwood, J. *et al.* **New alleles of the wheat domestication gene Q reveal multiple roles in growth and reproductive development.** *Development* (2017).

Co-authorship: Boden, S. A. *et al.* **Ppd-1 is a key regulator of inflorescence architecture and paired spikelet development in wheat**. *Nature Plants* **1**, 10.1038/nplants.2014.16 (2015).

Conferences

Invited Speaker: Combio, Brisbane, Australia, October 2016 ***Novel trait induction in elite wheat varieties***

Invited Speaker: EPSO/FESPB Plant Biology Congress, Prague, Czech Republic, June 2016 ***Novel trait induction in elite wheat varieties***

Invited Speaker: CSIRO 'Developing crops of the future workshop', Kiama, Australia, April 2016 ***Novel alleles of the major wheat domestication gene Q***

Poster presentation, networking and workshops: CSIRO 'PhD and postdoctoral forum', Brisbane, Australia, 2014,

Volume 144 (11) June 2017

Development

Table of Contents

Abbreviations

bp	base pair
CTAB	Cetyl trimethylammonium bromide
DNA	deoxyribonucleic acid
dNTP	deoxynucleoside triphosphate
EDTA	ethylenediamine tetra-acetic disodium salt
h	hours
IPTG	isopropyl-C-D-thiogalactoside
kb	kilobase-pairs
LB	Leuria-Bertani medium (in methods) low branching in chapter 3
min	minute(s)
miRNA	microRNA
mRNA	messenger RNA
PCR	polymerase chain reaction
RACE	rapid amplification of cDNA ends
RNA	ribonucleic acid
RNAi	RNA interference
RNase	ribonuclease
RT-PCR	reverse transcriptase polymerase chain reaction
qRT-PCR	quantitative real time polymerase chain reaction
qSL-PCR	quantitative stem-loop real time polymerase chain reaction
TBE	Tris-borate-EDTA
TE	Tris-EDTA
UV	ultraviolet
X-gal	5-bromo-4-chloro-3-indoyl-C-D-galactopyranoside

Abstract

The development of the wheat inflorescence, or spike, determines the number, size and shape of grain produced. Altering spike development has the potential to increase grain yield to support increasing global demands. Despite the importance of this specialized structure, little is known about the genes which underlie its development and thus contribute to grain output.

Yield potential in wheat can be modified by numerous developmental outcomes. The number of vegetative branches, known as tillers determines the number of spikes per plant. Similarly, the number of nodes within the spike determines the number of grain bearing structures called spikelets. Increasing the number of spikelets per node in the form of branching further increases yield potential. Finally, the fertility of florets, which are the grain bearing units found within spikelets determine the number of grain set. Optimising these inflorescence structures is key for maximising yield potential in wheat.

The important floral regulators, *PPD-1* and *FT* positively regulate floral transition and influence the rate of floral development. Increased expression of *PPD-1* leads to increases in *FT* expression and promotion of floral development. We have shown that loss-of-function mutations in both *PPD-1* and *FT* contribute to a reduction in expression of floral meristem identity genes, a delay in flowering, an increase in nodes within the inflorescence and the production of a unique form of inflorescence branch called a paired spikelet.

The important maize domestication gene *TB1* is responsible for a reduction in vegetative branching and the single stem structure of modern maize. We show that increased copies of wheat *TB1* reduce vegetative branches known as tillers as well as increase paired spikelet formation in wheat. We propose that TB1 interacts with FT in the inflorescence causing a similar reduction in meristem identity genes as we observed in *FT* and *Ppd-1* mutants.

The wheat domestication gene *Q,* an AP2 transcription factor, is one of only a handful of genes which is known to directly influence spike development in wheat. We have identified a novel gain-of-function mutation of *Q* which confers resistance to *miR172,* a microRNA that typically targets *AP2* transcripts for degradation. We show that increased *Q* levels are associated with several phenotypes including, delayed flowering, the formation of ectopic florets in place of glumes, the formation of paired spikelets and a reduction in internode elongation throughout the plant. AP2 transcription factors are reported to delay flowering in other plant species. Increased expression of *Q* is therefore the likely cause of a delay in flowering time and the formation of paired spikelets not dissimilar to what we observed in loss-of-function mutations of *FT* and *PPD-1*.

Taken together our results highlight a complex network of genes which regulate the number of grain producing units contributing to wheat yield. Many more genes regulating inflorescence development in wheat remain to be elucidated. With the recent release of the first wheat reference genome sequence, increased availability of reverse genetic resources and access to genome editing tools, it will be possible to identify novel gene function in wheat.

Chapter 1 - Introduction

Background

Globally, three major grass crops; rice, wheat and maize, provide around sixty per cent of the total calories consumed by humans (FAOSTAT, 2014). These cereal crops have all been selectively bred to maximise grain number and/or size within the flowering portion of the plant, the inflorescence. A combination of genetics, breeding programs, and improved farming practices have contributed to significant increases in agricultural yields over the past 50 years (Slafer, 2003, Hedden, 2003). Over the last decade it has become increasingly clear that the current rate of increase in cereal productivity will be insufficient to keep up with growing demands especially in light of climate change trends (Bassu et al., 2011). Defining the yield of crop species are the developmental processes that determine the functional components of the plant. In the case of cereals this includes the grain bearing inflorescence. An improved understanding and subsequent exploitation of the genetic factors influencing development processes in crop plants has the potential to contribute to significant increases in yield. This thesis will explore some of the genetic factors which influence inflorescence development in wheat and how best to uncover new gene function.

The grass inflorescence

Vegetative branching influences the number of inflorescences per plant

The vegetative architecture of a grass is defined by the arrangement of leaves on stems and the number of stems in the plant. In the major grass crops, additional stems (known as tillers), can form, with all stems and tillers having the potential to bear their own inflorescence **Figure 1**. In this way, vegetative development and inflorescence development are linked as tiller number can define inflorescence number.

The structural components of the grass inflorescence

The grass inflorescence is made up of a combination of stems known as rachises which feature a series of nodes (rachis nodes) either bearing additional rachis branches or a shorter branch type known as the spikelet. Spikelets are grass specific floral structures which contain florets and the reproductive structures necessary for grain production **Figure 1**.

Spikelets form either singly or in pairs, known as paired spikelets. The spikelet, features two sterile bracts known as glumes at its base, which are followed by a series of one or more florets. Each floret has a pair of bracts, the lemma and palea, which enclose the sexual organs. Each floret has the potential to bear a single grain. Variations in branching, the number of spikelets and their arrangement, and finally the number of florets per spikelet lead to the structural diversity of the many types of grass inflorescences **Figure 1**. (Doust, 2007, Kellogg, 2006, Perreta et al., 2009, Kellogg, 2007)

Elongation of internode tissue influences architecture

Internode elongation also determines the structure of the inflorescence. The final vegetative internode, known as the peduncle internode, and all internodes below it will define the position of the inflorescence above the leaves and the height of the plant. Similarly, within the inflorescence, elongation of rachis internodes will determine the distance between floral structures. Finally, within the spikelet, rachilla internodes can also vary in length, altering the compaction of the spikelets **Figure 1**.

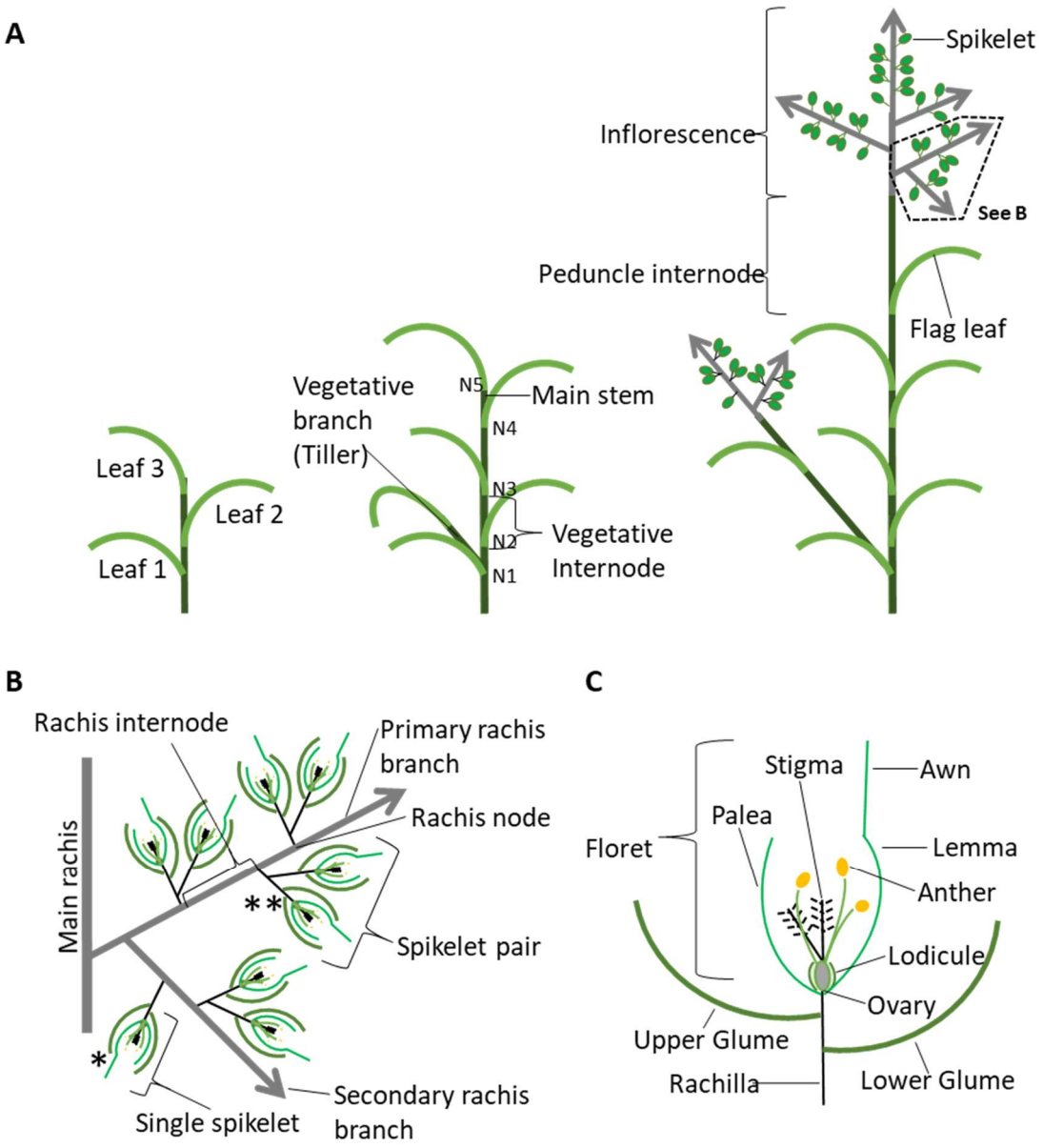

Figure 1 Schematic of archetypal grass vegetative and inflorescence architecture. **(A)** Whole plant schematics of archetypal grass structures including single leaves developing at nodes of stem, numbered in order of their development (left). Additional vegetative stems (tillers) can form at the vegetative nodes of other stems. Nodes of the main stem labelled N1-5 (middle). Elongation of vegetative internode tissue defines the length of the stem (middle). Inflorescences form in the apical tissue of vegetative stems (main or tillers) which have undergone floral transition. The inflorescence encompasses the stems, nodes and flowers which bear the grain. The final leaf developed before floral development occurs is known as the flag leaf and the final elongated internode before the inflorescence is known as the peduncle internode. **(B)** A developing archetypal inflorescence, showing a close up schematic of the first inflorescence branch (marked by a dotted box in panel A). Inflorescence structures are labelled indicating primary branches; those that form from the main or central inflorescence stem (rachis) and secondary rachis branches; those that form from the primary rachis branch. Subsequent higher order branching can occur in the grasses. Spikelets form on the rachis singly * or in specialised short branch structures not exceeding two spikelets per branch referred to as paired spikelets or spikelet pairs **.

The wheat inflorescence is distinct from rice and maize

The heavily cultivated grass crops, rice, maize and wheat, differ significantly in their inflorescence structure. Not surprisingly, phenotypic and genetic differences place these three species in separate subfamily groups (Gaut, 2002) sharing a common ancestor some 70 million years ago (Salse et al., 2008).

Rice inflorescence

The rice inflorescence, or panicle, has a central inflorescence axis that aborts after the production of several primary branches, which potentially bear secondary and then tertiary branches etc. All rachis branches bear several single spikelets, with each spikelet containing a single floret **Figure 2**. (Kellogg, 2007)

Maize inflorescence

Maize produces two distinct types of inflorescences: ears containing feminised flowers that produce grains, and tassels that produce pollen. Ears produce many short primary branches comprised of two spikelets, each containing a single developed floret. These 'spikelet pairs' are arranged in a spiral along the main inflorescence axis to generate many grains, or kernels in the typical cob shape of the ear. The tassel inflorescence consists of a central inflorescence axis with several long branches typically forming from the base of the inflorescence. Spikelet pairs cover the apical portion of the main rachis and primary rachis branches with each spikelet containing two male florets **Figure 2**. (Kellogg, 2007)

Wheat inflorescence

The wheat inflorescence or spike does not produce primary inflorescence branches. Instead the wheat inflorescence produces a series of spikelets in an alternating pattern on the main rachis before the main stem terminates in a single terminal spikelet. Additionally, the spikelets produced in wheat form an indeterminate number of florets unlike the fixed or determinate spikelets of rice and maize (Perreta et al., 2009). The model grass species *Brachypodium* bears an inflorescence which closely resembles that of wheat featuring terminal spikelets, spikelet indeterminacy and a single rachis **Figure 2**. (Kellogg, 2007)

Comparing the major grass crop inflorescences

Domesticated maize or corn forms a single stem with two unique inflorescence types. The tassel, bears spikelets arranged in pairs with each spikelet containing a pair of florets. In the case of the maize tassel, florets do not develop female reproductive components, instead acting to pollinate the second inflorescence type of maize, the cob. The maize tassel forms an indeterminate number of rachis nodes and therefore spikelets whereas the panicle of rice (excluding the central rachis) and spikes of wheat and *Brachypodium* feature terminal spikelets. The main central rachis of rice aborts instead of terminating as a spikelet. Rice, wheat and *Brachypodium* all feature vegetative branching with multiple tillers each potentially bearing their own inflorescence. Spikelets in rice, like in maize, are determinate. In contrast to maize, the rice spikelet forms only a single floret and bears all necessary components for fertile grain production. Fully developed wheat florets are also fertile but an indeterminate number are formed within each wheat spikelet leaving very small and microscopic floret tissues in the apical region of the spikelet that do not develop sufficiently to be fertile or bear grain. Typically, only the first 2-4 florets bear grain. Unlike the tassel of maize and

panicle of rice, the spike of wheat does not form additional rachis branches from the main stem, with spikelets forming immediately at the nodes of the central rachis **Figure 2**. (Bommert et al., 2005b, Vollbrecht et al., 2005, Kyozuka et al., 2014)

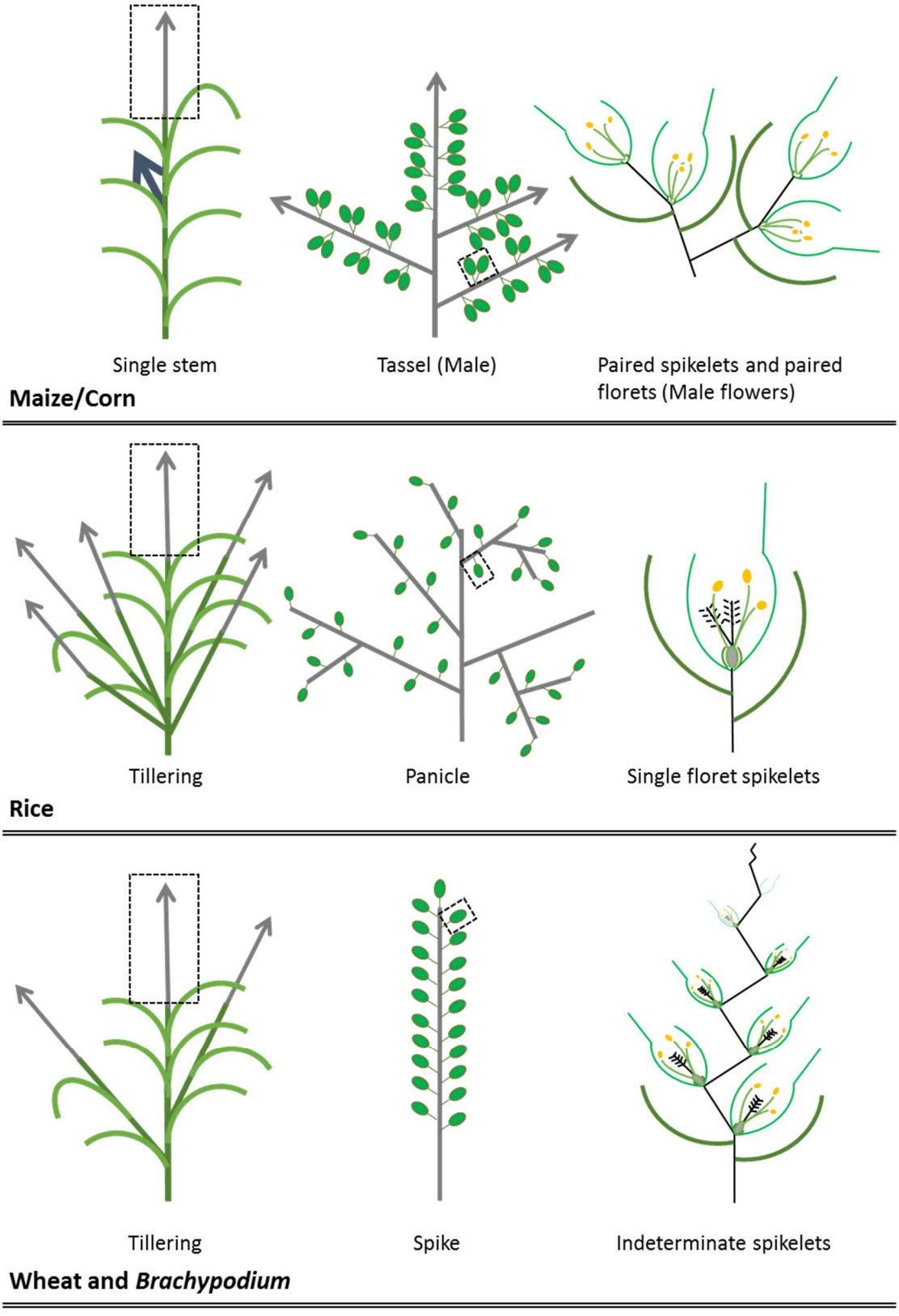

Figure 2 Schematic of vegetative (left), inflorescence (middle) and spikelet (right) structures of maize/corn, rice, and, wheat and *Brachypodium*. The names for inflorescences of the grasses are based on their structure and are shown in the middle of each schematic series. Structures are coordinated by colour to match the labelling in **Figure 1**. Structures marked out by dotted lines are enlarged in the adjacent schematic immediately to the right. The positioning of the maize cob is indicated by dark blue arrow.

The architecture of the grass inflorescence is controlled by meristem development and transition

Plant development is driven by groups of pluripotent cells called meristems. In the above ground portion of the plant, all additional organs and meristems (axillary meristems) are derived from the first shoot apical meristem (SAM) (Pautler et al., 2013, Tanaka et al., 2013).

Sections of the SAM are portioned to form a repeating series of units, called phytomers (Moore and Moser, 1995). Each phytomer consists of an internode, and a node region that contains the leaf primordium and an axillary meristem. The development of certain tissue types in each phytomer (the leaves and axillary meristem derived structures) is restricted to certain regions of the plant. Development of the leaf primordium, the axillary meristem and internode tissue is under strict genetic control. In the vegetative portion of the plant, leaf primordia develop into adult leaves and axillary meristems will either remain dormant or form tillers. Within the inflorescence, leaf primordia are repressed and axillary meristems either form rachis branches or spikelet structures. The specific architecture of the grass inflorescence is controlled through the manipulation of apical and lateral (axillary) meristem stages determining how and where certain structures form. Meristems are often named for the type of structures they produce (e.g. a grass meristem that gives rise to floral structures is called an inflorescence meristem) **Table 1.** (Pautler et al., 2013, Tanaka et al., 2013, Barton, 2010, Kyozuka et al., 2014).

Table 1 Meristem transition determines the number of branches, spikelets and florets in the inflorescence

<table>
<tr><td>Vegetative Meristem

(VM)</td><td>During the vegetative stage of development, leaves and axillary meristems are derived from cells of the shoot apical meristem. Leaf primordia are continually produced by shoot apical meristems and during the vegetative phase of growth these leaf primordia develop into adult leaves. Axillary meristems at this stage can be supressed or develop into tillers, which form their own series of leaves and axillary meristems like the original SAM. Eventually the apical meristems (main and tillers) receive signals to begin floral development. Figure 3

 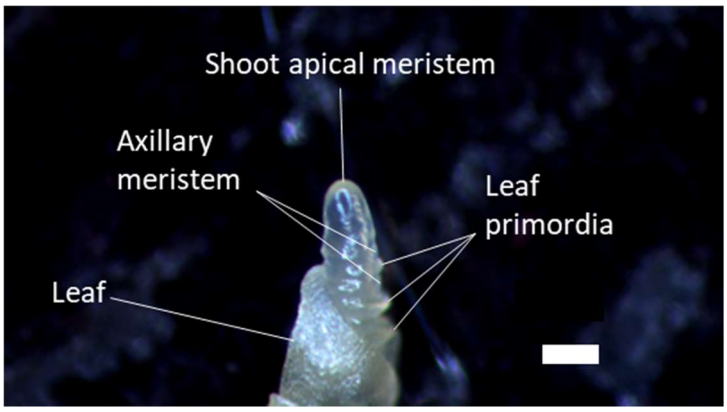

Figure 3 Shoot apical meristem of wheat with developing leaf primordia at basal nodes. At this stage of development, leaf primordia are developing and enlarged relative to the axillary meristems, which are suppressed. From the base of one leaf primordium to the base of the next leaf primordia is one phytomer unit. Apical nodes are too undeveloped to make out specific structures. Scale bar 200µm</td></tr>
<tr><td>Inflorescence Meristem

(IM)</td><td>Leaf primordia continue to be produced during inflorescence development. However, at this stage of development they remain supressed. In wheat, axillary meristems will go on to form the spikelet so are called spikelet meristems. In other grass species, axillary meristems can potentially behave like the apical meristem, causing an additional rachis branch with a series of axillary meristems to form. Consequently they are known as branch meristems. The positions of axillary meristems on the rachis are known as rachis nodes. In wheat, the SAM will eventually acquire spikelet meristem identity, forming the terminal spikelet preventing any additional axillary meristems from being formed. Figure 4</td></tr>
</table>

	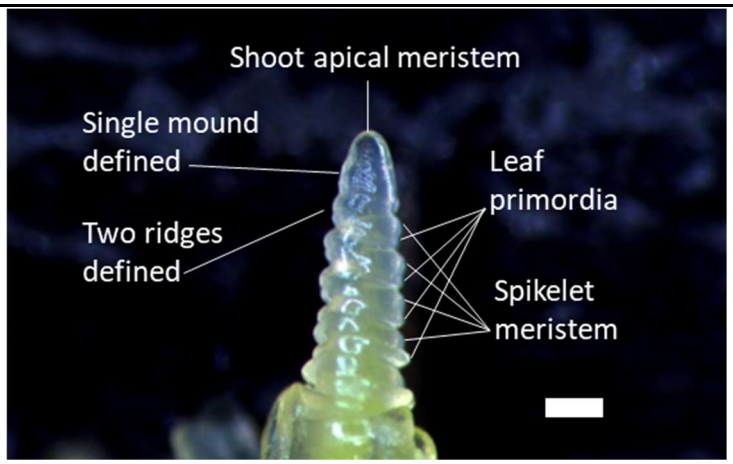 **Figure 4 Developing inflorescence of wheat during double ridge stage.** This is the first visual indication of a transition to inflorescence development. This stage is called double ridge for the clear enlarging of the two ridges of the leaf primordia and axillary meristems (spikelet meristems). Compared to the vegetative shoot apical meristem, axillary meristems appear enlarged at double ridge. Within the developing inflorescence, development of leaf primordia is supressed and axillary meristems go on to form floral structures. Scale bar 200µm
Branch Meristem (BM)	A branch meristem is essentially an axillary meristem that maintains the behaviour of an inflorescence meristem or floral SAM. Additional branch meristems or spikelet meristems form from the axillary meristems it defines. The process controlling whether an axillary meristem should branch or transition to a spikelet meristem is under strict genetic and environmental regulation. In wheat, the branch meristem is short lived or completely bypassed meaning rachises do not form at any node.
Spikelet Meristem (SM)	Once an axillary meristem has acquired spikelet meristem identity, the meristem will initiate the formation of spikelet structures, most notably a pair of leaf like bracts called glumes, which surround the subsequent floral organs. In wheat, the spikelet meristem is indeterminate and will continue to initiate floret meristems after the glumes are defined. Basal floret meristems develop earliest and form larger florets which are more likely to set grain. Apical florets are sequentially smaller and will eventually fail to set grain. In rice and maize, the spikelet meristem is determinate in that it produces a fixed number of florets. **Figure 5**

	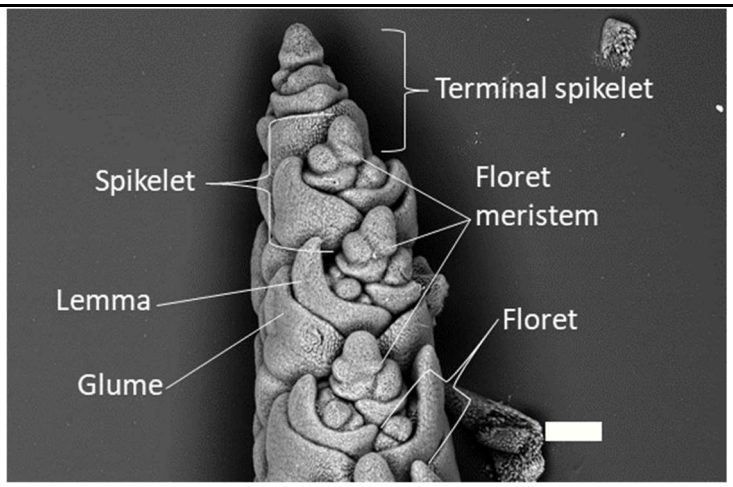 **Figure 5 Developing tip of a wheat inflorescence during floret formation.** By this stage of inflorescence development, spikelets are clearly defined and the basal florets within each spikelet feature differentiated floral structures. The apical portion of each spikelet features recently partitioned floret meristems and the indeterminate apex of the axillary meristem, which will continue to define florets. Scale bar 200µm
Floret Meristem (FM)	Following the definition of the glumes, each sequential node (rachilla node) of the wheat spikelet will produce a single floret containing the reproductive organs with the potential to bear a single grain.

The diverse range of inflorescence architectures in different cereals is largely determined by when and where branch meristems and inflorescence meristems transition to spikelet meristems. In all grasses, axillary meristems are defined from a subset of shoot apical meristem cells. Together, the identity or developmental stage of axillary meristems and the apical meristem as well as elongation of cells between axillary meristems (rachis internodes) define the structure of the inflorescence **Table 1.**

The rice inflorescence is produced by three axillary meristem identities: branch meristems produce the primary, secondary and tertiary branches, spikelet meristems give rise to spikelets, and floret meristems produce the florets.

In maize four different types of axillary meristem identity give rise to this inflorescence: branch meristems, spikelet pair meristems, spikelet meristems and finally floret meristems. The production of ears and tassels in the same plant demonstrates that changes in gene expression or activity can lead to changes in meristem identity and branching that contribute to dramatic differences in inflorescence architecture.

Wheat transitions immediately through, or bypasses the branched meristem identity and thus the axillary meristems produce spikelets and florets on a single rachis. This occurs in an alternating phyllotaxy with the SAM eventually terminating in a spikelet (the terminal spikelet) which is rotated 90 degrees relative to the spikelets that have arisen from axillar meristems **Figure 6.** (Ciaffi et al., 2011, Perreta et al., 2009, Kellogg, 2007)

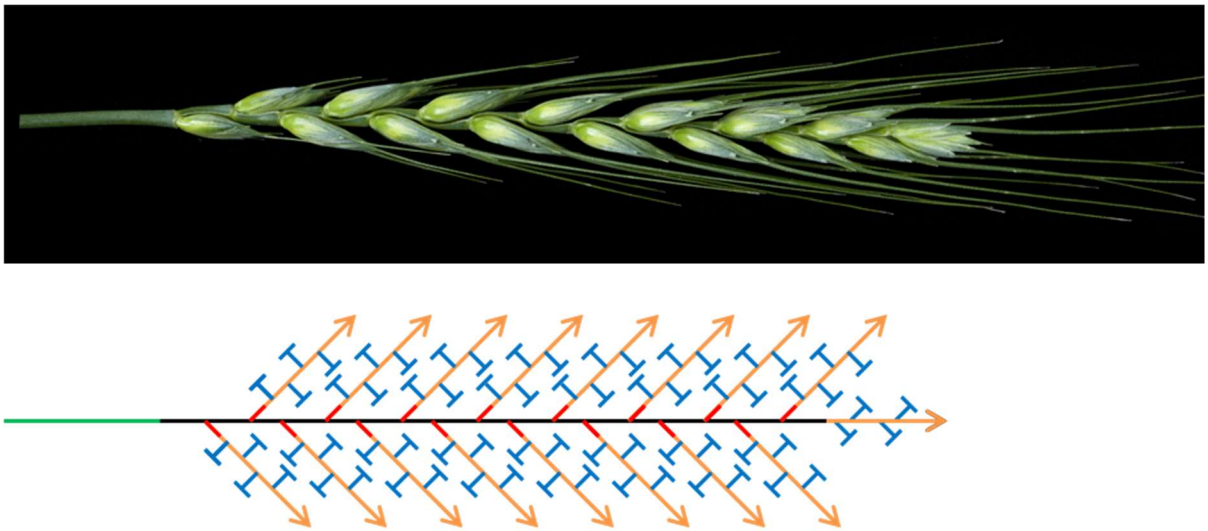

Figure 6 Wheat spike and schematic indicating the meristem states and their position in the developing Inflorescence. Vegetative, Inflorescence, Branch, Spikelet and **Floret** meristem positions are shown in bottom schematic. For clarity in the schematic, spikelets (excluding the terminal spikelet) are shown rotated 90 degrees relative to their natural position in the wheat spike (top image). Arrows represent indeterminate meristems (**Spikelet** Meristem). 'T' symbols indicate that a meristem is determinate and will produce a single defined structure (**Floral** Meristem).

Floral transition and rate of development in wheat are controlled through environmental integrators

A feature of many temperate plants is their ability to respond to their environment in a way that maximises their potential for setting seed/grain. In cropping systems, timing flowering to coincide with optimal seasonal conditions is essential for maximising yield. In wheat, several environmental sensors which modify flowering time have been utilised to tailor wheat varieties to specific growing regions (Trevaskis et al., 2007).

In wheat, a florally inductive signal which acts on the SAM, is required to transition from vegetative to reproductive development. The strength of the floral inductive signal affects the rate of inflorescence development and the number of floral organs deposited. Temperature, photoperiod and light quality (Gororo et al., 2001) all play roles in regulating floral transition and the strength of the floral signal and thus also influence the structure of the wheat inflorescence (Ugarte et al., 2010, Rahman and Wilson, 1977, Rahman and Wilson, 1978). A simple illustration of this process is the exposure of day length sensitive wheat plants to various photoperiods. Longer day lengths result in an earlier floral transition and an earlier transition of the SAM to terminal spikelet production. Consequently, fewer axillary meristems and spikelets are produced. In contrast, short day lengths result in a slower floral transition and inflorescences with more spikelets (Rahman et al., 1977).

Photoperiodic control of floral transition

The photoperiod dependent flowering pathway leads to flowering through interaction with the circadian clock of the plant and this is best understood in the model plant, *Arabidopsis thaliana*. In *Arabidopsis* the key circadian clock protein CONSTANS (CO), when in the presence of light, up-regulates expression of *FLOWERING LOCUS T* (*FT*) (Kobayashi et al., 1999). FT protein moves from the leaves to the shoot apical meristem (Corbesier et al., 2007). In the apical meristem FT interacts with FLOWERING LOCUS D (FLD) to activate the MADS-box floral meristem identity genes *APETALA 1* (*AP1*) and *LEAFY* (*LFY*) (Abe et al., 2005, Wigge et al., 2005). *FRUITFUL* (*FUL*), another MADS box floral meristem identity gene, functions redundantly with *AP1* to drive floral meristem identity (Alvarez-Buylla et al., 2006). Many identified floral meristem identity genes are MADS box transcription factors which are not only required for the vegetative to floral transition but also to determine the correct formation of floral structures (Alvarez-Buylla et al., 2006, Chu et al., 2010).

The photoperiodic control of flowering in *Arabidopsis* and wheat is dosage dependant with flowering time being modulated dynamically under changing photoperiods. Short photoperiods result in low *FT* dosage and late flowering while increasing photoperiod will increase *FT* dosage and reduce flowering time (Mockler et al., 2003, Chen et al., 2014). *Brachypodium* shows a similar response (Ream et al., 2014).

Sensing photoperiod and acting upstream of CO in *Arabidopsis* is PSEUDO-RESPONSE REGULATOR7 (PRR7). In wheat, a close homologue of *PRR7*, *PHOTOPERIOD1 (PPD1)* functions in a similar manner (Shimada et al., 2009). In wheat, gain-of-function mutations in the *PPD-1* gene have been identified on all three genomes. Each mutation causes early flowering irrespective of photoperiod, unlike wild alleles of *PPD-1*, which only promote flowering under long days (Beales et al., 2007,

Wilhelm et al., 2009, Díaz et al., 2012). Each of the gain-of-function *PPD-1* mutations identified results in over expression of *PPD-1*, which in turn leads to increased expression of *FT* and rapid flowering (Bentley et al., 2011). In contrast, loss of *ppd1* and *ft* function leads to late flowering and inflorescence architecture defects (Boden et al., 2015). The gain-of-function *PPD-1* alleles have been incorporated in what are known as photoperiod insensitive wheat varieties where accelerated flowering is observed (Beales et al., 2007, Shaw et al., 2012). Although other wild or photoperiod sensitive *PPD-1* homeoalleles can be present in these varieties the flowering time effect contributed by photoperiod sensitive homeoalleles is minor compared to the strong gain-of-function alleles (Wilhelm et al., 2009, Beales et al., 2007, Shaw et al., 2012).

Close homologues of some photoperiod pathway genes described in *Arabidopsis* are present in grass crop plants but not all share similar functions. Unlike in *Arabidopsis* and wheat, the rice orthologue of CO acts as an activator of the rice *FT* in short days and as an inhibitor in long days (Itoh et al., 2010). Maize is descended from the short-day grass *Teosinte*. However, modern corn varieties have been bred to be mostly photoperiod insensitive, tailoring their flowering time to modern cropping systems (Bortiri and Hake, 2007). Because responses to photoperiod can differ greatly between species it is best to consider the photoperiodic control of flowering within individual species.

Temperature influences floral transition and development

As well as photoperiod, flowering in *Arabidopsis* and temperate grasses including many wheat varieties, is strongly regulated by exposure to cold (vernalisation) (Trevaskis et al., 2007). The photoperiod and vernalisation pathways are well characterised in *Arabidopsis* and similar pathways are present in wheat (Turck et al., 2008, Distelfeld et al., 2009). In temperate wheat varieties, vernalisation is necessary to trigger floral

development and this requirement can only be overcome by very long periods under other floral promoting conditions like long days (Yan et al., 2003). Like photoperiod effects, the vernalisation response is dosage dependent. The longer the plant has spent in cold conditions, the greater the reduction in flowering time (Murai et al., 2003, Alonso-Peral et al., 2011).

Vernalisation insensitivity, seen in spring type wheat, is the result of expression of *VERNALISATION1 (VRN1)* in the absence of vernalisation. Increased *VRN1* expression can be achieved through insertions or deletions in the promoter region or first intron of *VRN1* (Trevaskis, 2010, Yan et al., 2004). In winter wheat varieties, *VRN1* expression is increased under cold conditions resulting in negative regulation of *VERNALISATION2 (VRN2).. VRN2* acts to repress *FT* until vernalisation has occurred, so in the absence of repression by *VRN2*, *FT* can promote flowering (Li and Dubcovsky, 2008). The spring wheat habit can also be brought about by loss-of-function mutations in *vrn2* (Bonnin et al., 2008, Distelfeld et al., 2009). *VRN1* also acts as a floral meristem identity gene and is promoted by *FT* as well as exposure to cold (Li and Dubcovsky, 2008). Therefore, *VRN1* expression can also be activated by the photoperiod pathway in an *FT* dependant manner (Preston and Kellogg, 2007, Li and Dubcovsky, 2008, Trevaskis et al., 2007). *FT* is considered a floral integrator as it can be activated by both the photoperiod and vernalisation pathways to promote flowering.

The Australian spring wheat variety, Sunstate, used to generate mutants featured in this study has a spring habit requiring no vernalisation, as well as photoperiod insensitivity resulting in a rapid floral transition. The flowering time of Sunstate is tailored to make best use of a short, dry, growing season.

Genetic control of inflorescence architecture

In wheat, *Brachypodium* and rice, a range of environmental factors and florigens (like *FT*) determine the strength of floral inductive signals which then influence inflorescence architecture. For example reductions in floral inductive signals lead to the formation of more rachis nodes and thus inflorescences bear more branches and/or spikelets (Zhang and Yuan, 2014, Rahman and Wilson, 1977, Rahman and Wilson, 1978, Ream et al., 2014). Besides these broad stroke type of influences, there are many other genetic factors, which when modified, can further alter meristem identities and maintenance, and ultimately, inflorescence architecture. These genetic factors can drastically change the numbers of, or types of inflorescence structures produced. Although inflorescence architectures between the grass crops are highly variable, often genes responsible for developmental changes in one species will be part of a similar developmental pathway in another species. Given the complexity of the wheat genomes, identifying mutants initially in rice, maize and *Brachypodium* can help us to identify potential gene targets in wheat.

Spikelet determinacy

One key aspect differentiating the wheat spike from other inflorescence forms is the presence of an indeterminate spikelet. Several mutants with altered spikelet determinacy have been generated in rice and maize (Laudencia-Chingcuanco and Hake, 2002, Gallavotti et al., 2010, Lee et al., 2007). In maize, mutants of *APETELLA2*-like (*AP2*-like) genes *INDETERMINATE SPIKELET 1(IDS1)* and *SISTER of INDETERMINATE SPIKELET 1 (SID1)* lose spikelet determinacy, producing a spikelet more similar to that of wheat (Chuck et al., 2008). Similar phenotypes have been observed in rice *AP2* mutants (Lee and An, 2012). Expression of many *AP2* genes has been shown to be strongly regulated by *microRNA172 (miR172)* in a variety of plant species including

grasses (Lauter et al., 2005, Varkonyi-Gasic et al., 2012, Brown and Bregitzer, 2011, Lee et al., 2014, Zhu et al., 2009).

miRNA regulation and inflorescence development

miRNAs are genomic encoded sequences which when transcribed are processed to generate short RNAs 21-24 nucleotides long (Chen, 2008). miRNAs act to regulate expression of their target genes by binding complementary sequences of gene transcript. Transcript is then targeted by an RNA-induced silencing complex. Once bound by the proteins in the silencing complex, miRNA targeted transcript can be either degraded or translation can be repressed by interference with the translational machinery (Zhang et al., 2006). Either outcome results in specific down regulation of a gene or class of genes. The plant specific miRNAs, miR172 and miR156 have both been implicated in regulating floral transition and inflorescence development (Jung et al., 2011). miR172 is broadly thought to act as a floral promotor whereas miR156 acts as a floral repressor (Lee et al., 2014, Jiao et al., 2010, Jung et al., 2014, Wu et al., 2009). Floral promotion by miR172 acts via repression of AP2s, which reduces their ability to antagonise flowering. miR156 negatively regulates SQUAMOSA PROMOTER BINDING PROTEIN-LIKE (SPLs) preventing them from promoting miR172 expression (Wu et al., 2009, Yu et al., 2012). Expression of miR156 is believed to decrease with the age of the plant, allowing for floral promotion by (Spanudakis and Jackson, 2014). The rice AP2-like genes *OsINDETERMINATE SPIKELET 1* (*OsIDS1*) and *OsSUPERNUMERARY BRACT (OsSNB*) inhibit flowering by negatively regulating *FT* (Lee et al., 2014). SPLs, AP2s and their regulatory miRNA appear to make up a regulatory feedback mechanism with AP2s acting to repress floral meristem identity and SPLs promoting floral meristem identity **Figure 7.**

Floral transition is promoted by floral meristem identity genes

MADS box genes play key roles during many stages of development including the definition of floral meristem identity (Fornara et al., 2004, Kobayashi et al., 2010, Kobayashi et al., 2012). In rice, *OsMADS18* is expressed highly in meristems, and overexpression induces accelerated growth of axillary shoot meristems and early flowering (Fornara et al., 2004). *OsMADS18* shares close homology to *OsFUL1* and other MADS box transcription factors which have been shown to have very similar overlapping functions in determining floral meristem identity (Kobayashi et al., 2012).

In rice, RNAi targeting of *OsMADS18* transcript showed no noticeable phenotype, suggesting functional redundancy with other rice MADS box genes (Fornara et al., 2004). Triple knockdown of *OsMADS14, 15* and *18* in a *PANICLE PHYTOMER 2* (OsPAP2) mutant resulted in severe flowering defects where the most severely affected transgenic lines were unable to transition from a vegetative to an inflorescence meristem (Kobayashi et al., 2012). Based on the severe flowering defects seen in the transgenic lines, *OsMADS14, 15, 18* and *PAP2* are all likely be inflorescence meristem identity genes required for the vegetative to inflorescene phase transition.

Conserved gene families across grass species allows for elucidation of general floral transition mechanisms

The photoperiod and vernalisation responses of temperate grasses like wheat, barley and *Brachypodium* are well described (Shaw et al., 2012, Beales et al., 2007, Casao et al., 2011, Ream et al., 2014). Based on conserved gene families in rice, maize, *Arabidopsis*, *Brachypodium* and wheat (Tanaka et al., 2013, Wang et al., 2015, Zhang and Yuan, 2014, Spanudakis and Jackson, 2014, Jung et al., 2014), we can expand on the previously described vernalisation and photoperiod pathways and infer a possible gene network which modulates floral transition in temperate grasses **Figure 7**.

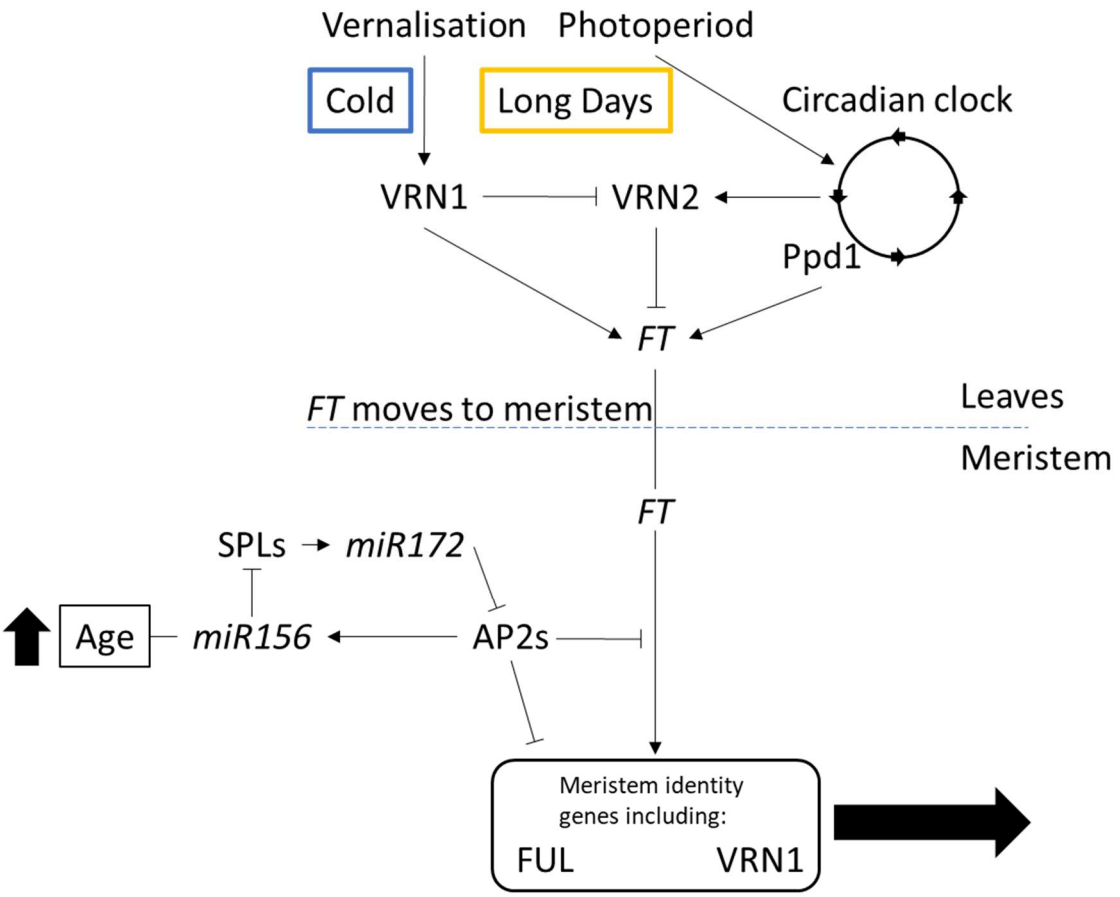

Figure 7 A general model of floral activation and regulation in temperate grasses. This model of floral transition regulation is based on a number of reviews spanning *Arabidopsis* and major grass species (Tanaka et al., 2013, Wang et al., 2015, Zhang and Yuan, 2014, Spanudakis and Jackson, 2014). For the purpose of this thesis, the model has been simplified to include only the gene families that will be discussed herein. There are many more proposed regulators of the floral transition that are not included in the model, including a wide range of hormones and genes. Note that in the grasses, there is a central role for *FT* in modulating floral meristem identity with its expression or activity being manipulated by multiple converging pathways.

Regulation of inflorescence/rachis branch formation

The AP2 *ETHYLENE RESPONSE* (ERF) transcription factors *BRANCHED SILKLESS1* (*BD1*) in maize, and *FRIZZY PANICLE* (*FZP*) in rice, are required for the timely transition of axillary meristems from branched/inflorescence to spikelet meristems. In *bd1* mutants, the maize tassel produces extra branches but is eventually able to produce a spikelet and determinate number of florets at the apex of each branch (Chuck et al., 2002). In rice, *FZP* produces a similar phenotype when mutated, but unlike maize *bd1,* severe mutant alleles of *fzp* are completely unable to transition from branch to spikelet production (Komatsu et al., 2003). Less severe alleles of *fzp* behave more like *bd1* producing some spikelets (Komatsu et al., 2003). In comparison to the tassel, the ear of *bd1* completely fails to acquire spikelet meristem identity (Chuck et al., 2002), a consequence of differentially regulated inflorescence determining genes in the tassel compared to the ear of maize.

The AP2-like genes, *OsIDS1* and *SNB* have been shown to act together to inhibit the expression of *FZP* thus regulating inflorescence branching in rice (Lee and An, 2012). In wheat, the production of secondary and higher order branching is rarely seen. This would suggest that a strong block on branching exists, perhaps as a consequence of multiple genetic copies of the wheat *FZP* orthologue.

The grass specific *RAMOSA* (from the Latin ‘ramus’ meaning ‘branch’) pathway of genes acts to control spikelet identity and branching in maize (Gallavotti et al., 2010, Bortiri et al., 2006, Satoh-Nagasawa et al., 2006, Vollbrecht et al., 2005). *RAMOSA2* (*RA2*) (lateral organ boundary domain transcription factor) and *RAMOSA3* (*RA3*) (trehalose-6-phosphate phosphatase) actively promote the expression of *RAMOSA1* (*RA1*) (Cys2-His2 zinc-finger transcription factor). *RA1* then forms a complex with *RAMOSA ENHANCER LOCUS 2* (*REL2*) (transcriptional co-repressor), and together

they act to define spikelet meristem identity. Mutations in any of the *RAMOSA* pathway genes lead to inflorescence branching similar to *bd1* mutants (Gallavotti et al., 2010, Vollbrecht et al., 2005, Satoh-Nagasawa et al., 2006, Bortiri et al., 2006).

A close homologue to *REL2*, *ABERRANT SPIKELET AND PANICLE1* (*ASP1*) has been described in rice with *asp1* mutants displaying numerous floral defects, reduced branching and precocious spikelet formation (Yoshida et al., 2012, Ikeda-Kawakatsu et al., 2012). Both *REL2* and *ASP1* share homology with the *Arabidopsis* gene *TOPLESS1* (*TPL1*). *TPL1* has been shown to act as a transcriptional co-repressor by recruiting histone deacetylation complexes (HDAC) which negatively regulate transcription via chromatin modification (Krogan and Long, 2009). Inhibiting HDAC mimics the phenotype of the *asp1* mutant suggesting that *ASP1* may function similarly to *TPL1* (Yoshida et al., 2012).

A common theme with the function of the aforementioned inflorescence branching regulators is a delayed or reduced capacity for them to promote axillary meristems to take on spikelet meristem identity, thus axillary meristems are more likely to behave like inflorescence or branch meristems.

Thesis outline

In the case of most cereal crops, basic developmental research is progressing faster than ever before thanks in part to improvements in, and accessibility to genetic sequencing tools and online databases sharing newly acquired genetic information. In comparison to research in the other cereal crops where many novel genes affecting yield traits have been elucidated, wheat research has progressed more slowly. This is not to say that selection for elite yield traits in wheat is not occurring, but often the specific genes responsible for controlling traits are not being identified at a sequence level. A lack of basic genetic knowledge exists in wheat due, in part, to the large hexaploid genome of bread wheat, and large tetraploid genome of durum or pasta wheat. Additionally, a proportion of the wheat genome consists of highly repetitive regions making the assembly of an accurate, continuous reference genome sequence technically difficult and too expensive for most small research budgets.

Although there are difficulties with working in a polyploid species like wheat, it is important that we understand the basic genetic control of yield traits within each crop species. An understanding of basic gene function will allow us to direct yield increases through targeted breeding incorporating new alleles of yield determining genes. An improved understanding of inflorescence development genes will unlock potential to subtly manipulate these genes to maximise yield outcomes in different growing regions.

Elucidating gene function in wheat, compared to the other diploid crop species (rice, maize and barley) is typically a time-consuming process. This thesis will explore ways to rapidly elucidate novel gene function in wheat by means of mutagenesis, transgenics, comparative genetics and modern sequencing technologies. By identifying genes that influence inflorescence development in wheat, the work presented here will highlight

potential genetic targets in which allelic variation could be introduced to enhance grain production in wheat.

Thesis layout

Chapter 3 will explore the genetic control of inflorescence branching in wheat. Figure 7 highlights that *PPD-1* regulated expression of *FT* is necessary to drive the floral transition of the meristem. Using mutants of *Brachypodium* and wheat we show that changes in expression or function of *PPD-1* and *FT* can modulate inflorescence branching. We show that transgenic wheat overexpressing *TaTB1* also leads to increased branching. Our work in wheat relating to *PPD-1, FT* and *TB1* has been published or is currently under review for publication. You can find these articles in the appendix section.

Chapter 4 looks at the function of the major wheat domestication gene *Q*, an AP2 transcription factor on chromosome 5A that in its domesticated form influences spike compaction, flowering time and grain separation from the spike at harvest. This chapter explores previously undescribed roles for *Q* in inflorescence development and the regulation of *Q* expression via its miR172-binding site. This work has been published and makes up the results section of this chapter. The published article can be found in the appendix section.

Chapter 5 uses two examples of wheat inflorescence phenotypes (one mutant and one a natural variant allele) with unknown genetic cause to describe the potential for uncovering causal genes using modern sequencing technologies. A changing landscape with unprecedented access to genetic resources in wheat, combined with a recently released wheat genome sequence should allow for rapid identification of gene function, improving our understanding of inflorescence development.

Chapter 2 - General materials and methods

Sterilisation, germination and planting

All wheat grain was harvested from mature, dry plants. Grain was removed from the wheat spike and cleaned by hand to prevent cross contamination of individual lines. After harvest, grain was 'after ripened' by storing at 37°C for 1-2 weeks to ensure uniform germination.

Grain were planted around 3cm deep in 'wheat special' soil mix, prepared by the CSIRO potting shed. No sterilisation was required when planting grain directly in soil. For detailed phenotyping and other experiments, plants were grown in native tube pots (12cm tall 300ml pots). Plants grown for mutant screening were either planted in rectangular wooden trays (60cm x 25cm) at high density, 48 or 96 plants per tray or grown in native tube pots. For all planting, better rates of germination and better plant health was achieved when soil was never allowed to sit in water. Once germinated, plants were watered enough to ensure that complete drying of soil would not occur. One gram of *Mini Osmocote*® fertiliser was applied per plant once the third leaf had emerged. Growth conditions are detailed in next section.

Plants grown for DNA extraction were plated evenly spaced in petri dishes on filter paper allowing approximately 1cm between grains. Sterile water containing Thiram (concentration as per manufacturer's instructions) was added to saturate filter paper and create a thin film of liquid above the paper; 4ml for a 10cm petri dish. Petri dishes were covered and sealed with *Parafilm*® to prevent evaporation. Plates were wrapped in foil and stored at 4°C for 48 hours before being transferred to 22°C to allow for germination. Once germination had occurred and first leaf had elongated around 2-3cm from the grain, leaves were harvested for DNA extraction. Seedlings were either transferred to soil or discarded. DNA extraction was also performed on leaf samples

taken from seedlings or adult plants grown in soil. The highest quality DNA extractions were achieved from seedling leaf samples.

Growth conditions

The following cabinet growth conditions were used. Plants were grown in controlled conditions for phenotyping and RNA extraction experiments.

Photoperiod	Main Lights	Dark
12h	12h at 22°C	12h at 16°C
16h	16h at 22°C	8h at 16°C

Light intensity Measured at 420µM m^{-1} s^{-1} 50cm below light source just above leaf canopy.

Plants were also grown in temperature controlled glasshouse and polyhouse conditions (24°C Day and 18°C night) for bulking seed, large scale phenotyping and mutagenesis screening. Plants were also grown for bulking seed and mutant screening in outdoor conditions under wire cage to protect from birds.

Wheat cross pollination

To ensure that self-pollination was not possible apical and basal spikelets were removed leaving only 10-12 spikelets on the central rachis nodes as these spikelets are typically at similar developmental stages. Florets were removed from the centre of remaining spikelets leaving only the first and second developed florets which are largest in size and have similar developmental timing. The palea and anthers were then removed from each floret, one floret at a time, ensuring that no anthers were missed. Emasculation was performed early in floral development soon after spikes had emerged and while anthers were still green. Emasculated spikes were covered with wax paper bags to prevent indiscriminate pollination from nearby plants. Emasculation was always performed on 'WT' varieties with donor pollen being supplied from mutant lines. The mutants in question carried semi dominant phenotypes and therefore successful crosses could easily be determined in the first generation. There were no cases where grain resulting

from crosses did not produce plants with intermediate mutant phenotypes indicating that the crossing method successfully avoided self-pollination. Plants for crossing were sown three at a time, twice a week for three weeks to ensure cross over of mature floral development between lines to be crossed. Mature pollen was applied to WT heads 2-3 times over a period of 3-5 days to maximise the chance of successful pollination. After each application of pollen, spikes were covered with their wax paper bags and the cross was recorded. For second and third applications of pollen, this process was repeated using the same donor plant each time.

DNA extraction

Adapted from cotton leaf extractions method (See below). Both 96 well-plate or individual tube extractions were performed using the same reagents but different volumes, centrifuges and spin speeds. For tube samples, liquid volumes added were doubled and all centrifugation was performed in desktop a micro centrifuge at maximum speed. Plate samples had volumes added as below and centrifugation steps were performed in large free standing or benchtop centrifuge at stated rpm with plate basket attachments.

All liquid volumes shown here are for plate method. For tube method, all volumes were doubled. Leaf samples were taken from young seedlings as a 3-4cm piece from the second or third leaf and added to 96 well plates or individual 2ml tubes with snap lids with a one or two ball bearings respectively. Samples were then frozen at -80°C before being shaken in a mixer mill/tissue lyser for at least 1min in racks cooled to -80°C. Shaking was repeated if leaf samples were not yet processed to a fine powder. 200ul of Cotton Lysis Buffer was added to each leaf sample before being shaken by hand or vortexed for 2mins. Samples were centrifuged for 2mins at 2000rpm (plates) or 1 minutes (Tubes) and then incubated at 65°C for 30-60mins. Samples were cooled in

standard freezer (approx. -20°C) for 10 mins before adding 150ul of chloroform:isoamyl alcohol (24:1) and shaking or vortexing for 1min. Samples were centrifuged for 10 minutes at 2000rpm (plates) or 5 minutes (tubes) then supernatant was carefully removed to fresh storage plate or 2ml snap lid tube. An equal volume of isopropanol was added to each sample before mixing and centrifuging for 30 minutes at 3000rpm (plates) or 20-30 minutes (tubes). All liquid was decanted from samples by inversion and light tapping on paper towel leaving the DNA pellet. The pellet of each sample was then 'washed' with 200ul of freshly prepared 70% ethanol then centrifuged at 3000rpm for 20 minutes (plates) or 15-20 minutes (tubes) before removal of ethanol by decanting or pipetting. Plates and tubes were left to dry completely at room temperature before adding 50ul of TE. DNA concentration of samples was assessed by spectrophotmeter (*NanoDrop*) and adjusted to a final concentration of 100ng/µl.

Cotton Lysis Buffer

Final concentration	**Add**
0.1M Tris-Cl pH8 (1M Stock)	20ml
1.4M NaCl	16.4g
0.02M EDTA pH 8 (0.5M stock)	8ml
2% (w/v) CTAB	4g
2% (w/v) PVP40	4g
Water	to 200ml
Autoclave	

PCR

Annealing temperatures in PCR protocols varied based on melting temperature of primer pairs.

Taq polymerase PCR

Per 20µl reaction: 1µl 100ng/µl DNA, 2µl 10xThermopol buffer (*NEB*), 0.6µl DMSO, 0.8µl 5mM dNTPs (*Promega*), 1µl 10µM Forward Primer, 1µl 10µM Reverse Primer, 0.2µl *Taq* DNA Polymerase (*NEB*), 12.4µl sterile water.

95°C 2min, (95°C 30sec, annealing 30sec, 72°C 1min per kb) 40 repeats, 72°C 10mins, 4-10°C hold

High fidelity PCR

Per 20µl reaction: 1µl 100ng/µl DNA, 4µl 5xGC Buffer (*NEB*), 1µl 5mM dNTPs (*Promega*), 1µl 10µM Forward Primer, 1µl 10µM Reverse Primer, 0.6µl DMSO, 0.2µl *Phusion* Polymerase (*NEB*), 11.8µl sterile water.

98°C 30sec, (98°C 10sec, annealing 30sec, 72°C 20sec per kb) 35 repeats, 72°C 10min, 4-10°C hold

Sequencing PCR

Per 10µl reaction: 2µl of gel purified DNA (concentration variable), 1µl 3.2µM either Forward or Reverse Primer, 3.5µl Sequencing Buffer, 1µl *Big Dye* (*Applied Biosystems*) sequencing mix, 2.5µl water.

96°C 1min, (96°C 5sec, 50°C 5sec, 60°C 4min) 30 repeats, 4-10°C hold

Colony PCR

Per 20µl reaction: Colony touched with tip of 200µl pipette tip and tapped once on bottom of PCR tube, 2µl 10xThermopol buffer (NEB), 0.8µl 5mM dNTPs (*Promega*), 0.2µl *Taq* DNA Polymerase (NEB), 1µl 10 µM M13 Forward Primer, 1µl 10 µM M13 Reverse Primer, 15µl sterile water.

95°C 2min, (95°C 30sec, 50-60°C 30sec, 72°C 1min per kb) 30 repeats, 72°C 10mins, 4-10°C hold

qPCR

Per 20µl reaction: 5µl cDNA sample, 2µl 10xPCR Reaction Buffer -$MgCl_2$ (*Invitrogen*), 1.4µl 50mM $MgCl_2$ (*Invitrogen*), 0.8µl 5mM dNTPs (*Promega*), 1µl SYBR Green (*Invitrogen*), 0.1µl *Platinum Taq* (*Invitrogen*), 2µl 5uM Forward and Reverse Primer mix, 7.7µl sterile reverse osmosis water.

Per 10ul Reaction: 5µl cDNA sample, 1µl 10xPCR Reaction Buffer -$MgCl_2$ (*Invitrogen*), 0.7µl 50mM $MgCl_2$ (*Invitrogen*), 0.4µl 5mM dNTPs (*Promega*), 0.5µl SYBR Green (*Invitrogen*), 0.05µl *Platinum Taq* (*Invitrogen*), 1µl 5uM Forward and Reverse Primer mix, 2.35µl sterile reverse osmosis water.

94°C 4min, (94°C 30sec, 55-62°C 15sec, 72°C 20sec (florescence acquisition)) 30 repeats, 40°C 2mins, 55-99°C (florescence acquisition for every °C)

Agarose gel electrophoresis

Gel was prepared to a concentration of 1% Agarose dissolved in 1xTBE. For visualisation of general PCR including *Taq* PCR and Colony PCR 1µl/50ml of *RedSafe*™ was added to gel moulds immediately prior to pouring gel. For visualisation of *Phusion* PCR which would be subject to band excision and gel extraction 2µl/50ml of *RedSafe*™ was added to gel mould immediately prior to pouring gel. Liquid Agarose solution was stored at 50°C for up to one month. Loading dye was added to PCR product prior to loading. Gels were run in 1xTBE (voltage and time variable). Gels were placed on UV trans-illuminator for visualisation and documentation. Gels requiring band excision were visualised on a dark reader. 2% Agarose was used to visualise and validate qPCR products.

PCR Gel Extraction

DNA bands were excised using straight edged disposable razors taking a minimum amount of gel with product. Gel extraction was performed as per QIAGEN Gel Extraction Kit protocol using all recommended and optional wash steps in a bench top microfuge. 30µl of Elution Buffer was used to elute bound DNA. Purified DNA was then stored at -20°C until ready for use.

Electroporation Transformation

XL1-Blue Competent cells suspended in glycerol were stored at -80°C and then transferred to prior to transformation. 1-1.5µl of ligation reaction was added to *XL1-Blue Competent* cells. Cells were transferred to a clean cuvette kept cool on ice. Cuvette was tapped to ensure contents were accumulated at the base then cuvette was placed in an electroporation device and shocked at 2200-2300V. 200-500µl of cold LB was added to cells in cuvette and then contents of cuvette were transferred back to original *eppendorf* tube. After 1 hour incubation at 37°C cells were placed on selective media. Cells to be selected on ampicillin were incubated for 15 minutes only.

For blue/white colony selection *Eppendorf* tubes were then placed in 37°C water bath for 15-30min. 50µl and 200µl of cell suspension were spread plated on Ampicillin plates each of which had been spread with 60µl X-gal [20mg/ml in dimethylformamide] and 6µl IPTG [0.8M] and allowed to dry before adding cells. Plates were sealed with *Parafilm*® then incubated overnight at 37°C. Plates were incubated overnight at 4°C before selecting white colonies.

Transformation of agrobacterium was performed as above except voltage was reduced to 2000V and post-electroshock incubation was at 28°C for 2 hours before plating.

Plated agrobacterium was grown at 28°C for 48 hours before screening for transformants.

Ligation of PCR product into *pGEM-T Easy* prior to sequencing

The A-overhang necessary for ligation into the *pGEM-T Easy* vector (*Promega*) was added to PCR product by combining 15.8µl of gel purified DNA to 0.2µl of *Taq Polymerase,* 2µl 5mM dNTPs, 2µl 10xThermopol buffer then incubating for 15min at 72°C. Ligation into *pGEM-T Easy* vector was prepared by combining 1µl *pGEM-T Easy,* 1µl *T4 DNA Ligase* (*Promega*), 5µl A-overhang product, 7µl 2xRapid Ligation Buffer (*Promega*) then incubated for 1hr at room temperature followed by incubation overnight at 4°C.

Preparing sequencing PCR product for sequencing submission

10µl of water was added to contents of Sequencing PCR. Contents were transferred to 1.5ml *eppendorf* tube. 3.5µl of 3.2M Sodium Acetate pH5.2 was added followed by 55µl of 100% ethanol. Tubes were mixed well and centrifuged for 30min at maximum speed in microfuge. Supernatant was removed carefully by pipetting from opposite side of pellet. 100µl of 70% ethanol was carefully added down side of tube opposite to pellet before spinning for 15min maximum speed in microfuge. As much supernatant was removed as possible from opposite side of pellet then tube contents were allowed to dry on bench top at room temperature or for quicker drying a vacuum centrifuge was used.

Tissue harvesting/ RNA extraction/ cDNA synthesis/ Expression analysis by qPCR

Meristems were harvested from the main stem of wheat plants at varying stages of inflorescence development/transition. Using a sterile razor blade approximately the top third of plant material was removed longitudinally from the area covering the apical meristem. Any remaining vegetative tissue was carefully removed to expose the meristem. Entire meristems were extracted without taking surrounding leaf tissue and then placed in 1.5ml or 2ml *eppendorf* tubes before immediately freezing in liquid nitrogen. Depending on the size of the apical meristems, 3-5 were harvested per tube to make one biological replicate. Stem tissue was harvested from the top 0.5cm of the peduncle internode immediately below the apical meristem. Tissue samples were stored at -80°C until needed.

Unless stated otherwise in our attached published materials and methods, RNA extraction from plant tissue was performed using the *Spectrum™ Plant Total RNA Kit* (*SIGMA-ALDRICH*) as per manufacturer's instructions. Prior to RNA extraction tissue samples were ground as per DNA extraction method and the entire contents of the tube was used in RNA extraction. Ball bearings were removed using a magnet after the addition and mixing with first buffer. RNA concentration was determined using *Spectrophotmeter* (*NanoDrop*).

cDNA synthesis was performed using *SuperScript™ III First-Strand Synthesis* (*Invitrogen*) as per manufacturer's instructions for 20µl reaction. cDNA was diluted tenfold by adding 80µl of sterile water before being stored at -20°C.

Unless stated otherwise in our attached published materials and methods, expression levels of target genes were determined by qPCR as per previously stated method. qPCR was performed using a *Rotor-Gene G* (*QIAGEN*) unless otherwise stated in associated

publications. Expression levels were normalised to housekeeping genes and shown relative to expression levels of 'Wild Type' sample. qPCR was performed on at least 3 biological replicates per tissue and genotype. Significance of expression differences between mutant and 'wild type' lines was assessed using a homoscedastic, single tailed, student's t-test.

Additional materials and methods

Additional materials and methods specific to each results chapter, including primer sequences, can be found in appendix in included publications.

Chapter 3 - Genetic control of inflorescence branching

Introduction

The grass inflorescence takes many species-specific forms. Much of this variation can be explained by differences in inflorescence branching. The degree of inflorescence branching is determined by the transition of axillary meristems from a branch or inflorescence meristem identity to a spikelet meristem identity. If the axillary meristem maintains a branch meristem or inflorescence meristem identity it will behave as an inflorescence meristem forming its own rachis with axillary meristems that themselves form branches or spikelets. The archetypal single rachis inflorescence of wheat is distinct from its grass crop relatives, maize and rice which produce branched inflorescences in their tassel and panicle respectively.

Axillary meristems of wheat rapidly transition to spikelet meristem identity preventing the formation of secondary rachises or primary and higher order branches (Poursarebani et al., 2015). Many spikelets (usually around 20) form along the main rachis of the wheat spike but typically the inflorescence does not branch to form an additional rachis or 'primary branch'. The model grass, B*rachypodium distachyon* has a similar inflorescence architecture to wheat with single indeterminate spikelets arranged on a single rachis. Loss of function in rice and maize ERF/AP2 genes *FZP* and *BD1* increase the degree of branching in these species. Similar loss of function mutations in related ERF/AP2 genes have been identified in *Brachypodium* and wheat which are sufficient to cause inflorescence branching (Derbyshire and Byrne, 2013, Dobrovolskaya et al., 2015).

This chapter will investigate two forms of branching, the first a true inflorescence meristem branch in which an axillary meristem behaves similarly to the apical inflorescence meristem producing its own rachis with a series of axillary meristems which form branches or spikelets **Figure 8**, **Figure 9**; the second is the paired spikelet which we believe to be a unique form of branch where two spikelets form at a single rachis node in a distinct phyllotaxy **Figure 8 Figure 12**. This chapter will build on unpublished and published data to better define inflorescence branching in wheat using wheat mutants, transgenic lines, *Brachypodium* as a model for the wheat inflorescence and the known genetic control of inflorescence architecture in other grass species.

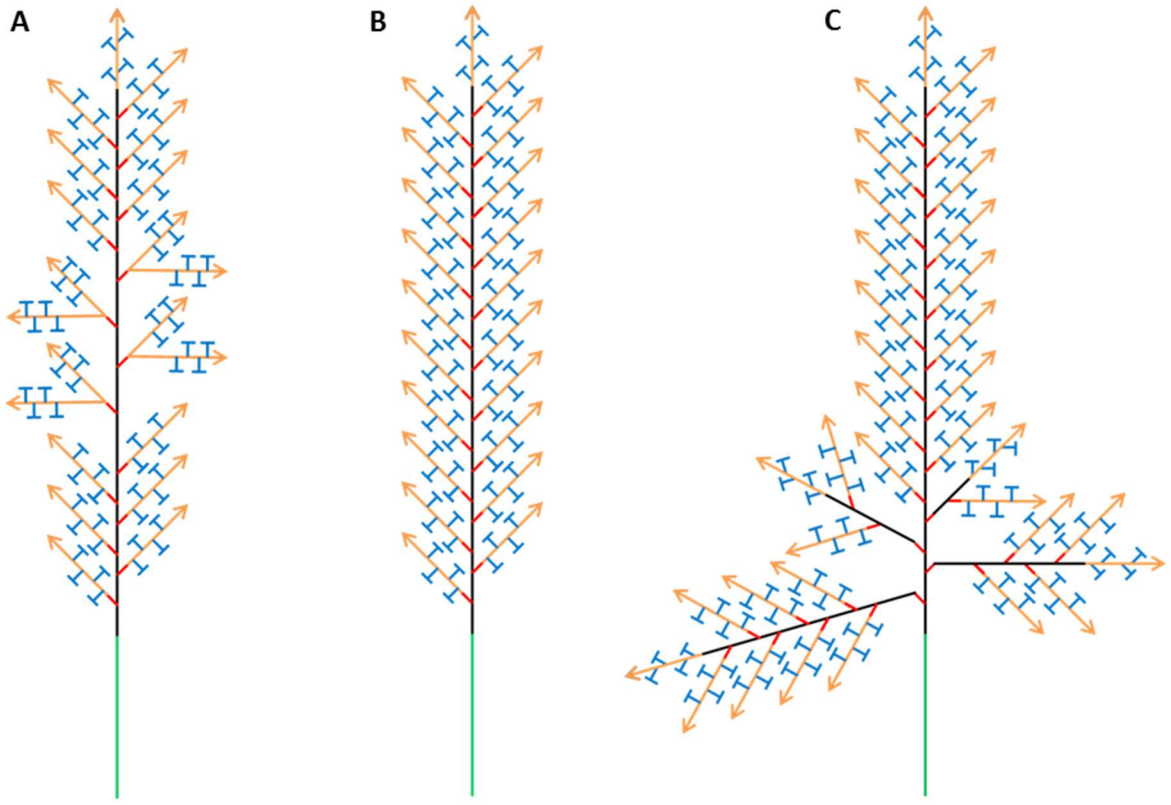

Figure 8 Wheat spike schematics (**A)** Wheat spike bearing paired spikelets (**B)** Archetypal wheat spike with single rachis and single spikelets (**C)** Branched spike with primary branches from the 1st, 2nd, 3rd and 4th rachis nodes (4 most basal nodes). The various meristem states and their position in the developing Inflorescence, Vegetative, Inflorescence, Branch, Spikelet and Floral Meristems. The transition to each meristem stage and the formation of axillary meristems is under environmental and genetic control. Arrows represent indeterminate meristems which form an undefined number of structures (Spikelet Meristem) whereas 'T' symbols indicate that a meristem is determinate and will be consumed producing a single structure (Floral Meristem).

Several genes have been shown to affect inflorescence branching in the grasses. In rice, gain of function mutations of *TAWAWA1 (TAW1)* produce highly branched inflorescences whereas loss of *TAW1* function is associated with smaller less branched inflorescences (Yoshida et al., 2013). *TAW1* appears to positively regulate *SHORT VEGETATIVE PHASE (SVP) MADS-box* transcription factors which are negative regulators of spikelet meristem identity. At the same time, *TAW1* negatively regulates expression of MADS-box transcription factors which themselves positively regulate spikelet meristem identity and spikelet organ formation. Thus, *TAW1* appears to regulate the formation of branching by determining rates of meristem transition in a manner similar to *FZP* (Yoshida et al., 2013, Komatsu et al., 2003). *TAW1* belongs to the ALOG gene family which is named after its earliest identified members (*Arabidopsis* LSH1 and *Oryza* G1) (Zhao et al., 2004, Yoshida et al., 2009). The first described ALOG gene in Arabidopsis, *LSH1*, was shown to elicit developmental changes in a photoreceptor dependant manner (Zhao et al., 2004). However, the role of light quality or photoperiod in regulating branching in *TAW1* has not been explored.

In maize, the *RAMOSA* transcription factors RA1, and RA2, together with RA3 (encoding a trehalose-6-phosphate phosphatase), positively regulate spikelet meristem determination and prevent the formation of long branches (Bortiri et al., 2006, Gallavotti et al., 2010, Satoh-Nagasawa et al., 2006). Loss of function *RA2* mutants feature disorganised inflorescences with higher degrees of branching and a reduction in paired spikelet formation (Bortiri et al., 2006). The maize ancestor teosinte initiates the development of a pair of spikelets but only one develops (Hubbard et al., 2002). Increased expression of the major domestication gene *TEOSINTE BRANCHED1* (*TB1*), relative to the pre-domestication form contributes a large amount of the developmental variation between teosinte and modern maize (Doebley et al., 1997). Domesticated *TB1* only accounts for some of the typical domesticated traits of maize with a small

proportion of complete paired spikelets forming when the domestication allele of *TB1* is crossed into teosinte (Doebley et al., 1995, Hubbard et al., 2002). Thus, the development of paired spikelets in maize is influenced by *TB1* but requires other genetic variation present in modern maize varieties before the vast majority of spikelet meristems develop as pairs.

Previous work relating to branched inflorescence architecture

Here, in the introduction to this chapter, I will briefly describe work relating to my honours research which is not represented in the literature but precedes and contributes to the new results and discussion points of this chapter. During my honours year, I described in detail the phenotypes of the *Brachypodium* mutant MB71 which features a highly branched inflorescence. The mutation causal to the observed phenotypes was found to be a large insertion before the transcriptional start site of an AP2/ERF transcription factor (Derbyshire and Byrne, 2013). The *AP2/ERF* gene appears to be orthologous to *FZP* in rice and *BD1* in maize, hereby referred to as *BdFZP* (*Brachypodium distachyon FZP*). While (Derbyshire and Byrne, 2013) conclude that the insertion responsible for the phenotypes of MB71 results in decreased expression of *BdFzp* (80% of WT), I did not observe expression differences during the double ridge stage of inflorescence development. While we cannot rule out that transcript levels are altered at some developmental stage in the mutant, it is also possible that the insertion which is close to the predicted translation start site is resulting in truncated transcript and protein synthesis.

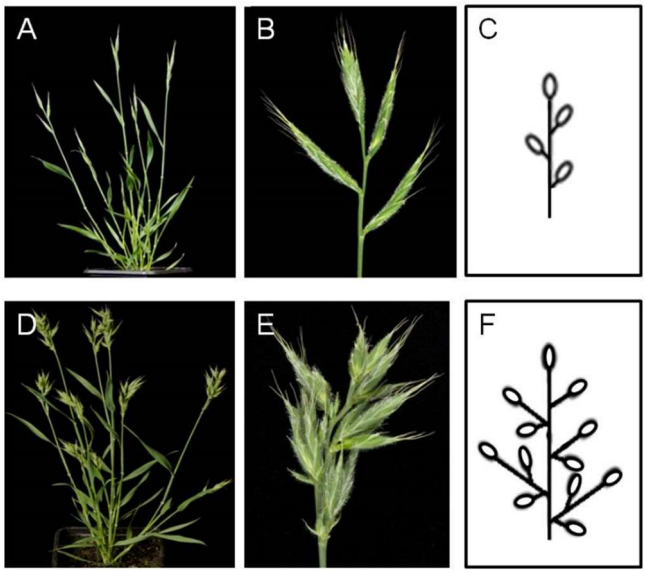

Figure 9 Bd21 and derived branched spike mutant MB71. (**A)** Bd21 whole plant. (**B)** Close up of Bd21 spike with four spikelets. **(C)** Schematic of Bd21 spike showing single spikelets at each of the three rachis nodes and a single terminal spikelet. (**D)** MB71 whole plant. (**E)** Close up of MB71 spike with multiple spikelets forming in branches off the main axis. (**F)** Schematic of MB71 spike showing the branching phenotype. Photos provided by Mary Byrne.

The branched inflorescence mutant MB71 was compared to its progenitor line Bd21 **Figure 9** in either one of four photoperiod conditions with fixed day and night temperatures **Figure 10**. To gauge the response to photoperiod without changing photosynthetic light quantity, 12 hours with full light plus photoperiods extended with incandescent light for 4 and 8 hours were used to provide 16 and 20 hour days. For Bd21 and MB71, spikes emerged later and produced more rachis nodes when plants were grown under shorter photoperiods, indicating that floral transition is promoted under long photoperiods. In comparison to Bd21, the spikes of MB71 plants emerged from the flag leaf later in all photoperiod conditions except for 20 hours **Figure 10 A**. Although spike emergence was similar between MB71 and Bd21 grown under 20h days, MB71 spikes showed signs of delayed development when compared to Bd21 spikes **Figure 10 E, F**. A delay in lateral spikelet development was also observed by Derbyshire and Bryne, 2013. This obvious developmental delay under all conditions indicates that MB71 has a delayed floral transition in comparison to Bd21. Delayed floral transition in MB71 in all conditions was associated with increased rachis node

number **Figure 10 B**, as well as an increase in spikelet number **Figure 10 C**. In MB71 multiple spikelets were present in branches at the basal rachis nodes whereas the apical rachis nodes were unfilled **Figure 10 D**, producing rudimentary structures but no complete spikelets, florets or grain. The number of spikelets per rachis node and the number of unfilled apical rachis nodes were increased in weakly inductive short day photoperiods (16h) compared to stronger florally inductive photoperiods (20h). Together these results indicate that loss of *BdFZP* function results in the delayed transition to spikelet meristem identity resulting in branched inflorescences and more rachis nodes on the primary axis of the inflorescence. A reduction in the number of filled rachis nodes under conditions which exaggerate these phenotypes (short days) indicates that there is a ceiling on the number of grain producing inflorescence structures that are able to develop. Growing MB71 in larger pots as well as removing all tillers but the main stem resulted in increased rachis node and grain filling in support of this observation. Similarly, we found that while grain number was increased in MB71 as a direct result of increased number of floral structures (spikelets and florets), grain size was also reduced. This highlights that, while we can increase grain number by altering rates of floral transition, this may not necessarily lead to yield increases. We have made similar observations in wheat where mutants with delays in flowering time and floral development produce more rachis nodes in the inflorescence and a greater number of grain which are smaller in size. In conclusion, genetic and phenotypic evidence suggests a link between *BdFZP*, flowering time and inflorescence development.

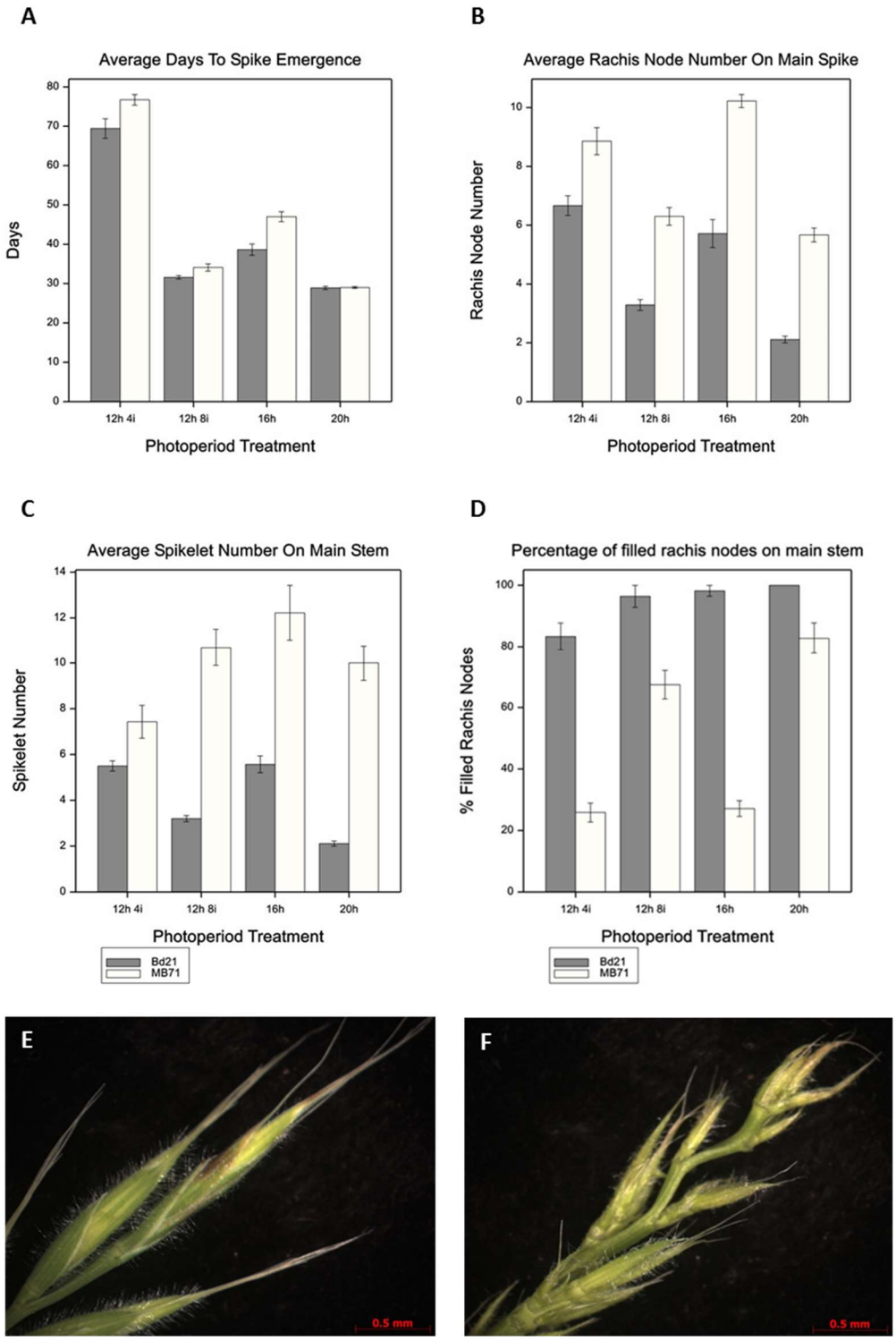

Figure 10 The branched spike *Brachypodium* mutant MB71 is delayed in inflorescence development. (A) Days until main spike emergence (**B)** the number of rachis nodes on the main stem, (**C)** the number of spikelets on the main stem and (**D)** the percentage of rachis nodes which were filled (spikelets present) on the main stem. Data is represented as the average with error bars representing standard error, n=10. X axis of figures indicates photoperiod length where h=daylight hours and i= length of incandescent light extension rich in far red light. (**E)** Main spike of Bd21 grown under 16 hour days just after spike emergence. (**F)** Main spike of MB71 grown under 20 hour days just after spike emergence showing delayed developmental stage of MB71 spikelets.

Results

Additional *Brachypodium FZP* mutants display delayed spike emergence and floral development

To confirm that loss-of-function mutations in *BdFZP* result in delayed inflorescence development in *Brachypodium* in an environment dependent manner, I ordered two additional *BdFZP* mutant lines from INRA (French National Institute for Agricultural Research**)** which have already been described to have a branched inflorescence presumably caused by the single nucleotide mutations and predicted amino acid changes in the AP2 binding domain of *BdFZP* (Dobrovolskaya et al., 2015). The mutants, named MS (multi spikelet) and DS (double spikelet) were so named for their typical degree of branching. However, branches with more than two spikelets could be observed in DS plants. The MS and DS plants were derived from mutant populations in the *Brachypodium* accession Bd21-3 whereas the MB71mutant was derived from Bd21. To ensure uniform growth between Bd21-3 and Bd21 backgrounds, all lines were vernalised for two weeks prior to growth in 16 hour days. While Bd21 does not require vernalisation to flower, it does respond to vernalisation with a slight reduction in flowering time (Ream et al., 2014). Comparable flowering times between Bd21 and Bd21-3 accessions have been shown to be achieved by two weeks of vernalisation (Ream et al., 2014).

Main spikes of both DS and MS plants emerged later than their parental line Bd21-3 **Figure 11A** and had a similar increase in rachis node number **Figure 11B**. Spikes of MB71 emerged later with more rachis nodes than those of Bd21 in agreement with our previous observations **Figure 10, Figure 11**. In addition to delayed spike emergence and increased Rachis node number, all mutants had spikes with less developed spikelets and florets upon emergence when compared to their parental lines . This is again consistent with our previous observations **Figure 10E, F**. To better assess this delay in development, we also scored the number of days until the florets of mutant spikes matched the developmental stage of just emerged parental spikes. Spikes of mutant lines were underdeveloped upon emergence from the flag leaf taking several days to match the developmental stage of just emerged WT/parental spike **Figure 11 A**.

As we did not perform crossing to isolate the three alleles in a common near-isogenic background, we cannot comment on the severity of phenotypes caused by the different mutant alleles of *BdFZP*. However, these observations strongly suggest that loss-of-function mutations in *BdFZP* lead to delays in inflorescence development. This is consistent with the proposed functional role of orthologous AP2/ERF transcription factors in promoting the transition of inflorescence and branch meristems to a spikelet meristem identity (Chuck et al., 2002, Komatsu et al., 2003).

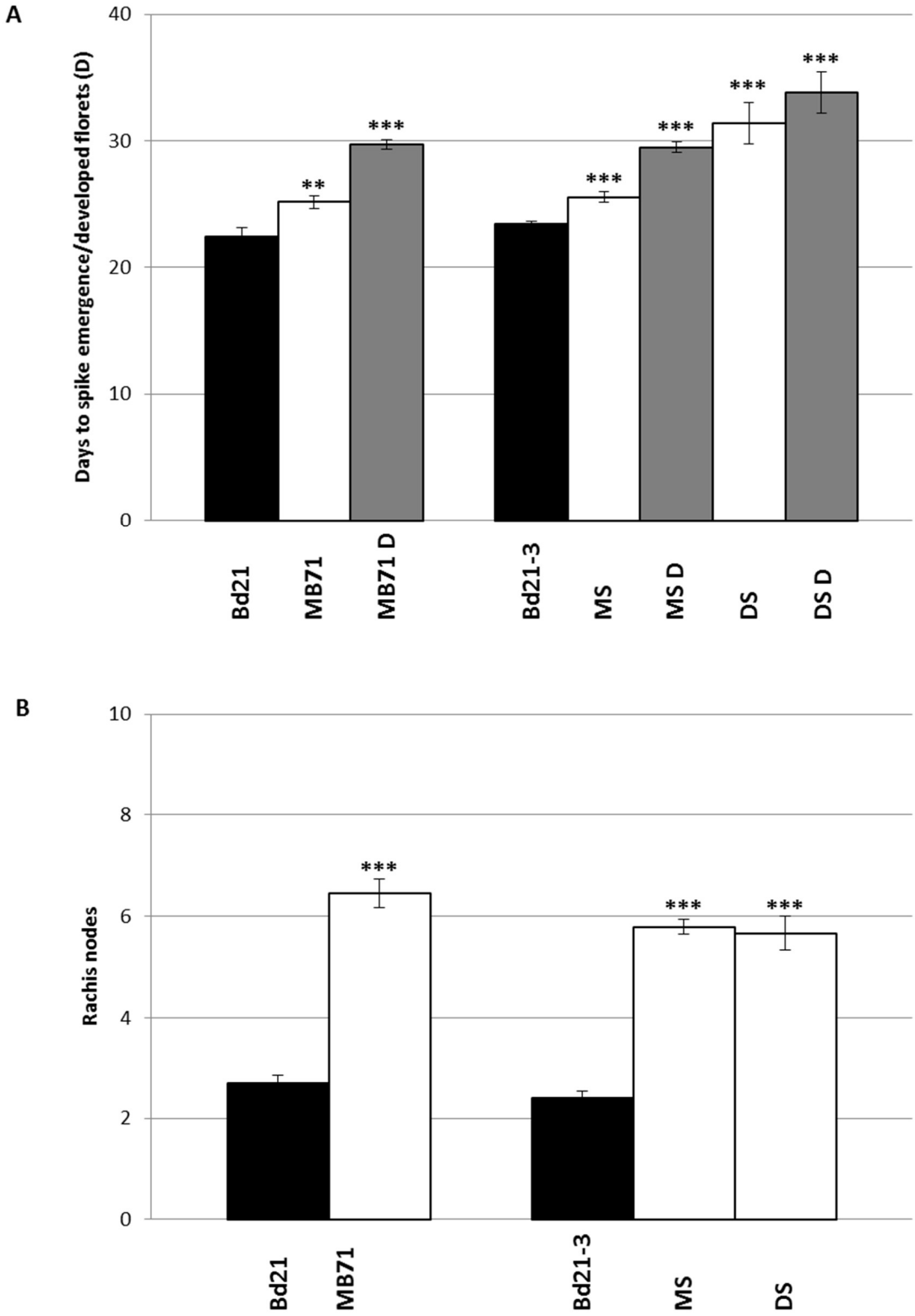

Figure 11 *BdFZP* mutants have delayed inflorescence development. A, Average number of days before emergence of the main spike from the flag leaf. Parental lines (black) shown to the left of derived mutants (white) in the same background. The number of days at which mutant spikes matched the level of spike development (D) of their parent lines at emergence is shown in grey. **B,** Average rachis node number on the main spike. Parental lines (black) shown to the left of derived mutants in the same background (white). n= 10, ** $P < 0.01$, *** $P < 0.001$.

Previous work relating to paired spikelet formation in wheat

This section specifically highlights work by collaborators which relates to the assessment of paired spikelet formation in wheat. It has been included in a separate results section to clearly define which work is mine and which work has been produced by others. Results described after this section (**Previous work relating to paired spikelet formation in wheat)** are my own contributions.

Wheat mutagenesis screens performed at CSIRO generated several mutant lines with a paired spikelet phenotype. Some of these mutants were late flowering indicative of a delayed floral development in comparison to their wild type-like siblings. We described the mutants and the paired spikelet trait in detail (Boden et al., 2015). We showed that paired spikelets arose in mutant lines because of reduced expression of the floral promoting gene *FT*. This effect could also be achieved by growing photoperiod sensitive wheat in short days where *FT* expression is reduced. In a similar manner to branch formation in *Brachypodium*, paired spikelet formation is dependent on the rate of floral transition with both types of structures arising under prolonged development of the inflorescence meristem. Paired spikelets come in one of two forms, rudimentary, possessing only a partial compliment of floret structures and no fertile florets or complete, where the secondary spikelet forms with fully developed florets **Figure 12**.

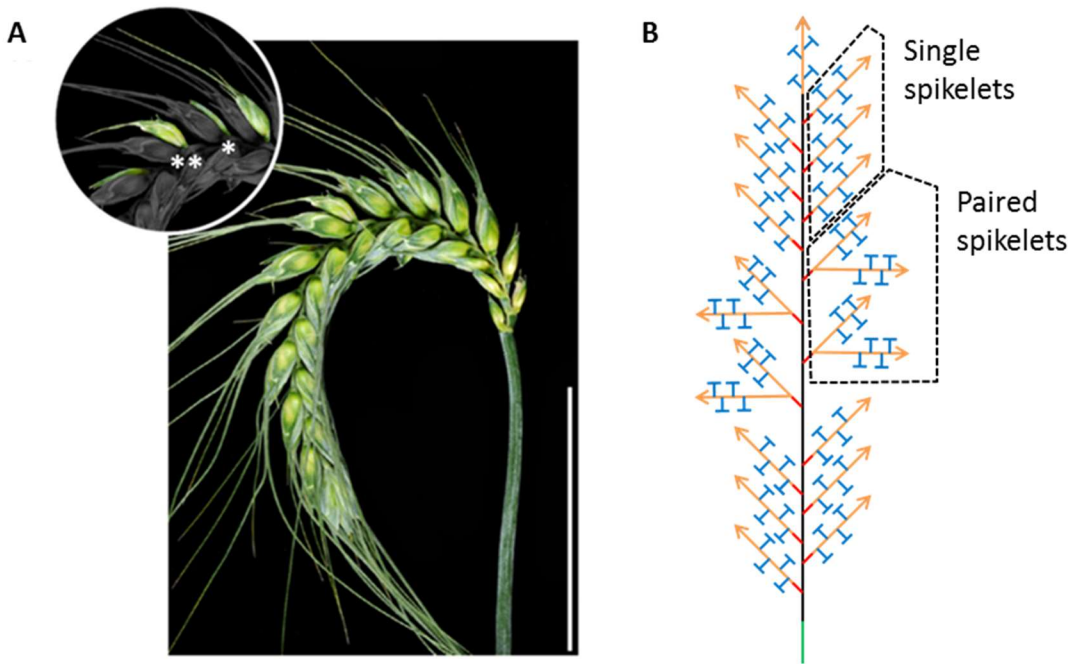

Figure 12 The paired spikelet phenotype of wheat. (A) Wheat spike with complete (**) and rudimentary (*) paired spikelets. **(B)** Schematic representation of paired spikelet producing wheat spike. The archetypal single spikelet per rachis node morphology of wheat is present in the apical and basal portions of the spike. Paired spikelets form with the highest frequency in central rachis node positions.

In addition to the paired spikelet flowering time mutants we described in (Boden et al., 2015) we also isolated a spikelet line with many paired spikelets from a four way cross of elite Australian wheat cultivars (MAGIC population). The paired spikelet line, 0053 was carried through multiple generations of single seed descent selecting for individuals segregating for high and low paired spikelet frequency. High and low branching (high and low paired spikelet) near isogenic sibling lines were established **Figure 13**.

The 0053 HB line which features a high proportion of paired spikelets also has fewer tillers compared to its low branching sibling line **Figure 13**. *FT* expression was comparable between the high and low branching lines (personal correspondence Scott Boden). However, there was a delay in inflorescence development and spike elongation in the high branching line which had smaller less developed spikes (terminal spikelet just defined) compared to the low branching line (post terminal spikelet development with elongating awns) in 8 leaf plants **Figure 13 E**.

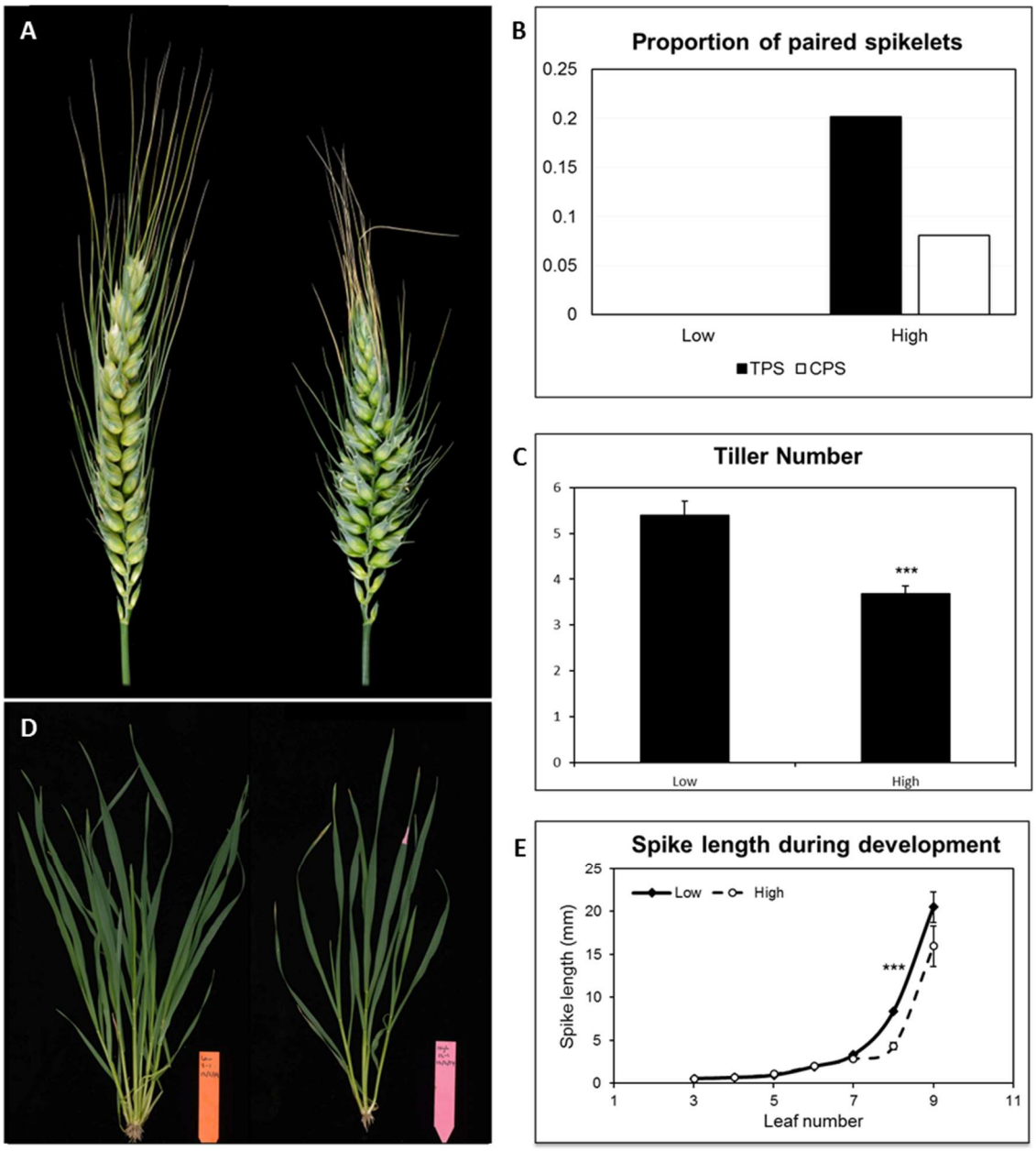

Figure 13 High frequency paired spikelet producing line was isolated from MAGIC population with reduced tiller number. (A) Spikes of low paired spikelet (0053 LB) (left), and high paired spikelet (0053 HB) (right) sibling lines. (**B)** The proportion of total (TPS, rudimentary plus complete) and complete paired spikelets (CPS) in 0053 high and low branching lines. (**C)** Tiller number of mature (after floral transition) 0053 low branching (left) and high branching (right) sibling lines. (**D)** Vegetative phenotypes of mature 0053 low branching (left) and high branching (right) sibling lines. (**E)** Spike length of 0053 high and low branching lines at leaf emergence stages. All data represents the mean result from 12 plants. Error is ± s.e.m. *** P < 0.001. Plants grown under 16 hour days.

DNA based SNP-Chip analysis performed by Matt Hayden (DPI Victoria) and Colin Cavanagh (CSIRO) suggested that the 0053 high branching line had extra copies of chromosome 4D. The analysis also revealed that of the four parents in the MAGIC population, the paired spikelet phenotype was most strongly associated with genomic regions derived from the Baxter wheat variety. Several QTL associated with the paired spikelet phenotype were detected. This analysis suggests that that causal genetic basis for increased paired spikelets in 0053 HB is chromosomal duplications of chromosome 4D derived from the Baxter wheat variety. Even though the duplicated region is large and contains many expressed genes, QTL analysis revealed relatively few QTL on chromosome 4D which are strongly associated with paired spikelet formation including a region containing the likely orthologue of *TB1*. Over expression of the maize *TB1* gene in wheat has been shown to reduce tiller formation in wheat (Lewis et al., 2008). With increases in *TB1* expression known to reduce tiller number in wheat and maize, *TB1* appeared to be a good candidate for a major contribution to tiller reduction and potentially paired spikelet production in the 0053 HB lines. Interestingly, Scott Boden (CSIRO) found that duplicated region of 4D contained a unique, Baxter specific allele of wheat *TB1* though we could not be confident that this allele would have a different effect than another duplicated allele of *TB1*. We decided to examine the effects of *TB1* dosage on paired spikelet formation further with the hypothesis that increased *TB1* dosage was responsible for reduced tiller formation as well as paired spikelet formation in the high branching 0053 line.

Misregulation of wheat floral transition genes leads to a unique branching phenotype known as paired spikelets

We described the paired spikelet phenotype in the context of a series of late flowering, paired spikelet producing lines. These lines were compared to their non-paired spikelet producing sibling (near-isogenic) or parental lines (Boden et al., 2015). Under short day conditions (12h) flowering time was reduced and a high frequency of paired spikelets were produced in comparison to non-paired spikelet producing sibling and parental lines under the same conditions. Reduced flowering time was associated with a reduction in *FT* expression in the paired spikelet producing lines characteristic of delayed floral transition early in the photoperiod sensing pathway (Boden et al., 2015). I characterised the expression of floral meristem identity genes in a subset of the paired spikelet producing lines.The flowering time mutant alleles used in the floral meristem identity gene expression analysis are summarised in **Table 2**.

Developing inflorescence tissue was harvested at double ridge with 5 inflorescences per genotype constituting a single biological replicate. Three biological replicates for each of the six genotypes were harvested. As flowering time was not uniform between genotypes and early and late flowering lines, the developmental stage of meristems in each genotype were checked daily to ensure harvesting at the same inflorescence development stage. Meristems were harvested at the double ridge stage. Expression of the following meristem identity genes were measured: Suppressor of *CONSTANS1 (SOC1), LEAFY (LFY), VERNALIZATION1 (VRN1), AGAMOUS-LIKE GENE1 (AGLG1), AGAMOUS-LIKE10* (*AGL10*) and *AGL29*. Each of these genes is thought to positively regulate floral meristem transition (Chen and Dubcovsky, 2012, Yan et al., 2003, Zhao et al., 2006, Kobayashi et al., 2012).

Expression of *LFY*, *VRN1*, *AGLG1*, *AGL10* and *AGL29* were reduced in all late flowering paired spikelet producing genotypes in comparison to their early flowering comparison lines. *SOC1* expression was reduced in response to reduced *PPD-1* function or expression but was not altered in the *ft* mutant suggesting *FT* independent regulation. Based on these results we concluded that paired spikelet development occurs via an *FT* dependant pathway where *PPD*-1 regulates *FT* expression and FT regulates the expression of floral meristem identity genes in the developing inflorescence. Reduced expression of floral meristem identity genes results in delayed transition of the axillary meristems of the inflorescence to a spikelet meristem identity increasing the proportion of nodes which develop paired spikelets.

Table 2 Expression of *Ppd-1* promotes expression of *FT* which promotes flowering in wheat. Genetic variation which increases expression of either *Ppd-1* or *FT* leads to earlier flowering whereas loss of function or reduced expression leads to later flowering. This table summarises the early flowering non-paired spikelet producing and late flowering paired spikelet producing alleles present in the subsequent expression analysis figure. All alleles are present in a common genetic background (Sunstate cultivar (SS)).

Non-paired spikelet Sunstate sibling	Paired spikelet sibling allele
Ppd-D1a **(photoperiod insensitive)** Misexpressed (Increased under non-inductive photoperiods) leading to promotion of FT and an early flowering spring habit.	***Ppd-D1a.2*** **(mutant)** Loss-of-function mutant has reduced promotion of FT leading to late flowering.
FT-B1 **(SS)** Normal allele of most abundantly expressed *FT* homeoallele.	***ft-B1*** **(mutant)** Complete deletion of *FT-B1* resulting in late flowering.
Ppd-D1a **(photoperiod insensitive)** Misexpressed (Increased under non-inductive photoperiods) leading to promotion of FT and an early flowering spring habit.	***Ppd-1*** **sensitive (naturally occurring/wild photoperiod sensitive allele)** Highly expressed in long days. Lowly expressed under short (12h) days. Plants with this allele are late flowering in short days relative to insensitive allele.

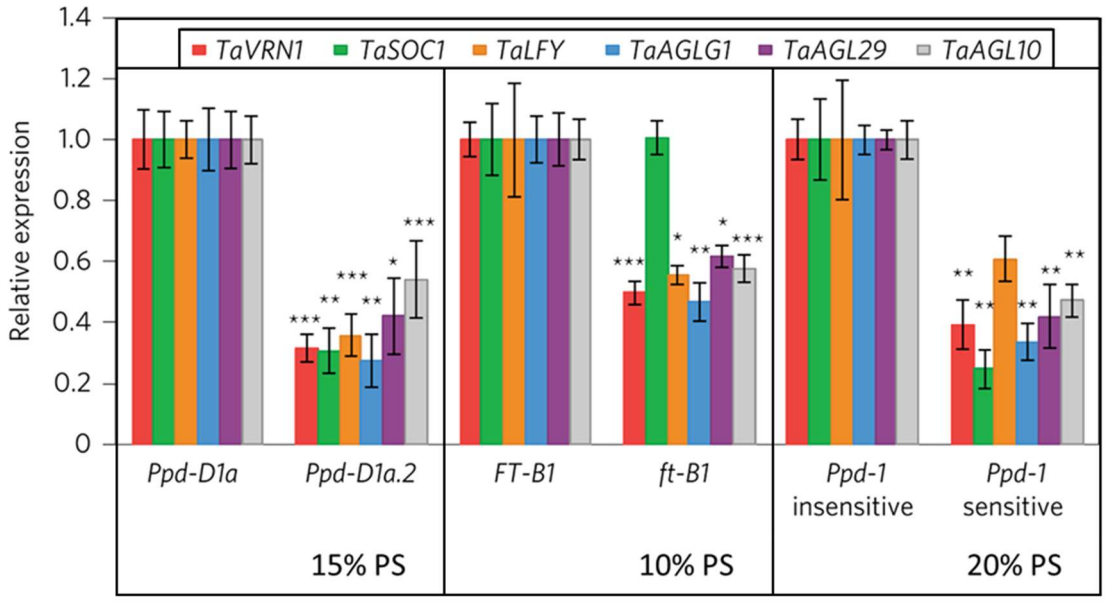

Figure 14 Attenuating the floral promoting signal in wheat leads to reduced expression of floral meristem identity genes and paired spikelet formation. Relative expression of floral meristem identity genes at double ridge in three paired spikelet producing lines and their parental (Sunstate) or sibling near isogenic lines. Lines differ by genetic allele as indicated on X axis. Paired spikelet (PS) frequency is indicated below paired spikelet producing alleles. All plants were grown in controlled conditions under a 12 hour photoperiod. Data are mean ±s.e.m. of three biological replicates.

*P<0.05; **P<0.01; ***P<0.001; for the *LFY* comparison in the *Ppd-1* insensitive/sensitive NIL lines, P=0.052.

High branching 0053 has increased expression of *TB1* and reduced expression of floral promoting genes compared to its low branching sibling

To confirm that duplications of chromosome 4D were leading to increased transcript abundance of *TB1*, I performed expression analysis on 0053 high and low branching cDNA samples provided by Scott Boden. RNA was extracted from developing inflorescences at double ridge. In addition to *TB1,* I also measured the expression level of the same suite of floral meristem identity genes we detected to be differentially expressed in the late flowering, paired spikelet lines shown in **Figure 11**. Expression of *TB1* was higher in high branching 0053 compared to its low branching sibling line **Figure 15**. In addition, expression of floral meristem identity genes was reduced in 0053 HB consistent with our previous findings suggesting increased *TB1* expression may be causal **Figure 15**.

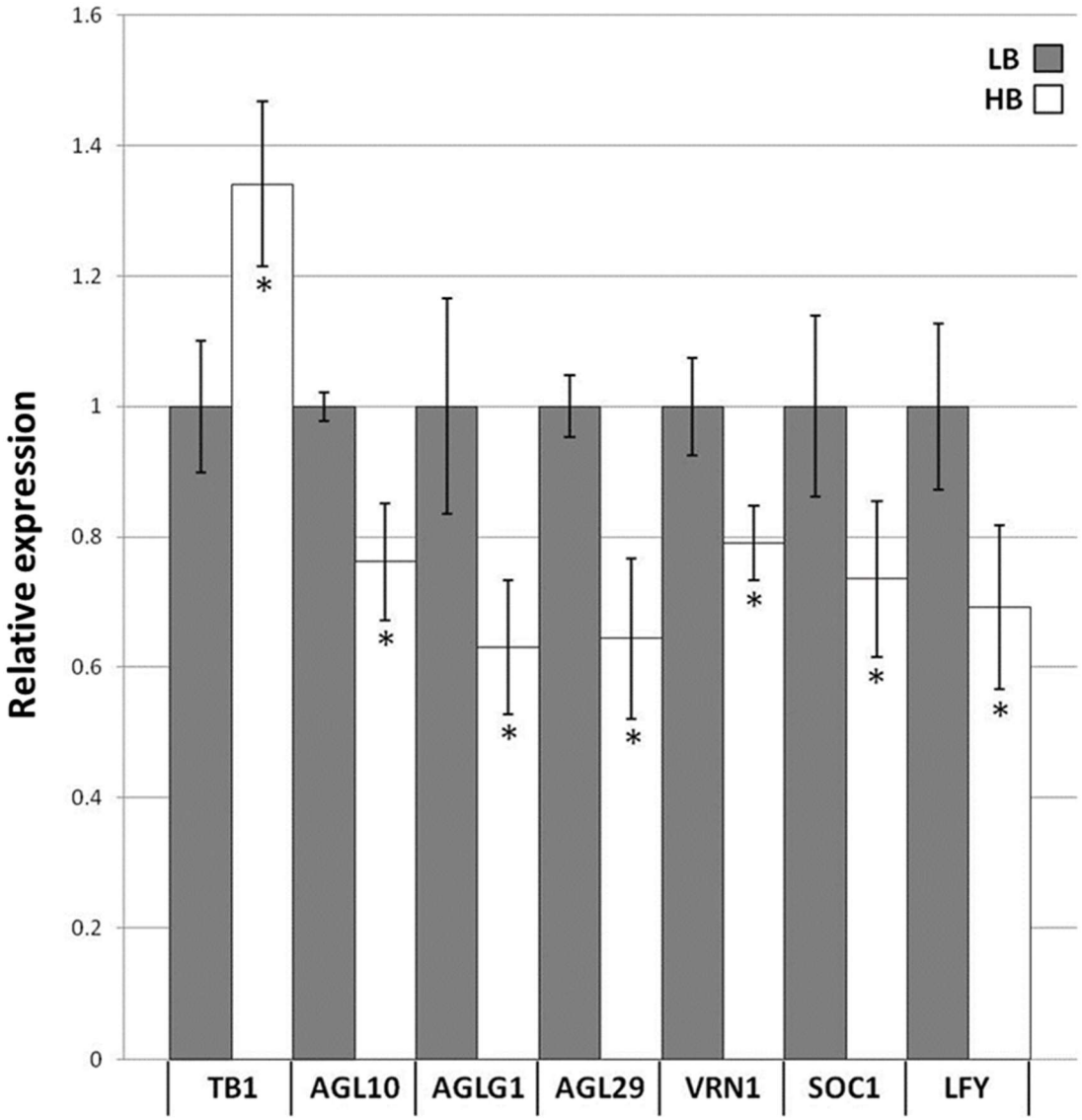

Figure 15 *TB1* expression is increased in 0053 HB compared to LB and expression of floral meristem identity genes is reduced. Normalised relative expression of *TB1* and floral meristem identity genes at double ridge in 0053 high and low branching sibling lines. Data are mean ±s.e.m. of three biological replicates. *P<0.05. Plants grown under 16 hour days.

Overexpression of *TaTB1* causes paired spikelet formation

To test that increased *TaTB1* transcript is sufficient to cause paired spikelet formation, I designed and ordered a restriction site edited version of the Baxter *TaTB1* coding sequence and cloned the gene into a maize ubiquitin overexpression construct. Unfortunately, transformed wheat callus failed to produce any shoots when transferred to shooting media. *TB1* negatively regulates tiller formation/outgrowth in maize so *TaTB1* may be repressing shoot formation when overexpressed in wheat callus. Control plants in the same round of tissue culture did generate shoots suggesting that lack of shoots in *TB1ox* transformants was construct specific. To prevent potential shoot suppression in *TB1ox* callus I combined the same Baxter *TB1* gene sequence with the *VRN1* promotor (Alonso-Peral et al., 2011). *VRN1* is expressed more strongly in the apical meristem and developing inflorescence and only weakly expressed in vegetative tissues (Alonso-Peral et al., 2011).

Callus from the wheat variety Fielder was transformed with the *VRN1pro*:*TaTB1* in a binary vector containing a bar selection gene or just the binary vector containing bar selection gene (Fielder control plants) (Thompson et al., 1987, Richardson et al., 2014). We obtained 42 plantlets arising from unique transformation events after growth on selective media. Rachis node number and paired spikelets were scored in all T0 transformants that reached maturity. Paired spikelets were detected in just over half of all T0 transformants **Figure 16**,

Figure 17, **Figure 18**, **Figure 19**. As expected, control plants did not produce a high frequency of paired spikelets with only a single rudimentary paired spikelet produced in 15 control spikes **Figure 19**. Expression of *TB1* was measured in adult leaf tissue of a subset of transgenic plants as well as controls. *TB1* transcript could be detected in all lines with higher expression being detected in some transgenic lines compared to

controls suggesting that the construct is able to achieve increased *TB1* expression levels **Figure 20**. Because the *VRN1* promotor is not highly active in leaf tissue these results only confirm that expression of *TB1* is occurring as a result of the construct, but we do not suggest this represents physiologically relevant expression as this would require extraction of developing spike tissue.

While expression of *TB1* under the control of the *VRN1* promotor does not necessarily tell us the consequence of increased levels of normally localised *TB1* (under native promotion), it does confirm that increased expression of *TB1* in the inflorescence is sufficient to increase in the frequency of paired spikelets. Based on these transgenic plants, it seems likely that the paired spikelet phenotype of 0053 HB is caused by a copy number and subsequent expression increase of *TB1*. It is not clear if the Baxter allele of *TB1* is required for paired spikelet formation or if paired spikelet formation could be achieved by increased expression of any functional *TB1* allele.

Unlike previous paired spikelet producing lines where paired spikelets form around the centre of the spike, the transgenic paired spikelet lines produce paired spikelets between the bottom quarter and centre of the spike. It is likely that this change is a consequence of the specific expression profile of the *VRN1* promotor. As we expect expression of *TB1* under the control of the *VRN1* promotor to be highest in the developing inflorescence we may expect that tiller number would be less severely reduced in these transgenic lines compared to 0053 HB. Plants out of tissue culture have highly variable tiller formation so we did not bother scoring tillering in T0 plants.

Some of the paired spikelet producing transgenic plants appeared to have compact spikes

Figure 17, **Figure 18** which may also be a consequence of increased *TB1* expression. Spikes of 0053 HB are also shorter than their low branching siblings but this may be a

consequence of altered rachis node number. Our preliminary results indicate that increased expression of *TB1* may have multiple effects on development.

Figure 16 Increased expression of *TB1* under the control of the *VRN1* promotor leads to paired spikelet formation in wheat. Spike of T0 transgenic (PC142) wheat plant with complete (**) and rudimentary (*) paired spikelets marked.

Figure 17 Increased expression of *TB1* under the control of the *VRN1* promotor leads to paired spikelet formation in wheat. Spikes of transgenic (PC142) wheat plants and control Fielder spike. Upright spikes on left hand side of each panel with the same spikes (right) bent to separate spikelets and expose spikelet pairs.

Figure 18 Increased expression of *TB1* under the control of the *VRN1* promotor leads to paired spikelet formation in wheat. Spikes of transgenic (PC142) wheat plants and control Fielder spike. Upright spikes on left hand side of each panel with the same spikes (right) bent to separate spikelets and expose spikelet pairs.

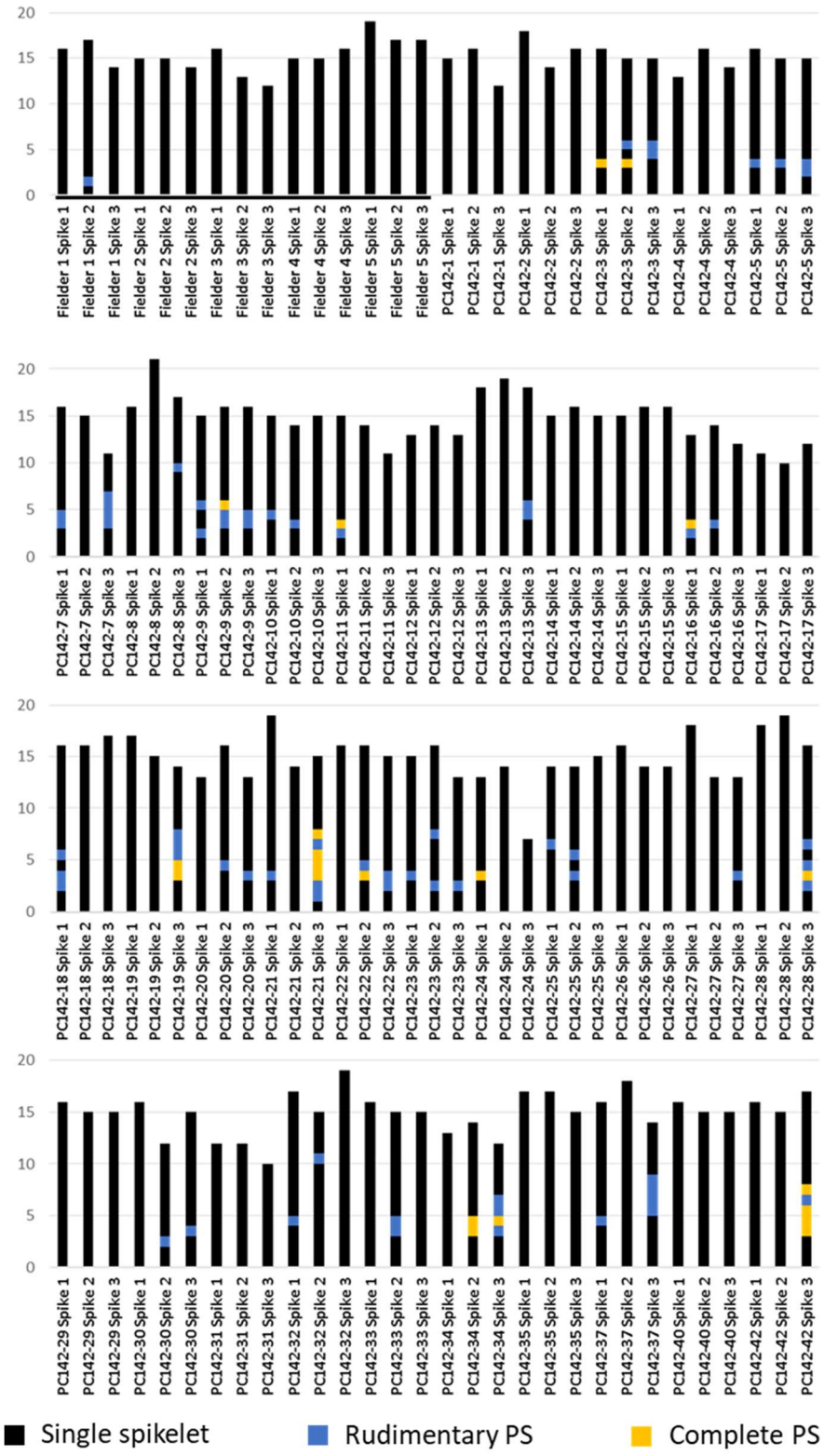

Figure 19 Rachis node number and position of paired spikelets in Fielder and *Tb1* over expressing T0 transformants. Rachis node number measured from the three most mature spikes of 5 control Fielder plants and T0 transgenic plants where Spike 1 is the main spike and spikes 2,3 are the most developed tillers. Total rachis node number is shown as cumulative stacked histogram where 1 is the first (most basal) rachis node and the highest number in each transgenic line is the terminal spikelet. The rachis node position of rudimentary paired spikelets (blue) and complete paired spikelets (yellow) is shown for each spike scored.

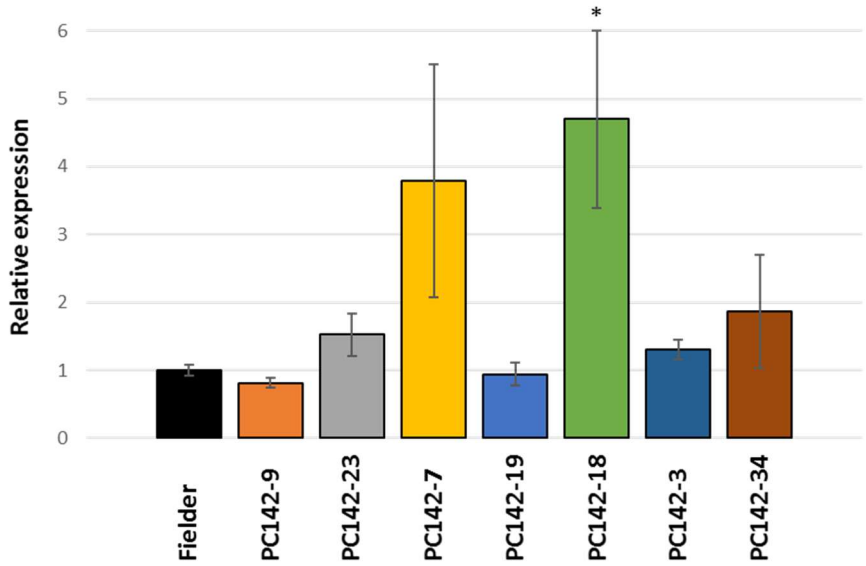

Figure 20 *TB1* is expressed in leaves of transgenic lines. Relative expression of *TB1* in control Fielder and T0 transgenic plants. RNA harvested from leaf tissue of mature plants. Data are mean ±s.e.m. of three biological replicates. *P<0.05.

We selected numerous paired spikelet producing T0 transgenic lines to grown on to the next generation. Paired spikelet formation appeared to be segregating in most T1 lines. Paired spikelet frequency ranged from occupying 0-55% of all rachis node positions. We screened for *TB1* copy number using a qPCR based assay targeting the D genome aversion of *TB1* and a control gene with a single gene copy. Control Fielder plants featured single haploid D genome copy of *TB1* as expected. *TB1* copy number was found to be variable amongst segregating T1 transgenic plants with one or more haploid copies present in each individual. To explore if increasing *TB1* copy number is associated with paired spikelet development, *TB1* copy number was plotted against % paired spikelets. In general, a positive relationship between *TB1* copy number and paired spikelet frequency was observed **Figure 21, Figure 22,** and **Figure 23**. In addition to changes in paired spikelet frequency with differing *TB1* copy number, plant height appeared to be reduced with increased copies of *TB1* **Figure 21, Figure 22,** and **Figure 23.** Consistent with this observation, mutations in maize *TB1* lead to increases in internode elongation (Hubbard et al., 2002). Furthermore, overexpression of maize *TB1* in wheat leads to reduction in plant height (Lewis et al., 2008).

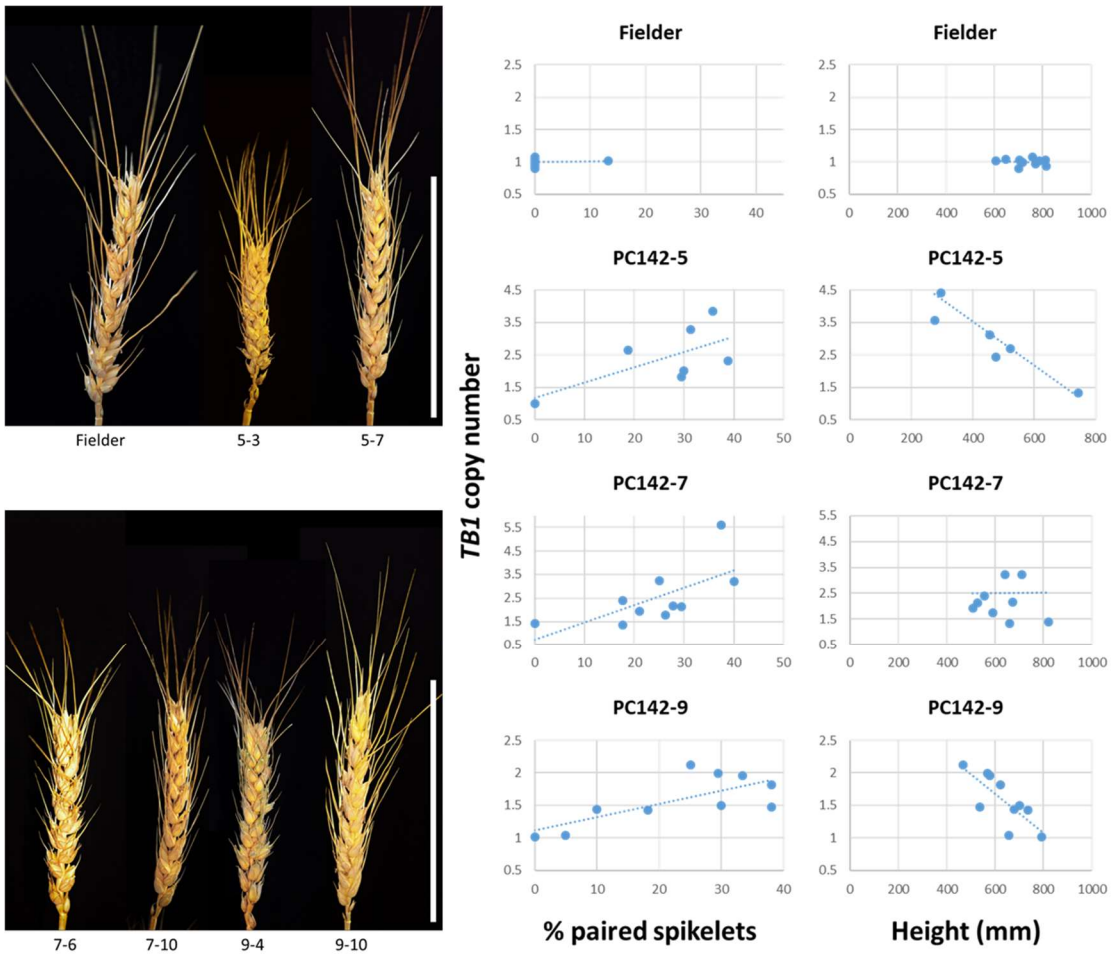

Figure 21 Increased *TB1* copy number is associated with the development of paired spikelets and a reduction in plant height. Images of control line (Fielder) and transgenic wheat lines showing example of high copy segregant individual with high paired spikelet frequency (left 5-3, 7-6, 9-4) and single copy segregant individual with low paired spikelet frequency (right 5-7, 7-10, 9-10). Scale bar= 10cm. X, Y scatter plots show effect of haploid complement of *TB1* (*TB1* copy number on percentage of rachis nodes which formed paired spikelets (% paired spikelets) and on plant height (mm). Line of best fit is plotted to indicate trend. Phenotypic data collected from main spike of each plant. *TB1* copy number determined for each plant by qPCR. For PC142-5 line n= 7. For all other lines n= 10

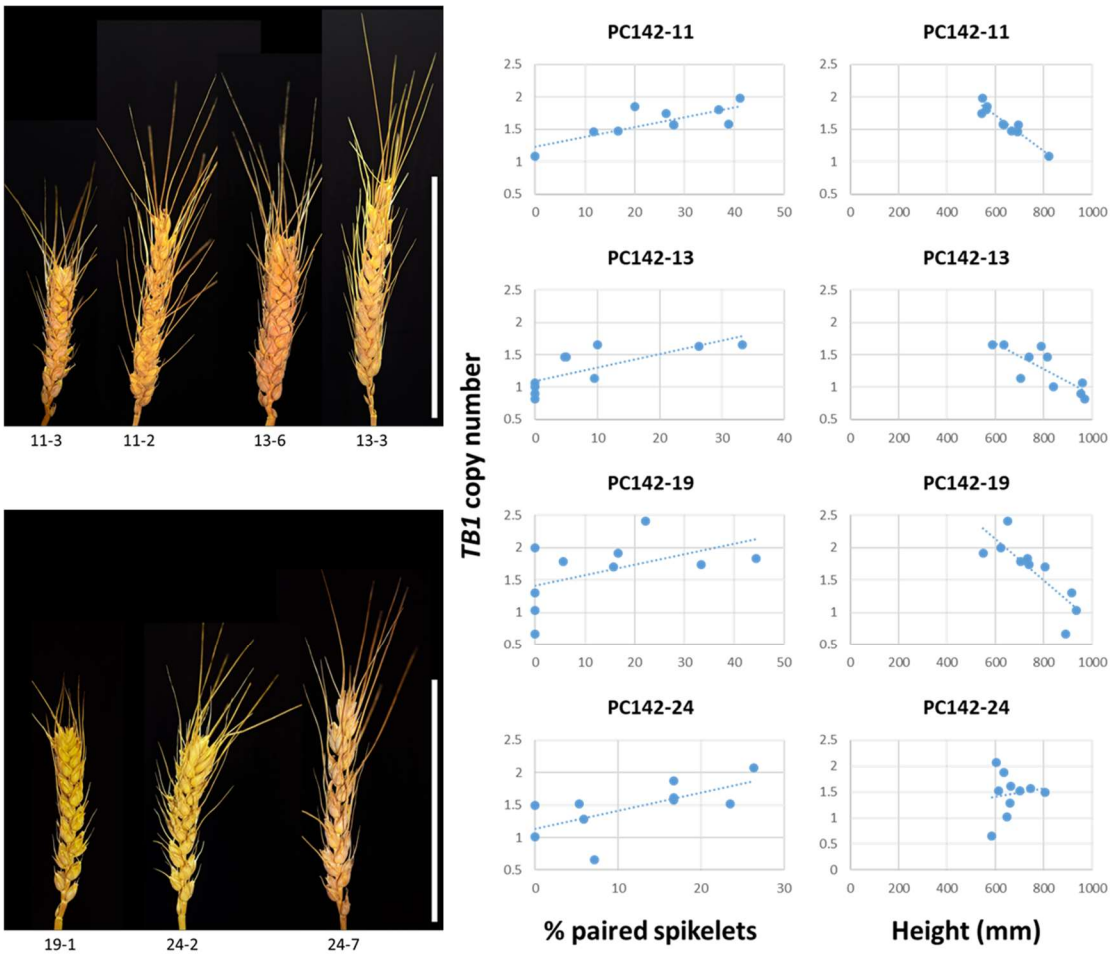

Figure 22 Increased *TB1* copy number is associated with the development of paired spikelets and a reduction in plant height. Images of transgenic wheat lines showing example of high copy segregant individual with high paired spikelet frequency (left 11-3, 13-6, 19-1, 24-2) and single copy segregant individual with low paired spikelet frequency (right 11-2, 13-3, 24-7). Scale bar= 10cm. X, Y scatter plots show effect of haploid complement of *TB1* (*TB1* copy number) on percentage of rachis nodes which formed paired spikelets (% paired spikelets) and on plant height (mm). Line of best fit is plotted to indicate trend. Phenotypic data collected from main spike of each plant. *TB1* copy number determined for each plant by qPCR. n= 10

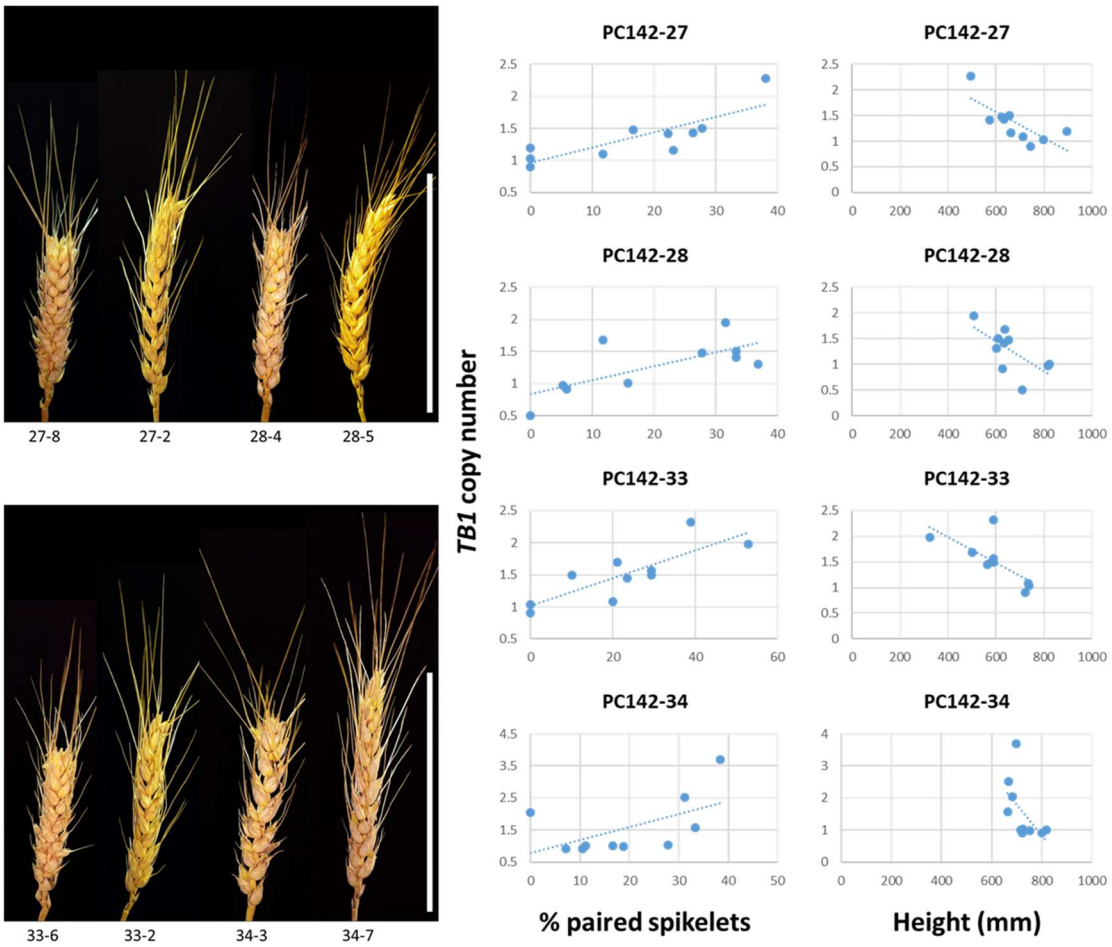

Figure 23 Increased *TB1* copy number is associated with the development of paired spikelets and a reduction in plant height. Images of transgenic wheat lines showing example of high copy segregant individual with high paired spikelet frequency (left 27-8, 28-4, 33-6, 34-3) and single copy segregant individual with low paired spikelet frequency (right 27-2, 28-5, 33-2, 34-7). Scale bar= 10cm. X, Y scatter plots show effect of haploid complement of *TB1* (*TB1* copy number) on percentage of rachis nodes which formed paired spikelets (% paired spikelets) and on plant height (mm). Line of best fit is plotted to indicate trend. Phenotypic data collected from main spike of each plant. *TB1* copy number determined for each plant by qPCR. n= 10

Discussion

At this point, before proceeding with the discussion section, I recommend you read our articles relating to the aforementioned results. They contain additional results from collaborators and are comprehensive assessments of the paired spikelet trait in wheat. The articles can be found in the appendix and are titled:

1. ***Ppd-1* is a key regulator of inflorescence architecture and paired spikelet development in wheat** (Co-author)
2. ***TEOSINTE BRANCHED1* regulates inflorescence architecture and development in bread wheat (*Triticum aestivum* L.)** (Equal first author)

Comparative genomics to identify inflorescence branching genes

It can be difficult to gauge how homologous developmental genes will function across different grass crop species given their markedly different inflorescence architectures. Examples of sequence and functional conservation in the AP2/ERF transcription factors support the notion that comparative genomics is a powerful tool for inferring gene function across the grasses (Komatsu et al., 2003, Derbyshire and Byrne, 2013, Dobrovolskaya et al., 2015, Poursarebani et al., 2015, Chuck et al., 2002), although we cannot expect that gene function will always be so readily conserved.

Environmental sensing modulates inflorescence development and floral transition

The interaction of environmental factors and meristem determining genes which together affect the rate of floral transition and eventually inflorescence architecture, represents a gap in many assessments of inflorescence development which instead typically focus on flowering time or architecture and not the combination of both.

The *BdFZP* mutants of *Brachypodium* and the *PPD-D1* and *FT* mutants of wheat described in this chapter all result in delayed inflorescence development leading to the formation of more nodes within the inflorescence as well as branch structures. Together, these branched mutants in *Brachypodium* and wheat highlight that floral transition, driven by environmental sensing mechanisms such as day length, is essential for determining rates of meristem transition.

The formation of inflorescence branches that behave like the main rachis producing several spikelet branches and a terminal spikelet in both *Brachypodium* and wheat has so far only been observed through the loss of function of their AP2/ERF transcription factors orthologous to rice *FZP*. In the case of wheat, multiple gene copies need to be mutated before additional rachises are formed with modifications in vernalisation and photoperiod effecting the expression of the trait. Unlike the formation of additional rachises which require specific mutations to occur, the paired spikelet branch in wheat can be exposed in a diverse set of wheat lines simply by providing weakly inductive floral signals. This effect appears to be influenced by genetic background with the appearance of and severity of paired spikelets varying between wheat lines. We have not observed these very specific paired spikelet branches in *Brachypodium* despite the otherwise similar inflorescence architecture to wheat though this trait may be present amongst the diverse set of *Brachypodium* landraces.

Paired spikelets appear to be developmentally distinct from rachis branches

The paired spikelet branch and the rachis branch of *FZP* mutants have very distinct phyllotaxies. Although a pair of spikelets can form at a single node in *FZP* mutants, the stacking of the spikelets is disorganised with each growing out in different directions, or maintaining the characteristic alternating phyllotaxy as in described wheat *FZP* mutants (Echeverry-Solarte et al., 2014, Dobrovolskaya et al., 2015, Poursarebani et al., 2015)The apparent disorganised spikelet phyllotaxy in wheat and *Brachypodium* mutants is potentially a consequence of spikelets developing too closely to each other and other branches, causing the branches and spikelets to twist and grow into each other as they develop. This seems likely to be the case as scanning electron microscope images of these mutants show branches with the characteristic alternating phyllotaxy of a primary rachis (Poursarebani et al., 2015).

Though the frequency of both types of branches is increased under weakly inductive floral signals, they appear to represent distinct developmental processes. If we consider *FZP* mutants to form true branches with the lateral meristem behaving like the primary apical inflorescence meristem, then the paired spikelet type of branch likely only ever acquires spikelet meristem at two positions per node and not a branch or inflorescence meristem identity to produce an additional rachis node. Otherwise we would expect to see more than two spikelets per rachis node under increasingly weakly inductive floral promoting conditions which is not the case in our observations. There are three possible mechanisms for paired spikelet formation. Firstly, paired spikelets may arise from the splitting of enlarged spikelet meristems thus forming a pair of uniform spikelets. This seems unlikely as the secondary spikelet develops much later than the primary spikelet. Secondly, they may represent the conversion of the leaf primordia (which is suppressed at each rachis node) to a spikelet meristem. However, we cannot exclude the third possibility that paired spikelets are a form of short rachis branch albeit with very tight regulation on axillary meristem identity that prevents more than two spikelets forming **Figure 24**.

In domesticated maize, spikelets typically arise in pairs. We cannot say for sure if the archetypal paired spikelet structures of maize and the paired spikelets we have observed in wheat are of similar developmental origin. In wheat, we have observed that the secondary spikelets making up a pair at a rachis node, seem to form sometime after the primary spikelet has defined florets (Boden et al., 2015, Greenwood et al., 2017). In contrast, SEMs of developing maize inflorescences show that the developmental stage of each spikelet in a spikelet appear is similarly timed (Laudencia-Chingcuanco and Hake, 2002). Comparisons between inflorescences of maize and wheat are complicated by differences in phyllotaxy and spikelet determinacy. Given the stark differences in inflorescence structure between wheat and maize it may not be possible to compare the

development of paired spikelets between these species. Analysis of this trait in a common ancestor would allow us to determine if it has a common origin or has arisen separately in the progenitors of wheat and maize.

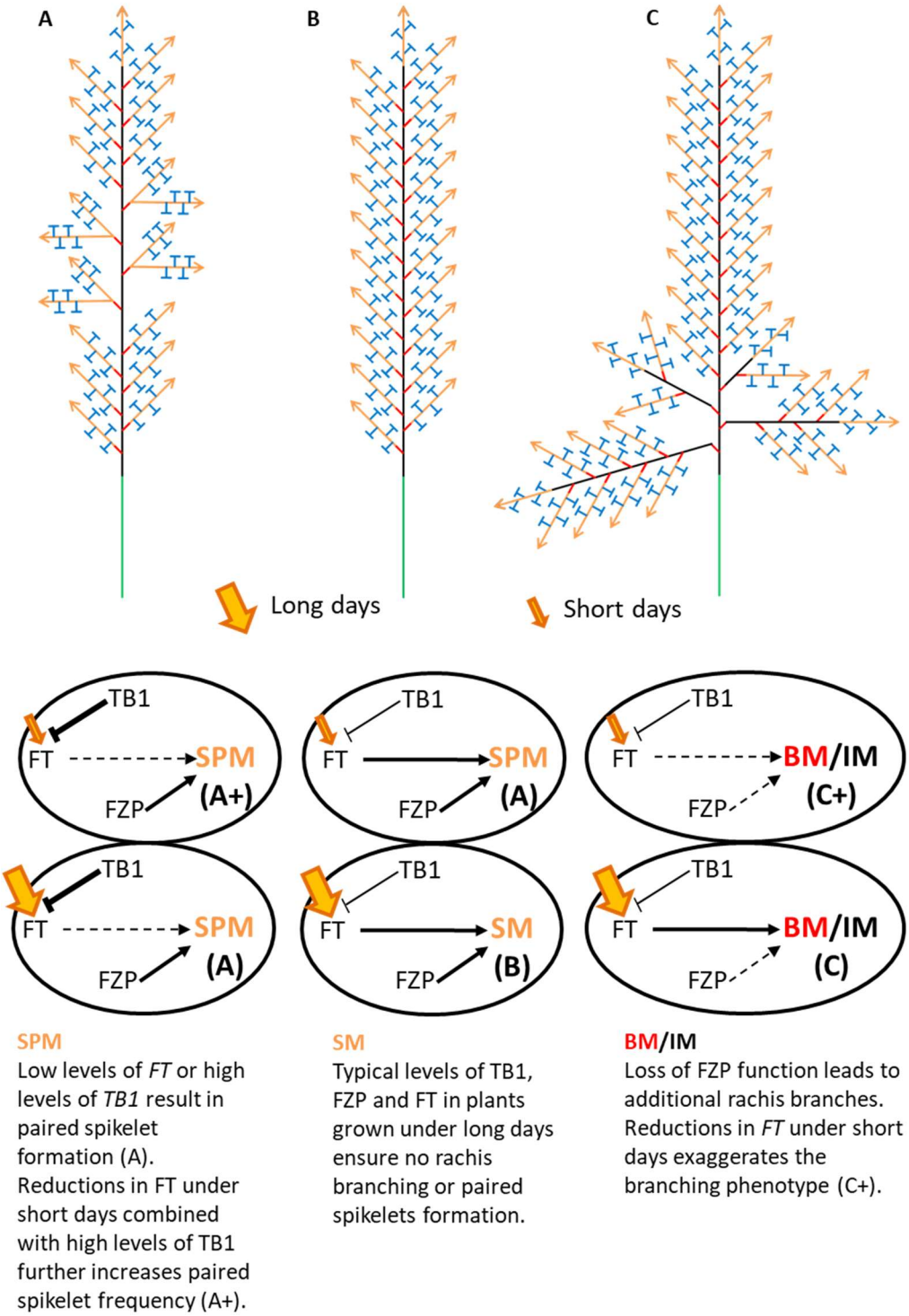

Figure 24 Mechanism of rachis branch and paired spikelet formation in wheat. These schematics show the consequence of different gene dosage and function on axillary meristem identity. Thick lines show high gene expression while thin lines show weaker gene expression. Dotted lines indicate loss of function or weak gene expression. In the case of paired spikelet formation (**A**), either an increase in TB1 levels or a reduction in FT levels is sufficient to cause paired spikelets to form. The development of an archetypal wheat inflorescence (**B**) depends on sufficiently high levels of FT, normal levels of TB1 and a stable form of FZP. The formation of rachis branches (**C**) requires loss-of-function in FZP with increased levels of branching occurring when levels of FT are also low. **SPM**: Spikelet pair meristem, **SM**: Spikelet meristem, **BM/IM**: Branch meristem/Inflorescence meristem.

Increased copies of *TB1* promote paired spikelet formation

Our results suggest that paired spikelet formation in wheat can be achieved through increased copy number (0053 HB) or expression (transgenics) of *TB1* in the developing inflorescence meristem. The Arabidopsis orthologue of TB1, BRC1, directly binds to and represses the floral activating function of FT (Niwa et al., 2013). If TB1 in wheat retains a similar interaction and florally repressive effect, this could account for the paired spikelet formation we observe. This model would fit with our observation that reduced levels of FT are associated with paired spikelet formation in wheat (Boden et al., 2015). Although we have observed that levels of FT were the same in developing inflorescences of 0053 high and low branching lines this does not account for possible protein-protein interactions (Appendix Dixon, L; Greenwood J. *et al.*). Recently we have shown that wheat TB1 and FT have a direct interaction suggesting that the floral repressive mechanism of BRC1 observed in Arabidopsis may be conserved (Appendix Dixon, L; Greenwood J. *et al.*).

TB1 appears to have distinct tissue specific functions in vegetative and inflorescence axillary meristem development, able to both repress tiller formation and promote paired spikelet formation. Because of these linked effects, it is difficult to determine genetic causality. Based on previous observations (Doebley et al., 1997, Takeda et al., 2003, Lewis et al., 2008), increased expression of *TB1* results in a reduction in tiller number but is TB1 directly influencing the inflorescence or is a reduction in tiller number changing resource partitioning to favour paired spikelet development? The inflorescence specific expression profile of *VRN1*pro:*TB1* transgenic plants is useful to assess the uncoupling of *TB1*'s roles. Our results suggest that increased *TB1* expression in the developing inflorescence where *VRN1* is most strongly expressed is sufficient to promote paired spikelet formation. This strongly implies that TB1 does in fact have a direct dual function in inflorescence and vegetative development. Assuming paired

spikelet formation is independent of tiller formation, we may also expect to identify paired spikelets in loss-of-function mutations of floral meristem identity genes which had reduced expression of these genes **Figure 14**, **Figure 15**, though multiple genes or their homeoalleles may need to be mutated/knocked out to overcome functional redundancy. If TB1 does indeed bind and antagonise FT function as our results suggest (Appendix Dixon, L; Greenwood J. *et al.*), the normal function of TB1 may be to balance vegetative and reproductive growth in response to environmental conditions which govern the floral signal.

What are the consequences of TB1s direct interaction with FT

The *ft* mutant we have described is late flowering and produces paired spikelets (Boden et al., 2015). With high levels of *TB1* also associated with paired spikelet formation and a detected interaction between TB1 and FT protein, we expect that TB1 may act to negatively regulate the floral promoting effect of FT (Appendix Dixon, L; Greenwood J. *et al.*). We did not detect differences in spike emergence between 0053HB and 0053LB lines despite their differences in TB1 copy number when grown under long days (Appendix Dixon, L; Greenwood J. *et al.*), although delays in flowering time of 0053HB compared to 0053LB have been observed when grown under short days (personal correspondence Steve Swain). When grown under long days, 0053HB does show a delay in inflorescence development but over time reaches a similar developmental stage as 0053LB (Appendix Dixon, L; Greenwood J. *et al.*). The chromosomal duplication in 0053HB which carries *TB1* could include other modifiers of flowering time making it difficult to accurately assess the interaction of TB1 and FT in these lines. Further analysis of the transgenic lines could be used to explore this although, in these lines *TB1* is not being expressed under its native promotor and may not accurately represent the plant wide function of TB1. Ultimately, performing mutagenesis in the 0053HB background to isolate loss-of-function alleles of TB1 with

reduced paired spikelet number would not only support that increased *TB1* dosage is leading to paired spikelet formation but would also elucidate any differences in flowering time associated with TB1 function.

The 0053 background carries a photoperiod sensitive allele of *PPD-1* originating from one of its parental donor varieties, Yitpi. We have shown that paired spikelet frequency increases under short day lengths when the photoperiod sensitive allele of *PPD-1* is present (Boden et al., 2015). While both the HB and LB line carry the same insensitive *PPD-1* allele, exposure to short day lengths could still be used to exaggerate additive flowering time differences and enhance the paired spikelet phenotype of 0053HB. Comparing paired spikelet frequency in the 0053HB line grown under short and long days will expose any additive effects of FT dosage on paired spikelet development in a high TB1 background (See **Figure 24**). Based on our previous result which suggest low levels of FT increase the number of paired spikelets, we expect that paired spikelet frequency would further increase under short days. If paired spikelet frequency does not differ between photoperiods in 0053HB plants, this would suggest that the high dosage of TB1 is sufficient to antagonise FT under long days and/or that paired spikelet frequency cannot be extended past a certain proportion of total rachis nodes.

TB1 appears to play an important role in regulating vegetative branching (tillering) and is therefore essential in defining the number of inflorescences per plant. This is clear in domesticated corn which features high expression of *TB1* and a restriction on vegetative branching leading to the development of only a single stem (Doebley et al., 1997). In two row barley (the primary form used for malting), loss-of-function alleles of the *TB1* orthologue *VRS1,* increase tiller formation and lateral spikelet fertility leading to fertile lateral florets as in six row barley (Ramsay et al., 2011). It is not clear how the TB1 model we propose in wheat applies to barley given that loss-of-function and not gain-of-function leads to increases in spikelet number. The lateral spikelets of barley are a

unique form of inflorescence structure and unlikely to be developmentally comparable to the spikelet pair we have observed in wheat although similar gene families may regulate their development.

The dual function of TB1 in regulating both vegetative and inflorescence branching represents an intriguing plant wide mechanism where high levels of *TB1* lead to less tillers and thus a reduction in inflorescences but then a higher number of spikelets within the remaining inflorescence structures. This dual role of TB1 may rely on an interaction with FT which may provide a mechanism for TB1 function to be altered with the onset of flowering potentially regulating tillering and inflorescence architecture differently under non-inductive and inductive floral conditions. Combining various gain and loss-of-function alleles of *TB1* and *FT,* and subsequent phenotyping would allow us to better understand the interaction between TB1 and FT.

Paired spikelet formation in wheat is under complex genetic control

TB1 and FT levels are unlikely to be completely responsible for modifying paired spikelet formation in wheat. Though low doses of FT and high doses of TB1 are conducive to paired spikelet formation, an assessment of diverse wheat varieties suggests that paired spikelet formation is background specific and likely several genes are interacting to regulate their formation. Indeed, we have observed that many QTL are associated with the presence of paired spikelets in wheat including a region near *TB1* and the semi-dwarfing gene *Rht-1* though we have confirmed that no association between *Rht-1* alleles and paired spikelet formation is present (Boden et al., 2015)(Appendix Dixon, L; Greenwood J. *et al.*). *PPD-1* represents a major QTL for paired spikelet regulation. We assume that modulation of *FT* expression by *PPD-1* represents a key mechanism for modifying paired spikelet development, but we cannot exclude the possibility that *PPD-1* is influencing other developmental pathways.

With respect to TB1, we have found that certain alleles were more strongly associated with paired spikelet formation (Appendix Dixon, L; Greenwood J. *et al.*). An incomplete association between TB1 alleles and paired spikelet formation indicates that TB1 is an important factor in paired spikelet development but not a complete developmental switch. Given that TB1 is a transcription factor, we expect that at the very least, other members which make up the transcriptional machinery and/or, downstream transcriptional targets are also potential regulators of paired spikelet development. Performing mutagenesis in wheat lines which produce paired spikelets and, subsequent screening for altered paired spikelet formation, could allow us to identify novel genes, or novel alleles of genes which also contribute to the development of paired spikelets. Similarly, transcriptome analysis comparing *TB1* overexpressing lines and null segregants would help us identify transcriptional targets which are likely to be contributing to paired spikelet formation.

Unifying inflorescence branching and paired spikelet formation

It is unclear how inflorescence meristem branching interacts with paired spikelet formation. Considering that both structures are influenced by rates of meristem transition (via FT), there are common aspects in each developmental pathway. The behaviour of a true meristem branch mirrors that of the original inflorescence meristem, which could simply be explained by a delay in the transition of an axillary meristem to a spikelet meristem. Paired spikelets on the other hand represent a specifically defined group of cells at a rachis node which do not develop any more than two spikelets even under changing rates of meristem transition. What regulates this meristem specificity is unknown, but axillary meristem size may play a role in the number of spikelet meristems defined. Supporting this theory, central rachis nodes of the spike typically

feature the highest proportion of paired spikelets and are also the earliest and largest nodes to develop compared to apical and basal rachis nodes (Boden et al., 2015, Greenwood et al., 2017). Increased meristem size leads to disorganisation of spikelet pair meristems in maize sometimes leading to triple spikelet formation (*thick tassel dwarf1*) (Bommert et al., 2005a). Furthermore, mutants in maize with increased meristem size show increased frequency of axillary structures (Bommert et al., 2013a, Bommert et al., 2013b). In backgrounds with active FZP, axillary meristems are unable to form additional rachis branches and this may be critical for limiting spikelet formation to pairs. Reducing *FT* expression, which delays floral transition, may allow larger meristems to form in the slowly developing inflorescence meristem. Either that or, a longer time spent in inflorescence development lends itself to defining an additional spikelet in the developing axillary meristem. Interestingly, the tassel of maize produces both rachis branches at basal rachis nodes and paired spikelets throughout the inflorescence suggesting tight and balanced regulation of axillary meristems (McSteen and Hake, 2001). Rachis branching in *Brachypodium* and Wheat also typically occurs at basal rachis nodes (Dobrovolskaya et al., 2015, Poursarebani et al., 2015).

A tendency for paired spikelets to form closer to the centre of the inflorescence and inflorescence/rachis branches to form at the base of the inflorescence may be the consequence of temporal changes in gene expression as well as spatial expression with defined spike regions having specific expression profiles. The developmental profile of the wheat spike lends to the hypothesis that

a) Branches form because of delayed transition to spikelet meristem identity. Basal nodes define spikelets later than central nodes predisposing them to rachis branching. Apical spikelets are likely to be subjected to higher dosage of *FT* which increases over time leading to a more rapid transition to spikelet meristem identity and reduced degree of branching.
b) Paired spikelets require large axillary meristems to form with the largest meristems around the centre of the developing inflorescence. Alternatively, central spikelets feature a specific set of genes which are conducive to paired spikelet formation independent of meristem size.

Combining branch formation and paired spikelet formation in a single wheat variety would provide important insight into the interaction of the development of these two specific structures. Considering that TB1 may have a direct inhibitory interaction with FT, we might expect that high TB1 dosage in an *fzp* mutant background would lead to compound increases in branching.

Summary

Modifying axillary meristem identity can take the archetypal single rachis of wheat and turn it into something that more closely resembles the branched inflorescences of other grasses. This process is tightly linked to the transition of axillary meristems to spikelet meristems. If these meristems do not receive the correct inductive signal, they are more likely to behave like the SAM and form an additional rachis with its own series of spikelets. The paired spikelet branch we have observed in wheat is distinct from the additional rachis branches we observed in *Brachypodium* and others have observed in wheat. Unique positioning of these two branch forms within the wheat inflorescence suggests that axillary meristems along the spike are differentially regulated.

Chapter 4 - New alleles of the wheat domestication gene Q reveal multiple roles in growth and reproductive development

Introduction

This chapter focusses on the major wheat domestication gene *Q,* an AP2 transcription factor that in its domesticated form confers a free threshing trait allowing grain to be easily separated from the spike at harvest. This work has been published in the peer reviewed journal, Development, therefore the results section of this chapter requires reading the published article which can be found in the appendix. The discussion section of this chapter will follow on from the published article.

The inflorescences of the major grass crops, rice, wheat, maize and barley have all been modified during domestication to produce larger quantities of grain with higher quality. In addition to grain number, size and quality, the easy separation of grain from the rest of the inflorescence (free threshing) is essential for efficient grain harvest as part of a farming system. The advantages of free threshing in wheat led to the selection of a single modern *Q* allele which is now present in all modern wheat varieties. *Q* and the pre-domestication allele, *q*, encode an AP2 transcription factor with the domesticated allele conferring a free threshing character as well as a subcompact (i.e. partially compact) spike.

Results

Please proceed to the appendix and read the article: **New alleles of the wheat domestication gene *Q* reveal multiple roles in growth and reproductive development** (Greenwood et al., 2017). All results presented in the appended manuscript are my own work. Jean Finnegan provided assistance with gathering some phenotypic data of *Q'* and revertant spikes.

Discussion

Modification of the AP2 transcription factor *Q*, or its downstream gene targets could refine yield traits

The AP2 transcription factor, *Q,* has become an essential component of domesticated wheat as evidenced by its widespread adoption and lack of known deviations from its domesticated form. When compared to pre-domesticated *q,* the presence of *Q* results in marked changes in vegetative and floral structures. A greater understanding of *Q* function presents an opportunity whereby new alleles of *Q,* or its transcriptional targets, could be utilised to generate novel and more ideal outcomes for cropping systems.

The allelic series of *Q* indicates that alternative *Q* allele variants may be better suited for use in elite wheat cultivars

The pleotropic phenotypes controlled by *Q* are modified to varying degrees in each of the *Q* alleles we have described. The domesticated form of (*Q*) is clearly an important allele thought to be maintained in all domesticated wheat varieties. The domesticated *Q* allele however, represents just one possible gain-of-function allele relative to pre-domesticated *Q* (*q*). The increased *Q* expression conferred by *Q* is an essential component of modern wheat but it is possible that slightly more or slightly less expression of *Q* would be optimal to performance. The *Q'* mutant we have described represents an extreme example where strong gain-of-function leads to less desirable traits indicating that too high an expression of *Q* is detrimental to floral development. A comparison of different gain of function *Q* mutations in a *q* background may reveal that a better balance of *Q* expression can be achieved compared to the widespread, domesticated form.

While the B genome version of *Q* is thought to be non-functional, the D genome version retains similar structure as the domesticated form on the A genome. However, the D

genome homeoallele of *Q* is lowly expressed. This is perhaps because it lacks a gain-of-function mutation in its miRNA-binding site like the A genome form. The D genome homeoallele of *Q* represents another target for the introduction of allelic variation. Given that gain-of-function mutations in the A genome version of *Q* are necessary to confer important agronomic traits, similar mutations should be screened in the D genome version to assess its agronomic contributions when expression is increased. Mutagenesis screening for *Q'* like phenotypes and subsequent sequencing of the D genome miRNA-binding site would allow for isolation of *QD* gain-of-function alleles, assuming gene function is conserved. Over expressing *QD* would help determine if *QA* and *QD* function similarly at comparable expression levels.

Alternative dwarfing pathways

In wheat, gibberellin (GA) promotes internode elongation by promoting proteasome dependent degradation of DELLA proteins (Achard and Genschik, 2009). Selection of semi-dwarfed, higher yielding wheat plants during the green revolution (Flintham et al., 1997) isolated naturally occurring variants of DELLA proteins which were resistant to GA-dependent degradation (Pearce et al., 2011). Many modern wheat varieties feature a semi-dwarfing habit because of GA resistant DELLAs, *Rht1a* and *Rht1b* (Pearce et al., 2011, Flintham et al., 1997). Similar dwarfing phenotypes can be generated by interrupting other aspects of the DELLA degradation pathway including GA synthesis (Ashikari et al., 2002, Chandler and Robertson, 1999). Unfortunately, growth repression by semi-dwarfing DELLA alleles adversely affects early plant vigour and reduces coleoptile elongation. Reduced coleoptile elongation limits sowing depth and availability to soil moisture. There has been considerable effort to isolate alternative dwarfing genes which retain the benefits of semi-dwarfing without the undesirable early developmental changes (Ahmad and Sorrells, 2002, Bai et al., 2004).

Increased *Q* expression leads to spike compaction and dwarfing. Interestingly, the *Q'* mutation does not appear to influence coleoptile length or leaf development when compared to SS-like siblings. While the spike compaction phenotypes and floral defects of *Q'* are too severe to be of any agronomic use, the fact that the dwarfing phenotypes of *Q'* are associated with the onset of floral development make AP2 transcription factors and their downstream targets interesting candidates for alternative-dwarfing. Combining dwarfing with the onset of flowering and internode elongation could be an ideal way of avoiding losses to early vigour and reductions in coleoptile length that are associated with *Rht1* dwarfing alleles. Introducing gain-of-function alleles of *Q* and other *AP2s* into wheat backgrounds without *Rht1* dwarfing alleles would allow us to properly assess the potential of these genes for alternative-dwarfing.

Driving tissue specific expression of *Q* in stems may be another way to achieve dwarfing while avoiding any unfavourable floral defects associated with increased *Q* expression in spikes. Besides the well described yield benefits of dwarfing in crops, increased stem thickness and dwarfing offers increased resistance to lodging (Foulkes et al., 2011). Lodging occurs when long stems are unable to withstand the weight of the inflorescence especially under adverse weather conditions often leading to crop losses (Verma et al., 2005, Pinthus and Levy, 1983).

Wheat hybrid development

There has been a widespread adoption of hybrid maize cropping systems. Crossing suitable parental lines generates vigorous, high yielding F1 plants that outperform the parent lines and subsequent generations. Hybrid maize represents a lucrative seed supply system requiring farmers to purchase F1 seed from the supplier each year. Attempts have been made to set up hybridisation systems in the other major grass crops, but it has been technically difficult to engineer parental lines which produce the requisite F1 traits and generate high numbers of F1 seed.

The basic components of a hybrid pair are to have a pollen donor and then a male sterile pollen recipient which will carry hybrid grain without self-fertilising any of its own progeny. The well described barley *AP2* (*HvAP2, CLY, ZEO*) has been shown to influence cleistogamy (floret opening). Typically, the flowers of wheat are cleistogamous (closed), effectively ensuring self-pollination. Non-cleistogamous flowering was present in barley lines with increased miR172 directed degradation of *HvAP2* (Nair et al., 2010). Like our allelic series of *Q*, varying levels of spike compaction have been observed in alleles of *HvAP2*, with increased expression being associated with spike compaction (Houston et al., 2013). While some conservation of function between *HvAP2* and *Q* is evident, we did not observe changes in cleistogamy in any of our *QA* alleles. Of the known *AP2* transcription factors in wheat, *Q* is not the likely orthologue of *HvAP2*. Instead, an *AP2* gene belonging to the group 2 chromosomes (*TaAP2*) bears striking sequence similarity to *HvAP2* so may share a more similar function (Ning et al., 2013). We might expect that increased regulatory targeting or loss-of-function of *TaAP2* would result in non-cleistogamous flowering.

Modified protein levels in gain-of-function *Q* have recently been reported

Recently, in a screen for altered grain quality, a gain-of-function *Q* mutant, phenotypically similar to *Q'* was found to have increased protein content including increased gluten (Xu et al., 2017 An overexpressed Q allele leads to increased spike density and improved processing quality: preprint online, not peer reviewed). Protein content, particularly the functional components of gluten are essential in defining the important dough and baking characteristics of bread. Gluten lends strength and elasticity allowing for a light airy structure during baking and a desirable chewy texture. Besides bread, these characteristics are also important in pasta and noodle making (Hruskova and Svec, 2009).

We observed reduced grain set in the severe gain-of-function mutations of *Q* (*Q'*) meaning these plants are unlikely to be agronomically viable (data not shown). A less severe miRNA-binding site mutation or the partial revertants isolated in the *Q'* background (i.e. *Q'-Rev2*) could be comparable to elite wheat varieties in terms of yield but may also feature altered grain quality profiles. Currently we are bulking grain samples from *Q'* and the SS-like segregant as well as the two *Q'* revertant alleles for grain quality assessment. It is possible that changes in grain composition in the reported gain-of-function *Q* are resulting in the observed protein increases. An assessment of grain size and composition should be performed to assess which grain components are contributing to milling traits. Analysis of grain composition and quality across our allelic series of *Q* would provide a comprehensive and controlled measure of the effect of *Q* alleles on grain quality.

Modifying spikelet determinacy in wheat

The indeterminate spikelet of wheat at harvest will typically contain several grains of varying sizes with the largest in either of the first two basal florets (most developed florets), continuing with reducing size in the successive florets of the rachilla before the florets are so underdeveloped that they do not bear any grain at all. This form of indeterminate floral development is unlikely to be the most suitable developmental path to maximise yield in a cropping system. Fixing the number of grain in each spikelet may present a way to improve the efficiency of the wheat spike and increase yield. Compared to wheat, the determinant spikelets of maize and rice typically fill their florets to produce a set number of grain per spikelet. In both maize and rice, spikelet determinacy is ensured by the correct function and regulation of *AP2s* (Chuck et al., 2007, Lee et al., 2007, Chuck et al., 2008, Zhu et al., 2009, Lee and An, 2012).

In the wild, plastic responses are useful for maximising seed survival. If some grain is lost due to damage, a grass could respond by branching (either vegetative or from the damaged inflorescence) to produce additional grain bearing units. The indeterminate spikelet may represent a means for an unbranched rachis to ensure some grain set even in the case of damage to part of the spike or spikelet. This utility may not be completely necessary in a cropping system where yield and quality are favoured and grain loss to damage is controlled. Furthermore, tillering grasses such as wheat will produce tillers in response to damage so already possess a means to recover lost yield. The question remains: does an indeterminate spikelet represent a waste of resources through the deposition of unfilled florets? Would it perhaps be more useful to have a wheat spike which set a determinate number of florets per spikelet?

In both rice and maize, altering *AP2s* can result in a loss of spikelet determinacy. Loss-of-function mutations in both species have been described which lead to spikelet indeterminacy (Lee et al., 2007, Chuck et al., 2008). We have shown that loss of function *Q* is associated with the sham ramification trait in wheat, resulting in many florets being produced per spikelet (Greenwood et al., 2017, Debernardi et al., 2017). In contrast, increased *Q* expression in *Q'* did not confer spikelet determinacy nor did it reduce the number of florets per spikelet when compared to SS-like siblings. A broader assessment of the function of other AP2s in wheat may reveal AP2s with the potential to alter this trait. A comparative study of AP2s and their downstream targets between grasses may indicate genes which are altered or missing and potentially associated with the manifestation of spikelet determinacy.

Improving our understanding of the *Q* developmental pathway

Altering *Q* function leads to many pleiotropic changes. Presumably, *Q* has a multitude of gene targets which are differentially regulated and contribute to the developmental changes we have observed in our *Q* alleles. A combination of Chromatin Immunoprecipitation Sequencing (CHIP-seq), to identify transcriptional targets, and RNA-seq, to identify differentially expressed genes would go a long way to improving our understanding of the types of genes that are regulated by *Q* and to what extent changes in *Q* expression lead to changes in downstream gene regulation. Identifying these downstream genes would allow us to use reverse genetic approaches to expose their individual developmental roles.

Recently, mutant databases have been established in tetraploid and hexaploid wheat which would allow for the isolation of loss-of-function alleles of *Q* gene targets (Krasileva et al., 2017). Combining mutants of each homeoallele in a common background, or alternatively, using CRSPR/Cas9 to perform targeted mutagenesis across homologous sequences would allow us to rapidly elucidate important developmental gene function. Concurrently, genes could be overexpressed to further explore their function.

AP2 genes can have diverse or overlapping functions and gene targets (Aukerman and Sakai, 2003, Schmid et al., 2003, Mlotshwa et al., 2006, Grigorova et al., 2011). With the emergence of more complete wheat genomic sequence it will be possible to identify additional *AP2* genes and determine if/what function is conserved between related genes. Simple mutagenesis to generate gain and loss-of-function alleles of these other *AP2* genes as we have done with *Q* would allow us to explore their role in flowering time, spikelet determinacy and internode elongation. These *AP2* genes may represent new avenues for modifying flowering time, spikelet determinacy, and lodicule swelling etc. without the need for targeting downstream genes. In addition, there is potential to identify which gene targets differ between different *AP2s* in wheat thus determining which downstream genes are important for which traits.

Summary

Q and its regulation by *miR172* represents an important pathway in wheat development. Our work, together with a side by side publication (Debernardi et al., 2017), indicates that the sequence of miR172-binding site of *Q* is not only important in regulation of the gene via *miR172*, but that changes in the miR172-binding site were the likely cause of the modern gain of function domesticated form. Furthermore, we have shown that transcription profiles of *Q* and *miR172* differ along the developing inflorescence potentially accounting for the differences in basal-apical phenotypes we observed. A comprehensive assessment of other *AP2* transcription factors and the interaction between *AP2s* and other flowering genes would go a long way towards improving our understanding of the complex genetic interactions which influence the floral transition and different stages of floral meristem identity.

Chapter 5 - Novel gene discovery

Introduction

Chapters 3 and 4 have discussed several novel wheat mutants with altered inflorescence architecture. While the developmental genes were already known, the new mutants revealed novel alleles that confer previously undescribed roles for those genes in wheat inflorescence development. This chapter will discuss the potential use of modern sequencing technologies to uncover previously unknown genes and their function in wheat.

Marker assisted map based cloning and QTL analyses are powerful tools for identifying chromosomal regions and eventually specific genes associated with particular traits. While these more traditional methods of gene discovery are relatively low cost, they can be very time consuming, requiring many generations and/or crosses to be performed to establish the necessary populations. Access to high throughput sequencing technologies has changed the way that researchers can approach gene discovery. It is now feasible in some species to re-sequence entire genomes to identify novel genetic variation.

Unfortunately, the wheat genome is many times larger than other crop species and model plant systems (Wu et al., 2010). Its large size means that whole genome sequencing requires many times more sequence information to achieve the same sequence coverage as in other species. This leads to costs which far exceed the budgets of most research projects. Even if it were possible to obtain high sequence coverage across the entire wheat genome, stitching together the many short sequence reads to form a contiguous genome sequence is a complex task. A large proportion of the wheat genome is made up of repetitive regions making it difficult to align sequence reads to a representative region (Garbus et al., 2015). In addition, the wheat genome is hexaploid with high sequence similarity between the three genomes making it difficult to accurately separate highly homologous reads (Lucas et al., 2014). With sequencing

options like RNAseq and Exon capture able to achieve high sequence coverage over genes at a lower cost than whole genome sequencing, it should be possible to fast track novel gene discovery in wheat (Ramirez-Gonzalez et al., 2015, Saintenac et al., 2011). When considering different sequencing methods, it is important to address the plant material that is available, what is its likely genetic makeup, what are you looking for and what are you comparing that to. This will govern the experimental design and the best gene discovery options.

Having the right material can simplify gene discovery

Chapters 3 and 4 have shown that mutagenesis is a powerful tool for identifying novel gene function in wheat. This approach is restricted to genes which behave in a semi-dominant or dosage dependant manner, as redundant gene families across the three wheat genomes have the potential to mask loss-of-function mutations. Working with dominant or semi-dominant alleles in wheat is technically simpler as the genetic component has effectively taken on a single gene mode of action. Whether a gene has a naturally arising dominant form, or dominance has been generated in a mutant screen, subsequent mutagenesis can then be used to knock out the dominant allele of a gene. The *Ppd-D1, FT* and *Q'* alleles discussed in previous chapters all represent genes with stronger function than their other homeoalleles allowing loss-of-function phenotypes related to these genes to manifest in mutant screens. This also means that if we identify any single gene effect with a dominant or semi-dominant habit in wheat, we are likely to be able to isolate revertant or loss-of-function phenotypes through secondary mutagenesis with a high likelihood that the second mutation causing loss-of-function is in the same gene or a related homeoalleles (if phenotype is related to gene dosage). In any method of gene discovery, multiple alleles, or in this case, derived revertant mutations are a powerful way to isolate the exact causal gene with a high degree of confidence and without the need for fine mapping or complementation. Performing

sequencing analysis on the multiple revertant alleles should identify a region or gene which contains mutations in all revertant lines. We are also able to exclude all non-causal mutations as they differ between revertants.

This type of approach has been utilised to isolate disease resistance genes (R genes) in wheat. A recently described technique called MutRenSeq takes advantage of multiple loss-of-function alleles to isolate disease resistance genes (Steuernage et al., 2016). The process of MutRenSeq involves creating loss-of-function mutants in disease-resistant wheat backgrounds then sequencing genomes or genes from both wild type resistant plants and those which have lost resistance. By comparing sequence of loss-of-function mutants to wild type, genes with mutations across loss-of-function lines can be identified as likely disease resistance genes. This process could be extended to any semi dominant/dominant wheat gene.

Once we have established our working loss-of-function/revertant mutant material, how then do we approach the task of high throughput sequencing as a means of gene discovery? As previously stated, whole genome sequencing in wheat is out of the question due to budget restrictions. RNA sequencing on the other hand is far more cost effective and allows us to focus on a much smaller subset of tissue specific expressed genes. Similarly, exon capture can be used to isolate a subset of the wheat genome, reducing alignment and analysis complexity.

RNA sequencing

The main caveat of RNA sequencing (RNAseq) is that gene expression and therefore the representation of genes of interest in the dataset is dependent on many factors. We must seriously consider what type of mutation is present; is it likely to be represented in transcript; what type of tissue the mutant gene is likely to be expressed in; and at what time during development? In our case we are interested in identifying genes which determine inflorescence architecture. We might consider that developing inflorescence tissue would carry expressed genes of interest. Depending on the trait however we may still need to settle on a specific developmental stage or a time series to capture a wider array of expressed genes. We must also consider that environment plays an important role in determining flowering time and inflorescence development. Genes which determine environmental sensing (light, temperature etc.) could potentially cause altered inflorescence development when mutated and these genes may or may not be expressed in the inflorescence. For example, *Ppd-1* and *FT* expression is highest in leaves while FT protein then acts to alter floral transition in the shoot apical meristem and developing inflorescence. RNA sequencing of developing inflorescence tissue may miss developmentally relevant genes such as these. At the very least, RNA extracted from the developing inflorescence provides information on the expression level of genes which are influencing inflorescence development but may not be the original cause of the mutant phenotypes.

Exon capture

Exon capture shares a similar caveat as RNAseq but with some distinct advantages. The biggest advantage is that harvest is not tissue specific as exon capture relies on genomic DNA. However, as the name suggests, exon regions are captured to be sequenced and a gene of interest must be represented in the probe set which is used to pull down exon regions if it is to be sequenced. Like RNAseq, exon capture cannot be used to identify mutations within promotor regions. Assuming the exon region is represented in the probe set and the mutation is in the exon region, exon capture is an extremely powerful tool for gene discovery in wheat which removes many of the bioinformatic headaches associated with sequencing of the large wheat genome. Exon capture may be best suited for identifying the revertant type mutations mentioned previously as these loss-of-function mutations are more likely to be present within the coding region of a gene. Furthermore, capture sets can be tailor made to isolate a specific class of genes to refine the scope of a project, improve depth of coverage and further simplify the bioinformatic analysis.

This results chapter will present two sets of wheat material which carry different floral traits (late flowering, awnless) with unknown genetic cause and discuss the procedure we have followed so far in attempt to isolate the causal mutations in each case. Unlike the previous chapters which presented a conclusive set of results relating to gene function, the work presented here is in varying stages of completion. The purpose of this chapter is to highlight the potential for high throughput sequencing to assist gene discovery in wheat.

Results

The late flowering mutant 1006

A late flowering mutant (SS1006 or 1006) was identified in a mutagenesis population of the Australian wheat cultivar Sunstate (SS) **Figure 25**. 1006 produces more rachis nodes than parental SS. However, unlike previously described late flowering mutants in chapter 3, 1006 does not produce paired spikelets at any rachis node position. Based on our previous results which suggest paired spikelets are formed by delaying the floral transition, it is unusual that paired spikelets are not formed in the late flowering 1006. This suggests that mutations in *Ppd*-1 and *FT* are unlikely to be causing the delay in flowering and perhaps a separate floral promoting pathway or meristem identity gene downstream of *FT* is responsible.

Typically, the differentiation of leaf nodes and rachis nodes is strongly linked to flowering time. Interestingly, when compared to other late flowering mutants, 1006 produces more rachis nodes in relation to the number of leaves deposited on the main stem **Figure 26**. This may indicate a prolonged duration of spike development compared to WT Sunstate and other derived mutant lines. 1006 produced an expected number of rachis nodes in relation to flowering time (anthesis) on trend with other flowering time mutants **Figure 27**. 1006 produced more rachis nodes than any other mutant from the same round of mutant screening.

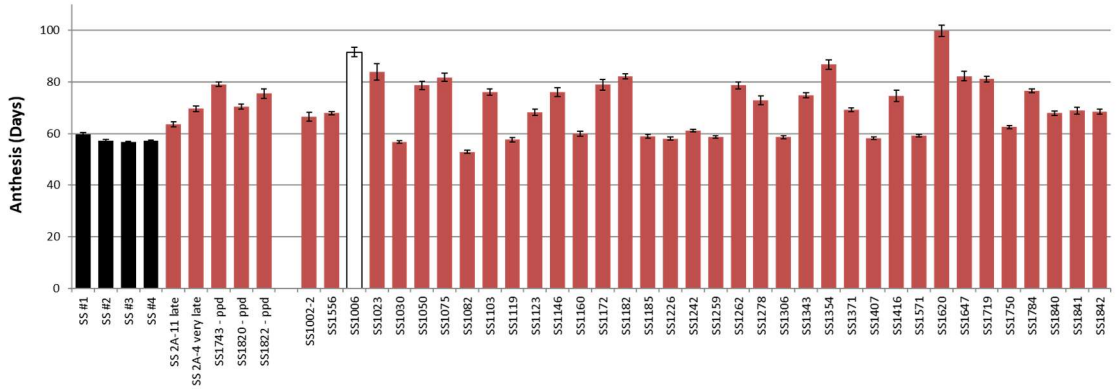

Figure 25 Number of days taken for Sunstate (SS) and derived flowering time mutants to reach anthesis. SS1006 (white) represents a very late flowering habit compared to other mutant lines and parental SS. Four groups of parental SS were scored (black). Flowering time mutants with known genetic cause, including Ppd-1 mutants, are shown on left hand side of figure adjacent to parental SS. N= 8 Plants grown in glasshouse conditions.

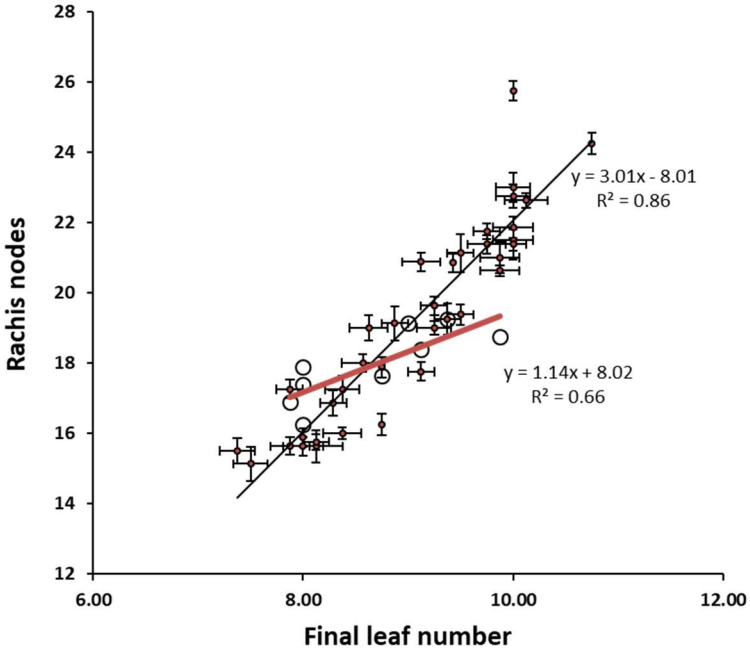

Figure 26 Final leaf number and number of rachis nodes of Sunstate (SS) and derived flowering time mutants. This data has been scored from the same set of plants as those in Figure 25. Parental SS and known flowering time mutant alleles are plotted as circles with line of best fit shown in red. Red points represent unknown flowering time mutants with line of best fit shown in black. Top plotted point represents 1006. 1006 produces more rachis nodes than other flowering time mutants with a similar final leaf number.

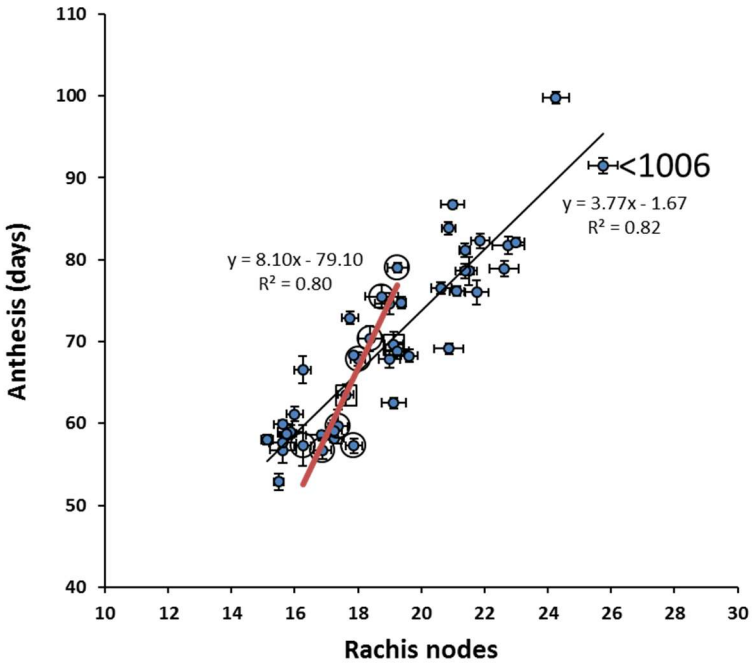

Figure 27 Number of rachis nodes and days until anthesis of Sunstate (SS) and derived flowering time mutants. Same dataset as anthesis plot Figure 25. Parental SS and known flowering time mutant alleles are plotted as circles with line of best fit shown in red. Blue points represent unknown flowering time mutants with line of best fit shown in black. 1006 point indicated by label (<1006). Flowering time and final rachis node number are generally well correlated with most lines plotting close to the line of best fit. 1006 produces the highest rachis node number of all the flowering time mutants isolated.

A lack of paired spikelets compared to many other flowering mutants indicate that the causal nature of the 1006 mutation may be in a novel flowering time, or meristem identity gene. As with *Q'*, we back-crossed the 1006 mutant to its progenitor line SS. Based on the segregation of the F2 population we were reasonably confident that late flowering in 1006 represented a single locus effect. Around a quarter of the population flowered as early as SS (between 4th-9th July N= 21) and around quarter flowered as late as 1006 (16th July or later N= 31). A broad spectrum of flowering time in the F2 population from early (SS-like flowering time) to late (1006-like flowering) indicated that the genetic effect may be behaving in a semi-dominant or dosage dependent manner to give intermediate flowering time phenotypes in the majority (approximately ½ N= 50) of the progeny **Figure 28**. Unlike the *Q'* mutation, 1006xSS F2 did not segregate

so clearly into distinct genetic classes. Instead, we observed crossing over of early and intermediate flowering times **Figure 28**.

Flowering time is often quite variable, even amongst near isogenic individuals grown under controlled conditions, making minor flowering time effects difficult to detect. Luckily the flowering time differences caused by the 1006 mutation are large. By isolating the tail ends of the segregating population, we can be reasonably confident we are isolating fixed early and late genetic classes. Plants which flowered early within the F2 and plants which flowered late were termed SS-like (early) and 1006-like (late), respectively. Twelve individuals were harvested from each genetic class for further analysis.

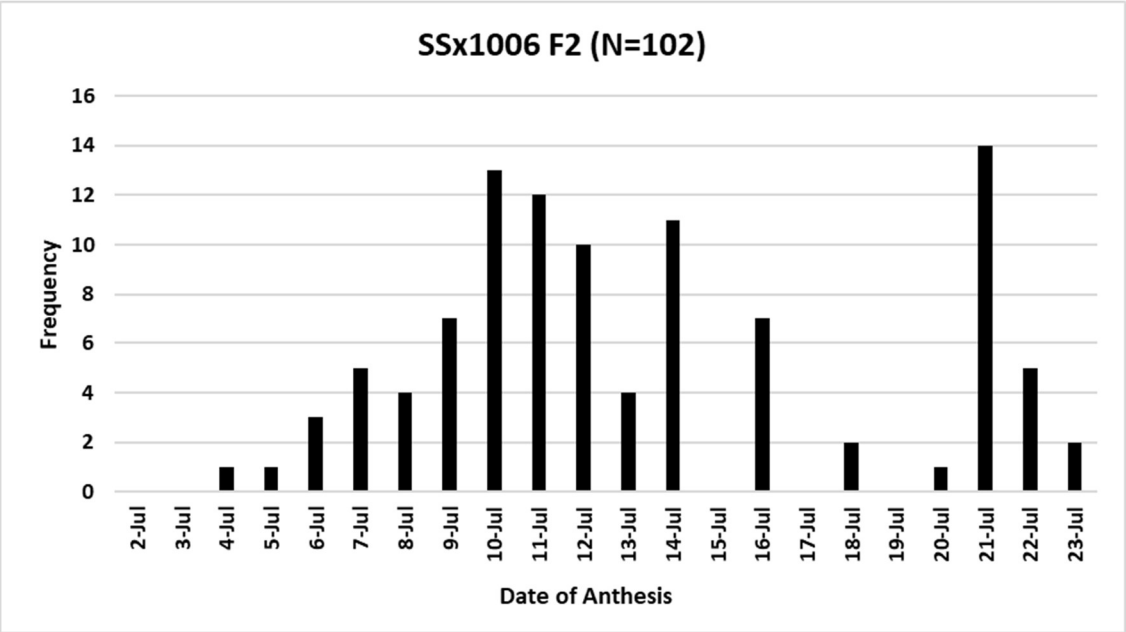

Figure 28 Segregating F2 population of 1006 backcrossed to Sunstate. Parental Sunstate grown alongside this population reached anthesis between the 4th and 10th of July. 1006 mutants grown alongside this population reached anthesis between the 16th and 22nd of July.

As with *Q'* we also performed a second round of mutagenesis on 1006 grain but failed to generate mutants which fully reverted to a SS-like flowering time, though overall reductions in flowering time were observed in some partial revertants. Given the range of potential flowering genes which could be targeted to cause earlier flowering in 1006 and the high variability of flowering time traits in general, we could not be confident that any of these partial revertants would represent mutations in a common gene. The revertants were not included in subsequent sequencing analyses. These revertants still represent useful material to clarify any future analysis which may identify a candidate mutation in 1006.

To identify potential candidate genes causing the 1006 phenotype, we decided to take a crude bulked segregant approach utilising the mutagen derived genetic diversity represented in the 12 early and late individuals harvested from the F2 population. All selected F2 lines were screened into F3 and F4 generations to ensure early and late phenotypes were maintained **Figure 29**. RNAseq was chosen over exon capture as this would allow us to determine which genes are differentially expressed between 1006 and SS-like plants while still potentially isolating the causal mutation. Even if we are unable to isolate the causal mutation in 1006, we will still be able to identify genes important for timely meristem development by comparing expression analysis between the two genetic classes. Performing RNAseq on multiple individuals from the early and late genetic classes allows us to eliminate non-causal SNPs as many of these would still be segregating or have segregated within the early and late populations. Assuming we would be able to isolate transcript containing SNPs linked to the causal mutation in 1006, these SNPs should be fixed in late flowering individuals and be fixed for the wild allele in early (SS-like) individuals.

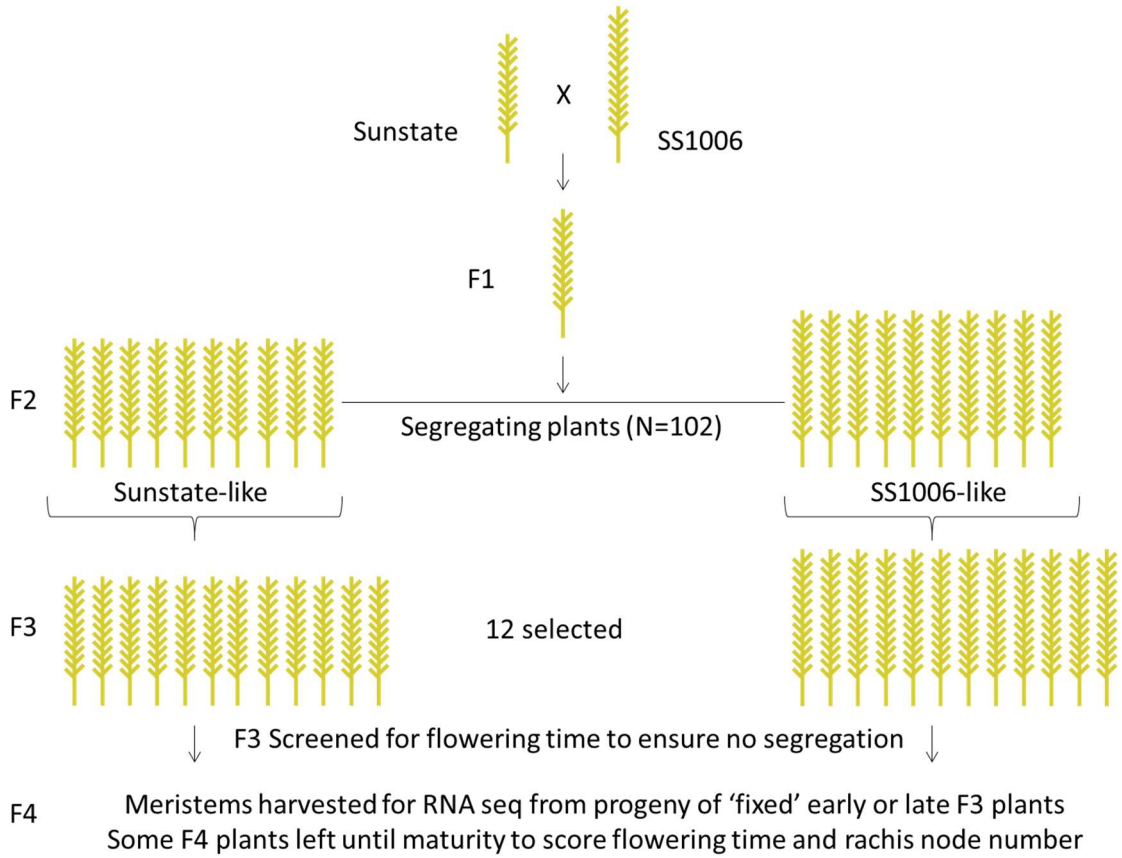

Figure 29 Schematic of establishing 1006 segregating population and segregant selection. Plants were selected from the tail ends of F2 segregating population. 12 plants were selected with an early flowering low rachis node habits and 12 were selected with a late flowering high rachis node number habit. Selected plants were screened for fixed growth habit in F3 population. Sufficient seed was harvested from F3 plants to perform meristem extractions for RNAseq in F4 population. Left over plants were scored to ensure retention of flowering habit before submitting RNA for library construction and sequencing.

The goals of the RNAseq experiment were to: identify differentially expressed transcript when comparing early and late individuals and, identify SNPs within sequenced transcript and then determine if any of the SNPs are wholly or partially linked (present in late lines but not early lines) with the late flowering phenotype of 1006. For expression analysis, two early and two late individuals were chosen. To facilitate statistical analysis for differential expression, three biological replicates were harvested from each of these chosen lines **Figure 31**.

For SNP detection, samples were combined from multiple individuals. Tissue was included from four lines in each of three early and three late samples to include all 12 individuals from each class without separate library preparation. We also included two biological replicate samples of non-mutagenised Sunstate **Figure 31**. Any SNPs detected which are not represented in parental non-mutagenised Sunstate are likely to have been introduced through mutagenesis. Similarly, SNPs present in late individuals but not early individuals may represent linked or causal mutations.

Selecting tissue and harvest time

As stated previously, the tissue type and time of harvest are important considerations when performing RNAseq. We sought to identify a developing inflorescence stage which would be likely to capture genes associated with floral transition and rate of inflorescence development. Developing inflorescences were harvested from SS-like and 1006-like individuals to assess their developmental rates. In line with the flowering time phenotype, 1006-like individuals initiated the development of floral shoot apical meristem structures later than SS-like individuals. Furthermore, 1006-like individuals had inflorescences which progressed through stages of development more slowly. Together, the developmental characteristics of 1006-like plants suggest that the genetic cause of floral delay is acting early and continuously to delay the onset of floral development and also to delay the continued rate of inflorescence development. The double ridge stage of inflorescence development represents inflorescence tissue which has differentiated into spikelet primordia at the base while maintaining an undifferentiated state at the apex. As the key traits of flowering time and final rachis node number are defined during double ridge we concluded that samples should be taken at this stage to best capture the genetic determinants of the 1006 phenotype **Figure 30**.

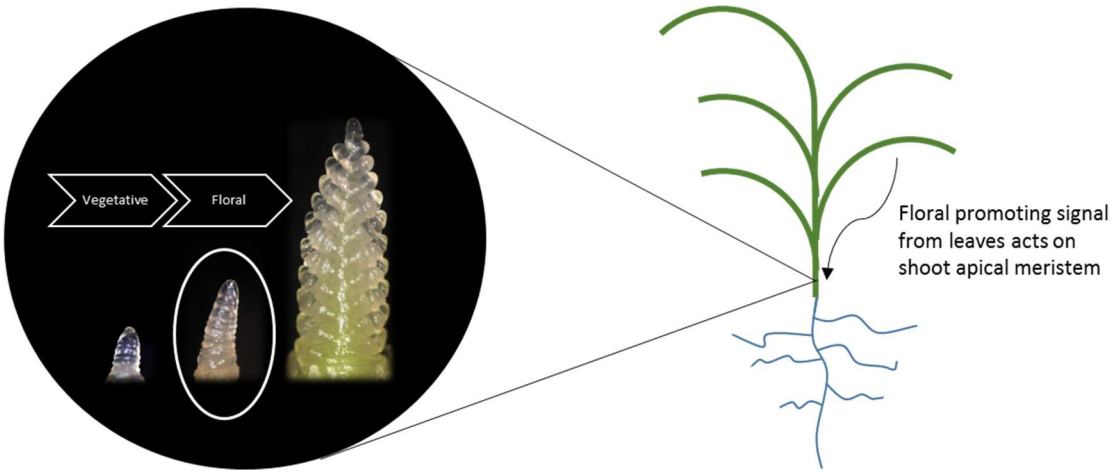

Figure 30 Schematic showing tissue type harvested for RNAseq experiment. Developing inflorescence meristems were harvested soon after floral transition at a stage known as double ridge shown in white circle. Terminal spikelet stage is shown on right hand side of black circle. We expected that our gene of interest would be acting during double ridge as this developmental stage is essential in defining the rachis node number and anthesis date of the plant. Harvesting inflorescence tissue potentially ignores many of the environmental integrator signals which drive the floral transition.

RNA sequencing and data analysis

RNA samples were sent to the Australian Genome Research Facility (AGRF) for library construction and sequencing. 125bp paired-end sequencing of 20 sample libraries was performed across two lanes on an *Illumina HiSeq 2500.* Each sample library was technically repeated in each of the two lanes. On average 12,291,860 paired-end sequence reads were generated per sample per lane **Figure 31**. Quality control and sequencing alignment was performed by Andrew Spriggs (CSIRO). Basic quality checks were performed using the QC-check tool in Biokanga. After quality control, filtering and trimming around one third of reads were discarded. The filter tool trims off the ends of reads where it finds adapter sequences present, filters out reads which are subsequently too short, filters out reads which contain too many unknown bases (Ns), filters out extra copies where forward and reverse pairs of reads together are exactly identical to other pairs (we expect randomly staggered starts/ends, so exact copies are most likely just an amplification effect, and redundant information), and filters out reads

that don't have some overlap with any other reads (a single completely unique read, with no support, is not going to be useful for any analysis). Filtered sequence reads were mapped to the publicly available wheat expressed sequence tag (EST) dataset. Around 75% of reads mapped uniquely to the EST dataset.

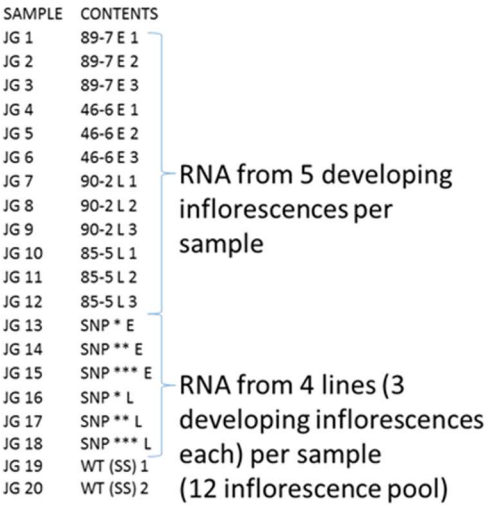

Lane	Sample Name	Paired Reads	Data Yield (bp)	Lane	Sample Name	Paired Reads	Data Yield (bp)
1	JG1	12,640,407	3.16 Gb	2	JG1	12,528,700	3.13 Gb
	JG2	12,969,443	3.24 Gb		JG2	12,891,023	3.22 Gb
	JG3	12,034,902	3.01 Gb		JG3	11,990,122	3.00 Gb
	JG4	12,640,417	3.16 Gb		JG4	12,562,239	3.14 Gb
	JG5	12,533,928	3.13 Gb		JG5	12,430,173	3.11 Gb
	JG6	11,524,097	2.88 Gb		JG6	11,463,777	2.87 Gb
	JG7	11,902,628	2.98 Gb		JG7	11,804,039	2.95 Gb
	JG8	11,902,520	2.98 Gb		JG8	11,829,545	2.96 Gb
	JG9	12,700,579	3.18 Gb		JG9	12,576,037	3.14 Gb
	JG10	12,425,498	3.11 Gb		JG10	12,314,294	3.08 Gb
	JG11	11,682,411	2.92 Gb		JG11	11,606,999	2.90 Gb
	JG12	11,762,495	2.94 Gb		JG12	11,655,722	2.91 Gb
	JG13	13,275,730	3.32 Gb		JG13	13,171,649	3.29 Gb
	JG14	12,532,181	3.13 Gb		JG14	12,426,719	3.11 Gb
	JG15	12,113,137	3.03 Gb		JG15	11,997,989	3.00 Gb
	JG16	11,920,139	2.98 Gb		JG16	11,853,365	2.96 Gb
	JG17	12,736,032	3.18 Gb		JG17	12,621,193	3.16 Gb
	JG18	12,166,837	3.04 Gb		JG18	11,960,547	2.99 Gb
	JG19	12,669,087	3.17 Gb		JG19	12,555,142	3.14 Gb
	JG20	12,756,925	3.19 Gb		JG20	12,545,747	3.14 Gb
				Total (both lanes)		491,674,414	122.92 Gb

Figure 31 RNA samples submitted for RNAseq and sequence yield generated. Samples 1-12 represent two sets of early and late lines with three biological replicates each to facilitate differential expression analysis. Samples 13-18 represent a pool of 12 early and 12 late lines across three samples for each growth habit to facilitate SNP detection across the early and late population. Samples 19-20 represent RNA from parental Sunstate included as a control and to determine which SNPs in the early and late lines were induced by mutagenesis.

Current analysis

Initially we performed SNP detection across the biological replicates of SS-like and 1006-like samples (JG1-12). We detected several SNPs which were present in only the 1006-like sequence reads. Of these SNPs, one was located within an intron sequence of a predicted gene which possessed high sequence similarity to a known flowering time gene in rice. Subsequent alignment and SNP detection of the pooled RNA samples from all 12 early and late individuals indicated that this particular SNP was segregating within the early and late sample population and therefore unlikely to be contributing to

delayed floral development in 1006. This false positive candidate from our initial analysis highlights the importance of including multiple segregated individuals to filter down the number of candidate genes. Similarly, including non-mutagenised Sunstate (JG19-20) allowed us to filter out SNPs which are naturally present, albeit at low frequency in our progenitor material.

Unfortunately, we did not detect any SNPs that were completely linked with the 1006-like late flowering habit. However, we did detect several SNPs with a potential partial linkage to the late flowering phenotype of 1006 being present in late flowering samples but not in early samples **Figure 32**. We included both SNPs which were likely induced by mutagenesis; not present in WT Sunstate, and; SNPs which were potentially still segregating in parental Sunstate. Induced SNPs (those resulting from mutagenesis) with potential partial linkage to 1006 were found on chromosome 2, 3 and 5 (highlighted in **Figure 32**).

RefID	Coord	EarlyPools SNP	EarlyPools Ref	EarlyIndv SNP	EarlyIndv Ref	LatePools SNP	LatePools Ref	LateIndv SNP	LateIndv Ref	WT SNP	WT Ref
1AL-3852696	687	6	0	12	0	6	4	10	6	4	3
1AS-3283893	8139	0	6	0	12	3	6	6	12	4	4
2AL-6390264	4695	0	6	0	12	3	6	7	12	2	3
2AS-3183635	432	0	6	0	12	4	6	7	12	0	4
2AS-5305160	9724	0	6	0	12	3	6	6	12	0	4
3AL-3834102	239	0	6	0	12	3	6	6	12	0	2
3AL-4393212	582	0	6	0	12	3	6	6	10	0	4
4AL-7169542	8596	0	6	0	12	3	6	6	12	3	4
4AL-7169542	8597	0	6	0	12	4	6	6	12	3	4
5AL-2119974	1785	6	0	12	0	6	5	11	9	4	0
5AL-2733412	8683	6	0	12	0	6	4	12	6	4	1
6AL-5753765	10452	0	6	0	12	3	6	6	12	3	4
7AS-4231081	3174	0	6	0	12	4	6	8	12	1	4
7AS-4231081	3189	0	6	0	12	4	6	8	12	1	4

Figure 32 SNPs identified with opposite representation in the early and late samples. Numbers in each SNP or Ref (Reference) column indicate the number of samples with sequence alignments of five reads or greater matching either the reference nucleotide of the EST dataset (Ref) or a SNP at a given position. Since pooled or individual samples were technically duplicated for sequencing, the sample numbers are doubled e.g. the 6 EarlyPool samples in this table are from three technically duplicated EarlyPool samples (Sample 13, 14, 15 Figure 31). Columns labelled WT represent non-mutagenised SS and therefore sequence profiles which do not match the fixed profiles of WT samples likely represent induced mutations derived from the original 1006 late flowering parent. A value of zero relative to adjacent SNP or Reference column for a set of samples indicates a particular nucleotide call is fixed in a set of samples. Sample sets with both SNP and Ref calls present exceeding the total sample number indicates that

lines are heterozygous e.g. LatePools and LateIndv samples are segregating for the SNPs presented here. Since these nucleotide sequences are fixed in Early lines, they may show partial linkage to the late flowering phenotype derived from 1006.

Future analysis

As of the 31/05/2017, the International Wheat Genome Sequencing Consortium have made the first version of the Wheat reference genome available to select research groups. As stated, our alignments have been made to publicly available wheat exon data sets. These exon data sets may not feature a full suite of genes especially considering varietal and tissue of origin differences between the samples making up this data set. Furthermore, the wheat exon dataset may not be correctly associated with relevant genome positions. Using the new wheat reference genome as a scaffold for aligning our RNA sequence reads may yield a higher proportion of reads aligned and provide us with more reliable physical location information which could help assess linkage of SNPs with our late flowering segregants.

Moving forward, we would like to align our sequencing data to the wheat reference genome. After aligning to the new wheat reference sequence, we would like to reassess our SNP detection as well as look for genes which are differentially expressed between 1006 and SS-like plants. To account for potential differences in gene representation between Chinese Spring (Wheat reference genome) and our Sunstate background, we would like to compare the wheat reference genome alignment to a de novo assembly of our transcript data. Gene sequence represented in our de novo assembly but not present in the reference genome would indicate to what extent the genetic make of Sunstate differs from Chinese Spring.

Near isogenic awn/awnless material

In wheat, a genetic association with awn length has been mapped to the *B1* locus on the long arm of Chromosome 5A near *VRN1* and *Q* (Yoshioka et al., 2017, Kato et al., 1998). Presence of the dominant *B1* locus in hexaploid wheat leads to a reduction in awn length. The near isogenic lines W11B+ and W11B- which have long awns (+) and short awns (-) respectively were established at CSIRO. Awnlessness was originally introduced into the Sunstate background when attempting to introduce a particular *VRN1* allele from an awnless wheat variety. Awnlessness was carried with the *VRN1* allele. Since the reported dominant *B1* locus is found near to *VRN1,* we assumed that co-segregation of *VRN1* and *B1* had occurred.

Genetic dominance of the *B1* locus should allow for the isolation of revertant alleles by simple mutagenesis. We performed sodium azide mutagenesis on approximately 2000 W11B- grain. Grain were harvested from M1 plants into approximately 20 pools. Pools consist of pooled grain from around 100 M1 plants. We isolated four presumed loss-of-function mutants in the F2 mutant population **Figure 33**. The four mutants were all derived from separate M1 pools so represent four unique mutation events leading to similar long awn phenotypes. Given the dominant function of the *B1* locus, we are confident that loss-of-function mutations within the *B1* gene will be responsible for some, if not all of the derived revertant phenotypes.

Figure 33 Near isogenic awned and awnless pair and revertant mutants derived from awnless parent. Mutagenesis was performed on W11B- grain and four unique awned revertants (2-1, 6-1, 11-1, 22-1) were isolated from the mutant population.

Uncovering the causal gene B1

Through direct sequencing of target genes in the *B1* region of parental awn/awnless lines and the derived revertants, we should be able to identify the causal gene. Unfortunately, no known awn development genes in the grasses have sequence similarity to predicted genes on wheat group 5 chromosomes though this may change with better representation of 5A sequence in the recently released wheat genome sequence. With direct sequencing of candidate genes not possible, we can consider a number of other options for gene discovery. Since we already know the chromosomal location of *B1*, our options to isolate the causal genetic mechanism can be more refined and are simplified. For example we can align reads only to this chromosome.

Exon capture, RNAseq or Chromosome sorting

The revertant lines we have isolated are likely to carry loss-of-function mutations within the causal *B1* gene. For this reason, we would expect that both exon capture and RNAseq would be able to identify the revertant mutations. As stated previously, both methods are complicated by the need for adequate representation of the gene. In the case of exon capture we require that a probe exists to pull down the *B1* gene and for RNAseq we are required to isolate the right tissue at the right time to capture *B1* transcript. Even if we are able to capture the gene with RNAseq there is no guarantee that the gene will be highly expressed allowing for SNPs to be confidently scored. Assuming representation of our gene of interest, exon capture is the simpler of the two methods to isolate revertant mutations. Even though the awned revertants are likely to contain many SNPs, only a small handful of genes or even a single gene will carry mutations in all four revertant lines. Since we now the chromosome location we can even narrow our candidate list to a small subset of genes on chromosome 5A. Besides exon capture, chromosome sorting can also be employed to reduce the wheat genome to single chromosome units. In this case, chromosome sorting is an attractive option as we know the chromosome which contains the gene of interest and we do not know for sure that the gene is represented in the exon capture probe set.

Discussion

Positional information removes bioinformatic complexity

A key purpose for our choice to use high throughput sequencing for gene discovery is to avoid the time-consuming process of generating large mapping populations. While map based cloning is a powerful tool for gene discovery, short project timeframes do not always allow for this tried and true technique to be employed. In theory, high throughput sequencing experiments using RNAseq or Exon capture should allow us to expedite gene discovery in much smaller populations of plants (Ramirez-Gonzalez et al., 2015, Trick et al., 2012). Even when taking a high throughput sequencing based approach as described in this chapter, knowing the chromosomal region associated with a mutation/trait is a very useful way to reduce analytical complexity. In comparison to the 1006 mutation which could be located anywhere, knowing the general chromosome location of the *B1* gene greatly narrows the range of potentially causal genes. A clear indication of the chromosomal position of a genetic effect allows you to exclude large regions of the genome from your analysis and thus exclude the many non-causal polymorphisms that will no doubt be identified in the analysis.

SNP discovery does not require separation of reads into three genomes but expression analysis does

Genes with high sequence similarity between the three wheat genomes make alignment of any one read to its representative gene difficult, hence the adoption of flow sorting and sequencing of individual chromosomes in wheat (Wu et al., 2010, Lucas et al., 2014). High sequence similarity can also become a problem when determining expression levels in wheat RNAseq experiments. For expression analysis, each read can only be associated with the expression of one homeoallele but may align to many. Often, reads with ambiguous alignment (to multiple reference locations) are discarded

removing potentially useful sequence information from analysis (Robert and Watson, 2015). When we consider the possibility for highly similar sequences between the three wheat genomes, discarding sequence reads could be particularly disruptive to analysis. For determining polymorphisms in mutant populations, aligning all common reads to a 'single' collapsed genome or to all possible alignment locations will still reveal the gene or gene family that a polymorphism is located in. Subsequent analysis through refined alignments or direct sequencing can then determine which gene homeoallele contains the mutation. Collapsing the wheat genome to combine highly similar home alleles to a single reference set may be used to simplify read alignment and also facilitate SNP detection. Even though SNP detection may identify multiple SNPs at any one gene position, SNPs associated with mutants can still be filtered against non-mutant sequence to determine which are causal and non-causal SNPs.

Mutagenesis to isolate multiple loss-of-function alleles in a single wheat gene

The MutRenSeq approach has been successful in isolating disease resistance genes in wheat (Steuernage et al., 2016). Like the mutants we have described, MutRenSeq relies on a single gene mode of action being present. Disease resistance which can come about through allelic variation in a single receptor gene is a field of research which can benefit greatly from this type of gene discovery approach (Steuernage et al., 2016). We propose that very similar techniques can be used to identify any gene which has a dosage dependant, semi-dominant or dominant contribution to any wheat phenotype. Through a candidate gene approach in *Ppd-1* and *Q* we were able to isolate numerous loss-of-function alleles, but these mutations could also have been isolated using Exon capture or RNAseq. Using Exon capture, RNAseq, whole chromosome sequencing or targeted sequencing it should be possible to rapidly isolate numerous novel wheat genes or allelic variants of genes which confer important yield traits provided they are controlled by semi-dominant, dominant or dosage dependent genetic effects.

The awn/awnless *B1* alleles are present in breeding material and mapping populations

It is important to consider that the *B1* and *b1* alleles inhibit and promote awn length respectively. Both alleles of *B1* are present in a diverse set of wheat varieties. Multi-parent advanced generation inter-cross (MAGIC) populations have been established in hexaploid wheat whose parents have different representations of the *B1* allele. MAGIC populations consist of many thousands of recombinant inbred lines (RIL) which carry a diverse mix of genetic material from up to 8 parental wheat lines (Gardner et al., 2016, Huang et al., 2012, Mackay et al., 2014). Mapping information of each parent and RIL combined with diverse phenotypic information can allow for the high-resolution trait-mapping down to relatively small regions containing a small number of genes (Bandillo et al., 2013). In the case of the *B1* gene in which we have loss-of-function mutations, direct sequencing of the small number of candidate genes in the revertant lines would be able to isolate the causal gene.

Exploiting natural diversity for genome wide association studies

There are many wheat landraces with differing flowering habits and inflorescence architecture traits. Performing exon capture or RNA sequencing across genetically diverse populations could be used to identify SNPs and other genetic variation that differentiate the population. This genetic variation can then be correlated with phenotypic data to help narrow the genetic associations to particular traits to small genomic regions (Huang et al., 2010, Sukumaran et al., 2015, Sun et al., 2017). Targeted sequencing of large diverse populations using RNAseq or exon capture would allow for high resolution mapping of different inflorescence traits. For example, the location of the awnless gene *B1* may be narrowed to only a handful of genes. Subsequent direct sequencing of these genes in the revertant lines we have generated would confirm the genetic cause of *B1*.

Summary

Flowering time and inflorescence architecture is controlled by numerous genetic factors and relatively few are known in wheat. With many more inflorescence architecture genes functionally described in other grass species, comparative genetics will be a powerful tool for elucidating gene function in wheat especially with the release of the first wheat reference genome sequence. In addition to reverse genetic screening, traditional forward genetic screens combined with high throughput sequencing should allow for novel gene discovery in wheat. Processes like RNA sequencing and Exon capture drastically reduce the subset of genetic material sequenced, essential when working in large genomes like wheat. Furthermore, these processes reduce cost while improving sequence coverage and allow even small research groups to employ high throughput sequencing for the identification of novel genetic variation in wheat.

Chapter 6 – General discussion

Mutagenesis is a powerful tool for elucidating gene function in wheat

In comparison to other grass species and model plant species where mutagenesis as part of forward genetic screening is a common tool for elucidating gene function, forward genetic screens for gene discovery in polyploid species are far less common. With the potential for extra redundant copies, mutagenesis typically fails to expose many genes which have a high level of functional redundancy (Lawrence and Pikaard, 2003). Therefore, observable mutant phenotypes in polyploids are more likely to be caused by semi-dominant or dominant mutations, or, through loss-of-function mutations in genes which already possess dominance or have acquired new function relative to their homologues on the other genomes (Beales et al., 2007, Pearce et al., 2011). The genes in which we have isolate mutant alleles, *Q, PPD-1* and *FT* are all examples of acquired dominant function relative to their other homeoalleles (Lv et al., 2014, Shaw et al., 2012, Greenwood et al., 2017, Debernardi et al., 2017, Boden et al., 2015). These agronomically important genes are evidence that gene dosage has been an important avenue for introducing genetic and phenotypic variation in wheat.

Huge potential exists in elucidating and exploiting the function of the somewhat hidden suite of redundant wheat genes. Comparative genetics is perhaps our most powerful tool for indicating which sets of genes are worth targeting for functional analysis in wheat. The upcoming release of a 'complete' reference sequence for wheat will enhance our capacity to perform important comparative studies to better adapt knowledge from other grass crop species. Utilising new molecular tools such as CRSPR/Cas9 to perform targeted modifications in a set of homologous wheat genes will provide us with the opportunity to examine loss of function mutants which would otherwise be hidden by traditional forward genetic screens (Wang et al., 2014).

We and others have shown that mutagenesis in wheat has a proven ability to produce strong detectable phenotypes albeit in genes with semi-dominant or dominant function or whose function is dosage dependant (Chandler and Harding, 2013, Boden et al., 2015, Greenwood et al., 2017, Sanchez-Martin et al., 2016, Steuernage et al., 2016).

Although there can be some technical difficulties associated with working in a polyploid species, polyploidy allows for higher mutagenic loads be tolerated with a lower risk of losing a full homeoalleles complement of essential gene function (Uauy et al., 2009). Because of this, wheat is actually an ideal model system for isolating certain types of mutations including those in unique alleles of disease receptor genes, gain-of-function mutations and mutations in genes which have acquired unique function relative to their related homeoalleles. In addition to surviving high mutagenic load, fewer mutant plants need to be screened to isolate loss-of-function mutations of single gene effects thanks to higher mutation rates compared to diploid organisms (Uauy et al., 2009).

Still, in wheat, it is unlikely to isolate phenotypic variation derived from mutations in genes with redundant copies. Leveraging the high mutation capacity of wheat, mutant stock collections have been established in both hexaploid and tetraploid wheat (Krasileva et al., 2017). This important reverse genetic resource allows researchers to query a gene of interest and order mutant lines which can then be crossed to combine multiple mutant alleles across the genomes into a common background. Emerging gene editing tools could also be employed to serve this function but any positive agronomic outcomes may be regulated as genetically modified (Khatodia et al., 2016).

Where possible wheat research should utilise emerging reverse genetic resources. Given the low cost and simplicity of performing mutagenesis in wheat, researches should also consider generating their own mutant material in local breeding lines to explore induced

genetic variation in diverse and agriculturally relevant backgrounds, particularly for forward genetic screens.

Environment is a powerful tool for studying inflorescence development

Changes in flowering time in response to environmental changes are well documented (Greenup et al., 2009) but rarely is inflorescence development shown in the context of altered environmental conditions despite changes in flowering time also altering inflorescence architecture. Modifying, day length, light quality and temperature all modulate the rate of floral development (Gororo et al., 2001) and are therefore a powerful tool for studying inflorescence architecture phenotypes in wheat. As we have shown in *Brachypodium*, the use of weakly inductive floral signals can be used to exaggerate inflorescence branching in *fzp* mutants. Similarly, in wheat, we have shown weakly inductive photoperiods can be used to exaggerate the frequency of paired spikelet's in photoperiod sensitive backgrounds (Boden et al., 2015). The future study of inflorescence development would benefit from the use of modified environmental conditions to expose weak genetic effects particularly when screening mutant populations. With easy access to many wheat varieties of differing environmental and floral transition responses, the integration (crossing) of environmental influence and floral promoting signals can be studied in detail.

A complex network controlling floral transition and inflorescence development

As discussed in chapter 4, *AP2* transcription factors have been shown to have a generally florally repressive effect negatively regulating the floral promoting effects of *FT* and floral meristem identity genes like *SOC1* and *AGAMOUS* (*AG).* The general floral repressive role of *AP2* transcription factors is counteracted by negative feedback from some floral meristem identity genes as well as by the highly conserved *miR172* (Krogan et al., 2012, Jung et al., 2014, Yant et al., 2010, Tao et al., 2012, Huang et al., 2016) **Figure 34**.

Based on the known function of *AP2s* in *Arabidopsis,* the florally antagonistic interactions of *Q* should be explored in the mutants we have generated. Querying flowering time and expression profiles of our *Q* allelic series through different inflorescence development stages would help determine which genes are regulated by *Q* and to what extent changes in *Q* expression and function modify these interactions. We know very little about *Q* transcriptional targets. CHIP-seq could be used to determine *Q* gene targets. In addition, Q protein localisation within developing inflorescence tissue should be determined using immunolocalisation methods (Sauer and Friml, 2010). Given that *Q* and other *AP2s* are important in determining the development of specific sets of floral structures (Jung et al., 2014, Aukerman and Sakai, 2003, Huang et al., 2016, Mlotshwa et al., 2006, Huijser and Schmid, 2011), immunolocalisation would help resolve in which tissues and at which stage of development this action is necessary. Extending this type of tissue specific and temporal resolution to other developmental genes would allow us to determine what different overlapping gradients of different genes are important in defining the unique floral structures of wheat and other grass crops.

The rice *AP2* genes *SNB* and *IDS1* have been shown to inhibit *FZP* and promote inflorescence branching. Double mutants of *snb* and *ids1* show increased *FZP* expression and reduced branching consistent with the role of FZP in driving transition to spikelet meristem identity (Lee and An, 2012). It is not clear whether *AP2s* are directly interacting and inhibiting *FZP* or rather acting through the described floral antagonistic *AP2* pathway via *FT* and/or floral meristem identity genes. Both direct negative interaction with *FZP* or negative regulation of floral transition would be sufficient to promote branching in rice. In wheat, which does not typically form inflorescence branches, this interaction has not been observed. Though, based on the interaction between *Brachypodium fzp* mutants and changes in the floral promoting signal we may expect that the combination of *ap2* mutations and *fzp* would also reduce branching severity and this may extend to wheat. With *fzp* mutants available in wheat (Dobrovolskaya et al., 2015, Poursarebani et al., 2015) this interaction could also be explored by crossing *fzp* mutants with our loss and gain-of-function *Q* alleles. In addition, combining different combinations of available *FZP, Q, FT, TB1 and PPD-1* alleles would allow us to identify some of the possible complex genetic interactions in this network based on altered developmental profiles.

We could further expand our understanding of floral regulatory mechanisms in wheat through altered expression of *miR156.* In *Arabidopsis* regulatory feedback between *AP2s, miR156* and *miR172* are important in defining floral development (Jung et al., 2011, Wu et al., 2009) (See **Figure 34**). Creating transgenic wheat plants which either overexpress *miR156* or over express mimics of *miR156* target sites (to reduce functional *miR156*) would expand our understanding of this important feedback loop in wheat and improve our understanding of *AP2* regulation beyond the conserved targeting by *miR172*. In both rice and wheat, targets of *miR156, SPLs,* have been shown to positively regulate *TB1* expression (Lu et al., 2013, Liu et al., 2017). Thus, we can accommodate a

general regulatory model encompassing all the wheat genes we have discussed in chapters 3 and 4 **Figure 34**. These genetic interactions are likely far more complicated than shown in **Figure 34** with many TFs coming together at different dosages with overlapping expression profiles across developing meristems likely to be important in determining the formation of specific inflorescence structures. With the genetic material we have available in wheat, we can begin to explore these complex interactions and improve our understanding of inflorescence development not only in wheat, but all grass crops.

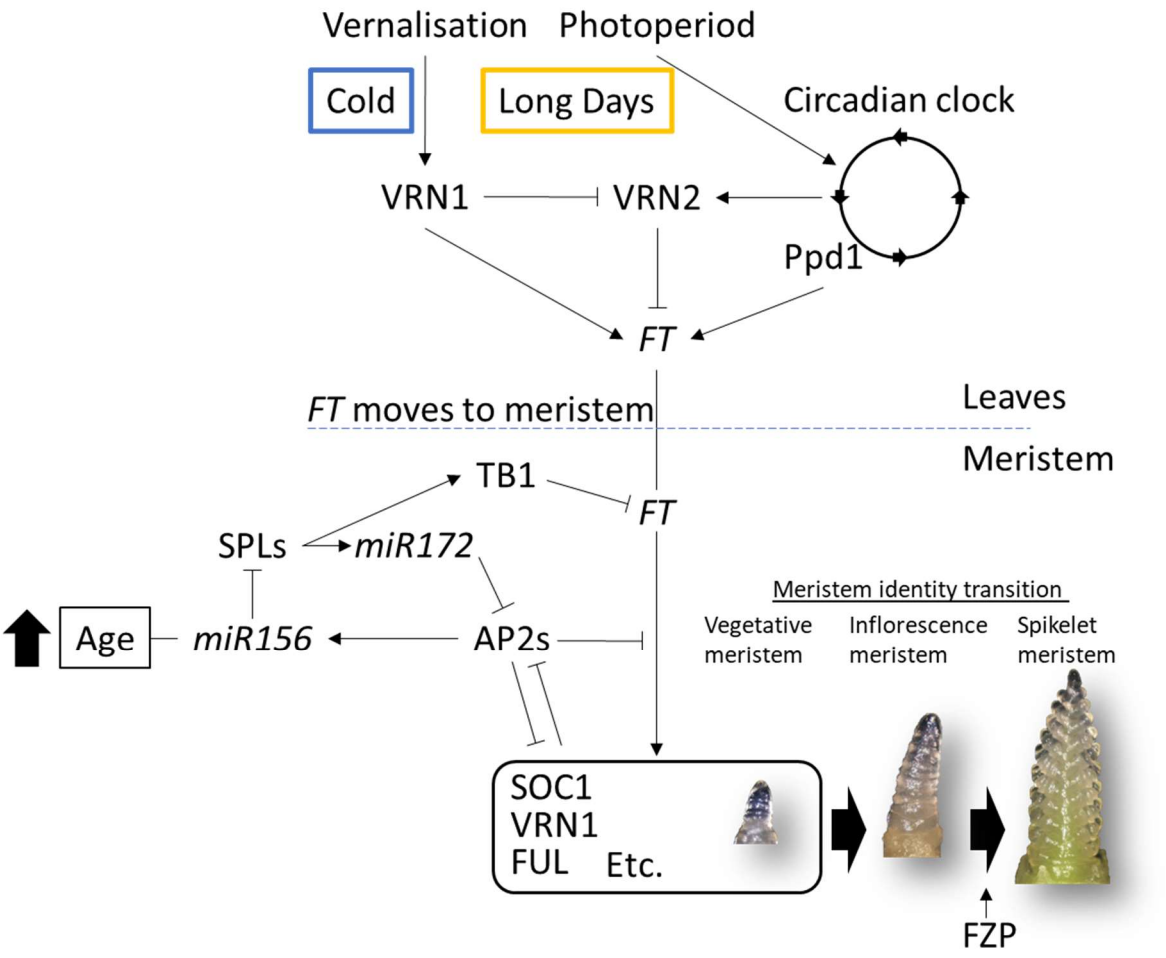

Figure 34 General floral regulatory pathway in temperate wheat. This general model of floral transition and regulation of inflorescence development is based on a number of reviews and research articles spanning Arabidopsis and major grass species. Upregulation of FT expression after exposure to cold and growth in long days leads to promotion of floral meristem identity genes and inflorescence development in the SAM. Low doses of FT delay this process or are non-florally inductive. Floral meristem identity genes and the floral promoting effects of FT are antagonised by TB1 and AP2s. TB1 and AP2s are regulated by complex genetic networks to ensure correct floral development. Besides influencing meristem transition, TB1 and AP2s also influence meristem identity and/or floral patterning determining where specific floral structures form within the inflorescence. FZP and genes which promote spikelet meristem identity are required to promote the formation of spikelets rather than inflorescence/rachis branches. (Krogan et al., 2012, Jung et al., 2014, Yant et al., 2010, Tao et al., 2012, Huang et al., 2016, Greenup et al., 2009, Komatsu et al., 2003, Lu et al., 2013, Liu et al., 2017).

Altering inflorescence architecture

Besides comprising a complex and interesting developmental pathway, the genes we have described in this thesis and those presented in **Figure 34** all present molecular targets for altering inflorescence architecture in wheat and thus altering yield potential. The yield potential, or the number of grain producing units is a critical component in determining wheat yield. Delaying flowering time and increasing rachis branching would result in an elaborate wheat spike with high yield potential (Poursarebani et al., 2015, Boden et al., 2015). Whether the plant could capitalise on such an increase in yield potential will require experimental validation under field conditions.

Inflorescence architecture and yield potential

During domestication and through the continued selection for higher yielding crops many genes influencing floral transition have been altered to generate plants which flower in a predictable manner (Meyer and Purugganan, 2013). For example, Australian spring wheat is early flowering so grain can be set before a water limited, dry, hot, summer (Richards et al., 2014). Early flowering limits yield potential by reducing the number of grain producing units developed. However, when conditions only allow for a reduced number of grain to be set, yield potential must be reduced accordingly. Flowering time typically influences the total number of grain producing units, but also the number of vegetative tissues including leaves and tillers (Miralles and Richards, 2000). Leaves represent a major source of carbon fixation and tillers determine the total number of spikes per plant. Thus, the transition to and rate of inflorescence development is an essential determinant of yield potential by defining the overall architecture of the plant as well as the number of grain producing units per spike.

Modifying genes which determine the architecture and rate of inflorescence development downstream of *FT* may present a way of uncoupling inflorescence and

vegetative development as the effects of some of these genes may influence inflorescence architecture without modifying vegetative structures (Miralles and Richards, 2000). Uncoupling vegetative and inflorescence development is one potential avenue for manipulating source and sink ratios to maximise yield potential. Modifications to pathways involved in environmental sensing or early in the floral transition pathway on the other hand like the well described *Ppd-1* and *FT*, will modulate both vegetative and inflorescence development.

Whether yield potential is modified through whole plant developmental changes or through the uncoupling of vegetative and inflorescence development, will increasing the number of grain producing units in the inflorescence necessarily lead to yield improvements? The simple answer is, no, at least not large changes, even though it is possible to greatly increase yield potential by modifying inflorescence architecture. Subtle modifications to flowering time to better suit wheat varieties to particular growing environments may prove more successful in maximising yield.

Although the focus of this thesis has been inflorescence development and we have not explored yield measurements in field conditions, it has become clear that increasing the number of floral units in the inflorescence may not be an effective means for increasing yield. In every instance where we have increased grain number e.g. in late flowering mutants of wheat, paired spikelet producing lines or the branched spike mutants of *Brachypodium*, the increase in grain number was typically associated with a reduction in grain size. This type of trade off makes a lot of sense, if the capacity of the plant to fill grain is not increased with grain number then yield must stagnate. The plant may need more photosynthetic capacity, more nitrogen, phosphorus, more water, deeper roots or a longer growing season to be able to add bulk to the increased grain number. Larger inflorescences alone are unlikely to produce significant yield increases under current cropping systems, but potentially combined with changes in farming practices or

altered molecular pathways to improve assimilate availability to the spike, the capacity for grain filling of high yield potential crops can be improved.

Closing statement

Inflorescence architecture is determined by the strength of floral promoting signals which drive the transition from meristems which produce vegetative tissues to those that produce floral tissues. Importantly, these floral promoting signals influence the rate of inflorescence development which ultimately changes the number of grain producing units that are defined. Fast rates of inflorescence development generally result in simpler inflorescence structures with fewer grain producing units while slow rates of inflorescence development result in more elaborate inflorescence types. Variation in the genes which drive floral transition or determine meristem identity in wheat can alter the archetypal single rachis inflorescence to one that produces additional rachis branches, unique structures called spikelet pairs and increase the total number of grain bearing spikelets. Genes governing inflorescence development are important targets for maximising yield potential in the grass crops.

References

Abe, M., Kobayashi, Y., Yamamoto, S., Daimon, Y., Yamaguchi, A., Ikeda, Y., Ichinoki, H., Notaguchi, M., Goto, K. & Araki, T. 2005. FD, a bZIP protein mediating signals from the floral pathway integrator FT at the shoot apex. *Science,* **309,** 1052-1056.

Achard, P. & Genschik, P. 2009. Releasing the brakes of plant growth: how GAs shutdown DELLA proteins. *J Exp Bot,* **60,** 1085-92.

Ahmad, M. & Sorrells, M. E. 2002. Distribution of microsatellite alleles linked to Rht8 dwarfing gene in wheat. *Euphytica,* **123,** 235-240.

Alonso-Peral, M. M., Oliver, S. N., Casao, M. C., Greenup, A. A. & Trevaskis, B. 2011. The Promoter of the Cereal VERNALIZATION1 Gene Is Sufficient for Transcriptional Induction by Prolonged Cold. *Plos One,* **6**.

Alvarez-Buylla, E. R., García-Ponce, B. & Garay-Arroyo, A. 2006. Unique and redundant functional domains of APETALA1 and CAULIFLOWER, two recently duplicated Arabidopsis thaliana floral MADS-box genes. *Journal of Experimental Botany,* **57,** 3099-3107.

Ashikari, M., Sasaki, A., Ueguchi-Tanaka, M., Itoh, H., Nishimura, A., Datta, S., Ishiyama, K., Saito, T., Kobayashi, M., Khush, G. S., Kitano, H. & Matsuoka, M. 2002. Loss-of-function of a rice gibberellin biosynthetic gene, GA20 oxidase (GA20ox-2), led to the rice 'green revolution'. *Breeding Science,* **52,** 143-150.

Aukerman, M. J. & Sakai, H. 2003. Regulation of flowering time and floral organ identity by a MicroRNA and its APETALA2-like target genes. *Plant Cell,* **15,** 2730-41.

Bai, G. H., Das, M. K., Carver, B. F., Xu, X. Y. & Krenzer, E. G. 2004. Covariation for microsatellite marker alleles associated with Rht8 and coleoptile length in winter wheat. *Crop Science,* **44,** 1187-1194.

Bandillo, N., Raghavan, C., Muyco, P. A., Sevilla, M. A., Lobina, I. T., Dilla-Ermita, C. J., Tung, C. W., McCouch, S., Thomson, M., Mauleon, R., Singh, R. K., Gregorio, G., Redona, E. & Leung, H. 2013. Multi-parent advanced generation inter-cross (MAGIC) populations in rice: progress and potential for genetics research and breeding. *Rice (N Y),* **6,** 11.

Barton, M. K. 2010. Twenty years on: the inner workings of the shoot apical meristem, a developmental dynamo. *Dev Biol,* **341,** 95-113.

Bassu, S., Asseng, S. & Richards, R. 2011. Yield benefits of triticale traits for wheat under current and future climates. *Field Crops Research,* **124,** 14-24.

Beales, J., Turner, A., Griffiths, S., Snape, J. W. & Laurie, D. A. 2007. A Pseudo-Response Regulator is misexpressed in the photoperiod insensitive Ppd-D1a mutant of wheat (Triticum aestivum L.). *Theoretical and Applied Genetics,* **115,** 721-733.

Bentley, A. R., Turner, A. S., Gosman, N., Leigh, F. J., Maccaferri, M., Dreisigacker, S., Greenland, A. & Laurie, D. A. 2011. Frequency of photoperiod-insensitive Ppd-A1a alleles in tetraploid, hexaploid and synthetic hexaploid wheat germplasm. *Plant Breeding,* **130,** 10-15.

Boden, S. A., Cavanagh, C., Cullis, B. R., Ramm, K., Greenwood, J., Jean Finnegan, E., Trevaskis, B. & Swain, S. M. 2015. Ppd-1 is a key regulator of inflorescence architecture and paired spikelet development in wheat. *Nature Plants,* **1,** 14016.

Bommert, P., Je, B. I., Goldshmidt, A. & Jackson, D. 2013a. The maize Galpha gene COMPACT PLANT2 functions in CLAVATA signalling to control shoot meristem size. *Nature,* **502,** 555-8.

Bommert, P., Lunde, C., Nardmann, J., Vollbrecht, E., Running, M., Jackson, D., Hake, S. & Werr, W. 2005a. thick tassel dwarf1 encodes a putative maize ortholog of the Arabidopsis CLAVATA1 leucine-rich repeat receptor-like kinase. *Development,* **132,** 1235-45.

Bommert, P., Nagasawa, N. S. & Jackson, D. 2013b. Quantitative variation in maize kernel row number is controlled by the FASCIATED EAR2 locus. *Nat Genet,* **45,** 334-7.

Bommert, P., Satoh-Nagasawa, N., Jackson, D. & Hirano, H. Y. 2005b. Genetics and evolution of inflorescence and flower development in grasses. *Plant and Cell Physiology,* **46,** 69-78.

Bonnin, I., Rousset, M., Madur, D., Sourdille, P., Dupuits, C., Brunel, D. & Goldringer, I. 2008. FT genome A and D polymorphisms are associated with the variation of earliness components in hexaploid wheat. *Theoretical and Applied Genetics,* **116,** 383-394.

Bortiri, E., Chuck, G., Vollbrecht, E., Rocheford, T., Martienssen, R. & Hake, S. 2006. ramosa2 encodes a LATERAL ORGAN BOUNDARY domain protein that determines the fate of stem cells in branch meristems of maize. *Plant Cell,* **18,** 574-85.

Bortiri, E. & Hake, S. 2007. Flowering and determinacy in maize. *Journal of Experimental Botany,* **58,** 909-916.

Brown, R. H. & Bregitzer, P. 2011. A Ds insertional mutant of a barley miR172 gene results in indeterminate spikelet development. *Crop Science,* **51,** 1664-1672.

Casao, M. C., Igartua, E., Karsai, I., Lasa, J. M., Gracia, M. P. & Casas, A. M. 2011. Expression analysis of vernalization and day-length response genes in barley (Hordeum vulgare L.) indicates that VRNH2 is a repressor of PPDH2 (HvFT3) under long days. *J Exp Bot,* **62,** 1939-49.

Chandler, P. M. & Harding, C. A. 2013. 'Overgrowth' mutants in barley and wheat: new alleles and phenotypes of the 'Green Revolution' Della gene. *Journal of Experimental Botany,* **64,** 1603-1613.

Chandler, P. M. & Robertson, M. 1999. Gibberellin dose-response curves and the characterization of dwarf mutants of barley. *Plant Physiol,* **120,** 623-32.

Chen, A. & Dubcovsky, J. 2012. Wheat TILLING mutants show that the vernalization gene VRN1 down-regulates the flowering repressor VRN2 in leaves but is not essential for flowering. *PLoS Genet,* **8,** e1003134.

Chen, A., Li, C. X., Hu, W., Lau, M. Y., Lin, H. Q., Rockwell, N. C., Martin, S. S., Jernstedt, J. A., Lagarias, J. C. & Dubcovsky, J. 2014. PHYTOCHROME C plays a major role in the acceleration of wheat flowering under long-day photoperiod. *Proceedings of the National Academy of Sciences of the United States of America,* **111,** 10037-10044.

Chen, X. 2008. MicroRNA metabolism in plants. *Curr Top Microbiol Immunol,* **320,** 117-36.

Chu, T., Xie, H., Xu, Y. & Ma, R. 2010. Regulation pattern of the FRUITFULL (FUL) gene of Arabidopsis thaliana. *Shengwu Gongcheng Xuebao/Chinese Journal of Biotechnology,* **26,** 1546-1554.

Chuck, G., Meeley, R. & Hake, S. 2008. Floral meristem initiation and meristem cell fate are regulated by the maize AP2 genes ids1 and sid1. *Development,* **135,** 3013-9.

Chuck, G., Meeley, R., Irish, E., Sakai, H. & Hake, S. 2007. The maize tasselseed4 microRNA controls sex determination and meristem cell fate by targeting Tasselseed6/indeterminate spikelet1. *Nat Genet,* **39,** 1517-21.

Chuck, G., Muszynski, M., Kellogg, E., Hake, S. & Schmidt, R. J. 2002. The control of spikelet meristem identity by the branched silkless1 gene in maize. *Science,* **298,** 1238-1241.

Ciaffi, M., Paolacci, A. R., Tanzarella, O. A. & Porceddu, E. 2011. Molecular aspects of flower development in grasses. *Sex Plant Reprod,* **24,** 247-82.

Corbesier, L., Vincent, C., Jang, S., Fornara, F., Fan, Q., Searle, I., Giakountis, A., Farrona, S., Gissot, L., Turnbull, C. & Coupland, G. 2007. FT protein movement contributes to long-distance signaling in floral induction of Arabidopsis. *Science,* **316,** 1030-1033.

Debernardi, J. M., Lin, H. Q., Chuck, G., Faris, J. D. & Dubcovsky, J. 2017. microRNA172 plays a crucial role in wheat spike morphogenesis and grain threshability. *Development,* **144,** 1966-1975.

Derbyshire, P. & Byrne, M. E. 2013. MORE SPIKELETS1 is required for spikelet fate in the inflorescence of Brachypodium. *Plant Physiol,* **161,** 1291-302.

Díaz, A., Zikhali, M., Turner, A. S., Isaac, P. & Laurie, D. A. 2012. Copy number variation affecting the photoperiod-B1 and vernalization-A1 genes is associated with altered flowering time in wheat (Triticum aestivum). *PLoS ONE,* **7**.

Distelfeld, A., Li, C. & Dubcovsky, J. 2009. Regulation of flowering in temperate cereals. *Current Opinion in Plant Biology,* **12,** 178-184.

Dobrovolskaya, O., Pont, C., Sibout, R., Martinek, P., Badaeva, E., Murat, F., Chosson, A., Watanabe, N., Prat, E., Gautier, N., Gautier, V., Poncet, C., Orlov, Y. L., Krasnikov, A. A., Berges, H., Salina, E., Laikova, L. & Salse, J. 2015. FRIZZY PANICLE Drives Supernumerary Spikelets in Bread Wheat. *Plant Physiology,* **167,** 189-199.

Doebley, J., Stec, A. & Gustus, C. 1995. Teosinte Branched1 and the Origin of Maize - Evidence for Epistasis and the Evolution of Dominance. *Genetics,* **141,** 333-346.

Doebley, J., Stec, A. & Hubbard, L. 1997. The evolution of apical dominance in maize. *Nature,* **386,** 485-488.

Doust, A. N. 2007. Grass architecture: genetic and environmental control of branching. *Current Opinion in Plant Biology,* **10,** 21-25.

Echeverry-Solarte, M., Kumar, A., Kianian, S., Mantovani, E. E., Simsek, S., Alamri, M. S. & Mergoum, M. 2014. Genome-Wide Genetic Dissection of Supernumerary Spikelet and Related Traits in Common Wheat. *The Plant Genome,* **7,** 0.

FAOSTAT. 2014. *FAOSTAT* [Online]. Food and Agriculture Organization of the United Nations

Available: http://faostat.fao.org/ [Accessed 2014].

Flintham, J. E., Borner, A., Worland, A. J. & Gale, M. D. 1997. Optimizing wheat grain yield: Effects of Rht (gibberellin-insensitive) dwarfing genes. *Journal of Agricultural Science,* **128,** 11-25.

Fornara, F., Pařenicová, L., Falasca, G., Pelucchi, N., Masiero, S., Ciannamea, S., Lopez-Dee, Z., Altamura, M. M., Colombo, L. & Kater, M. M. 2004. Functional characterization of OsMADS18, a member of the AP1/SQUA subfamily of MADS box genes. *Plant Physiology,* **135,** 2207-2219.

Foulkes, M. J., Slafer, G. A., Davies, W. J., Berry, P. M., Sylvester-Bradley, R., Martre, P., Calderini, D. F., Griffiths, S. & Reynolds, M. P. 2011. Raising

yield potential of wheat. III. Optimizing partitioning to grain while maintaining lodging resistance. *Journal of Experimental Botany,* **62,** 469-486.

Gallavotti, A., Long, J. A., Stanfield, S., Yang, X., Jackson, D., Vollbrecht, E. & Schmidt, R. J. 2010. The control of axillary meristem fate in the maize ramosa pathway. *Development,* **137,** 2849-56.

Garbus, I., Romero, J. R., Valarik, M., Vanzurova, H., Karafiatova, M., Caccamo, M., Dolezel, J., Tranquilli, G., Helguera, M. & Echenique, V. 2015. Characterization of repetitive DNA landscape in wheat homeologous group 4 chromosomes. *Bmc Genomics,* **16**.

Gardner, K. A., Wittern, L. M. & Mackay, I. J. 2016. A highly recombined, high-density, eight-founder wheat MAGIC map reveals extensive segregation distortion and genomic locations of introgression segments. *Plant Biotechnology Journal,* **14,** 1406-1417.

Gaut, B. S. 2002. Evolutionary dynamics of grass genomes. *New Phytologist,* **154,** 15-28.

Gororo, N. N., Flood, R. G., Eastwood, R. F. & Eagles, H. A. 2001. Photoperiod and vernalization responses in Triticum turgidum x T. tauschii Synthetic hexaploid wheats. *Annals of Botany,* **88,** 947-952.

Greenup, A., Peacock, W. J., Dennis, E. S. & Trevaskis, B. 2009. The molecular biology of seasonal flowering-responses in Arabidopsis and the cereals. *Annals of Botany,* **103,** 1165-1172.

Greenwood, J. R., Finnegan, E. J., Watanabe, N., Trevaskis, B. & Swain, S. M. 2017. New alleles of the wheat domestication gene Q reveal multiple roles in growth and reproductive development. *Development,* **144,** 1959-1965.

Grigorova, B., Mara, C., Hollender, C., Sijacic, P., Chen, X. & Liu, Z. 2011. LEUNIG and SEUSS co-repressors regulate miR172 expression in Arabidopsis flowers. *Development,* **138,** 2451-6.

Hedden, P. 2003. The genes of the Green Revolution. *Trends in Genetics,* **19,** 5-9.

Houston, K., McKim, S. M., Comadran, J., Bonar, N., Druka, I., Uzrek, N., Cirillo, E., Guzy-Wrobelska, J., Collins, N. C., Halpin, C., Hansson, M., Dockter, C., Druka, A. & Waugh, R. 2013. Variation in the interaction between alleles of HvAPETALA2 and microRNA172 determines the density of grains on the barley inflorescence. *Proc Natl Acad Sci U S A,* **110,** 16675-80.

Hruskova, M. & Svec, I. 2009. Wheat Hardness in Relation to Other Quality Factors. *Czech Journal of Food Sciences,* **27,** 240-248.

Huang, B. E., George, A. W., Forrest, K. L., Kilian, A., Hayden, M. J., Morell, M. K. & Cavanagh, C. R. 2012. A multiparent advanced generation inter-cross population for genetic analysis in wheat. *Plant Biotechnology Journal,* **10,** 826-839.

Huang, X., Wei, X., Sang, T., Zhao, Q., Feng, Q., Zhao, Y., Li, C., Zhu, C., Lu, T., Zhang, Z., Li, M., Fan, D., Guo, Y., Wang, A., Wang, L., Deng, L., Li, W., Lu, Y., Weng, Q., Liu, K., Huang, T., Zhou, T., Jing, Y., Li, W., Lin, Z., Buckler, E. S., Qian, Q., Zhang, Q. F., Li, J. & Han, B. 2010. Genome-wide association studies of 14 agronomic traits in rice landraces. *Nat Genet,* **42,** 961-7.

Huang, Z., Shi, T., Zheng, B., Yumul, R. E., Liu, X., You, C., Gao, Z., Xiao, L. & Chen, X. 2016. APETALA2 antagonizes the transcriptional activity of AGAMOUS in regulating floral stem cells in Arabidopsis thaliana. *New Phytol*.

Hubbard, L., McSteen, P., Doebley, J. & Hake, S. 2002. Expression patterns and mutant phenotype of teosinte branched1 correlate with growth suppression in maize and teosinte. *Genetics,* **162,** 1927-1935.

Huijser, P. & Schmid, M. 2011. The control of developmental phase transitions in plants. *Development,* **138,** 4117-4129.

Ikeda-Kawakatsu, K., Maekawa, M., Izawa, T., Itoh, J. I. & Nagato, Y. 2012. ABERRANT PANICLE ORGANIZATION 2/RFL, the rice ortholog of Arabidopsis LEAFY, suppresses the transition from inflorescence meristem to floral meristem through interaction with APO1. *Plant Journal,* **69,** 168-180.

Itoh, H., Nonoue, Y., Yano, M. & Izawa, T. 2010. A pair of floral regulators sets critical day length for Hd3a florigen expression in rice. *Nature Genetics,* **42,** 635-638.

Jiao, Y., Wang, Y., Xue, D., Wang, J., Yan, M., Liu, G., Dong, G., Zeng, D., Lu, Z., Zhu, X., Qian, Q. & Li, J. 2010. Regulation of OsSPL14 by OsmiR156 defines ideal plant architecture in rice. *Nature Genetics,* **42,** 541-544.

Jung, J. H., Lee, S., Yun, J., Lee, M. & Park, C. M. 2014. The miR172 target TOE3 represses AGAMOUS expression during Arabidopsis floral patterning. *Plant Science,* **215,** 29-38.

Jung, J. H., Seo, P. J., Kang, S. K. & Park, C. M. 2011. miR172 signals are incorporated into the miR156 signaling pathway at the SPL3/4/5 genes in Arabidopsis developmental transitions. *Plant Mol Biol,* **76,** 35-45.

Kato, K., Miura, H., Akiyama, M., Kuroshima, M. & Sawada, S. 1998. RFLP mapping of the three major genes, Vrn1, Q and B1, on the long arm of chromosome 5A of wheat. *Euphytica,* **101,** 91-95.

Kellogg, E. A. 2006. Beyond taxonomy: Prospects for understanding morphological diversity in the grasses (Poaceae). *Darwiniana,* **44,** 7-17.

Kellogg, E. A. 2007. Floral displays: genetic control of grass inflorescences. *Curr Opin Plant Biol,* **10,** 26-31.

Khatodia, S., Bhatotia, K., Passricha, N., Khurana, S. M. & Tuteja, N. 2016. The CRISPR/Cas Genome-Editing Tool: Application in Improvement of Crops. *Front Plant Sci,* **7,** 506.

Kobayashi, K., Maekawa, M., Miyao, A., Hirochika, H. & Kyozuka, J. 2010. PANICLE PHYTOMER2 (PAP2), encoding a SEPALLATA subfamily MADS-box protein, positively controls spikelet meristem identity in rice. *Plant Cell Physiol,* **51,** 47-57.

Kobayashi, K., Yasuno, N., Sato, Y., Yoda, M., Yamazaki, R., Kimizu, M., Yoshida, H., Nagamura, Y. & Kyozuka, J. 2012. Inflorescence meristem identity in rice is specified by overlapping functions of three AP1/FUL-Like MADS box genes and PAP2, a SEPALLATA MADS Box gene. *Plant Cell,* **24,** 1848-59.

Kobayashi, Y., Kaya, H., Goto, K., Iwabuchi, M. & Araki, T. 1999. A pair of related genes with antagonistic roles in mediating flowering signals. *Science,* **286,** 1960-1962.

Komatsu, M., Chujo, A., Nagato, Y., Shimamoto, K. & Kyozuka, J. 2003. Frizzy panicle is required to prevent the formation of axillary meristems and to establish floral meristem identity in rice spikelets. *Development,* **130,** 3841-3850.

Krasileva, K. V., Vasquez-Gross, H. A., Howell, T., Bailey, P., Paraiso, F., Clissold, L., Simmonds, J., Ramirez-Gonzalez, R. H., Wang, X., Borrill, P., Fosker, C., Ayling, S., Phillips, A. L., Uauy, C. & Dubcovsky, J. 2017. Uncovering hidden variation in polyploid wheat. *Proc Natl Acad Sci U S A,* **114,** E913-E921.

Krogan, N. T., Hogan, K. & Long, J. A. 2012. APETALA2 negatively regulates multiple floral organ identity genes in Arabidopsis by recruiting the co-repressor TOPLESS and the histone deacetylase HDA19. *Development,* **139,** 4180-90.

Krogan, N. T. & Long, J. A. 2009. Why so repressed? Turning off transcription during plant growth and development. *Current Opinion in Plant Biology,* **12,** 628-636.
Kyozuka, J., Tokunaga, H. & Yoshida, A. 2014. Control of grass inflorescence form by the fine-tuning of meristem phase change. *Curr Opin Plant Biol,* **17,** 110-5.
Laudencia-Chingcuanco, D. & Hake, S. 2002. The indeterminate floral apex1 gene regulates meristem determinacy and identity in the maize inflorescence. *Development,* **129,** 2629-2638.
Lauter, N., Kampani, A., Carlson, S., Goebel, M. & Moose, S. P. 2005. microRNA172 down-regulates glossy15 to promote vegetative phase change in maize. *Proceedings of the National Academy of Sciences of the United States of America,* **102,** 9412-9417.
Lawrence, R. J. & Pikaard, C. S. 2003. Transgene-induced RNA interference: a strategy for overcoming gene redundancy in polyploids to generate loss-of-function mutations. *Plant Journal,* **36,** 114-121.
Lee, D. Y. & An, G. 2012. Two AP2 family genes, supernumerary bract (SNB) and Osindeterminate spikelet 1 (OsIDS1), synergistically control inflorescence architecture and floral meristem establishment in rice. *Plant J,* **69,** 445-61.
Lee, D. Y., Lee, J., Moon, S., Park, S. Y. & An, G. 2007. The rice heterochronic gene SUPERNUMERARY BRACT regulates the transition from spikelet meristem to floral meristem. *Plant J,* **49,** 64-78.
Lee, Y. S., Lee, D. Y., Cho, L. H. & An, G. 2014. Rice miR172 induces flowering by suppressing OsIDS1 and SNB, two AP2 genes that negatively regulate expression of Ehd1 and florigens. *Rice,* **7**.
Lewis, J. M., Mackintosh, C. A., Shin, S., Gilding, E., Kravchenko, S., Baldridge, G., Zeyen, R. & Muehlbauer, G. J. 2008. Overexpression of the maize Teosinte Branched1 gene in wheat suppresses tiller development. *Plant Cell Reports,* **27,** 1217-1225.
Li, C. & Dubcovsky, J. 2008. Wheat FT protein regulates VRN1 transcription through interactions with FDL2. *Plant J,* **55,** 543-54.
Liu, J., Cheng, X., Liu, P. & Sun, J. 2017. miR156-Targeted SBP-Box Transcription Factors Interact with DWARF53 to Regulate TEOSINTE BRANCHED1 and BARREN STALK1 Expression in Bread Wheat. *Plant Physiol,* **174,** 1931-1948.
Lu, Z. F., Yu, H., Xiong, G. S., Wang, J., Jiao, Y. Q., Liu, G. F., Jing, Y. H., Meng, X. B., Hu, X. M., Qian, Q., Fu, X. D., Wang, Y. H. & Li, J. Y. 2013. Genome-Wide Binding Analysis of the Transcription Activator IDEAL PLANT ARCHITECTURE1 Reveals a Complex Network Regulating Rice Plant Architecture. *Plant Cell,* **25,** 3743-3759.
Lucas, S. J., Akpinar, B. A., Simkova, H., Kubalakova, M., Dolezel, J. & Budak, H. 2014. Next-generation sequencing of flow-sorted wheat chromosome 5D reveals lineage-specific translocations and widespread gene duplications. *Bmc Genomics,* **15**.
Lv, B., Nitcher, R., Han, X. L., Wang, S. Y., Ni, F., Li, K., Pearce, S., Wu, J. J., Dubcovsky, J. & Fu, D. L. 2014. Characterization of FLOWERING LOCUS T1 (FT1) Gene in Brachypodium and Wheat. *Plos One,* **9**.
Mackay, I. J., Bansept-Basler, P., Barber, T., Bentley, A. R., Cockram, J., Gosman, N., Greenland, A. J., Horsnell, R., Howells, R., O'Sullivan, D. M., Rose, G. A. & Howell, P. J. 2014. An Eight-Parent Multiparent Advanced Generation Inter-Cross Population for Winter-Sown Wheat: Creation, Properties, and Validation. *G3-Genes Genomes Genetics,* **4,** 1603-1610.
McSteen, P. & Hake, S. 2001. barren inflorescence2 regulates axillary meristem development in the maize inflorescence. *Development,* **128,** 2881-2891.

Meyer, R. S. & Purugganan, M. D. 2013. Evolution of crop species: genetics of domestication and diversification. *Nature Reviews Genetics,* **14,** 840-852.

Miralles, D. J. & Richards, R. A. 2000. Responses of leaf and tiller emergence and primordium initiation in wheat and barley to interchanged photoperiod. *Annals of Botany,* **85,** 655-663.

Mlotshwa, S., Yang, Z., Kim, Y. & Chen, X. 2006. Floral patterning defects induced by Arabidopsis APETALA2 and microRNA172 expression in Nicotiana benthamiana. *Plant Mol Biol,* **61,** 781-93.

Mockler, T., Yang, H. Y., Yu, X. H., Parikh, D., Cheng, Y. C., Dolan, S. & Lin, C. T. 2003. Regulation of photoperiodic flowering by Arabidopsis photoreceptors. *Proceedings of the National Academy of Sciences of the United States of America,* **100,** 2140-2145.

Moore, K. J. & Moser, L. E. 1995. Quantifying Developmental Morphology of Perennial Grasses. *Crop Science,* **35,** 37-43.

Murai, K., Miyamae, M., Kato, H., Takumi, S. & Ogihara, Y. 2003. WAP1, a wheat APETALA1 homolog, plays a central role in the phase transition from vegetative to reproductive growth. *Plant Cell Physiol,* **44,** 1255-65.

Nair, S. K., Wang, N., Turuspekov, Y., Pourkheirandish, M., Sinsuwongwat, S., Chen, G., Sameri, M., Tagiri, A., Honda, I., Watanabe, Y., Kanamori, H., Wicker, T., Stein, N., Nagamura, Y., Matsumoto, T. & Komatsuda, T. 2010. Cleistogamous flowering in barley arises from the suppression of microRNA-guided HvAP2 mRNA cleavage. *Proc Natl Acad Sci U S A,* **107,** 490-5.

Ning, S., Wang, N., Sakuma, S., Pourkheirandish, M., Wu, J., Matsumoto, T., Koba, T. & Komatsuda, T. 2013. Structure, transcription and post-transcriptional regulation of the bread wheat orthologs of the barley cleistogamy gene Cly1. *Theor Appl Genet,* **126,** 1273-83.

Niwa, M., Daimon, Y., Kurotani, K., Higo, A., Pruneda-Paz, J. L., Breton, G., Mitsuda, N., Kay, S. A., Ohme-Takagi, M., Endo, M. & Araki, T. 2013. BRANCHED1 interacts with FLOWERING LOCUS T to repress the floral transition of the axillary meristems in Arabidopsis. *Plant Cell,* **25,** 1228-42.

Pautler, M., Tanaka, W., Hirano, H. Y. & Jackson, D. 2013. Grass meristems I: shoot apical meristem maintenance, axillary meristem determinacy and the floral transition. *Plant Cell Physiol,* **54,** 302-12.

Pearce, S., Saville, R., Vaughan, S. P., Chandler, P. M., Wilhelm, E. P., Sparks, C. A., Al-Kaff, N., Korolev, A., Boulton, M. I., Phillips, A. L., Hedden, P., Nicholson, P. & Thomas, S. G. 2011. Molecular Characterization of Rht-1 Dwarfing Genes in Hexaploid Wheat. *Plant Physiology,* **157,** 1820-1831.

Perreta, M. G., Ramos, J. C. & Vegetti, A. C. 2009. Development and Structure of the Grass Inflorescence. *The Botanical Review,* **75,** 377-396.

Pinthus, M. J. & Levy, A. A. 1983. The relationship between the Rht 1 and Rht 2 dwarfing genes and grain weight in Triticum aestivum L. spring wheat. *Theor Appl Genet,* **66,** 153-7.

Poursarebani, N., Seidensticker, T., Koppolu, R., Trautewig, C., Gawronski, P., Bini, F., Govind, G., Rutten, T., Sakuma, S., Tagiri, A., Wolde, G. M., Youssef, H. M., Battal, A., Ciannamea, S., Fusca, T., Nussbaumer, T., Pozzi, C., Borner, A., Lundqvist, U., Komatsuda, T., Salvi, S., Tuberosa, R., Uauy, C., Sreenivasulu, N., Rossini, L. & Schnurbusch, T. 2015. The Genetic Basis of Composite Spike Form in Barley and 'Miracle-Wheat'. *Genetics,* **201,** 155-65.

Preston, J. C. & Kellogg, E. A. 2007. Conservation and divergence of APETALA1/FRUITFULL-like gene function in grasses: Evidence from gene expression analyses. *Plant Journal,* **52,** 69-81.

Rahman, M., Wilson, J. & Aitken, Y. 1977. Determination of Spikelet Number in Wheat. *Australian Journal of Agriculture,* **28,** 575-581.

Rahman, M. S. & Wilson, J. H. 1977. Determination of Spikelet Number in Wheat .1. Effect of Varying Photoperiod on Ear Development. *Australian Journal of Agricultural Research,* **28,** 565-574.

Rahman, M. S. & Wilson, J. H. 1978. Determination of Spikelet Number in Wheat .3. Effect of Varying Temperature on Ear Development. *Australian Journal of Agricultural Research,* **29,** 459-467.

Ramirez-Gonzalez, R. H., Segovia, V., Bird, N., Fenwick, P., Holdgate, S., Berry, S., Jack, P., Caccamo, M. & Uauy, C. 2015. RNA-Seq bulked segregant analysis enables the identification of high-resolution genetic markers for breeding in hexaploid wheat. *Plant Biotechnology Journal,* **13,** 613-624.

Ramsay, L., Comadran, J., Druka, A., Marshall, D. F., Thomas, W. T., Macaulay, M., MacKenzie, K., Simpson, C., Fuller, J., Bonar, N., Hayes, P. M., Lundqvist, U., Franckowiak, J. D., Close, T. J., Muehlbauer, G. J. & Waugh, R. 2011. INTERMEDIUM-C, a modifier of lateral spikelet fertility in barley, is an ortholog of the maize domestication gene TEOSINTE BRANCHED 1. *Nat Genet,* **43,** 169-72.

Ream, T. S., Woods, D. P., Schwartz, C. J., Sanabria, C. P., Mahoy, J. A., Walters, E. M., Kaeppler, H. F. & Amasino, R. M. 2014. Interaction of photoperiod and vernalization determines flowering time of Brachypodium distachyon. *Plant Physiol,* **164,** 694-709.

Richards, R. A., Hunt, J. R., Kirkegaard, J. A. & Passioura, J. B. 2014. Yield improvement and adaptation of wheat to water-limited environments in Australia-a case study. *Crop & Pasture Science,* **65,** 676-689.

Richardson, T., Thistleton, J., Higgins, T. J., Howitt, C. & Ayliffe, M. 2014. Efficient Agrobacterium transformation of elite wheat germplasm without selection. *Plant Cell Tissue and Organ Culture,* **119,** 647-659.

Robert, C. & Watson, M. 2015. Errors in RNA-Seq quantification affect genes of relevance to human disease. *Genome Biology,* **16**.

Saintenac, C., Jiang, D. Y. & Akhunov, E. D. 2011. Targeted analysis of nucleotide and copy number variation by exon capture in allotetraploid wheat genome. *Genome Biology,* **12**.

Salse, J., Bolot, S., Throude, M., Jouffe, V., Piegu, B., Quraishi, U. M., Calcagno, T., Cooke, R., Delseny, M. & Feuillet, C. 2008. Identification and characterization of shared duplications between rice and wheat provide new insight into grass genome evolution. *Plant Cell,* **20,** 11-24.

Sanchez-Martin, J., Steuernagel, B., Ghosh, S., Herren, G., Hurni, S., Adamski, N., Vrana, J., Kubalakova, M., Krattinger, S. G., Wicker, T., Dolezel, J., Keller, B. & Wulff, B. B. 2016. Rapid gene isolation in barley and wheat by mutant chromosome sequencing. *Genome Biol,* **17,** 221.

Satoh-Nagasawa, N., Nagasawa, N., Malcomber, S., Sakai, H. & Jackson, D. 2006. A trehalose metabolic enzyme controls inflorescence architecture in maize. *Nature,* **441,** 227-230.

Sauer, M. & Friml, J. 2010. Immunolocalization of proteins in plants. *Methods Mol Biol,* **655,** 253-63.

Schmid, M., Uhlenhaut, N. H., Godard, F., Demar, M., Bressan, R., Weigel, D. & Lohmann, J. U. 2003. Dissection of floral induction pathways using global expression analysis. *Development,* **130,** 6001-12.

Shaw, L. M., Turner, A. S. & Laurie, D. A. 2012. The impact of photoperiod insensitive Ppd-1a mutations on the photoperiod pathway across the three genomes of hexaploid wheat (Triticum aestivum). *Plant Journal,* **71,** 71-84.

Shimada, S., Ogawa, T., Kitagawa, S., Suzuki, T., Ikari, C., Shitsukawa, N., Abe, T., Kawahigashi, H., Kikuchi, R., Handa, H. & Murai, K. 2009. A genetic network of flowering-time genes in wheat leaves, in which an APETALA1/FRUITFULL-like gene, VRN1, is upstream of FLOWERING LOCUS T. *Plant Journal,* **58,** 668-681.

Slafer, G. A. 2003. Genetic basis of yield as viewed from a crop physiologist's perspective. *Annals of Applied Biology,* **142,** 117-128.

Spanudakis, E. & Jackson, S. 2014. The role of microRNAs in the control of flowering time. *Journal of Experimental Botany,* **65,** 365-380.

Steuernage, B., Periyannan, S. K., Hernandez-Pinzon, I., Witek, K., Rouse, M. N., Yu, G. T., Hatta, A., Ayliffe, M., Bariana, H., Jones, J. D. G., Lagudah, E. S. & Wulff, B. B. H. 2016. Rapid cloning of disease-resistance genes in plants using mutagenesis and sequence capture. *Nature Biotechnology,* **34,** 652-655.

Sukumaran, S., Dreisigacker, S., Lopes, M., Chavez, P. & Reynolds, M. P. 2015. Genome-wide association study for grain yield and related traits in an elite spring wheat population grown in temperate irrigated environments. *Theoretical and Applied Genetics,* **128,** 353-363.

Sun, C., Zhang, F., Yan, X., Zhang, X., Dong, Z., Cui, D. & Chen, F. 2017. Genome-wide association study for 13 agronomic traits reveals distribution of superior alleles in bread wheat from the Yellow and Huai Valley of China. *Plant Biotechnol J.*

Takeda, T., Suwa, Y., Suzuki, M., Kitano, H., Ueguchi-Tanaka, M., Ashikari, M., Matsuoka, M. & Ueguchi, C. 2003. The OsTB1 gene negatively regulates lateral branching in rice. *Plant Journal,* **33,** 513-520.

Tanaka, W., Pautler, M., Jackson, D. & Hirano, H. Y. 2013. Grass meristems II: inflorescence architecture, flower development and meristem fate. *Plant Cell Physiol,* **54,** 313-24.

Tao, Z., Shen, L. S., Liu, C., Liu, L., Yan, Y. Y. & Yu, H. 2012. Genome-wide identification of SOC1 and SVP targets during the floral transition in Arabidopsis. *Plant Journal,* **70,** 549-561.

Thompson, C. J., Movva, N. R., Tizard, R., Crameri, R., Davies, J. E., Lauwereys, M. & Botterman, J. 1987. Characterization of the Herbicide-Resistance Gene Bar from Streptomyces-Hygroscopicus. *Embo Journal,* **6,** 2519-2523.

Trevaskis, B. 2010. Goldacre Paper: The central role of the VERNALIZATION1 gene in the vernalization response of cereals. *Functional Plant Biology,* **37,** 479-487.

Trevaskis, B., Hemming, M. N., Dennis, E. S. & Peacock, W. J. 2007. The molecular basis of vernalization-induced flowering in cereals. *Trends Plant Sci,* **12,** 352-7.

Trick, M., Adamski, N. M., Mugford, S. G., Jiang, C. C., Febrer, M. & Uauy, C. 2012. Combining SNP discovery from next-generation sequencing data with bulked segregant analysis (BSA) to fine-map genes in polyploid wheat. *Bmc Plant Biology,* **12**.

Turck, F., Fornara, F. & Coupland, G. 2008. Regulation and identity of florigen: Flowering Locus T moves center stage.

Uauy, C., Paraiso, F., Colasuonno, P., Tran, R. K., Tsai, H., Berardi, S., Comai, L. & Dubcovsky, J. 2009. A modified TILLING approach to detect induced mutations in tetraploid and hexaploid wheat. *Bmc Plant Biology,* **9**.

Ugarte, C. C., Trupkin, S. A., Ghiglione, H., Slafer, G. & Casal, J. J. 2010. Low red/far-red ratios delay spike and stem growth in wheat. *Journal of Experimental Botany,* **61,** 3151-3162.

Varkonyi-Gasic, E., Lough, R. H., Moss, S. M. A., Wu, R. & Hellens, R. P. 2012. Kiwifruit floral gene APETALA2 is alternatively spliced and accumulates in

aberrant indeterminate flowers in the absence of miR172. *Plant Molecular Biology,* **78,** 417-429.

Verma, V., Worland, A. J., Sayers, E. J., Fish, L., Caligari, P. D. S. & Snape, J. W. 2005. Identification and characterization of quantitative trait loci related to lodging resistance and associated traits in bread wheat. *Plant Breeding,* **124,** 234-241.

Vollbrecht, E., Springer, P. S., Goh, L., Buckler, E. S. t. & Martienssen, R. 2005. Architecture of floral branch systems in maize and related grasses. *Nature,* **436,** 1119-26.

Wang, L., Sun, S. Y., Jin, J. Y., Fu, D. B., Yang, X. F., Weng, X. Y., Xu, C. G., Li, X. H., Xiao, J. H. & Zhang, Q. F. 2015. Coordinated regulation of vegetative and reproductive branching in rice. *Proceedings of the National Academy of Sciences of the United States of America,* **112,** 15504-15509.

Wang, Y. P., Cheng, X., Shan, Q. W., Zhang, Y., Liu, J. X., Gao, C. X. & Qiu, J. L. 2014. Simultaneous editing of three homoeoalleles in hexaploid bread wheat confers heritable resistance to powdery mildew. *Nature Biotechnology,* **32,** 947-951.

Wigge, P. A., Kim, M. C., Jaeger, K. E., Busch, W., Schmid, M., Lohmann, J. U. & Weigel, D. 2005. Integration of spatial and temporal information during floral induction in Arabidopsis. *Science,* **309,** 1056-1059.

Wilhelm, E. P., Turner, A. S. & Laurie, D. A. 2009. Photoperiod insensitive Ppd-A1a mutations in tetraploid wheat (Triticum durum Desf.). *Theoretical and Applied Genetics,* **118,** 285-294.

Wu, G., Park, M. Y., Conway, S. R., Wang, J. W., Weigel, D. & Poethig, R. S. 2009. The sequential action of miR156 and miR172 regulates developmental timing in Arabidopsis. *Cell,* **138,** 750-9.

Wu, S. W., Xiao, Y., Zheng, X., Cai, Y. F., Dolezel, J., Liu, B. H., Yang, L., Song, M. F., Zhou, P., Zhou, Y., Meng, F. H., Wang, S. H., Liu, H. W., Zhai, H. Q. & Yang, J. P. 2010. Chromosome sorting and its applications in common wheat (Triticum aestivum) genome sequencing. *Chinese Science Bulletin,* **55,** 1463-1468.

Yan, L., Helguera, M., Kato, K., Fukuyama, S., Sherman, J. & Dubcovsky, J. 2004. Allelic variation at the VRN-1 promoter region in polyploid wheat. *Theoretical and Applied Genetics,* **109,** 1677-1686.

Yan, L., Loukoianov, A., Tranquilli, G., Helguera, M., Fahima, T. & Dubcovsky, J. 2003. Positional cloning of the wheat vernalization gene VRN1. *Proceedings of the National Academy of Sciences of the United States of America,* **100,** 6263-6268.

Yant, L., Mathieu, J., Dinh, T. T., Ott, F., Lanz, C., Wollmann, H., Chen, X. & Schmid, M. 2010. Orchestration of the floral transition and floral development in Arabidopsis by the bifunctional transcription factor APETALA2. *Plant Cell,* **22,** 2156-70.

Yoshida, A., Ohmori, Y., Kitano, H., Taguchi-Shiobara, F. & Hirano, H. Y. 2012. ABERRANT SPIKELET and PANICLE1, encoding a TOPLESS-related transcriptional co-repressor, is involved in the regulation of meristem fate in rice. *Plant Journal,* **70,** 327-339.

Yoshida, A., Sasao, M., Yasuno, N., Takagi, K., Daimon, Y., Chen, R., Yamazaki, R., Tokunaga, H., Kitaguchi, Y., Sato, Y., Nagamura, Y., Ushijima, T., Kumamaru, T., Iida, S., Maekawa, M. & Kyozuka, J. 2013. TAWAWA1, a regulator of rice inflorescence architecture, functions through the suppression of meristem phase transition. *Proc Natl Acad Sci U S A,* **110,** 767-72.

Yoshida, A., Suzaki, T., Tanaka, W. & Hirano, H. Y. 2009. The homeotic gene long sterile lemma (G1) specifies sterile lemma identity in the rice spikelet. *Proc Natl Acad Sci U S A,* **106,** 20103-8.

Yoshioka, M., Iehisa, J. C. M., Ohno, R., Kimura, T., Enoki, H., Nishimura, S., Nasuda, S. & Takumi, S. 2017. Three dominant awnless genes in common wheat: Fine mapping, interaction and contribution to diversity in awn shape and length. *PLoS One,* **12,** e0176148.

Yu, S., Galvao, V. C., Zhang, Y. C., Horrer, D., Zhang, T. Q., Hao, Y. H., Feng, Y. Q., Wang, S., Schmid, M. & Wang, J. W. 2012. Gibberellin Regulates the Arabidopsis Floral Transition through miR156-Targeted SQUAMOSA PROMOTER BINDING-LIKE Transcription Factors. *Plant Cell,* **24,** 3320-3332.

Zhang, B., Pan, X., Cobb, G. P. & Anderson, T. A. 2006. Plant microRNA: a small regulatory molecule with big impact. *Dev Biol,* **289,** 3-16.

Zhang, D. B. & Yuan, Z. 2014. Molecular Control of Grass Inflorescence Development. *Annual Review of Plant Biology, Vol 65,* **65,** 553-+.

Zhao, L., Nakazawa, M., Takase, T., Manabe, K., Kobayashi, M., Seki, M., Shinozaki, K. & Matsui, M. 2004. Overexpression of LSH1, a member of an uncharacterised gene family, causes enhanced light regulation of seedling development. *Plant Journal,* **37,** 694-706.

Zhao, T., Ni, Z., Dai, Y., Yao, Y., Nie, X. & Sun, Q. 2006. Characterization and expression of 42 MADS-box genes in wheat (Triticum aestivum L.). *Mol Genet Genomics,* **276,** 334-50.

Zhu, Q. H., Upadhyaya, N. M., Gubler, F. & Helliwell, C. A. 2009. Over-expression of miR172 causes loss of spikelet determinacy and floral organ abnormalities in rice (Oryza sativa). *BMC Plant Biol,* **9,** 149.

Appendix

nature plants

LETTERS

PUBLISHED: 26 JANUARY 2015 | ARTICLE NUMBER: 14016 | DOI: 10.1038/NPLANTS.2014.16

Ppd-1 is a key regulator of inflorescence architecture and paired spikelet development in wheat

Scott A. Boden[1†], Colin Cavanagh[1†], Brian R. Cullis[2,3], Kerrie Ramm[1], Julian Greenwood[1,4], E. Jean Finnegan[1], Ben Trevaskis[1] and Steve M. Swain[1*]

The domestication of cereal crops such as wheat, maize, rice and barley has included the modification of inflorescence architecture to improve grain yield and ease harvesting[1]. Yield increases have often been achieved through modifying the number and arrangement of spikelets, which are specialized reproductive branches that form part of the inflorescence. Multiple genes that control spikelet development have been identified in maize, rice and barley[2–5]. However, little is known about the genetic underpinnings of this process in wheat. Here, we describe a modified spikelet arrangement in wheat, termed paired spikelets. Combining comprehensive QTL and mutant analyses, we show that *Photoperiod-1* (*Ppd-1*), a pseudo-response regulator gene that controls photoperiod-dependent floral induction, has a major inhibitory effect on paired spikelet formation by regulating the expression of *FLOWERING LOCUS T* (*FT*)[6,7]. These findings show that modulated expression of the two important flowering genes, *Ppd-1* and *FT*, can be used to form a wheat inflorescence with a more elaborate arrangement and increased number of grain producing spikelets.

Grains of the cereal crops wheat, maize and rice are a major source of human nutrition. Continuing population growth and rising competition for arable land are increasing the demand for development of novel ways to improve grain yield per plant. Studies in rice have demonstrated that changes in the number and arrangement of spikelets, which are specialized inflorescence branches that bear grain-producing florets, can increase the plant's yield[3,4]. Modifying the number and arrangement of spikelets on the wheat inflorescence could therefore be a strategy to improve yield potential in this important crop. The architecture of the wheat inflorescence (spike) is relatively simple compared with the branched inflorescences of rice (panicle) and maize (tassel and ear). It is characteristically unbranched and forms single spikelets on opposite sides of the central rachis in an alternating phyllotaxy, with a single terminal spikelet at the distal end of the spike. The spikelets of the wheat spike are indeterminate and typically produce three or four fertile florets, in contrast to the determinate spikelets of rice and maize that bear only one or two florets.

Although the archetypal wheat inflorescence is a relatively simple structure, and a number of variations have been reported[8,9], almost nothing is known about the causal molecular pathways. In general, two types of variation exist, both of which have the potential to produce more spikelets and grains per inflorescence. In the first, spikelets form on the main inflorescence as usual, but one, or more, of the basal spikelets is replaced by long lateral branches, each forming their own spikelets and florets[8,9], reminiscent of the rice panicle or maize tassel. The second broad type of inflorescence branching includes a range of modifications that may or may not be related in developmental terms, which involve the production of two or more spikelets at a single node, without the formation of a long branch. One example of this type of branching, and the focus of this study, is the 'paired spikelet', which is distinct from the 'multirow spikes'[10] and has been referred to as 'banana spikelets', 'twin spikelets' and 'opposite supernumerary spikelets' (Fig. 1a)[8,11]. Paired spikelets are characterized by the formation of a second spikelet immediately adjacent to and directly below (abaxial) a typical single spikelet, similar to the primary and secondary spikelets that form the 'spikelet pair' in maize and other members of the Andropogoneae. The second spikelet appears in a number of forms, from rudimentary structures that do not form grain through to complete spikelets that form a number of grain[11] (Fig. 1a). Although some studies have investigated the genetic factors that contribute to various forms of inflorescence branching in wheat[10,12,13], the genes that regulate paired spikelet development are unknown.

We first characterized development of this trait using a group of modern cultivars that are known to represent broad genetic variation from Australia and around the world[14,15]. We defined two classes of paired spikelets (Fig. 1a): complete paired spikelets, in which the secondary spikelet contained at least one floret with all floral organs that regularly set seed, and rudimentary paired spikelets in which the secondary spikelet was present in various forms, including cup-like, spine and protoglume structures, and secondary spikelets with florets at different stages of development but no grains[11]. Scanning electron microscopy (SEM) of the abaxial surface of glumes from rudimentary and complete secondary spikelets supported the conclusion that these structures are variations of the same phenomenon, as glumes from all types of secondary spikelets were very similar to each other and to those of primary spikelets, with all being devoid of long thin trichomes that are present on leaves (Supplementary Fig. 1). This result is distinct from the elongated glumes of maize *Tunicate* mutants, which contain many trichomes due to a persistence of vegetative state in the inflorescence[16]. The frequency of paired spikelets was greatest at the centre of the inflorescence (Fig. 1b), particularly for complete paired spikelets, demonstrating that their distribution is distinct

[1]CSIRO Agriculture Flagship, GPO Box 1600, Canberra, ACT 2601, Australia. [2]National Institute for Applied Statistics Research Australia (NIASRA), School of Mathematics & Applied Statistics, University of Wollongong, New South Wales, 2522, Australia. [3]CSIRO Digital Productivity Flagship, GPO Box 1600, Canberra, ACT 2601, Australia. [4]Research School of Biology, The Australian National University, Canberra, ACT 0200, Australia. †Present address: Department of Crop Genetics, John Innes Centre, Norwich, NR4 7UH, UK (S.A.B.), Innovation Center, Bayer CropScience NV, Technologie Park 38, 9052 Zwijnaarde, Belgium (C.C.). *e-mail: steve.swain@csiro.au

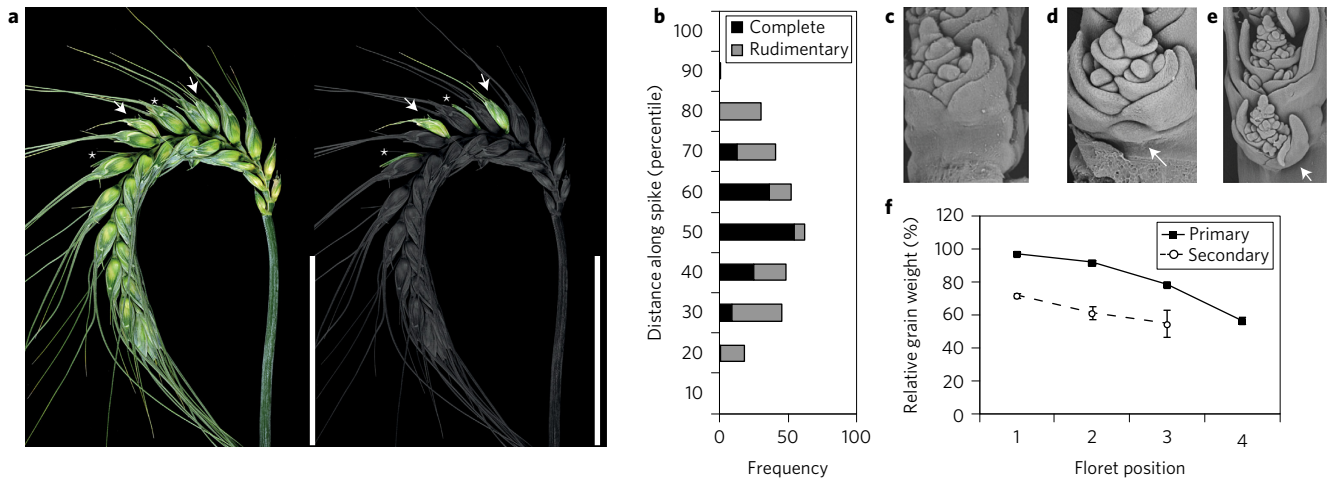

Figure 1 | Characterization of paired spikelets. a, Wheat spike with complete (arrow) and rudimentary (asterisk) paired spikelets. Right-hand panel highlights secondary (green) and primary (grey) spikelets. Scale bar, 5 cm. **b**, Distribution of rudimentary (grey) and complete (black) paired spikelets along the spike. Rachis node position is indicated as a percentile of the total rachis nodes: the bottom, mid-point and top of the spike are indicated as 10th, 50th and 90th percentiles, respectively. **c**–**e**, SEM images of **c**, a typical spikelet without a secondary spikelet, **d**, a raised cluster of cells (arrow) distal to the base of the typical spikelet, and **e**, a secondary spikelet with fully formed florets (arrow) distal to the base of the primary spikelet. **f**, Comparative grain weights of each floret from the primary spikelet (black, solid line) and the secondary spikelet (white circle, broken line), expressed as a percentage of the heaviest grain within the primary spikelet. Data are the mean ± s.e.m. ($n = 12$ plants).

from the long primary branches of the maize tassel and rice panicle that occur towards the base of the inflorescence. Further analysis confirmed that there is a statistically significant relationship between the rachis node position and the occurrence of a paired spikelet, with the central nodes having the highest probability (0.77–0.9, $P < 0.001$) of containing a paired spikelet (Supplementary Fig. 2). A similar distribution was also observed for grain number per secondary spikelet (Supplementary Fig. 3), as is commonly observed for primary spikelets of an archetypal spike, suggesting that primary and secondary spikelets share common regulatory pathways. This conclusion was supported by SEM analysis of immature inflorescences from genotypes known to produce paired spikelets. Secondary spikelets were found to initiate during early stages of inflorescence development at a time when the number of rachis nodes is being determined (prior to terminal spikelet) and primary spikelets develop. Paired spikelets were observed during these early stages as a range of structures, from a raised cluster of cells that contain no organs through to a secondary spikelet with fully formed florets (Fig. 1c–e). As commonly observed in typical primary spikelets, grain weight from secondary spikelets with fully formed florets progressively decreased at each increasing floret position (Fig. 1f; Supplementary Fig. 4; $P < 0.001$).

To gain insight into the genetic determinants that control paired spikelet formation we conducted a quantitative trait locus (QTL) analysis using a four-way multiparent advanced generation intercross (MAGIC) population derived from four elite wheat cultivars[15]. Paired spikelets were measured in five experiments, which included glasshouse and field grown plants over three successive years (2009–2011; Supplementary Table 1). Owing to the binomial distribution of this trait coupled with the low frequency of plants that displayed paired spikelets, a hybrid approach to QTL mapping was developed, implementing methods presented previously[17–19], but placed within the framework of a generalized linear mixed model (as described in Supplementary methods). Using the 90,000 single nucleotide polymorphism wheat array, 1,417 individuals were genotyped and a map consisting of 2,630 uniquely positioned markers was used for QTL analysis across the five experiments (Supplementary Table 2). These markers explained a high proportion (73–100%) of the genetic variance for this trait in four out of five experiments, and in all experiments the final QTL analysis explained 82–100% of total marker variance (Supplementary Table 3). From all five experiments, we identified 104 QTLs (Fig. 2; Supplementary Tables 4–6), which were refined to 18 putative QTLs on the basis of co-located markers associating with paired spikelets in at least two experiments (Supplementary Table 6). The mean marker position for each of these 18 putative regions was then used to identify those with a significant additive genetic effect across the five experiments (1A, 1B, 2D, 3A, 3B, 4D, 5B; Fig. 2; Supplementary Table 7) and to determine QTL that had a strong environmental contribution (1B, 1D, 2A, 4A, 5B, 6A, 7A; Supplementary Table 7). The QTLs on 1B, 2D, 3A and 5B are particularly interesting because they display a high LOD (logarithm of odds) score and/or appear in multiple experiments, with the 2D QTL having the single-highest LOD score of 11.32 (Fig. 2; Supplementary Table 6). The region on 2D was identified using a marker residing in the *Photoperiod-1* (*Ppd-D1*) flowering gene, and, interestingly, it was the QTL with the strongest single effect of a founder allele (Supplementary Table 8), identified as the photoperiod sensitive *Ppd-D1d* allele that contains a deletion in exon 7 (Supplementary Table 10)[14]. Given the significant genetic contribution identified for *Ppd-D1* and previous reports of photoperiod influencing formation of additional spikelets at individual rachis nodes[8,9], we decided to focus on variation in this gene as a potential explanation for the QTL on chromosome 2D.

Ppd-1 is a member of the pseudo-response regulator (PRR) gene family whose proteins contain a CCT (CONSTANS, CONSTANS-like, TIMING OF CAB1 (TOC1) and pseudo-receiver domain[6,7]. PRRs are important components of the circadian clock that directly regulate expression of core oscillator genes, and they also interact with NUCLEAR FACTOR-Y transcription factors[20,21]. In temperate cereals, allelic variation in *Ppd-1* influences sensitivity to long-day (LD) photoperiods; loss-of-function alleles confer a delayed flowering response upon transition from short-day (SD) to LD conditions, and gain-of-function insensitive alleles promote a constitutive LD response in all photoperiods[6,7,22–24]. To investigate the potential role of *Ppd-1* in paired spikelet development, we compared inflorescence phenotypes of near isogenic lines (NILs) in a common genetic background (Sunstate; BC4F3) that were either photoperiod

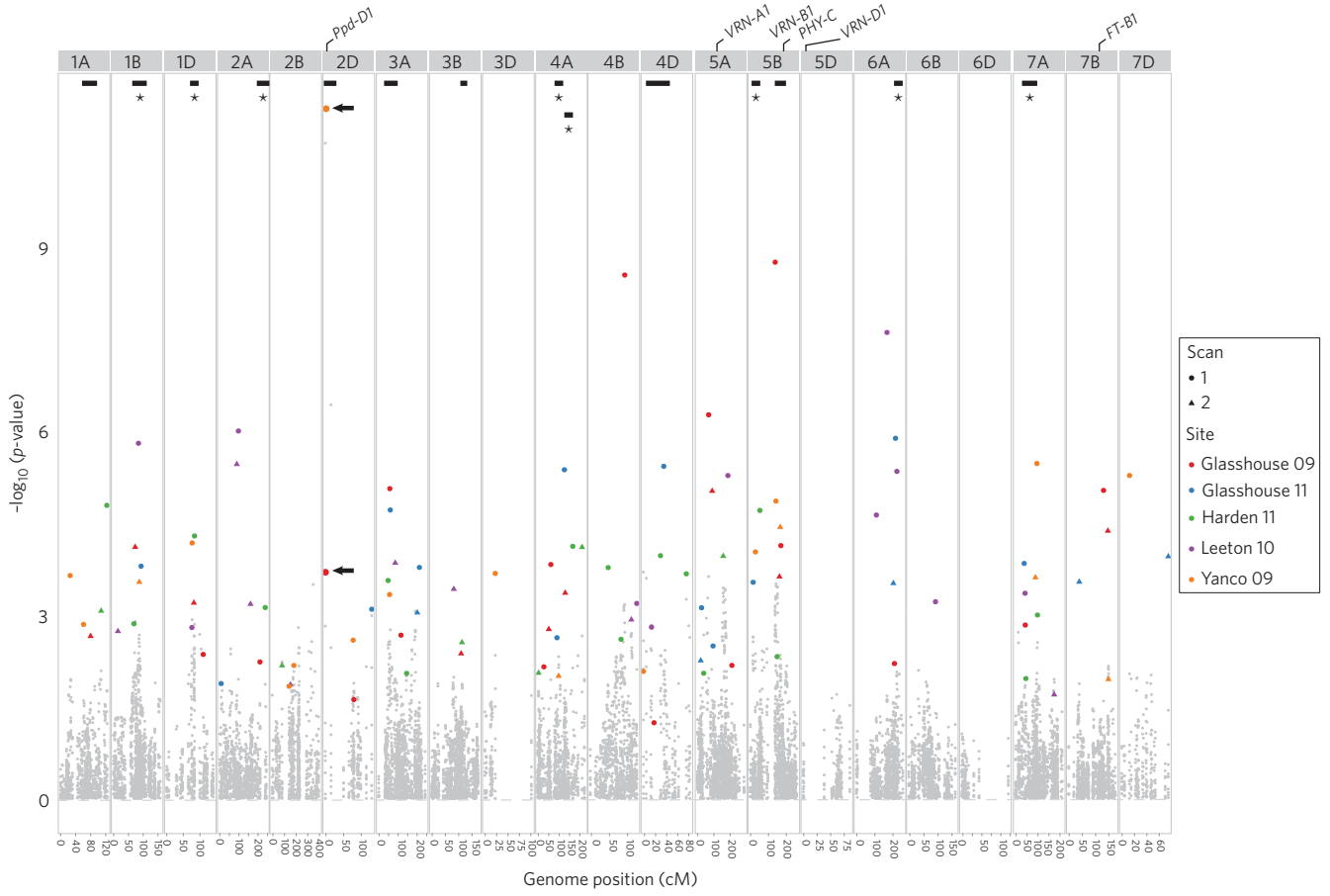

Figure 2 | Genome-wide plot displaying the 104 QTL (coloured dots/triangles) that contribute to paired spikelet development using the four-way MAGIC population across five independent experiments (five different colours). Coloured symbols identify significant markers identified in the final multi-QTL model, M3, and the black arrows indicate the QTL identified using the *Ppd-D1* marker. Grey dots represent non-significant markers from models M0 and M1 (Supplementary Methods). Black bars span regions of significant additive genetic effect across five experiments and black bars with asterisks indicate QTL with a significant experimental (environment) effect. Locations for *Ppd-D1*, *VRN-A1*, *VRN-B1*, *PHY-C* and *FT-B1* are indicated.

insensitive (flower early regardless of photoperiod) or strongly photoperiod sensitive (flower earlier in LD than SD photoperiods). The insensitive line contained the *Ppd-D1a* allele present in two of the four MAGIC parents[7,14] and three copies of the *Ppd-B1* gene[22], whereas the sensitive NIL contained a sensitive *Ppd-D1* allele found in one of the MAGIC parents (*Ppd-D1b*) and a single copy of *Ppd-B1* (Supplementary Tables 9 and 10). Under SD conditions (12 h light/12 h dark), the sensitive NIL flowered much later (~36 days) and produced a high frequency of paired spikelets (20% of rachis nodes) compared with the early flowering insensitive NIL that did not produce any paired spikelets (Fig. 3a and Supplementary Fig. 5). The sensitive NIL also formed more rachis nodes, and displayed elongated basal rachis internodes, relative to the insensitive line (Fig. 3a). Under LD conditions (16 h light/8 h dark), paired spikelet formation was suppressed in the sensitive NIL, and both the insensitive and the sensitive NILs flowered earlier and produced fewer rachis nodes, relative to plants grown in SD photoperiods (Fig. 3b and Supplementary Fig. 6). Taken together, these results suggest that LD photoperiods and *Ppd-1* alleles that elicit a constitutive LD response suppress paired spikelet development. The suppressive effect of LD in the sensitive NIL is not a consequence of increased expression of *Ppd-1* under LD relative to SD, as we did not detect any significant difference in transcript levels for *Ppd-D1* and *Ppd-B1* between the two photoperiods, and *Ppd-A1* was very weakly expressed (Supplementary Fig. 7). Photoperiod transfer experiments using the photoperiod-responsive MAGIC parent line Yitpi (Supplementary Tables 9 and 10) further demonstrated that LD photoperiods suppress formation of paired spikelets relative to SD photoperiods (Fig. 3c). This experiment also showed that LD photoperiods suppress paired spikelet formation and limit rachis node development between the stages of double ridge and 5 days after double ridge (Fig. 3c), confirming a photoperiod dependence of paired spikelet formation during early inflorescence development.

Further confirmation of the role for *Ppd-1* in regulating paired spikelet development was obtained in a forward genetics screen using the cultivar 'Sunstate', which contains the photoperiod-insensitive *Ppd-D1a* allele (Supplementary Table 9)[14]. By screening approximately 8,400 M2 plants under SD conditions, we identified a class of mutant that displayed paired spikelets, was late flowering and exhibited inflorescence architecture traits characteristic of the SD-grown photoperiod-sensitive NIL (Fig. 4 and Supplementary Fig. 8). Within this class, we identified three independent lines containing mutations in *Ppd-D1* that produce transcripts predicted to be incapable of generating a functional protein (Supplementary Fig. 9). Under SD conditions, all three mutants produced paired spikelets, which were mostly rudimentary, and displayed inflorescence phenotypes that were not seen in the Sunstate progenitor, including increased number of rachis nodes and elongated basal rachis internodes (Fig. 4b–g). Under LD conditions, the inflorescence architecture phenotypes were largely suppressed, indicating that *Ppd-A1* and *Ppd-B1* provide sufficient photoperiod responsiveness in the absence of Ppd-D1 (Supplementary Fig. 10). As expected,

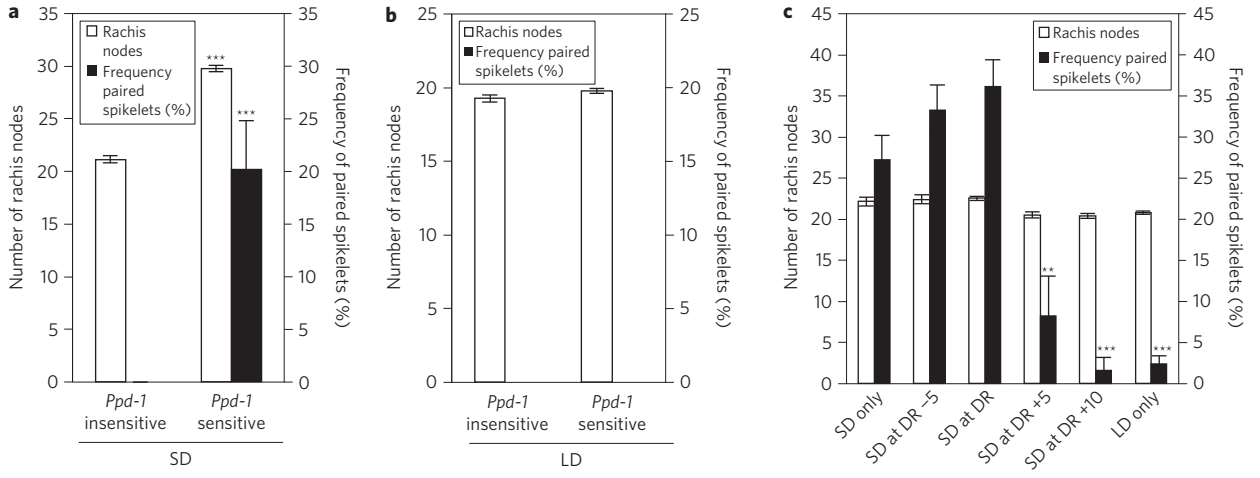

Figure 3 | The effect of allelic variation for *Ppd-1* and photoperiod on inflorescence architecture. a, Rachis node numbers and paired spikelet frequency from the main inflorescence of the *Ppd-1* NILs under SD photoperiods and **b**, LD photoperiods. **c**, Rachis node numbers and paired spikelet frequency as a percentage of total rachis nodes from the main inflorescence of plants grown under varying photoperiod regimes, with plants transferred from LD to SD at the developmental stages indicated. SD, short days; LD, long days; DR, double ridge. Data are the mean ± s.e.m. (n = 8–10 plants). $^{**}P < 0.01$; $^{***}P < 0.001$.

expression of *Ppd-A1* or *Ppd-B1* was not attenuated in the *Ppd-D1a* mutants, although *Ppd-B1* transcript levels were higher in *Ppd-D1a.1* and *Ppd-D1a.3*, suggesting that aberrantly spliced *Ppd-D1* transcripts may affect transcription or mRNA stability of *Ppd-B1* (Supplementary Fig. 11). These results confirm that insensitive alleles of *Ppd-D1* suppress formation of paired spikelets.

Given the association between paired spikelet development and late flowering in the *Ppd-1* NILs and the *Ppd-D1a* mutants, we investigated the effect of *Ppd-D1* on paired spikelets further by monitoring changes in expression of key flowering genes. *FLOWERING LOCUS T* (*FT*) is a central component of the flowering pathway whose expression is typically limited to inductive photoperiods, although variation in *Ppd-1* sensitivity in wheat disrupts the dependence of LD photoperiods for *FT* expression[7,23]. In plants containing the insensitive *Ppd-D1a* allele, we detected increased levels of *Ppd-D1* transcripts during the night-time of a SD, relative to *Ppd-D1* in the photoperiod-sensitive plants (Fig. 5a). The insensitive plants also displayed increased levels of *FT* transcripts at 2 h and 13 h after dawn, relative to the sensitive NIL (Fig. 5b), and *FT* expression increased in both the insensitive and sensitive NIL when grown under LD conditions (Supplementary Fig. 12). Moreover, *FT* transcript levels were lower in each of the *Ppd-D1a* mutants, relative to the progenitor containing a functional *Ppd-D1* protein (Fig. 5c). Taken together with our analysis of inflorescence architecture in these plants, our results demonstrate that paired spikelet development is associated with reduced expression of *FT* during early spike development. FT protein is produced in the leaf and transported to the shoot apical meristem where it triggers expression of meristem identity genes that regulate meristem fate to initiate the inflorescence and associated floral organs. We hypothesized that low expression of *FT* facilitates paired spikelet development via attenuated induction of meristem identity genes in the developing inflorescence. To address this hypothesis, we assessed paired spikelet development in a wheat mutant (also in the Sunstate background) that no longer contains *FT-B1* (E.J.F., unpublished observations), the most abundantly expressed *FT* homoeoallele[23]. We found that deletion of *FT-B1* enabled formation of paired spikelets, even in a background genotype that contained an insensitive *Ppd-D1a* allele, confirming that insensitive alleles of *Ppd-1* suppress paired spikelet development through a *FT*-dependent pathway (Fig. 5d–f). Although a QTL was identified in the region of the *FT* gene (Fig. 2, Chromosome Group 7), there is no known allelic variation for *FT-B1* in the MAGIC population that can be linked to the paired spikelet phenotype at present. A role for FT was further supported by analysis of meristem identity genes that are expressed in cereal meristems during initiation of spikelet growth[25–27], which corresponds to the stage when paired spikelets form. We analysed expression of genes within the developing inflorescence of the *Ppd-D1a.2* and *ft-B1* mutants, relative to their respective progenitors, and in the *Ppd-1* NILs. The genes included *SUPPRESSOR*

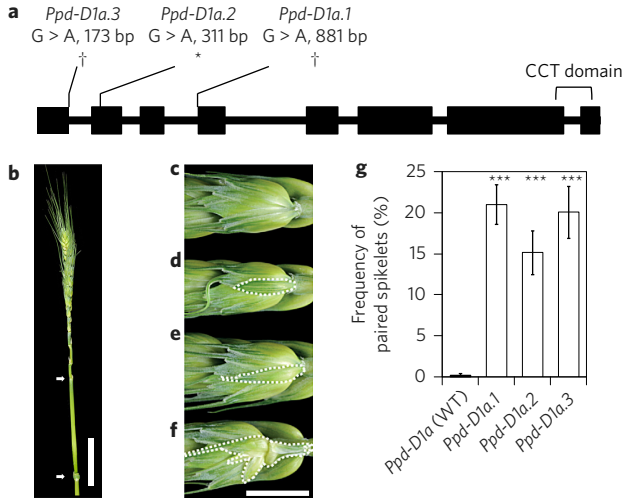

Figure 4 | Identification and phenotyping of *Ppd-D1a* mutants. **a**, Schematic of *Ppd-D1* gene structure: exons (rectangles) and introns (lines). *Ppd-D1a.2*—G > A conversion at 311 bp in exon 2 (W68*; premature stop codon). *Ppd-D1a.1* and *Ppd-D1a.3*—G > A conversions at the intron 3/exon 4 junction (881 bp) and the exon 1/intron 1 junction (173 bp), respectively, which prevent correct splicing of premature mRNA. *Premature stop codon; †mutation at splice site, base pair position is relative to start codon. **b**–**f**, Inflorescence phenotypes of the *Ppd-D1a.2* mutant with elongated basal internodes (**b**, arrows); typical primary spikelet (**c**), rudimentary (**d**–**e**) and complete (**f**) paired spikelets. Secondary spikelet shown within dashed white line. Scale bars: **b**, 5 cm; **c**–**f**, 1 cm. **g**, Frequency of paired spikelets in *Ppd-D1a* mutants grown under SD photoperiod. Data are mean ± s.e.m. (n = 8). $^{***}P < 0.001$.

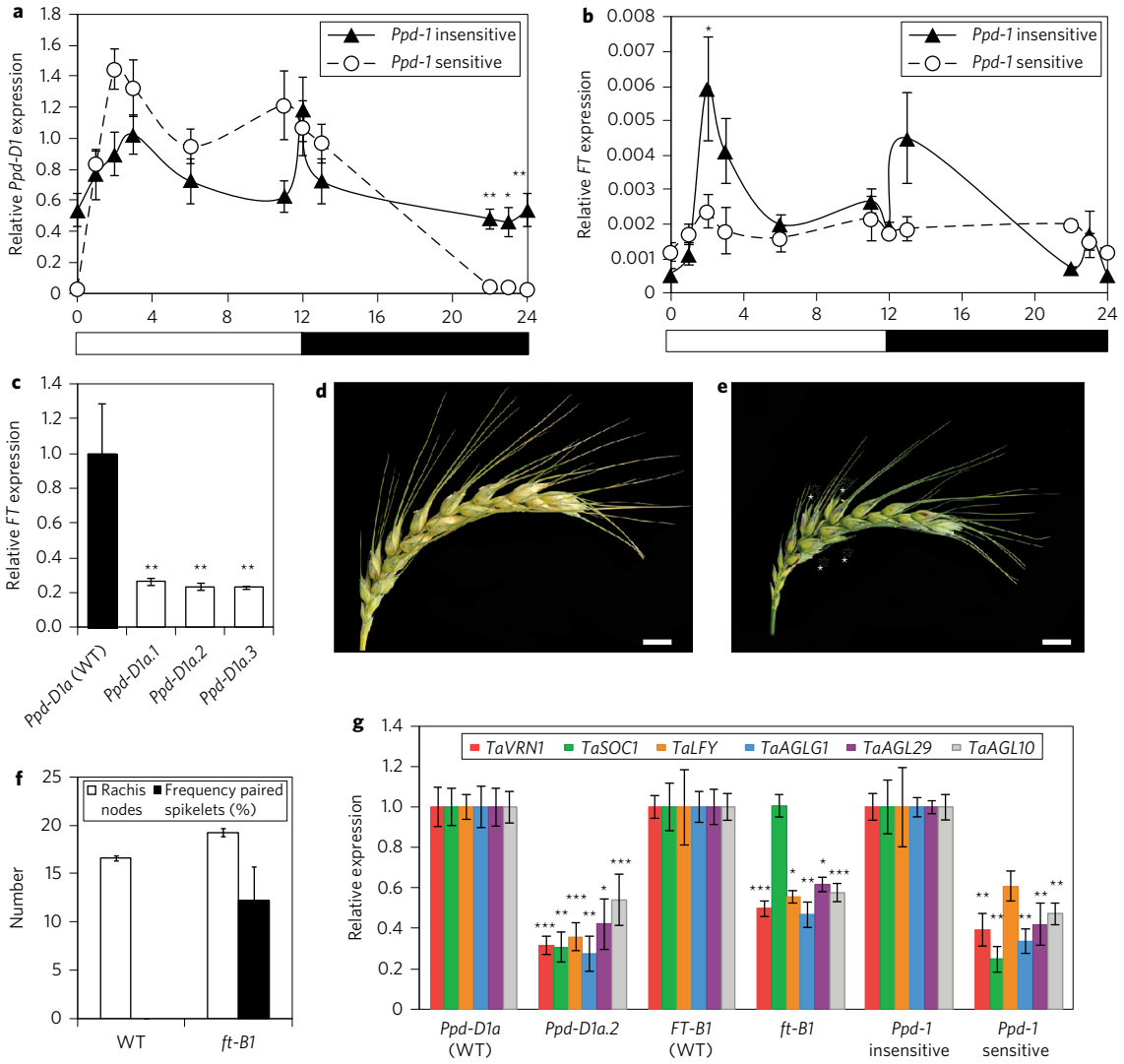

Figure 5 | Deletion of *FT-B1* promotes paired spikelet development. a–b, Diurnal expression analysis over a 24-h period for *Ppd-D1* (**a**) and *FT* (**b**) in the insensitive (solid line) and sensitive (broken line) *Ppd-1* NILs under a SD photoperiod. Daylight (white rectangles); night-time (black rectangles); dawn (0 h). **c**, *FT* expression in *Ppd-D1a* mutants, relative to the progenitor (Sunstate). Data are mean ± s.e.m. of three biological replicates. **d–f**, Spikes of progenitor (**d**) (Sunstate) and *FT-B1* deletion mutant (**e**) (*ft-B1*) (asterisks highlight paired spikelets), with measurements (**f**) of rachis nodes and paired spikelet frequency. Scale bars, 1 cm; data are mean ± s.e.m. ($n = 8$ plants). **g**, Expression of meristem identity genes in the *Ppd-D1a.2* and *ft-b1* mutants, relative to their respective wild-type progenitors, and in the *Ppd-1* NILs. Data are mean ± s.e.m. of three biological replicates. $^*P < 0.05$; $^{**}P < 0.01$; $^{***}P < 0.001$; for the *LFY* comparison in the *Ppd-1* NIL lines, $P = 0.052$.

OF CONSTANS1 (*SOC1*), *LEAFY* (*LFY*), *VERNALIZATION1* (*VRN1*), *AGAMOUS-LIKE GENE1* (*AGLG1*), *AGAMOUS-LIKE10* (*AGL10*) and *AGL29* (refs 25–27). In each of the genotypes that develops paired spikelets (*Ppd-D1a.2* and *ft-B1* mutants, sensitive NIL), we detected reduced transcript levels for *LFY*, *VRN1*, *AGLG1*, *AGL10* and *AGL29*, relative to the corresponding genotypes that suppress paired spikelet formation (wild-type progenitors and the insensitive NIL) (Fig. 5g). *SOC1* transcript levels were also significantly lower in the *Ppd-1* genotypes that form paired spikelets, relative to the genotypes that suppress their development (Fig. 5g). Based on these results, we conclude that the regulation of paired spikelet development by *Ppd-1* occurs via an *FT*-dependent pathway, which mediates the expression of meristem identity genes in the developing inflorescence.

In summary, we conclude that *Ppd-1* has an important role in regulating the formation of paired spikelets by modulating the strength of the floral promoting signal (*FT*) during early reproductive development. Our analysis suggests that the wheat spike is intrinsically capable of producing paired spikelets, which appear developmentally similar to the spikelet pairs of maize, if grown under conditions that produce a weakly inductive floral signal that leads to reduced expression of spikelet meristem identity genes. These results could be explained by a simple model whereby a weak floral signal facilitates slightly delayed conversion of inflorescence axillary meristems to spikelet meristems, so that a short branch comprising a lateral (secondary) and terminal (primary) spikelet forms instead of a single spikelet. This model will be further investigated by characterization of paired spikelet mutants identified in this study that contain an intact *Ppd-D1a* sequence, which may include mutations that attenuate expression of meristem identity genes. Tissue-specific complementation of the *Ppd-D1a* and *ft-B1* mutants, and altered expression of meristem identity genes, would also provide additional evidence for gene function and potentially allow us to confirm this hypothesis. This explanation is consistent with models for spikelet pair development in maize[28], and is similar to the inverse relationship observed between the number

of inflorescence branches and the strength of the floral promoting signal in rice[29]. These results may also help determine the pathways regulating inflorescence architecture in barley; although *Ppd-H1* and *FT1* have not been implicated in the control of two- and six-row spike forms, it is possible that attenuated expression of flowering genes is associated with the spikelet phenotype of the barley *flo* mutants[30], which resemble paired spikelets of wheat. Our results demonstrate that *Ppd-1* and *FT* have broader functions during inflorescence development in wheat beyond the initial vegetative to reproductive transition, and suggest that appropriate modifications of these genes could be used to form a wheat spike with a more elaborate arrangement and increased number of grain producing spikelets.

Methods

Methods and any associated references are available in the Supplementary Information.

Received 4 July 2014; accepted 5 December 2014; published 26 January 2015

References

1. Doebley, J., Gaut, B. S. & Smith, B. D. The molecular genetics of crop domestication. *Cell* **127,** 1309–1321 (2006).
2. Vollbrecht, E., Springer, P. S., Goh, L., Buckler, E. S. IV & Martienssen, R. Architecture of floral branch systems in maize and related grasses. *Nature* **436,** 1119–1126 (2005).
3. Ashikari, M. *et al.* Cytokinin oxidase regulates rice grain production. *Science* **309,** 741–745 (2005).
4. Miura, K. *et al. OsSPL14* promotes panicle branching and higher grain productivity in rice. *Nature Genet.* **42,** 545–549 (2010).
5. Ramsay, L. *et al.* INTERMEDIUM-C, a modifier of lateral spikelet fertility in barley, is an ortholog of the maize domestication gene *TEOSINTE BRANCHED 1*. *Nature Genet.* **43,** 169–172 (2011).
6. Turner, A., Beales, J., Faure, S., Dunford & Laurie, D. A. The pseudo-response regulator *Ppd-H1* provides adaptation to photoperiod in barley. *Science* **310,** 1031–1034 (2005).
7. Beales, J., Turner, A., Griffiths, S., Snape, J. W. & Laurie, D. A. A *Pseudo-Response Regulator* is misexpressed in the photoperiod insensitive *Ppd-D1a* mutant of wheat (*Triticum aestivum* L.). *Theor. Appl. Genet.* **115,** 721–733 (2007).
8. Sharman, B. C. Branched heads in wheat and wheat hybrids. *Nature* **153,** 497–498 (1944).
9. Sharman, B. C. Interpretation of the morphology of various naturally occurring abnormalities of the inflorescence of wheat (*Triticum*). *Can. J. Bot.* **45,** 2073–2080 (1967).
10. Dobrovolskaya, O. *et al. FRIZZY PANICLE* drives supernumerary spikelets in bread wheat (*T. aestivum* L.). *Plant Physiol.* http://dx.doi.org/10.1104/pp.114.250043 (2014).
11. Yen, C. & Yang, J. L. The essential nature of organs in Gramineae, multiple secondary axes theory: A new concept. *J. Sichuan Agric. Univ.* **10,** 544–565 (1992).
12. Koric, S. *Branching genes in Triticum aestivum*. Proc. Int. Wheat Genet. Symp. 4th, Colorado, Missouri, 283–288 (1973).
13. Pennell, A. L. & Halloran, G. M. Inheritance of supernumerary spikelets in wheat. *Euphytica* **32,** 767–776 (1983).
14. Eagles, H. A., Cane, K. & Vallance, N. The flow of alleles of important photoperiod and vernalisation genes through Australian wheat. *Crop Pasture Sci.* **60,** 646 (2009).
15. Huang, B. E. *et al.* A multiparent advanced generation inter-cross population for genetic analysis in wheat. *Plant Biotech. J.* **10,** 826–839 (2012).
16. Wingen, L. U. *et al.* Molecular genetic basis of pod corn (*Tunicate maize*). *Proc. Natl Acad. Sci. USA* **109,** 7115–7120 (2012).
17. Verbyla, A. P., Cullis, B. R. & Thompson, R. The analysis of QTL by simultaneous use of the full linkage map. *Theor. Appl. Genet.* **116,** 95–111 (2007).
18. Pastina, M. M. *et al.* A mixed model QTL analysis for sugarcane multiple-harvest-location trial data. *Theor. Appl. Genet.* **124,** 835–849 (2011).
19. Verbyla, A. P., Taylor, J. D. & Verbyla, K. L. RWGAIM: an efficient high-dimensional random whole genome average (QTL) interval mapping approach. *Genet. Res.* **94,** 291–306 (2013).
20. Nakamichi, N., Kita, M., Ito, S., Yamashino, T. & Mizuno, T. PSEUDO-RESPONSE REGULATORS, PRR9, PRR7 and PRR5, together play essential roles close to the circadian clock of *Arabidopsis thaliana*. *Plant Cell Physiol.* **46,** 686–698 (2005).
21. Li, C., Distelfeld, A., Comis, A. & Dubcovsky, J. Wheat flowering repressor VRN2 and promoter CO2 compete for interactions with NUCLEAR FACTOR-Y complexes. *Plant J.* **67,** 763–773 (2011).
22. Díaz, A., Zikhali, M., Turner, A. S., Isaac, P. & Laurie, D. A. Copy number variation affecting the *Photoperiod-B1* and *Vernalization-A1* genes is associated with altered flowering time in wheat (*Triticum aestivum*). *PLoS ONE* **7,** e33234 (2012).
23. Shaw, L. M., Turner, A. S. & Laurie, D. A. The impact of photoperiod insensitive *Ppd-1a* mutations on the photoperiod pathway across the three genomes of hexaploid wheat (*Triticum aestivum*). *Plant J.* **71,** 71–84 (2012).
24. Shaw, L. M., Turner, A. S., Herry, L., Griffiths, S. & Laurie, D. A. Mutant alleles of *Photoperiod-1* in wheat (*Triticum aestivum* L.) that confer a late flowering phenotype in long days. *PLoS ONE* **8,** e79459 (2013).
25. Yan, L. *et al.* Positional cloning of the wheat vernalization gene *VRN1*. *Proc. Natl Acad. Sci. USA* **100,** 6263–6268 (2003).
26. Zhao, T. *et al.* Characterization and expression of 42 MADS-box genes in wheat (*Triticum aestivum* L.). *Mol. Genet. Genomics* **276,** 334–350 (2006).
27. Kobayashi, K. *et al.* Inflorescence meristem identity in rice is specified by overlapping functions of three *AP1/FUL*-like MADS box genes and *PAP2*, a *SEPALLATA* MADS box gene. *Plant Cell* **24,** 1848–1859 (2012).
28. McSteen, P., Laudencia-Chingcuanco, D. & Colasanti, J. A floret by any other name: control of meristem identity in maize. *Trends Plant Sci.* **5,** 61–66 (2000).
29. Endo-Higashi, N. & Izawa, T. Flowering time genes *Heading Date 1* and *Early Heading Date 1* together control panicle development in rice. *Plant Cell Physiol.* **52,** 1083–1094 (2011).
30. Forster, B. P. *et al.* The barley phytomer. *Ann. Bot.* **100,** 725–733 (2007).

Acknowledgements

We thank Bjorg Sherman for technical assistance with plant husbandry, Mark Talbot for expert assistance with scanning electron microscopy and Carl Davies for photography. We thank Lindsay Shaw and Megan Hemming for helpful discussions. A CSIRO O.C.E. Postdoctoral Fellowship funded S.A.B.

Author contributions

S.A.B., C.C., K.R., J.G., E.J.F., B.T. and S.M.S. performed experiments and collected phenotypic information. C.C. and B.R.C. designed the MAGIC experiments, performed QTL and statistical analysis. S.A.B., E.J.F., B.T. and S.M.S. contributed new materials. All authors contributed to the preparation of the manuscript.

Additional information

Supplementary information is available online. Reprints and permissions information is available online at www.nature.com/reprints. Correspondence and requests for materials should be addressed to S.M.S.

Competing interests

The authors declare no competing financial interests.

TEOSINTE BRANCHED1 regulates inflorescence architecture and development in bread wheat (*Triticum aestivum* L.)

Laura E. Dixon[1†], Julian R. Greenwood[2†], Stefano Bencivenga[1], Peng Zhang[3], James Cockram[4], Gregory Mellers[4], Kerrie Ramm[2], Colin Cavanagh[2††], Steve M. Swain[2], Scott A. Boden[1*]

1. Department of Crop Genetics, John Innes Centre, Norwich Research Park, Norwich, NR4 7UH, United Kingdom.
2. CSIRO Agriculture and Food, Canberra, ACT, 2601, Australia.
3. Plant Breeding Institute, School of Life and Environmental Sciences, University of Sydney, Cobbitty, NSW 2570, Australia.
4. John Bingham Laboratory, National Institute of Agricultural Botany (NIAB), Cambridge, CB3 0LE, United Kingdom.

Laura E. Dixon (laura.dixon@jic.ac.uk)
Julian R. Greenwood (julian.greenwood@csiro.au)
Stefano Bencivenga (stefano.bencivenga@jic.ac.uk)
Peng Zhang (peng.zhang@sydney.edu.au)
James Cockram (james.cockram@niab.com)
Gregory Mellers (greg.mellers@niab.com)
Kerrie Ramm (kerrie.ramm@csiro.au)
Colin Cavanagh (colin.cavanagh@bayer.com)
Steve M. Swain (steve.swain@csiro.au)
Scott A. Boden (scott.boden@jic.ac.uk)

* To whom correspondence should be addressed: Scott A. Boden
Email: scott.boden@jic.ac.uk; Phone: +44 01603 450051

† - These authors contributed equally to this work.

†† - Present address: Bayer CropScience SA-NV, J.E. Mommaertslaan 14, 1831 Diegem, Machelen, Belgium

Short title: *TB1* regulates wheat inflorescence architecture

Please contact Scott A. Boden for material distribution requests.

Abstract: The flowers of major cereals are arranged on reproductive branches known as spikelets, which group together to form an inflorescence. Diversity for inflorescence architecture has been exploited during domestication to increase crop yields, and genetic variation for this trait has potential to further boost grain production. Multiple genes that regulate inflorescence architecture have been identified by studying alleles that modify gene activity or dosage; however, little is known in wheat. Here, we show *TEOSINTE BRANCHED1* (*TB1*) regulates inflorescence architecture in bread wheat (*Triticum aestivum* L.) by investigating lines that display a form of inflorescence branching known as 'paired spikelets'. We show that TB1 interacts with FLOWERING LOCUS T and that increased dosage of *TB1* alters inflorescence architecture and growth rate by reducing expression of meristem identity genes, with allelic diversity for *TB1* found to associate genetically with paired spikelet development in modern cultivars. We propose *TB1* coordinates formation of axillary spikelets during the vegetative to floral transition, and that alleles known to modify dosage or function of *TB1* could help increase wheat yields.

Introduction

A grass inflorescence is a group of seed-producing flowers that are arranged on specialised branches, known as spikelets. A plant's reproductive success is strongly influenced by the number and arrangement of spikelets and flowers that form on an inflorescence, known as inflorescence architecture, as this determines the maximum number of sites available for seed production. Consequently, diversity for inflorescence architecture has been important during the domestication of crop plants, as modifications that increase flower number have helped improve yields (Meyer & Purugganan 2013; Zhang & Yuan 2014). This diversity is often influenced genetically by alleles that alter the dosage of genes involved in spikelet and floret development (Doebley et al. 1997; Simons et al. 2005; Miura et al. 2010; Jiao et al. 2010; Yoshida et al. 2012; Houston et al. 2013; Zhu et al. 2013; Park et al. 2014; Greenwood et al. 2017; Debernardi et al. 2017; Soyk et al. 2017). An increased understanding of the genes that regulate spikelet and floret development, and selection of alleles that alter the activity of these genes, can therefore be used as a tool to increase crop yields (Miura et al. 2010; Jiao et al. 2010; Yoshida et al. 2012; Park et al. 2014; L. Wang et al. 2015; Soyk et al. 2017).

Bread wheat (*Triticum aestivum* L.) produces an inflorescence with a unique architecture among crops, forming single spikelets on opposite sides of a central rachis in an alternating phyllotaxy and a terminal spikelet at the apex, with each spikelet producing multiple florets. The number of spikelets that form on an inflorescence and the number of

fertile florets in each spikelet are two major determinants of yield, which are influenced by the rate of inflorescence development (Rawson 1970; Miralles et al. 2000; Slafer 2003; Gonzalez et al. 2011). Despite the importance of these traits for grain production and the potential for improvements to contribute to yield increases required to feed the world's growing population, very little is known about how they are regulated genetically (Reynolds et al. 2009; González-Navarro et al. 2015). Recent studies have investigated wheat lines with modified inflorescence architectures to identify genes that contribute to spikelet development, including our analysis of 'paired spikelets' (Dobrovolskaya et al. 2014; Boden et al. 2015; Poursarebani et al. 2015). Paired spikelets are a form of supernumerary spikelets characterised by the formation of two precisely positioned spikelets at a given rachis node rather than the typical single spikelet (Boden et al. 2015; Sharman 1944), which are distinct from other supernumerary spikelet structures including long lateral branches that form at the base of an inflorescence, and multi-rowed spikelets characterised by the formation of multiple spikelets at individual nodes (Dobrovolskaya et al. 2014; Poursarebani et al. 2015; Sharman 1967). Paired spikelet development is regulated by multiple genes, with quantitative trait loci (QTL) analysis of a four parent multi-parent advanced generation intercross (MAGIC) population detecting 18 QTL that contribute to this trait (Boden et al. 2015). One of the QTL detected in this study was underpinned by *Photoperiod-1* (*Ppd-1*), a pseudo-response regulator gene that controls photoperiod response pathways in wheat (Beales et al. 2007). We found that *Ppd-1* regulates inflorescence architecture by controlling the expression of the central regulator of flowering, *FLOWERING LOCUS T* (*FT*), which modulates the strength of the flowering signal perceived in the developing inflorescence. Alleles of *Ppd-1* and *FT* that produce a weak flowering signal facilitated paired spikelet production through reduced expression of genes that regulate spikelet development, relative to *Ppd-1* and *FT* alleles that produce a strong flowering signal and suppress paired spikelet formation (Boden et al. 2015).

In this study, we have investigated a pair of near-isogenic lines (NILs) developed from the MAGIC population to identify that a homologue of the maize domestication gene, *TEOSINTE BRANCHED1* (*TB1*), regulates wheat inflorescence architecture in a dosage-dependent manner. We show that TB1 protein interacts with FT, and that increased dosage of *TB1* promotes paired spikelet production and delays inflorescence growth by reducing expression of meristem identity genes during early developmental stages. We also identify variant alleles for *TB1* on the B and D wheat genomes, and show that these

alleles are at least partially responsible for diversity of inflorescence architecture in modern wheat cultivars.

Results

To identify genes that regulate inflorescence architecture in wheat, we investigated a pair of near-isogenic lines (NILs) derived from a single line of a four parent multi-parent advanced generation intercross (MAGIC) population for spring wheat (Huang et al. 2012). This line (MAGIC line 0053) was chosen because individuals within field plots displayed either wild-type inflorescences or inflorescences with multiple paired spikelets, suggesting that alleles for one or more gene(s) regulating spikelet architecture were segregating within this line. Seeds were independently selected from plants with wild-type (WT) and paired spikelet producing inflorescences over multiple generations (Supplementary Figure 1) to produce true-breeding lines that formed either wild-type inflorescences, or highly-branched inflorescences with multiple paired spikelets (Figure 1; Figure 1A), which will henceforth be referred to as *highly-branched* (*hb*). In *hb* plants, 43.3 ± 3.8% of nodes on the inflorescence (a.k.a. rachis nodes) produced paired spikelets, with 28.7 ± 3.9% of all nodes containing fertile secondary spikelets (Figure 1B). Paired spikelets were found most frequently at central nodes of the inflorescence (Supplementary Figure 2), which is consistent with our previous analysis of this trait (Boden et al. 2015). As paired spikelet development is facilitated by genetic and environmental conditions that delay flowering, and is associated with an increase in the number of sites available for spikelet production, we tested if flowering time and rachis node numbers were affected in *hb* plants, relative to WT (Sharman 1944; Boden et al. 2015). Under long-day photoperiods (16 h light/ 8 h dark), we observed no difference in the number of days until inflorescence emergence or the number of rachis nodes between the two genotypes, confirming that paired spikelet production is independent of flowering-time in these lines (Figure 1C, D). We did however notice a slight increase in the total leaf number of *hb* plants, relative to WT, suggesting inflorescence development is delayed in *hb* plants (Figure 1E). To investigate this further, we compared rates of inflorescence development and growth in *hb* plants, relative to WT plants, at intervals defined by leaf emergence from leaf 3 (L3) until leaf 8 (L8; Figure 1F, G). No significant difference in morphology or growth was detected between WT and *hb* inflorescences during early developmental stages (L3-L4; Figure 1F, G). However, growth of *hb* inflorescences was delayed at stages L5 and L6 which is when the terminal spikelet forms and spikelet primordia begin developing florets; this delay explains the increase in leaf number of *hb* plants (Figure 1E, G). Growth of *hb* inflorescences was delayed

dramatically at the L7 stage, relative to WT, which was allayed by L8 when there was no difference in inflorescence length detected between the two genotypes (Figure 1G; Supplementary Figure 3). There was also no significant difference in the length of mature inflorescences between the two genotypes (insert of Figure 1G). In addition to the inflorescence phenotypes, we found that *hb* plants produced fewer tillers than WT plants (Figure 1H, I). Dissection of leaf sheaths surrounding immature tillers showed that the *hb* plants produced tiller buds at each vegetative node that were smaller than those produced in WT plants (Supplementary Figure 4), suggesting that the reduced tiller numbers in the *hb* plants were due to suppressed outgrowth of the tiller buds rather than failure to develop tillers. Taken together, these results suggest that there is a pleiotropic effect on growth of lateral organs from the main shoot in *hb* plants, relative to WT.

To identify the genetic factor(s) contributing to the inflorescence and plant architecture phenotypes of the *hb* NIL, we initially performed genotype analysis using the 90,000 single nucleotide polymorphism wheat array (S. Wang et al. 2014), which suggested there was a partial or complete duplication of chromosome 4D (data not shown). To investigate this further, we performed cytogenetic analysis of chromosomes from WT and *hb* plants, which showed that the *hb* line is tetrasomic for chromosome 4D (Figure 2; Figure 2A, B). Our previous analysis of quantitative trait loci (QTL) that contribute to paired spikelet development within the four parent MAGIC population detected a QTL with a significant additive genetic effect on the short arm of chromosome 4D (4DS), which was detected using a marker positioned within the major Green Revolution gene, *Rht-D1* (*Reduced height-D1; Rht-2*) (Boden et al. 2015). Dominant dwarfing alleles for *Rht-1* and *Rht-2* (*Rht-B1b* and *Rht-D1b*, respectively) restrict plant growth and impede inflorescence development by reducing the plant's sensitivity to the growth promoting hormone, gibberellin (GA) (Pearce et al. 2011; Hedden 2013; Boden et al. 2014). Both the WT and *hb* lines contain the *Rht-B1b* (dwarfing) and *Rht-D1a* (WT) alleles, and we hypothesised that reduced sensitivity to GA *via* increased dosage of *Rht-D1a* may facilitate paired spikelet development by restricting growth of spikelet meristems and the developing inflorescence. To test this hypothesis, we examined inflorescence architecture in a pair of NILs that contained either the WT *Rht-D1a* allele or the dwarfing *Rht-D1b*, and in *Rht-D1c* (*Rht10*) lines that contain multiple copies of *Rht-D1a* (Pearce et al. 2011), relative to its NIL that contains a single copy. We did not detect paired spikelets in either of these genotypes, suggesting that increased dosage of *Rht-D1* is not responsible for the modified inflorescence architecture of the *hb* line (Supplementary Figure 5). Through our analysis of

Rht-D1 and the surrounding genetic region underlying the QTL on 4D, we noticed that a wheat homologue of an important maize domestication gene, *TEOSINTE BRANCHED1* (*TB1*), is closely linked to *Rht-D1* (Figure 2C). *TB1* encodes a class II TCP (TEOSINTE BRANCHED1, CYCLOIDEA, PCF1) transcription factor, which is a member of a plant-specific family of transcription factors that bind to promoter regions of genes known to regulate developmental processes including branching, floral symmetry, leaf development and germination (Doebley et al. 1997; Luo et al. 1996; Kosugi & Ohashi 1997; Tatematsu et al. 2008). *TB1* homologues regulate tiller number and influence inflorescence architecture traits in maize, rice and barley (Doebley et al. 1995; Doebley et al. 1997; Takeda et al. 2003; Studer et al. 2011; Ramsay et al. 2011), with the dominant *Tb1* allele of domesticated maize restricting growth of lateral branches *via* increased gene expression, relative to the *tb1* allele of the wild progenitor, teosinte (*Zea mays* ssp. *parviglumis*) (Doebley et al. 1997); we therefore hypothesised that increased dosage of the wheat *TB1* homologue from the D genome (*TB-D1*) may be responsible for the paired spikelet and tiller phenotypes of *hb* plants. Using digital droplet PCR (ddPCR), we confirmed that *hb* plants contain a haploid complement of two copies for *TB-D1*, and WT plants contain one copy (Figure 2D). We then compared expression levels for *TB1* from the A (*TB-A1*), B (*TB-B1*) and D genomes in WT and *hb* plants at defined stages of inflorescence development and in vegetative tissues that included tiller buds, emerging tillers, leaves, roots and germinating seedlings. We observed that *TB-B1* and *TB-D1* are expressed predominantly in developing inflorescences and tillers, relative to leaves, roots and seedlings, and that *TB-A1* is expressed significantly lower than *TB-B1* and *TB-D1* (Figure 2E, F; $p < 0.0001$). We found that *TB-D1* transcript levels are significantly higher in developing inflorescences of *hb* plants, relative to WT, at the double ridge stage of development that is pivotal for paired spikelet formation (Boden et al. 2015) and during the L5-L7 developmental stages when inflorescence growth is delayed in *hb* plants (Figure 1F, 2E). We also detected a significant increase in *TB-D1* transcripts in tiller buds and emerging tillers of *hb* plants, relative to WT, while no significant difference in *TB-D1* transcript levels were detected between the two genotypes in roots, leaves or germinating seedlings (Figure 2F). These results demonstrate that *TB-D1* transcript levels are significantly higher in tissues of the *hb* plants that display architecture phenotypes, relative to WT plants, which was not observed for most other genes that are in proximity to *TB-D1* on chromosome 4D (Supplementary Figure 6). These results are therefore consistent with increased expression of *TB-D1* promoting paired spikelet development and suppressing tiller outgrowth.

To confirm genetically that increased dosage of *TB-D1* promotes paired spikelet development, we generated transgenic lines that expressed *TB-D1* using the well characterised promoter of *VERNALIZATION1* (*VRN1*) (Alonso-Peral et al. 2011), in the genetic background of Fielder that forms paired spikelets at a very low frequency. *VRN1* encodes a MADS-box transcription factor that is expressed robustly in the developing inflorescence during the vegetative to reproductive transition, including the double ridge stage when paired spikelets form (Yan et al. 2003; Alonso-Peral et al. 2011; Boden et al. 2015). This experiment therefore increased the number of genomic copies for *TB-D1*, and promoted expression of the additional copies of *TB-D1* within the inflorescence at stages pivotal for paired spikelet development. From this experiment, we identified 14 independent *pVRN1:TB-D1* transgenic lines that formed paired spikelet-producing inflorescences (Figure 3; Figure 3A, B; Supplementary Figure 7, Supplementary Table 1). Genotype analysis of T_1 transgenic lines confirmed that paired spikelet-producing plants contained 1.5 or 2 haploid copies of *TB-D1*, while null transgenic plants and control Fielder plants that contained 1 haploid copy of *TB-D1* did not form paired spikelets, or did so at a very low frequency (Figure 3A-C, Supplementary Figure 7, Supplementary Table 1). Within the 14 transgenic lines, secondary spikelets were found to occur at 8-34% of the rachis nodes, and each line produced plants that contained fertile secondary spikelets (Figure 3A, B, Supplementary Table 1). These results confirm our hypothesis that increased dosage of *TB1* promotes paired spikelet development. This conclusion was further supported by analysis of plants from a revertant line that derived spontaneously from an individual *hb* plant, which no longer formed paired spikelets, produced more tillers and were significantly taller than *hb* plants (Fig. 3D-F; Supplementary Table 2). We hypothesised that the increased height of these plants was caused by loss of the dwarfing *Rht-B1b* allele, and that the absence of paired spikelets and increased tiller numbers occurred through loss of the closely linked *TB-B1,* possibly through loss of chromosome 4B. Marker analysis confirmed that *TB-B1* and *Rht-B1b* were indeed absent in the revertant lines (Figure 3G, Supplementary Figure 8). Taken together with the expression analysis, we conclude that increased dosage of *TB1*, with contributions from both the wheat D and B genomes, promotes paired spikelet development and reduces outgrowth of tillers in *hb* plants.

To identify how increased *TB1* dosage may promote paired spikelet development, we surveyed the literature for molecular interactions that involve *TB1* orthologues and associate with genetic pathways known to influence inflorescence architecture. In

Arabidopsis, rice and wheat, the central integrator of flowering, FT, interacts with FLOWERING LOCUS D (FD, or FDL in wheat) and 14-3-3 proteins to form a floral activating complex, which induces expression of floral meristem identity genes (Abe et al. 2005; Wigge et al. 2005; Taoka et al. 2011; Li et al. 2015). It has also been shown that the Arabidopsis homologue of *TB1*, *BRANCHED1* (*BRC1*) (Aguilar-Martinez et al. 2007), negatively regulates the floral transition of axillary branches by interacting with FT and suppressing its ability to promote expression of floral meristem identity genes (Niwa et al. 2013). As we have shown previously that deletion of *FT-B1* promotes paired spikelet development (Boden et al. 2015), we hypothesised that TB-D1 interacts with FT and that increased dosage of *TB-D1* facilitates paired spikelet development by reducing the availability of FT to promote floral transition events within the developing inflorescence, including expression of spikelet meristem identity genes. To test this hypothesis, we performed yeast two-hybrid (Y2H) and bimolecular fluorescence complementation (BiFC) analysis to determine if TB-D1 and FT proteins interact. Both the Y2H and BiFC analyses demonstrated that TB-D1 interacts directly with FT, while no interaction was detected in control experiments, which included a truncated version of TB-D1 (TB1Δ) that lacks the first 115 amino acids of TB1, a region demonstrated previously to be essential for the interaction between BRC1 and FT from Arabidopsis (Figure 4; Figure 4A-C; Supplementary Figure 9) (Niwa et al. 2013). We then tested if increased dosage of *TB-D1* affects expression of genes that regulate spikelet development by analysing transcript levels of meristem identity genes from developing inflorescences of WT and *hb* plants (Figure 4D). These genes included *VRN1*, *SOC1*, *AGAMOUS-LIKE GENE1* (*AGLG1*), *AGAMOUS-LIKE10* (*AGL10*) and *AGL29*, whose expression was found previously to be reduced in inflorescences of paired spikelet producing lines, including a mutant containing a deletion of *FT-B1* (Boden et al. 2015). We found that transcript levels for all meristem identity genes were significantly reduced during early developmental stages in inflorescences of *hb* plants, relative to those of WT plants (except for *VRN1* at the DR stage), which included stages pivotal for paired spikelet development (Figure 4D). At the leaf 7 developmental stage, transcript levels for *VRN1*, *SOC1*, *AGL10* and *AGL29* were not significantly different in WT and *hb* plants, which is consistent with the observed completion of spikelet and floret development in *hb* inflorescences at the L7 stage in preparation for growth between emergence of L7 and 8 (Figure 1F-G, 4D). We confirmed that these changes in activity of meristem identity genes were not caused by reduced expression of *FT* in *hb* plants, relative to WT (Supplementary Figure 10). Based on these results, we conclude that TB1 interacts with FT and that increased dosage of TB1

promotes paired spikelet development and delays inflorescence growth between the L5 and L7 stages by reducing the expression of spikelet meristem identity genes.

As *TB1* contributes to important yield traits including inflorescence architecture and growth, we hypothesised that there are allelic variants for *TB1* among modern wheat cultivars, which contribute to variation in spikelet development. To test this hypothesis and determine if a *TB1* allele may be responsible for the paired spikelet QTL detected previously on chromosomes 4B and 4D (Boden et al. 2015), we sequenced *TB-B1* and *TB-D1* from the cultivars used to generate the four parent spring wheat MAGIC population: Baxter, Chara, Westonia and Yitpi. No sequence polymorphism was detected for *TB-B1* amongst the four cultivars; however, one polymorphism was detected in the open reading frame of *TB-D1* from Baxter, which is a non-synonymous mutation (G-328 bp-T; D110Y) at the beginning of the conserved TCP domain (Figure 5; Figure 5A; Supplementary Figure 11-12). Interestingly, our previous analysis identified Baxter as the cultivar that contributes a positive genetic effect for the paired spikelet QTL on chromosome 4D, detected using the marker for *Rht-D1* that is in proximity to *TB-D1* (Boden et al. 2015). Taken together, these results suggest that the Baxter allele for *TB-D1* (referred to as *TB-D1b*) may be responsible for the paired spikelet QTL detected on chromosome 4D. To gain further evidence of allelic variation for *TB1*, we surveyed 230 modern winter wheat cultivars for paired spikelet development over two growing seasons (Supplementary Figure 13, Supplementary Tables 3, Supplementary Data Set 1). We identified 96 cultivars that produce paired spikelets, including Abbot, Ambrosia, Einstein, Gladiator, and Hyperion that form secondary spikelets at 20-35% of rachis nodes (Supplementary Figure 13, Supplementary Table 3). Digital droplet PCR and sequence analysis for *TB-B1* and *TB-D1* on a subset of these cultivars showed that there is no CNV for *TB-B1* or *TB-D1* (Supplementary Figure 14), and no sequence variant alleles for *TB-D1*. We did however detect an allele for *TB-B1* (referred to as *TB-B1b*) that contains five sequence polymorphisms in complete linkage disequilibrium, including two synonymous mutations (G-198 bp-A, G-912 bp-A) and three non-synonymous mutations (C-309 bp-G, S103R; A-663 bp-T, K221N; C-812 bp-T, A271V) (Figure 5B, Supplementary Figure 15-16). KASP-based marker analysis showed that the *TB-B1b* allele is widely distributed across a geo-referenced panel of 264 European wheat varieties (the GEDIFLUX panel), and was observed most frequently in cultivars of Great Britain, Belgium and France (Figure 5C, Supplementary Tables 4, Supplementary Data Set 2). We also identified that both the *TB-B1a* (WT; reference sequence) and *TB-B1b* alleles are present among the founder

genotypes used to generate the eight parent UK winter wheat MAGIC population, with Rialto, Robigus and Soissons containing the *TB-B1a* allele and Alchemy, Brompton, Claire, Hereward and Xi 19 containing the *TB-B1b* allele (Supplementary Table 4). We hypothesised, therefore, that phenotype and genetic analyses for paired spikelets within this MAGIC population would identify a QTL on chromosome 4B in the region proximal to *TB-B1*. Paired spikelet measurements were recorded for field grown replicated trials over two successive years (643 lines with two replicates in 2015 and 493 lines with two replicates in 2016), with broad sense heritability estimated at 72.4% and 94.1% for 2015 and 2016, respectively. In both years, genetic mapping identified a highly significant QTL in a region of chromosome 4B that included *TB-B1*, which was bound by markers wsnp_BF482960B_Ta_1_4 (47.64 cM, chr 4B position 28954488 bp) and RAC875_c27536_611 (48.65 cM, chr 4B position 32250720 bp) and explained 6% and 7.5% of phenotypic variance (R^2) in the 2015 and 2016 trials, respectively (Figure 5D, Supplementary Figure 17, Supplementary Tables 5, 6). This analysis identified that alleles donated by Rialto, Robigus and Soissons are predicted to contribute positively towards the paired spikelet trait, suggesting that the *TB-B1a* allele facilitates paired spikelet development (Supplementary Table 6). This conclusion was supported by *TB-B1* specific marker analysis of a subset of 212 MAGIC lines that formed either wild-type or paired spikelet-producing inflorescences, which confirmed the *TB-B1a* allele is associated genetically with paired spikelet development (McNemar's Test, $p < 0.05$; Supplementary Table 7). To test if the non-synonymous mutations of *TB-B1b* alter the function of TB-B1, we performed Y2H analysis to determine if TB-B1a and TB-B1b both interact with FT. We detected that both proteins interact with FT; however, analysis of serial dilutions indicated that the interaction between TB-B1a and FT is slightly stronger than the interaction between TB-B1b and FT (Figure 5E). These results show that variant *TB1* alleles are present on the B and D genomes of winter and spring wheat, respectively, and that diversity for *TB1* modulates inflorescence architecture in modern wheat cultivars.

Discussion

Inflorescence architecture contributes significantly to seed production in plants, and is a major determinant of crop yield. Seed production can be increased by developing inflorescences with more elaborate branching patterns, which can be achieved by breeding with alleles that modify the activity of genes involved in spikelet or floret development (Miura et al. 2010; Jiao et al. 2010; Yoshida et al. 2012; Bommert et al. 2013; Meyer & Purugganan 2013; Zhu et al. 2013; Park et al. 2014; Poursarebani et al. 2015;

Soyk et al. 2017). In this study, we have shown that increased dosage of *TB1* promotes inflorescence branching in the form of paired spikelets, and that allelic diversity for *TB1* is associated with spikelet architecture traits in modern wheat cultivars.

Our analysis of the near-isogenic and transgenic lines demonstrates that increased dosage of *TB1* promotes paired spikelet development, which is associated with reduced expression of spikelet meristem identity genes. The reduced expression of the meristem identity genes is consistent with our previous analysis of paired spikelet-producing genotypes that have loss-of-function alleles for key flowering genes, including *Ppd-D1* and *FT* (Boden et al. 2015). Based on these results, and protein interaction experiments that show TB1 interacts with FT, we propose a model for *TB1*-dependent regulation of inflorescence architecture (Figure 6), whereby increased dosage of *TB1* facilitates paired spikelet development by reducing the availability of FT to form part of the floral activating complex and promote expression of spikelet meristem identity genes (Taoka et al. 2011; Boden et al. 2015; Li et al. 2015). This effect of increased *TB1* dosage is consistent with studies of the Arabidopsis *TB1* homologue, *BRC1*, which showed BRC1 is a negative regulator of flowering that interacts with FT and restricts the expression of floral meristem identity genes within axillary meristems (Niwa et al. 2013). We propose that this role for *TB1* is conserved in wheat, where it helps regulate the development of axillary spikelet meristems from the inflorescence meristem during the vegetative to floral transition. At standard levels, *TB1* facilitates formation of unbranched primary spikelets along the inflorescence; however, when *TB1* levels are increased, the maturation of spikelet meristems is delayed, which results in development of a short branch that is limited to two spikelets (Figure 6). This effect of increased *TB1* levels is consistent with studies performed in rice and tomato, which have demonstrated that inflorescences with more elaborate branching patterns and increased yields can be developed by reducing the activity of flowering signals and extending the duration of meristem maturation (Park et al. 2012; Yoshida et al. 2012; Kyozuka et al. 2014; Park et al. 2014; L. Wang et al. 2015; Lemmon et al. 2016; Soyk et al. 2017).

Our observation that increased dosage of *TB1* promotes paired spikelet development and reduces tiller numbers in wheat suggests that there is a conserved role for this gene in regulating inflorescence and plant architecture of cereals. In maize, the *Tb1* allele of domesticated cultivars is expressed constitutively, relative to the *tb1* allele of teosinte, and it suppresses development and growth of axillary branches (Doebley et al. 1997; Hubbard et al. 2002). Consequently, the *Tb1* allele modifies plant architecture by suppressing tiller

development to produce a monoculm plant, which is consistent with observations in barley, rice and wheat that show *TB1* negatively regulates tiller outgrowth (Doebley et al. 1995; Doebley et al. 1997; Hubbard et al. 2002; Takeda et al. 2003; Lewis et al. 2008; Ramsay et al. 2011). In regard to inflorescence architecture, the *Tb1* allele contributes to development of maize ears with cupules that contain two spikelets, relative to the less active *tb1* allele of teosinte that is associated with formation of single spikelet cupules (Doebley et al. 1995). Taken together with results shown here, these reports suggest that *TB1* has a conserved role among cereals in regulating development and growth of axillary meristems, and that increased dosage of *TB1* within the developing inflorescence promotes formation of spikelet pairs rather than single spikelets. This conclusion is supported by a report of wheat plants over-expressing the maize *TB1* gene that produced fewer tillers and formed inflorescences with an increased number and density of rachis nodes and many small spikelets containing incomplete florets, which is consistent with a description of paired spikelets (Lewis et al. 2008). This effect of *TB1* dosage on spikelet architecture may also explain the six-rowed spikelet phenotype of barley lines that contain loss-of-function alleles of the barley *TB1* homologue, *INTERMEDIUM-C* (*INT-C/HvTB1*). Mutant alleles of *HvTB1* increase fertility of lateral spikelets, which are sterile in two-rowed barley that contain the wild-type allele of *HvTB1* (Ramsay et al. 2011). Taken together with results presented here and those of *BRC1* in Arabidopsis, the improved fertility of lateral spikelets in barley lines that carry mutant alleles of *HvTB1* may be explained by increased expression of meristem identity genes within the lateral spikelets. Further investigation of meristem identity gene expression in inflorescences of maize and barley NILs that contain variant alleles of *Tb1* and *INT-C*, respectively, would determine if the *TB1*-dependent mechanism for regulating spikelet architecture is conserved among cereals.

In addition to the inflorescence architecture phenotypes shown here, an important observation from this study is that inflorescence growth was delayed in the *hb* NIL, relative to WT, between emergence of leaf 5 and leaf 7. Inflorescence growth rate contributes significantly to floret fertility, and is therefore an important component of yield (Miralles et al. 2000; Slafer 2003; Reynolds et al. 2009). Wheat plants typically produce 10-12 floret primordia per spikelet, yet only 2-4 of these primordia survive to produce grain; hence, optimisation of floret fertility is a key objective for improving wheat yield (Reynolds et al. 2009; González et al. 2011; González-Navarro et al. 2015; Guo & Schnurbusch 2015). The delayed inflorescence growth of the *hb* NIL, relative to WT, suggests that *TB1* dosage influences the rate of inflorescence growth during early developmental stages. It remains

to be determined whether this phenotype is directly linked to TB1 function, or is a consequence of secondary spikelet development in these lines. However, this result, along with the rapid inflorescence growth that occurs between emergence of leaf 6 and 8, suggests that wheat inflorescences undergo a transition from a phase of axillary organ development to a period of growth in between the terminal spikelet and white anther stages. The timing of this transition correlates developmentally with the stage when the maximum number of viable floret primordia is observed (Guo & Schnurbusch 2015), suggesting that this may be a point during development when the peak sink potential of the inflorescence is established prior to initiation of inflorescence growth. Comparative analysis of gene expression and metabolite levels in inflorescences of WT and *hb* NILs during these developmental stages will therefore be useful for identifying molecular pathways that influence the rate of inflorescence growth and floret fertility.

An important outcome of this research is the identification of variant alleles for *TB1* on the B and D wheat genomes that regulate inflorescence architecture in modern wheat cultivars. We identified an alternate allele for *TB-D1* in spring wheat, which is a candidate gene for a spikelet architecture QTL detected previously on chromosome 4D (Boden et al. 2015). We also identified a variant allele for *TB-B1* in winter wheat that contains five sequence polymorphisms (*TB-B1b*), and demonstrated that allelic diversity for *TB-B1* contributes to the most significant paired spikelet QTL in the winter wheat MAGIC population. Yeast two-hybrid analysis was performed to investigate the comparative strength of the interaction between FT and TB-B1a versus FT and TB-B1b, which suggested that TB-B1a interacts more strongly with FT than does TB-B1b. Taken together with our genetic analysis of the two *TB-B1* alleles, this result supports our conclusion that increased activity of TB1 promotes paired spikelet development by modulating the function of FT (Figure 6). An intriguing outcome from our analysis of multiple wheat cultivars is that many were found to produce paired spikelets, which is surprising given that paired spikelets are undesired within breeding programs because florets of the secondary spikelets often produce small grain that reduce the uniformity of grain size (*Crop Committee Handbook*, AHDB, 2013). Taken together with our analysis of *TB1*, this phenomenon may be explained by alleles that promote paired spikelet development also contributing beneficial effects for important yield components of plant development, such as inflorescence growth, floret fertility or tiller number. Interestingly, we observed that the *TB-B1b* allele appears more frequently in winter wheat cultivars of the UK, France and Belgium, relative to other regions of Europe; this finding suggests that there may be an

adaptive advantage for this allele under certain environmental conditions, which is consistent with the proposed role for *tb1* regulating the plasticity of plant architecture traits of teosinte in response to changes in the local environment (Doebley et al. 1995). Further characterisation of these alleles through generation of NILs, or development of CRISPR/Cas9 transgenic lines that target individual polymorphisms within the *TB-B1b* allele, will be important for determining the effect of these mutations on inflorescence and plant architecture. Nonetheless, these results show that variant *TB1* alleles are present on the B and D genomes of winter and spring wheat, respectively, and that diversity for *TB1* modulates inflorescence architecture in modern wheat cultivars.

In summary, we conclude that *TB1* is a key regulator of inflorescence and plant architecture in wheat, which influences development of axillary spikelets by modulating FT-dependent activation of meristem identity genes. Our demonstration that increased dosage of *TB1* promotes paired spikelet development is consistent with reports from other crops showing the more elaborate inflorescence branching can be achieved using alleles that modify dosage of gene activity (Doebley et al. 1995; Miura et al. 2010; Jiao et al. 2010; Park et al. 2012; Yoshida et al. 2012; Bommert et al. 2013; Houston et al. 2013; Zhu et al. 2013; Park et al. 2014; L. Wang et al. 2015; Soyk et al. 2017). In the case of *TB1*, these results point towards a conserved role for this gene regulating the determinacy and development of axillary spikelet meristems in cereals (Doebley et al. 1995). These results therefore highlight the potential for alleles that modify *TB1* activity to increase the number of flowers available for seed production, which is important given our increasing need to identify new genetic traits that will increase yields of our staple crop plants (Reynolds et al. 2009; Fischer et al. 2014).

Materials and methods

Plant materials and growth conditions

Hexaploid wheat (*Triticum aestivum* L.) used in this study included the following genotypes: MAGIC line 0053, from which the near isogenic lines (NIL) termed ‘wild-type’ and ‘*hb*’ were derived (wild-type (WT) refer to lines of MAGIC line 0053 that form regular inflorescences; Supplementary Fig. 1); tall revertant NIL derived from the ‘*hb*’ NIL; transgenic lines expressing *TB-D1* using the *VRN1* promoter generated in the *cv.* Fielder genetic background (see details below); *Rht* NILs (BC_6F_3 NILs in the *cv.* Paragon background, containing either the *Rht-D1b* dwarf allele from *cv.* Alchemy, or the *Rht-D1a*

allele from *cv.* Paragon); *Rht-D1c* (a.k.a *Rht10*) (Pearce et al. 2011); and multiple wheat cultivars listed in Supplementary Tables 3-4 and Supplementary Data Set 1.

Wild-type and *hb* plants used for phenotype analysis and gene expression studies were grown in controlled growth chambers under short day (SD; 10 h light/ 14 h dark) or long day (LD; 16 h light/ 8 h dark) photoperiods, with a day temperature of 20 ºC and a night temperature of 15 ºC. Winter wheat varieties surveyed for paired spikelet phenotypes were grown at field sites of KWS based in Thriplow, Cambridgeshire, England (52º06'00.6''N, 0º05'29.1''E) in 1 m^2 plots. Phenotype data for the winter wheat varieties were collected over two growing seasons (2015 and 2016).

The 'NIAB Elite MAGIC' bread wheat population has been previously described (Mackay et al. 2014), and F_8 seed was sourced from NIAB, UK. The paired spikelet phenotype was assessed, following previously published protocols (Boden et al. 2015) but with fertile or infertile classifications for complete PS (resulting in 0-3 scores). PS phenotypes were scored in two field trials; both of which were undertaken at NIAB (Cambridgeshire, UK, 52°13'19"N, 0°5'46"E). The first consisted of 643 progeny (2 replicates) and the 8 founders (2 replicates), sown in autumn 2014 and phenotyped at maturity in 2015 (the '2015 trial'). The second trial used 493 progeny (2 replicates) and the 8 founders (≥4 replicates), sown in autumn 2015 and phenotyped at maturity in 2016 (the '2016 trial'). Each replicate in both trials was sown as two adjacent rows of 1 m each within 1 m^2 plots of 6 rows total.

Inflorescence architecture measurements

Rachis node and paired spikelet measurements were recorded for the inflorescences of the main stem and first tiller. Paired spikelet measurements for each plant have been normalised by calculating the frequency of rachis nodes that contain paired spikelets, represented as a percentage. Data shown for WT and *hb* plants is the average ± S.E.M. of at least 8 plants. Data shown for winter wheat varieties is the average ± S.E.M. of 4 plants, and these varieties were scored in 2 growing seasons. Data shown for *hb* and tall revertant lines is the average ± S.E.M. of at least 3 plants. Data shown for positive transgenic plants is average ± s.d. of 3-4 plants, and for null transgenic plants the data is average ± s.d. of 2-4 plants and average ± s.d. of 10 plants for *cv.* Fielder.

Flowering time measurements

Developmental flowering time by total leaf number was determined by counting leaves of the main stem until emergence of the flag leaf. Heading date was measured as the number of days since germination when the inflorescence first emerged from the sheath

475 on the main stem (Zadoks scale, *Z* = 47). Three independent flowering time experiments
476 were performed, with 10-20 plants measured in each experiment.

477

478 **Dissection of inflorescences and tillers**

479 Developing inflorescences and immature tillers were isolated with a binocular dissecting
480 microscope and then digitally photographed on a Leica MZ16 Stereo dissecting
481 microscope with a Leica DFC420 colour camera (Leica, Milton Keynes, UK). Developing
482 inflorescences were harvested at developmental stages determined by sequential
483 emergence of leaves from germination. Lengths of inflorescences were determined at
484 each developmental stage using Fiji Software (Schindelin et al. 2012), with the embedded
485 scale used as a reference. Two independent experiments were performed, with at least 4
486 inflorescences measured at each developmental stage. For tiller dissections, 6-8 plants
487 were examined of each genotype, with two independent experiments performed.

488 **Paired spikelet distribution analysis**

489 Paired spikelet distribution analysis was performed as described previously (Boden et al.
490 2015), with 12 inflorescences from 6 plants (6 main stems and 6 tiller inflorescences)
491 collected and phenotyped from each of the WT and *hb* genotypes.

492 **Fluorescence in situ hybridization (FISH) analysis**

493 Lines were characterised by FISH as described previously (Zhang et al. 2004). Plasmid
494 clone pSc119.2 contains highly repetitive sequences from rye, *Secale cereale* L.
495 (Bedbrook et al. 1980), whereas clone pAs1 contains a repetitive sequence that belongs to
496 the *Afa* family isolated from *Aegilops tauschii* Coss. (Rayburn and Gill, 1986). Using two
497 clones simultaneously, all B and D genome chromosomes and chromosomes 1A, 4A and
498 5A of hexaploid wheat can be identified[8]. One microgram of plasmid DNA of pSc119.2 and
499 pAs1 was labeled with fluorescein-12-dUTP (fluoresces green) and rhodamine-5-dUTP
500 (fluoresces red), respectively, using nick translation in accordance with the manufacturer's
501 protocol (Roche Diagnostic Australia, Sydney, Australia). The hybridisation and post-
502 hybridisation washes were conducted as described previously (Zhang et al. 2004).
503 Chromosomes were counterstained with 4′, 6-diamidino-2-phenylindole (DAPI) (Life
504 Technologies Australia, Thermo Fischer Scientific, Melbourne, Australia) and pseudo-
505 colored blue. Chromosome preparations were analyzed with a Zeiss Axio Imager
506 epifluorescence microscope (Carl Zeiss Microimaging, Jena, Germany). Images were
507 captured with a Retiga EXi CCD (charge-coupled device) camera (QImaging) operated

with Image-Pro Plus 7.0 software (Media Cybernetics Inc., Rockville, USA) and processed with Photoshop version 8.0 software (Adobe Systems).

DNA extractions and sequence analysis

Nucleotide sequences for *TB-A1, TB-B1* and *TB-D1* were obtained by BLAST search from the Ensembl Plants website, using the maize TB1 protein sequence as a query sequence. Genomic DNA extractions were performed as described previously (Paterson et al. 1993). Clones of *TB-B1* and *TB-D1* were amplified using Phusion DNA polymerase (New England Biolabs, Hitchin, UK), and the following oligonucleotides: *TB-B1*: ATGTTTCCTTTCTATGATTCCC, CATCCGGTTCTTTTCCC-TAGT and CGAGGGGAAGAAGCAGGTG, CACAAATAATCCATTGAACAAAGC; *TB-D1*: CTCTTC-CACCCGCAGACAC, TCAGTAGG- GCTGCGAGTTG. DNA fragments were sequenced using Big-Dye Terminator Sequencing v3.1 Ready Reaction Kit (Perkin Elmer, Applied BioSystems, Thermo Fischer Scientific, Loughborough, UK), or with Mix2Seq Kit (Eurofins, Ebersberg, Germany). Multiple nucleotide and protein sequence alignments of *TB-A1*, *TB-B1* and *TB-D1* were performed using MUSCLE. Pair-wise nucleotide and protein sequence alignments of *cv.* Chinese Spring reference sequences for *TB-B1* and *TB-D1* with alleles identified from other wheat varieties were performed using EMBOSS Needle, which were formatted in Microsoft Word. *TB-B1* and *TB-D1* alleles from wheat cultivars that contain sequence polymorphisms relative to the reference sequences from Chinese Spring were named *TB-B1b* and *TB-D1b*, following convention for naming alternate alleles for other wheat genes.

RNA extraction and expression analysis

RNA was extracted from tiller, root, young emerging leaf, mature leaf and seedling tissue using the SPECTRUM Plant Total RNA Kit (Sigma-Aldrich, Gillingham, UK), and from developing inflorescences using the RNeasy Plant Mini Kit (Qiagen, Manchester, UK). 'Tiller buds' refer to immature tillers that were transparent or light green in colour for which no leaf blade had begun to emerge, while 'Emerging tillers' refer to young tillers where leaf blade tissue was beginning to emerge from the coleoptile-like tissue. RNA was extracted from developing inflorescences at the double ridge stage, and inflorescences harvested at complete emergence of leaf 5, leaf 6 and leaf 7. Analysis of *FT* expression was performed using RNA extracted from leaves of WT and *hb* plants, which were grown under a SD photoperiod until the leaf 5 stage and then transferred to LD photoperiod for 7 days. Synthesis of cDNA and quantitative RT-PCR were performed as described previously (Boden et al. 2014). Oligonucleotides for quantitative RT-PCR analysis are provided in

Supplementary Table 8. Expression of candidate genes in leaves, roots, tillers and seedlings were normalised using RNA polymerase 15 kDa sub-unit (*TaRP15*; Shaw et al. 2012), and with Traes_6DS_BE8B5E56D.1 (Borrill et al. 2016) in developing inflorescences. All quantitative RT-PCR data points are the average of at least three biological replicates, with two technical replicates performed in each reaction.

Kompetitive Allele Specific PCR (KASP) analysis

Oligonucleotides for KASP analysis were designed using Polymarker (http://polymarker.tgac.ac.uk), and contained the standard FAM or HEX compatible tails (FAM tail: 5` GAAGGTGA-CCAAGTTCATGCT 3`; HEX tail: 5` GAAGGTCGGAG TCAACGGATT 3`). Oligonucleotide sequences are provided in Supplementary Table 9. The KASP assay was performed as described previously (Ramirez-Gonzalez et al. 2015), with the following modifications: assays were set up as 2.4-µL reactions [1.8µL template (10–20 ng of DNA) dried to assay plate, 1.18 µL of V4 2x Kaspar mix (LGC Group, Teddington, UK), 1.18µL dH_2O and 0.032 µL primer mix]; and the PCR cycling included hotstart at 95 °C for 15 min, followed by ten touchdown cycles (95 °C for 20 s; touchdown 65 °C, −1 °C per cycle, 25 s), then followed by 40 cycles of amplification (95 °C for 10 s; 57 °C for 60 s).

Droplet Digital PCR Reactions and data analysis

Droplet Digital PCR (ddPCR) was performed to determine gene copy numbers for *TB-B1* and *TB-D1*, in reference to *TaCONSTANS2* (*TaCO2)* that has a single copy on each of the three wheat genomes. Oligonucleotide sequences are provided in Supplementary Table 10. The ddPCR reaction mix included: 10 µL of 2X QX200 ddPCR EvaGreen Supermix (Bio-Rad, Watford, United Kingdom), 6 µL of genomic DNA template (2.5 ng/µL; 15 ng), 2 µL of mixed oligonucleotides (2 µM each), 0.2 µL of *Hind*III-HF (New England Biolabs), in a 20 µL reaction volume. Droplets were generated in 8-well cartridges, using the QX200 droplet generator (Bio-Rad). Water-in-oil emulsions were transferred to a 96-well plate and amplified in a C1000 Touch Thermal Cycler (Bio-Rad). Thermal cycling conditions were: 7 min at 95 °C; 40 cycles of a three-step thermal profile comprising of 30 s at 94 °C, 30 s at 60 °C and 1 min at 72 °C, with ramp rate 2.0 °C/s. After cycling, each sample was incubated at 90 °C for 5 min and then cooled to 4 °C. Plates were then transferred to the QX200 droplet reader (Bio-Rad). Data acquisition and analysis was performed using QuantaSoft (Bio-Rad) software to quantify numbers of positive droplets containing amplicons and negative droplets without amplicons. Calculations for copy number of *TB-B1* and *TB-D1* were performed in Microsoft Excel. As oligonucleotides for *TaCO2*

annealed to sequence and produced amplicons from the A, B and D genomes, gene copy numbers for *TB-B1* and *TB-D1* were determined by dividing the number of positive droplets for *TB-B1* and *TB-D1* by one-third of the number of positive droplets for *TaCO2*.

Construct design and wheat transformation

The construct used to generate *pVRN1:TB-D1* transgenic plants contained *TB-D1* with the G328T SNP present in *cv.* Baxter, WT and *hb* lines, as well as synonymous mutations (C30G, G309T and C1023G) that modified restriction sites to facilitate cloning and construct design. *Nco* I and *Not* I sites flanking the start and stop codon positions, respectively, were used to clone *TB-D1* into the *KR PRO 5* plasmid containing the *VRN1* promoter (Alonso-Peral et al. 2011) and the kanamycin resistance gene for selection. The *pVRN1:TB-D1* cassette was cloned into the *vecBarII* construct containing the *Tn7* Spectinomycin resistance gene, and the *BAR* open reading frame under the regulatory control of the *CaMV 35S* promoter and the *Agrobacterium tumefaciens* octopine synthase terminator sequences.

Transgenic wheat plants were generated by *Agrobacterium*-mediated transformation of the hexaploid wheat *cv.* Fielder, as described previously (Ishida et al. 2015; Richardson et al. 2014). Genomic DNA extractions were performed as described previously (Paterson et al. 1993), and genotype analysis of T_1 transgenic lines was performed as described previously using qRT-PCR (Mieog et al. 2013; Boden et al. 2014) and the $2^{-\Delta\Delta CT}$ method to determine relative copy number for *TB-D1*. Amplicons of *TB-D1* were amplified using oligonucleotides shown in Supplementary Table 10, and were normalised to *Epsilon Cyclase-A1* (oligonucleotides in Supplementary Table 10), which is present once on the '*A*' genome of wheat (Mieog et al. 2013). Normalised levels of *TB-D1* for each transgenic plant were then normalised to those identified for *cv.* Fielder, to determine relative copy numbers of *TB-D1* for each transgenic line. Data for qRT-PCR is the average of 2 technical replicates, with 100 ng of template DNA per reaction. Reactions were performed using the BIO-RAD CFX384 Real-Time System (Bio-Rad).

Yeast two-hybrid analysis

Yeast two-hybrid assays were performed at 28 °C in the yeast strain AH109 (Clontech, Saint-Germain-en-Laye, France) using the co-transformation technique (Egea-Cortines et al. 1999). Open reading frames of full length *TB-D1, TB-B1a*, *TB-B1b* and *FT*, and a truncated version of *TB-D1* (*TB1*Δ) that encodes a protein lacking the first 114 amino acids of the full-length protein, were cloned into the Gateway vector GAL4 system (*pGADT7* and

pGBKT7; Clontech) passing through *pDONR207* (Life Technologies, ThermoFischer Scientific, Loughborough, UK). Strength of protein interactions was tested on selective yeast synthetic dropout medium (YSD) lacking Leucine (L), Tryptophan (W), Adenine (A), and Histidine (H), supplemented with different concentrations of 3-aminotriazole (3-AT; 2.5 mM, 5 mM and 10mM). Images were taken 7 days after plating on the selective media.

Bimolecular fluorescence complementation analysis

Open reading frames of full length *TB-D1* and *FT*, and truncated *TB1* (*TB1*Δ) in *pDONR207* (Life Technologies) generated for the yeast-two-hybrid assay, were each cloned into *pYFPN43* and *pYFPC43*. *pEAQ-HT* vector (Sainsbury et al. 2009), which expresses the silencing suppressor *p19* of tomato bushy stunt virus, was added to the vector combination. BiFC was performed in *Nicotiana benthamiana* as described previously (Belda-Palazon et al. 2012). Images were taken with a Zeiss LSM780 confocal microscope 72 hours after infiltration.

Genetic analysis of NIAB Elite MAGIC population

Trial entries were arrayed in an incomplete block design using the software Block Designs U (http://www.expdesigns.co.uk). Paired spikelet phenotype data were analysed using GenStat (16th Edition, VSNi, UK) with a generalised linear mixed model (GLMM) employing a Poisson distribution with a logarithmic link function (Bolker et al. 2009) providing best linear unbiased estimate (BLUE) values. Broad sense heritability for the replicated trials was calculated as per equation one (Tenesa & Haley 2013); where σ_g^2 is the genotypic variance and σ^2 is the residual error variance with r replicates.

$$H^2 = \frac{\sigma_g^2}{\sigma_g^2 + \frac{\sigma^2}{r}} = \frac{V_g}{V_p} \qquad \text{Equation One}$$

In total, 643 F_5 lines from the 'NIAB Elite MAGIC' wheat population (Mackay et al. 2014) were genotyped using a wheat Illumina 90k iSelect array (Illumina, CA, USA) designed by Wang et al. (S. Wang et al. 2014) generating 18,601 polymorphic markers mapped to 7,369 unique genetic map locations (Gardner et al. 2016). Using these markers, a high confidence subset of identity by descent (IBD) segments were calculated in a three-point probabilistic manner (Huang & George 2011) for their parental contributions over the 7,369 uniquely mapped markers. Founder probabilities were assigned with a 33% threshold, as identity-by-descent relationships among the founders complicate direct observation of true parental origin. The resulting founder haplotype probabilities were used for composite interval mapping analysis.

642

643 QTL analysis was performed using an identity by descent composite interval mapping
644 (IBD-CIM) method (Milner et al. 2016). IBD-CIM was performed using the mpIM function of
645 the R package mpMap (Huang & George 2011). Primarily, a linear model was fitted for
646 estimation of the QTL fixed effects for every founder at each hypothetical QTL position
647 (with the founder 'Xi19' arbitrarily fixed as the reference haplotype). Simple interval
648 mapping (SIM) was run and then the inclusion of marker covariates was determined by a
649 forward selection process in an Akaike Information Criterion (AIC) dependent manner, up
650 to a maximum of five covariates. To determine significance thresholds, a null distribution is
651 formed with the same variance as the trial's score data and the significance threshold is
652 then determined empirically. The proportion of phenotypic variance explained by any given
653 QTL, accounting for all other QTL, is the square of the semi-partial correlation coefficient
654 (Milner et al. 2016) QTL nomenclature follows recommended rules, as listed in the
655 GrainGenes catalogue. (https://wheat.pw.usda.gov/ggpages/wgc/ 98/Intro.htm).

656 Genetic markers of interest were aligned to the unannotated IWGSC RefSeq v1.0
657 reference wheat genome sequence (cv. Chinese Spring 42, www.wheatgenome.org/)
658 using BLASTn with a maximum E-value threshold of 0.1 (Altschul et al. 1990). Annotation
659 within target regions was undertaken using GMap (Wu & Watanabe 2005) to map high-
660 confidence TGAC v1 gene models (Clavijo et al. 2017) (*cv.* Chinese Spring 42, Earlham
661 Institute) to IWGSC RefSeq v1.0 using 95% minimum identity and 80% minimum coverage
662 thresholds. The highest scoring BLASTx hit for the resulting gene models in wheat from
663 the SwissProt (UniProt Consortium 2016) database were identified with a maximum E-
664 value threshold of one (Supplementary Table 7).

665 **Statistical analysis**

666 Differences between treatments were tested by two-tailed Student's *t*-test. Results in
667 figures are shown as means ± standard error, except for Fig. 2h-i which is the mean ±
668 standard deviation because some null transgenic lines contained only two individuals. For
669 the *TB-B1* specific marker analysis of 212 UK winter wheat MAGIC lines, a McNemar's
670 test was performed using 1 degree of freedom.

671 **Accession numbers**

672 Accession numbers for all genes investigated in this study are provided in Supplementary
673 Tables 8 and 10.

674 **Supplemental Data Files**

675 Supplementary Table 1: Phenotype information for transgenic *pVRN1:TB1* lines, with
676 controls.

677 Supplementary Table 2: Phenotype information for *hb* revertant lines, relative to *hb*.

678 Supplementary Table 3: Proportion of rachis nodes with paired spikelets in subset of
679 modern wheat cultivars.

680 Supplementary Table 4: *TB-B1* alleles of modern winter wheat cultivars investigated in this
681 study.

682 Supplementary Table 5. Summary of paired spikelet QTL identified in the 'NIAB Elite
683 MAGIC' population using IBD-CIM.

684 Supplementary Table 6: Summary of predicted effect of seven founder alleles for QTL on
685 chromosome 4B, relative to Xi 19.

686 Supplementary Table 7: Summary of *TB-B1* specific KASP marker analysis of a subset of
687 212 NIAB MAGIC lines.

688 Supplementary Table 8: Oligonucleotide sequences used in qRT-PCR assays.

689 Supplementary Table 9: Oligonucleotide sequences used in KASP marker assays.

690 Supplementary Table 10: Oligonucleotide sequences used in digital droplet PCR (ddPCR)
691 assays.

692 Supplementary Figure 1: Schematic outlining pedigree of WT and *hb* lines from MAGIC
693 line 0053.

694 Supplementary Figure 2: Paired spikelets occur most frequently within the central region of
695 *hb* inflorescences.

696 Supplementary Figure 3: WT and *hb* inflorescences at the leaf 8 developmental stage.

697 Supplementary Figure 4: Immature tillers of WT and *hb* plants.

698 Supplementary Figure 5: Inflorescence architecture phenotypes of *Rht-D1* NILs.

699 Supplementary Figure 6: Expression analysis of genes from chromosome group 4 that are
700 in proximity to *Rht-1* and *TB1*.

701 Supplementary Figure 7: Inflorescence architecture phenotypes of *pVRN1:TB1* transgenic
702 plants.

703 Supplementary Figure 8: KASP marker analysis of *Rht-B1* in *hb* and revertant lines.

704 Supplementary Figure 9: TEOSINTE BRANCHED1 interacts with FLOWERING LOCUS T.

Supplementary Figure 10: Expression analysis of *FLOWERING LOCUS T* in WT and *hb* plants.

Supplementary Figure 11: Alignment of coding nucleotide sequence (CDS) for *TB-D1a* and *TB-D1b* alleles.

Supplementary Figure 12: Alignment of predicted amino acid sequence for TB-D1a and TB-D1b.

Supplementary Figure 13: Paired spikelet development in modern winter wheat cultivars.

Supplementary Figure 14: Analysis of copy number variation for *TB-D1* and *TB-B1* in winter wheat.

Supplementary Figure 15: Alignment of coding nucleotide sequence (CDS) for *TB-B1a* and *TB-B1b* alleles.

Supplementary Figure 16: Alignment of amino acid sequence for TB-B1a and TB-B1b .

Supplementary Figure 17: Chromosome-wide CIM scans displaying 4B QTL that contribute to paired spikelet development in the UK wheat MAGIC population.

Supplementary Data Set 1: Paired spikelet phenotypes for modern winter wheat cultivars.

Supplementary Data Set 2: Summary of *TB-B1* allele genotypes for GEDIFLUX population.

Author contributions

SAB, LED, JRG and SMS designed the research. SAB and LED performed phenotype and genotype analyses of WT and *hb* plants, modern wheat cultivars and MAGIC lines, and conducted expression analysis. JG analysed transgenic plants and performed expression analysis. SB performed Y2H and BiFC assays. PZ performed FISH experiments. JC and GM collected MAGIC phenotype data and performed QTL analysis. SMS, KR and CC performed initial genotype analysis and characterization of MAGIC line 0053. SAB, LED and JRG wrote the manuscript.

Acknowledgements

We acknowledge the BBSRC (BBS/E/J/000C0677; BB/M011666/1 and BB/N00518X/1), the Royal Society (UF150081), International Wheat Yield Partnership and a CSIRO O.C.E. Fellowship for funding this research. We also acknowledge: Grant Calder, Sara Simonini, Simon Griffiths, Richard Goram (all JIC), Matthew Moscou and Inma Hernandez-Pinzon

(TSL), and Beatrice Corsi (NIAB) for technical assistance, Ben Trevaskis (CSIRO) for the *VRN1* promoter, Jacob Lage and Nicholas Bird (KWS) for access to field trials of modern wheat cultivars, and Keith Gardner (NIAB) for genetic mapping guidance. We thank the Wheat Genetic Improvement Network for access to the GEDIFLUX collection.

Competing interests

The authors declare that there are no competing interests.

References

Abe M, Kobayashi Y, Yamamoto S, Daimon Y, Yamaguchi A, Ikeda Y, Ichinoki H, Notaguchi M, Goto K, Araki T. 2005. FD, a bZIP protein mediating signals from the floral pathway integrator FT at the shoot apex. *Science* 309: 1052–1056.

Aguilar-Martinez JA, Poza-Carrion C, Cubas P. 2007. Arabidopsis *BRANCHED1* acts as an integrator of branching signals within axillary buds. *The Plant Cell* 19: 458–472.

Alonso-Peral MM, Oliver SN, Casao MC, Greenup AA, Trevaskis B. 2011. The promoter of the cereal VERNALIZATION1 gene is sufficient for transcriptional induction by prolonged cold. *PLoS ONE* 6: e29456.

Altschul, S, Gish, W, Miller, W. 1990. Basic local alignment search tool. *Journal of Molecular Biology* 215, 403–410 (1990).

Beales J, Turner A, Griffiths S, Snape JW, Laurie DA. 2007. A Pseudo-Response Regulator is misexpressed in the photoperiod insensitive *Ppd-D1a* mutant of wheat (*Triticum aestivum* L.). *Theoretical and Applied Genetics* 115: 721–733.

Bedbrook, JR, Jones, J, O'Dell, M, Thompson, R, Flavell, RB. 1980. A molecular description of telomeric heterochromatin in *Secale* species. *Cell* 19, 545–560.

Belda-Palazon B, Ruiz L, Marti E, Tarrage S, Tiburcio AF, Culianez F, Farras R, Carrasco P, Ferrando A. 2012. Aminopropyltransferases involved in polyamine biosynthesis localize preferentially in the nucleus of plant cells. *PLoS ONE* 7: e46907.

Boden SA, Cavanagh C, Cullis BR, Ramm K, Greenwood J, Finnegan EJ, Ben Trevaskis, Swain SM. 2015. *Ppd-1* is a key regulator of inflorescence architecture and paired spikelet development in wheat. *Nature Plants* 1:14016.

Boden SA, Weiss D, Ross JJ, Davies NW, Trevaskis B, Chandler PM, Swain SM. 2014. *EARLY FLOWERING3* regulates flowering in spring barley by mediating gibberellin production and *FLOWERING LOCUS T* expression. *The Plant Cell* 26: 1557–1569.

Bolker BM, Brooks ME, Clark CJ, Geange SW, Poulsen JR, Stevens MHH, White J-SS.

2009. Generalized linear mixed models: a practical guide for ecology and evolution. *Trends in Ecology and Evolution* 24: 127–135.

Bommert P, Nagasawa NS, Jackson D. 2013. Quantitative variation in maize kernel row number is controlled by the *FASCIATED EAR2* locus. *Nature Genetics* 45: 334–337.

Borrill P, Ramirez-Gonzalez R, Uauy C. 2016. expVIP: a customizable RNA-seq data analysis and visualization platform. *Plant Physiology* 170: 2172–2186.

Clavijo BJ, Venturini L, Schudoma C, Accinelli GG, Kaithakottil G, Wright J, Borrill P, Kettleborough G, Heavens D, Chapman, H *et al.* 2017. An improved assembly and annotation of the allohexaploid wheat genome identifies complete families of agronomic genes and provides genomic evidence for chromosomal translocations. *Genome Research*: doi:10.1101/gr.217117.116.

Consortium TU. 2016. UniProt: the universal protein knowledgebase. *Nucleic Acids Research* 45: D158–D169.

Crop Committee Handbook. 2013. *Crop Committee Handbook*. Agriculture and Horticulture Development Board Cereals and Oilseeds.

Debernardi JM, Lin H, Chuck G, Faris JD, Dubcovsky J. 2017. microRNA172 plays a crucial role in wheat spike morphogenesis and grain threshability. *Development* 144: 1966–1975.

Dobrovolskaya O, Pont C, Sibout R, Martinek P, Badaeva E, Murat F, Chosson A, Watanabe N, Prat E, Gautier N, *et al.* 2014. *FRIZZY PANICLE* drives supernumerary spikelets in bread wheat (*T. aestivum* L.). *Plant Physiology* 167: 189–199.

Doebley J, Stec A, Gustus C. 1995. *teosinte branched1* and the origin of maize: Evidence for epistasis and the evolution of dominance. *Genetics* 141: 333–346.

Doebley J, Stec A, Hubbard L. 1997. The evolution of apical dominance in maize. *Nature* 386: 485–488.

Egea-Cortines M, Saedler H, Sommer H. 1999. Ternary complex formation between the MADS-box proteins SQUAMOSA, DEFICIENS and GLOBOSA is involved in the control of floral architecture in *Antirrhinum majus*. *The EMBO Journal* 18: 5370–5379.

Fischer T, Byerlee D, Edmeades G. 2014. *Crop yields and global food security*. Australian Centre of International Agricultural Research.

Gardner KA, Wittern LM, Mackay IJ. 2016. A highly recombined, high-density, eight-founder wheat MAGIC map reveals extensive segregation distortion and genomic locations of introgression segments. *Plant Biotechnology Journal* 14: 1406–1417.

Gonzalez FG, Miralles DJ, Slafer GA. 2011. Wheat floret survival as related to pre-anthesis spike growth. *Journal of Experimental Botany* 62: 4889–4901.

González-Navarro OE, Griffiths S, Molero G, Reynolds MP, Slafer GA. 2015. Dynamics of floret development determining differences in spike fertility in an elite population of wheat. *Field Crops Research* 172: 21–31.

Greenwood JR, Finnegan EJ, Watanabe N, Trevaskis B, Swain SM. 2017. New alleles of the wheat domestication gene *Q* reveal multiple roles in growth and reproductive development. *Development* 144: 1959–1965.

Guo Z, Schnurbusch T. 2015. Variation of floret fertility in hexaploid wheat revealed by tiller removal. *Journal of Experimental Botany* 66: 5945–5958.

Hedden P. 2013. The genes of the Green Revolution. *Trends in Genetics* 19: 5–9.

Houston K, McKim SM, Comadran J, Bonar N, Druka I, Uzrek N, Cirillo E, Guzy-Wrobelska J, Collins NC, Halpin C, *et al.* 2013. Variation in the interaction between alleles of HvAPETALA2 and microRNA172 determines the density of grains on the barley inflorescence. *Proceedings of the National Academy of Sciences of USA* 110: 16675–16680.

Huang BE, George AW. 2011. R/mpMap: a computational platform for the genetic analysis of multiparent recombinant inbred lines. *Biochemistry* 27: 727–729.

Huang BE, George AW, Forrest KL, Kilian A, Hayden MJ, Morell MK, Cavanagh CR. 2012. A multiparent advanced generation inter-cross population for genetic analysis in wheat. *Plant Biotechnology Journal* 10: 826–839.

Hubbard L, McSteen P, Doebley J, Hake S. 2002. Expression patterns and mutant phenotype of teosinte branched1 correlate with growth suppression in maize and teosinte. *Genetics* 162: 1927–1935.

Ishida Y, Tsunashima M, Hiei Y, Komari T. 2015. Wheat transformation. Wang K ed. *Agrobacterium* protocols: methods in molecular biology. Springer, 189–198.

Jiao Y, Wang Y, Xue D, Wang J, Yan M, Liu G, Dong G, Zeng D, Lu Z, Zhu X, *et al.* 2010. Regulation of *OsSPL14* by *OsmiR156* defines ideal plant architecture in rice. *Nature Genetics* 42: 541–544.

Kosugi S, Ohashi Y. 1997. PCFI and PCF2 specifically bind to *cis* elements in the rice proliferating cell nuclear antigen gene. *The Plant Cell* 9: 1607–1619.

Kyozuka J, Tokunaga H, Yoshida A. 2014. Control of grass inflorescence form by the fine-tuning of meristem phase change. *Current Opinion in Plant Biology* 17: 110–115.

Lemmon ZH, Park SJ, Jiang K, Van Eck J, Schatz MC, Lippman ZB. 2016. The evolution of inflorescence diversity in the nightshades and heterochrony during meristem maturation. *Genome Research* 26: 1676–1686.

Lewis JM, Mackintosh CA, Shin S, Gilding E, Kravchenko S, Baldridge G, Zeyen R,

838 Muehlbauer GJ. 2008. Overexpression of the maize *Teosinte Branched1* gene in wheat
839 suppresses tiller development. *Plant Cell Reports* 27: 1217–1225.

840 Li C, Lin H, Dubcovsky J. 2015. Factorial combinations of protein interactions generate a
841 multiplicity of florigen activation complexes in wheat and barley. *The Plant Journal* 84: 70–
842 82.

843 Luo D, Carpenter R, Vincent C, Copsey L, Coen E. 1996. Origin of floral asymmetry in
844 *Antirrhinum*. *Nature* 383: 794–799.

845 Mackay IJ, Bansept-Balser P, Barber T, Bentley AR, Cockram J, Gosman N, Greenland
846 AJ, Horsnell R, Howells R, O'Sullivan D, *et al.* 2014. An eight-parent multiparent advanced
847 generation inter-cross Population for winter-sown wheat: creation, properties, and
848 validation. *G3-Genes, Genomes, Genetics* 4: 1603–1610.

849 Meyer RS, Purugganan MD. 2013. Evolution of crop species: genetics of domestication
850 and diversification. *Nature Reviews Genetics* 14: 840–852.

851 Mieog JC, Howitt CA, Ral J-P. 2013. Fast-tracking development of homozygous transgenic
852 cereal lines using a simple and highly flexible real-time PCR assay. *BMC Plant Biology* 13:
853 71.

854 Milner SG, Maccaferri M, Huang BE, Mantovani P, Massi A, Frascaroli E, Tuberosa R,
855 Salvi S. 2016. A multiparental cross population for mapping QTL for agronomic traits in
856 durum wheat (*Triticum turgidum* ssp. durum). *Plant Biotechnology Journal* 14: 735–748.

857 Miralles D, Richards RA, Slafer GA. 2000. Duration of the stem elongation period
858 influences the number of fertile florets in wheat and barley. *Australian Journal of Plant*
859 *Physiology* 27: 931–940.

860 Miura K, Ikeda M, Matsubara A, Song X-J, Ito M, Asano K, Matsuoka M, Kitano H, Ashikari
861 M. 2010. *OsSPL14* promotes panicle branching and higher grain productivity in rice.
862 *Nature Genetics* 42: 545–549.

863 Niwa M, Daimon Y, Kurotani KI, Higo A, Pruneda-Paz JL, Breton G, Mitsuda N, Kay SA,
864 Ohme-Takagi M, Endo M, *et al.* 2013. BRANCHED1 interacts with FLOWERING LOCUS
865 T to repress the floral transition of the axillary meristems in *Arabidopsis*. *The Plant Cell* 25:
866 1228–1242.

867 Park SJ, Jiang K, Schatz MC, Lippman ZB. 2012. Rate of meristem maturation determines
868 inflroescence architecture in tomato. *Proceedings of the National Academy of Sciences of*
869 *USA* 109: 639–644.

870 Park SJ, Jiang K, Tal L, Yichie Y, Gar O, Zamir D, Eshed Y, Lippman ZB. 2014.
871 Optimization of crop productivity in tomato using induced mutations in the florigen
872 pathway. *Nature Genetics* 46: 1337–1342.

873 Paterson, AH, Brubaker, CL, Wendel, JF 1993. A rapid method for extraction of cotton

(*Gossypium* ssp.) genomic DNA suitable for RFLP and PCR analysis. *Plant Molecular Biology Reporter* 11: 122-127.

Pearce S, Saville R, Vaughan SP, Chandler PM, Wilhelm EP, Sparks CA, Al-Kaff N, Korolev A, Boulton MI, Phillips AL, *et al.* 2011. Molecular characterization of *Rht-1* dwarfing genes in hexaploid wheat. *Plant Physiology* 157: 1820–1831.

Poursarebani N, Seidensticker T, Koppolu R, Trautewig C, Gawronski P, Bini F, Govind G, Rutten T, Sakuma S, Tagiri A, *et al.* 2015. The genetic basis of composite spike form in barley and 'Miracle-Wheat'. *Genetics* 201: 155–165.

Ramirez-Gonzalez R, Segovia V, Bird N, Fenwick P, Holdgate S, Berry S, Jack P, Caccamo M, Uauy C. 2015. RNA-Seq bulked segregant analysis enables the identification of high-resolution genetic markers for breeding in hexaploid wheat. *Plant Biotechnology Journal* 13: 613–624.

Ramsay L, Comadran J, Druka A, Marshall DF, Thomas WTB, Macaulay M, MacKenzie K, Simpson C, Fuller J, Bonar N, *et al.* 2011. *INTERMEDIUM-C*, a modifier of lateral spikelet fertility in barley, is an ortholog of the maize domestication gene *TEOSINTE BRANCHED 1*. *Nature Genetics* 43: 169–172.

Rawson HM. 1970. Spikelet number, its control and relation to yield per ear in wheat. *Australian Journal of Biological Science* 23: 1–15.

Rayburn, AL, Gill, BS. 1986. Isolation of a D-genome specific repeated DNA sequence from *Aegilops squarrosa*. *Plant Mol. Biol. Rep.* 4, 102–109.

Reynolds M, Foulkes MJ, Slafer GA, Berry P, Parry MAJ, Snape JW, Angus WJ. 2009. Raising yield potential in wheat. *Journal of Experimental Botany* 60: 1899–1918.

Richardson, T, Thistleton, J, Higgins, TJ, Howitt, C, Ayliffe, M. 2014. Efficient *Agrobacterium* transformation of elite wheat germplasm without selection. *Plant Cell Tissue Organ Culture* 119, 647- 659.

Sainsbury F, Thuenemann EC, Lomonossoff GP. 2009. *pEAQ*: versatile expression vectors for easy and quick transient expression of heterologous proteins in plants. *Plant Biotechnology Journal* 7: 682–693.

Schindelin J, Arganda-Carreras I, Frise E, Kaynig V, Longair M, Pietzsch T, Preibisch S, Rueden C, Saalfield S, Schmid B, *et al.* 2012. Fiji: an open-source platform for biological-image analysis. *Nature Methods* 9: 676–682.

Sharman BC. 1944. Branched heads in wheat and wheat hybrids. *Nature*: 497–498.

Sharman BC. 1967. Interpretation of the morphology of various naturally occurring abnormalities of the inflorescence of wheat *(Triticum*). *Canadian Journal of Botany* 45: 2073–2080.

Shaw LM, Turner AS, Laurie DA. 2012. The impact of photoperiod insensitive *Ppd-1a*

mutations on the photoperiod pathway across the three genomes of hexaploid wheat (*Triticum aestivum*). *The Plant Journal* 71: 71–84.

Simons KJ, Fellers JP, Trick HN, Zhang Z, Tai Y-S, Gill BS, Faris JD. 2005. Molecular characterization of the major wheat domestication gene *Q*. *Genetics* 172: 547–555.

Slafer GA. 2003. Genetic basis of yield as viewed from a crop physiologist's perspective. *Annals of Applied Biology* 142: 117–128.

Soyk S, Lemmon ZH, Oved M, Fisher J, Liberatore KL, Park SJ, Goren A, Jiang K, Ramos A, van der Knaap E, *et al.* 2017. Bypassing negative epistasis on yield in tomato imposed by a domestication gene. *Cell* 169: 1142–1155.

Studer A, Zhao Q, Ross-Ibarra J, Doebley J. 2011. Identification of a functional transposon insertion in the maize domestication gene. *Nature Genetics* 43: 1160–1163.

Takeda T, Suwa Y, Suzuki M, Kitano H, Ueguchi-Tanaka M, Ashikari M, Matsuoka M, Ueguchi C. 2003. The OsTB1 gene negatively regulates lateral branching in rice. *The Plant Journal*: 513–520.

Taoka K-I, Ohki I, Tsuji H, Furuita K, Hayashi K, Yanase T, Yamaguchi M, Nakashima C, Purwestri YA, Tamaki S, *et al.* 2011. 14-3-3 proteins act as intracellular receptors for rice Hd3a florigen. *Nature* 476: 332–335.

Tatematsu K, Nakabayashi K, Kamiya Y, Nambara E. 2008. Transcription factor AtTCP14 regulates embryonic growth potential during seed germination in Arabidopsis thaliana. *The Plant Journal* 53: 42–52.

Tenesa A, Haley CS. 2013. The heritability of human disease: estimation, uses and abuses. *Nature Reviews Genetics* 14: 139–149.

Wang L, Sun S, Jin J, Fu D, Yang X, Weng X, Xu C, Li X, Xiao J, Zhang Q. 2015. Coordinated regulation of vegetative and reproductive branching in rice. *Proceedings of the National Academy of Sciences of USA* 112: 15504–15509.

Wang S, Wong D, Forrest K, Allen A, Chao S, Huang BE, Maccaferri M, Salvi S, Milner SG, Cattivelli L, *et al.* 2014. Characterization of polyploid wheat genomic diversity using a high-density 90 000 single nucleotide polymorphism array. *Plant Biotechnology Journal* 12:787-796.

Wigge PA, Kim MC, Jaeger KE, Busch W, Schmid M, Lohmann JU, Weigel D. 2005. Integration of spatial and temporal information during floral induction in Arabidopsis. *Science* 309: 1056–1059.

Wu TD, Watanabe CK. 2005. GMAP: a genomic mapping and alignment program for mRNA and EST sequences. *Biochemistry* 21: 1859–1875.

Yan L, Loukoianov A, Tranquilli G, Helguera M, Fahima T, Dubcovsky J. 2003. Positional

945 cloning of the wheat vernalization gene *VRN1*. *Proceedings of the National Academy of*
946 *Sciences of USA*100: 6263–6268.

947 Yoshida A, Sasao M, Yasuno N, Takagi K, Daimon Y, Chen R, Yamazaki R, Tokunaga H,
948 Kitaguchi Y, Sato Y, *et al.* 2012. *TAWAWA1*, a regulator of rice inflorescence architecture,
949 functions through suppression of meristem phase transition. *Proceedings of the National*
950 *Academy of Sciences of USA* 110: 767–772.

951 Zhang D, Yuan Z. 2014. Molecular control of grass inflorescence development. *Annual*
952 *Review of Plant Biology* 65: 553-578

953 Zhang P, Li W, Fellers JP, Friebe B. 2004. BAC-FISH in wheat identifies chromosome
954 landmarks consisting of different types of transposable elements. *Chromosoma* 112: 288–
955 299.

956 Zhu Z, Tan L, Fu Y, Liu F, Cai H, Xie D, Wu F, Wu J, Matsumoto T, Sun C. 2013. Genetic
957 control of inflorescence architecture during rice domestication. *Nature Communications* 4:
958 2200.

959 **Figure legends**
960
961 **Figure 1: Inflorescence architecture and development and tiller number are modified**
962 **in *highly-branched* (*hb*) plants. A**) Wild-type (WT) and *hb* inflorescences, with secondary
963 spikelets highlighted in blue. Scale bar 1 cm. **B**) Frequency of total paired spikelets (TPS)
964 and complete fertile paired spikelets (CPS) and **C**) rachis node numbers of WT and *hb*
965 inflorescences. **D, E**) Flowering time of WT and *hb* plants, measured by **D**) days to
966 anthesis and **E**) total leaf number. **F, G**) Inflorescence development phenotypes of WT
967 (black) and *hb* (blue) plants, measured at intervals defined by leaf emergence. Insert
968 shown in (**G**) is mature inflorescence length for WT (black) and *hb* (blue). Scale bar, 1 mm.
969 **H, I**) Tiller numbers of WT and *hb* plants. Scale bar 10 cm. Data are mean ± s.e.m. (n = 8
970 plants for **B – E**; **I**; n = 4 for **G,** n = 10 for **G** insert). All images are representatives of
971 individuals used for quantification. **p < 0.01; ***p < 0.001.

972 **Figure 2: Genetic characterization and expression analysis reveals increased**
973 **dosage of *TB-D1* in *hb* NILs. A, B**) FISH analysis of (**A**) WT and (**B**) *hb* lines, copies of
974 chromosome 4D are labeled. **C**) Schematic diagram of chromosome 4DS region in
975 proximity to *Rht-D1.* **D**) Digital droplet PCR analysis of haploid gene copy number for *TB-*
976 *D1* in WT and *hb* lines. **E**) Relative expression of *TB-A1*, *TB-B1* and *TB-D1* in developing
977 inflorescences of WT (solid bars) and *hb* (white bars) plants, at double ridge (DR, grey),
978 leaf 5 (L5, blue), leaf 6 (L6, green) and leaf 7 (L7, magenta) developmental stages.

Expression is relative to *TB-B1* in WT. **F**) Expression analysis of *TB-A1* (grey), *TB-B1* (red) and *TB-D1* (purple) in vegetative tissues of WT (solid bars) and *hb* (white bars) plants. Data of ddPCR and expression analyses are mean ± s.e.m. of 3-4 biological replicates. *$p < 0.05$; **$p < 0.01$

Figure 3: Increased dosage of *TB1* promotes paired spikelet development. A) Inflorescences of *pVRN1:TB1* transgenic plants, and the WT untransformed control (Fielder). **B**) Frequency of paired spikelets and (**C**) *TB-D1* haploid gene copy number for *pVRN1:TB1* transgenic plants (white) and control (grey, null transgenic; black, Fielder) lines. **D-F**) Plant (**D**) and inflorescence (**E**) architecture phenotypes of *hb* and revertant lines, with (**F**) quantification of paired spkelets per inflorescence and tiller numbers per plant. Secondary spikelets highlighted in blue. **G**) KASP marker analysis of *TB-B1* in *hb* (red) and revertant (magenta) lines, along with no template control (NTC, black). Scale bars, 10 cm (**D**) and 1 cm (**A**, **E**). All images are representatives of individuals used for quantification. Data of ddPCR and expression analyses are mean ± s.e.m. of 3-4 biological replicates. Data for transgenic lines are mean ± s.d. of 2-4 plants per transgenic genotype, 10 plants for (WT) Fielder. ***$p < 0.001$.

Figure 4: TB1 interacts with FLOWERING LOCUS T and modulates expression of meristem identity genes. A) Yeast two-hybrid (Y2H) assay between TB1 and FT, including control reactions with truncated TB-D1 (TB1Δ) and empty vectors (Ø), grown on varying selective media. **B**) Bimolecular fluorescence complementation (BiFC) assay for TB1 and FT, and control reactions including truncated TB-D1 (TB1Δ) and empty vectors (Ø). **C**) Schematic of full-length TB1 and truncated TB1 (TB1Δ) proteins used for Y2H and BiFC assays; TCP and R refer to domains of TB1 protein, numbers indicate amino acid positions. **D**) Expression of meristem identity genes in developing inflorescences of *hb* (white bars), relative to WT (solid bars), at double ridge (DR, grey), leaf 5 (L5, blue), leaf 6 (L6, green) and leaf 7 (L7, magenta) developmental stages. Data are mean ± s.e.m. of 4 biological replicates. *$p < 0.05$; **$p < 0.01$.

Figure 5: Allelic variation for *TB-B1* and *TB-D1* contributes to inflorescence architecture diversity in spring and winter wheat. A-B) Schematic diagrams of variant alleles for *TB-D1* (**A**, *TB-D1b*) from spring wheat and *TB-B1* (**B**, *TB-B1b*) from winter wheat, with positions of polymorphisms (indicated in red text) and molecular effect indicated (Syn., synonymous). TCP and R refer to genic regions that encode domains of the TB1 protein. **C**) Geographical distribution of *TB-B1a* (purple) and *TB-B1b* (red) alleles

in European wheat cultivars of the GEDIFLUX collection. **D**) Genome-wide composite interval mapping scan displaying QTL that contribute to paired spikelet development from the UK winter wheat MAGIC population from the (2015 trial, including a highly significant QTL on chromosome 4B (indicated by yellow star). Red line indicates threshold of high significance ($p < 0.01$). **E**) Y2H assay between TB-B1 alleles (TB-B1a and TB-B1b) and FT, including control reactions with empty vectors (Ø), grown on varying selective media. A 10-fold serial dilution was performed for each interaction experiment.

Figure 6: A model explaining the effect of increased dosage of TB1 on spikelet development in wheat. Increased levels of TB1 restrict the interaction of FT with other members of the floral activating complex (FDL and 14-3-3), which reduces expression of meristem identity genes (e.g. *VRN1*) and facilitates paired spikelet development. At standard levels of TB1, the floral activating complex promotes robust expression of meristem identity genes, and paired spikelet development is suppressed.

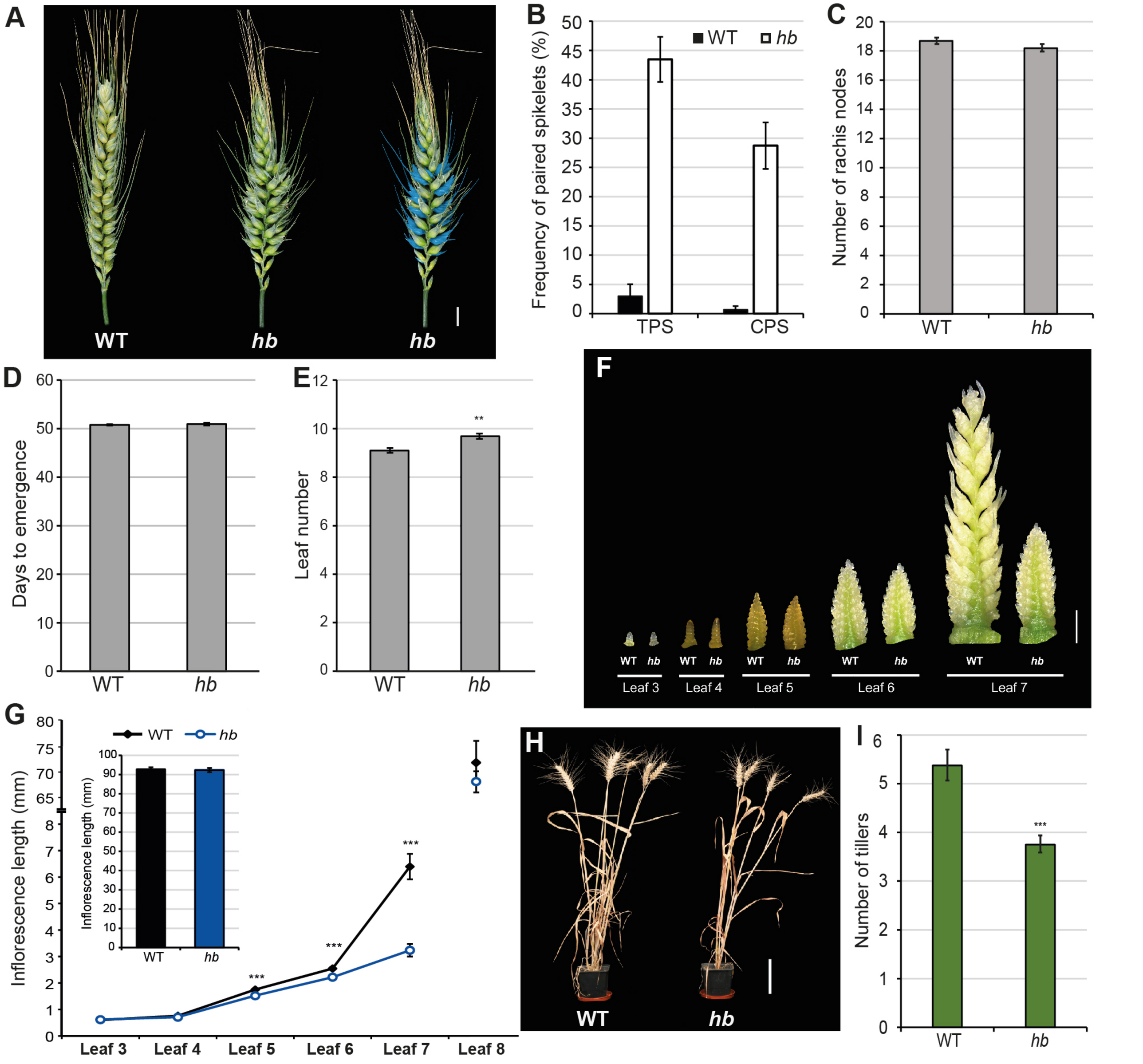

Figure 1: Inflorescence architecture and development and tiller number are modified in *highly-branched* (*hb*) plants. A) Wild-type (WT) and *hb* inflorescences, with secondary spikelets highlighted in blue. Scale bar 1 cm. **B**) Frequency of total paired spikelets (TPS) and complete fertile paired spikelets (CPS) and **C**) rachis node numbers of WT and *hb* inflorescences. **D, E**) Flowering time of WT and *hb* plants, measured by **D**) days to anthesis and **E**) total leaf number. **F, G**) Inflorescence development phenotypes of WT (black) and *hb* (blue) plants, measured at intervals defined by leaf emergence. Insert shown in (**G**) is mature inflorescence length for WT (black) and *hb* (blue). Scale bar, 1 mm. **H, I**) Tiller numbers of WT and *hb* plants. Scale bar 10 cm. Data are mean ± s.e.m. (n = 8 plants for **B – E**; **I**; n = 4 for **G,** n = 10 for **G** insert). All images are representatives of individuals used for quantification. $^{**}p < 0.01$; $^{***}p < 0.001$.

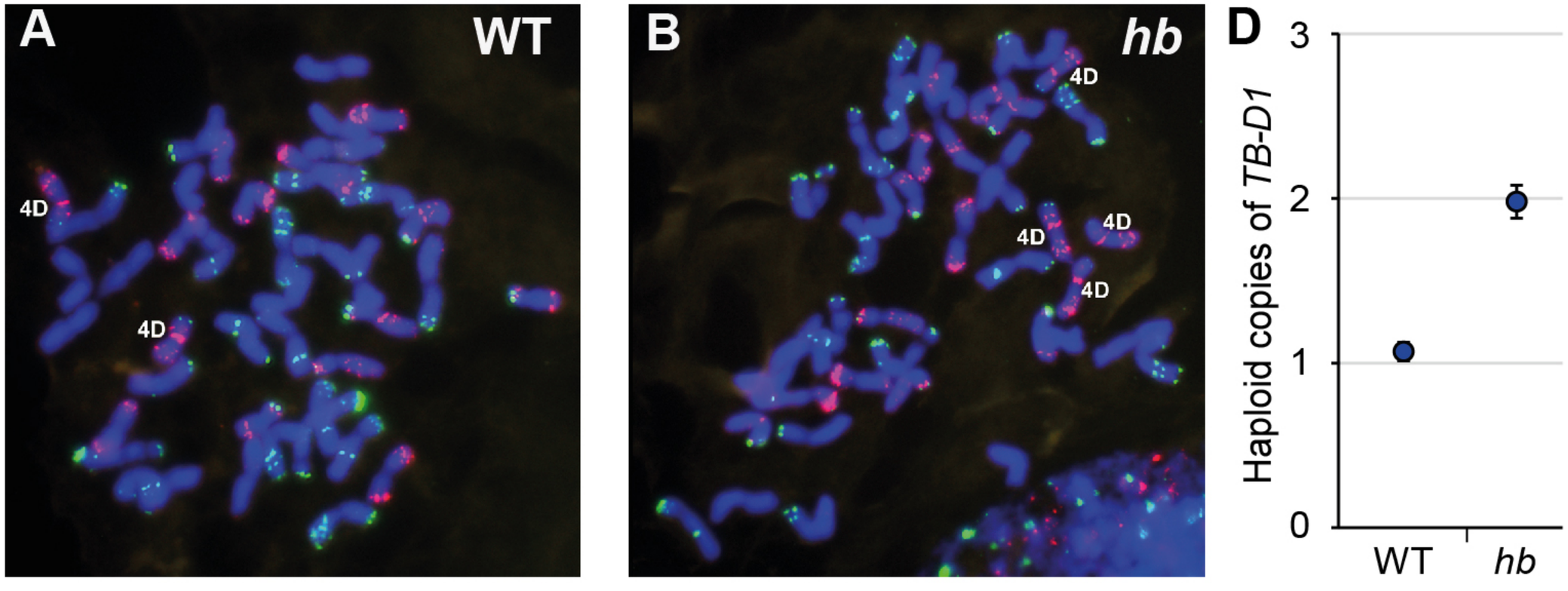

Figure 2: Genetic characterization and expression analysis reveals increased dosage of *TB-D1* in *hb* NILs. A, B) FISH analysis of (**A**) WT and (**B**) *hb* lines, copies of chromosome 4D are labeled. **C**) Schematic diagram of chromosome 4DS region in proximity to *Rht-D1.* **D**) Digital droplet PCR analysis of haploid gene copy number for *TB-D1* in WT and *hb* lines. **E**) Relative expression of *TB-A1*, *TB-B1* and *TB-D1* in developing inflorescences of WT (solid bars) and *hb* (white bars) plants, at double ridge (DR, grey), leaf 5 (L5, blue), leaf 6 (L6, green) and leaf 7 (L7, magenta) developmental stages. Expression is relative to *TB-B1* in WT. **F**) Expression analysis of *TB-A1* (grey), *TB-B1* (red) and *TB-D1* (purple) in vegetative tissues of WT (solid bars) and *hb* (white bars) plants. Data of ddPCR and expression analyses are mean ± s.e.m. of 3-4 biological replicates. *$p < 0.05$; **$p < 0.01$

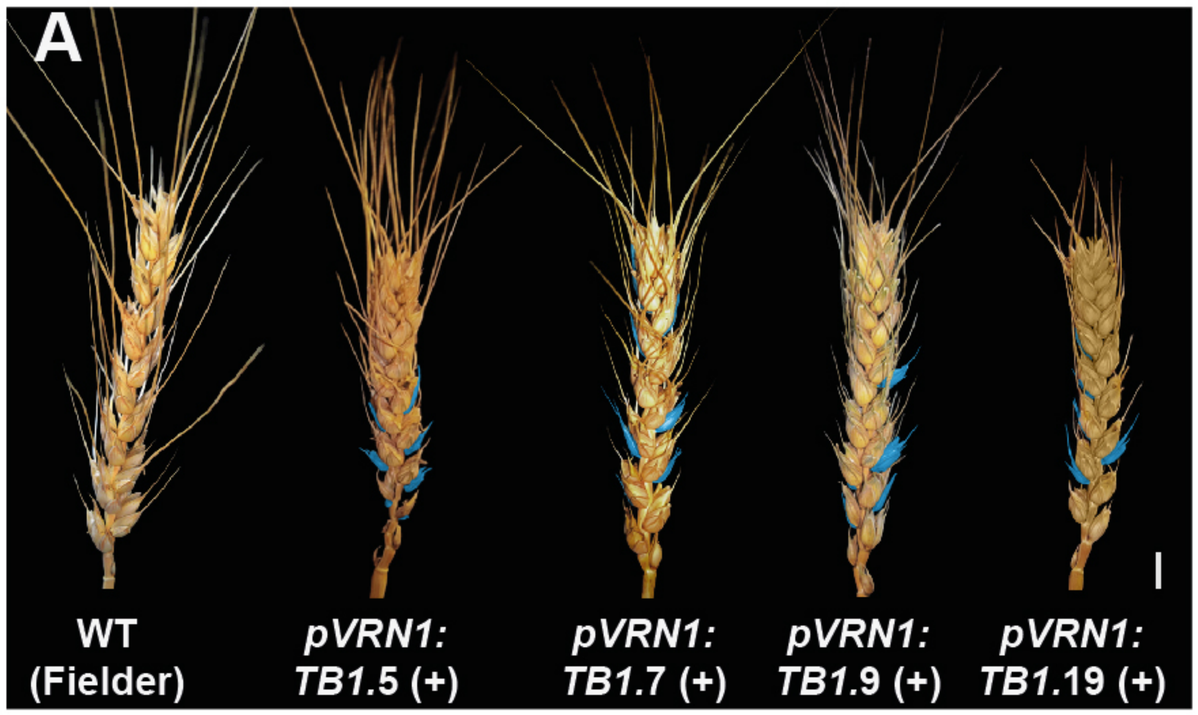

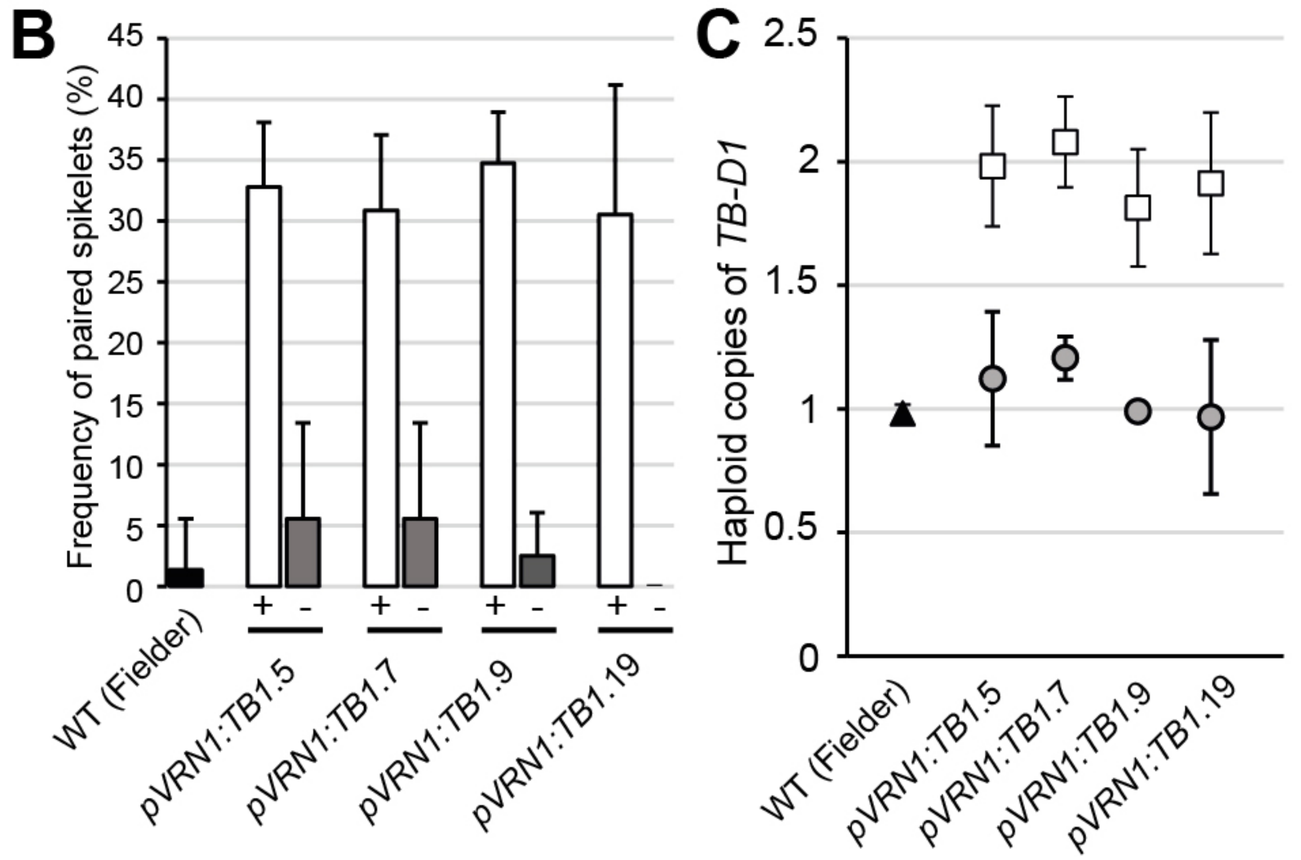

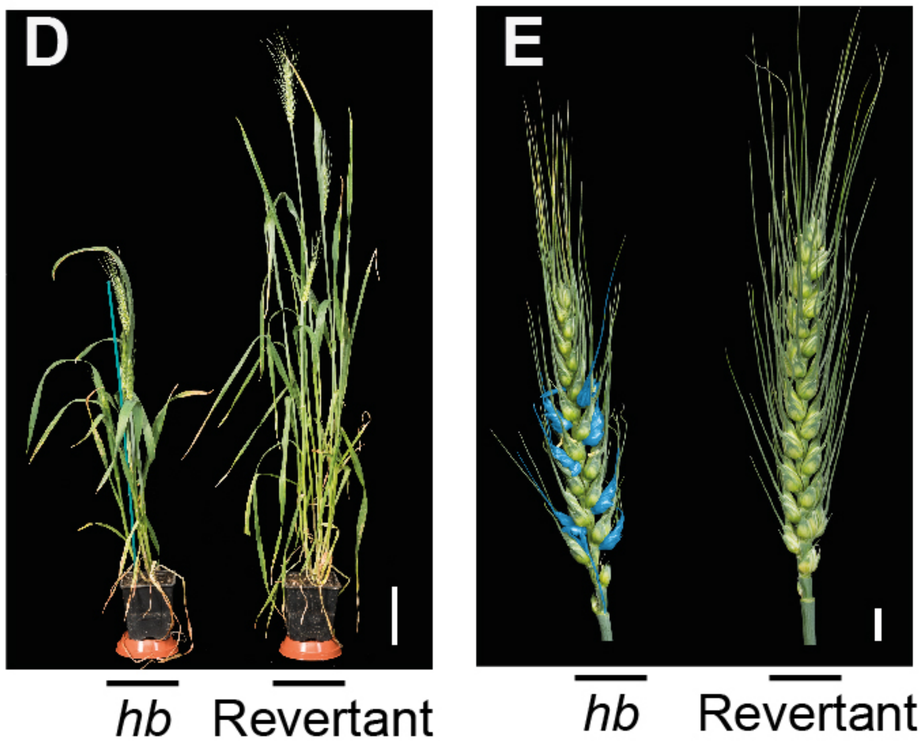

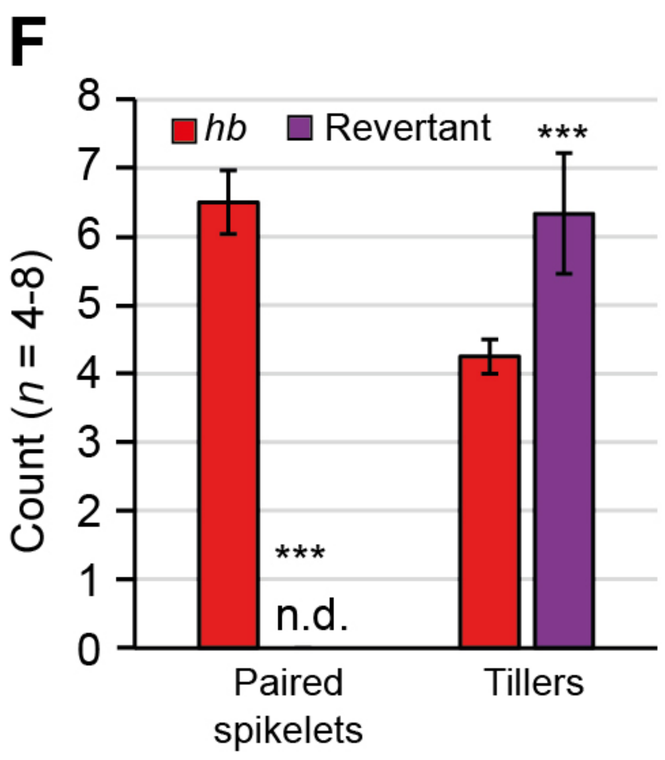

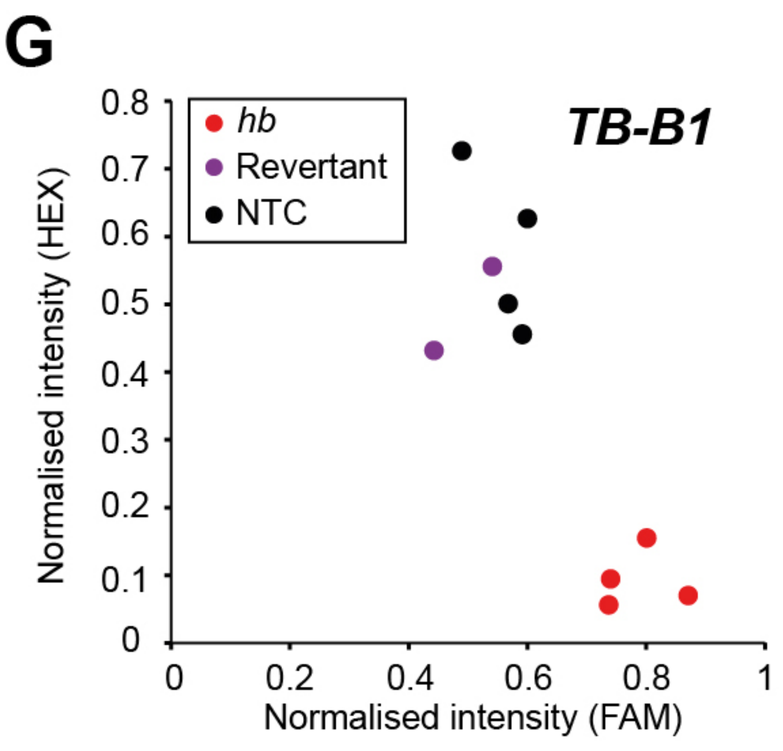

Figure 3: Increased dosage of *TB1* promotes paired spikelet development. A) Mature inflorescences of *pVRN1:TB1* transgenic plants, and the WT untransformed control (Fielder). **B**) Frequency of paired spikelets and (**C**) *TB-D1* haploid gene copy number for *pVRN1:TB1* transgenic plants (white) and control (grey, null transgenic; black, Fielder) lines. **D-F**) Plant (**D**) and inflorescence (**E**) architecture phenotypes of *hb* and revertant lines, with (**F**) quantification of paired spkelets per inflorescence and tiller numbers per plant. Secondary spikelets highlighted in blue. **G**) KASP marker analysis of *TB-B1* in *hb* (red) and revertant (magenta) lines, along with no template control (NTC, black). Scale bars, 10 cm (**D**) and 1 cm (**A**, **E**). All images are representatives of individuals used for quantification. Data of ddPCR and expression analyses are mean ± s.e.m. of 3-4 biological replicates. Data for transgenic lines are mean ± s.d. of 2-4 plants per transgenic genotype, 10 plants for (WT) Fielder. ***$p < 0.001$.

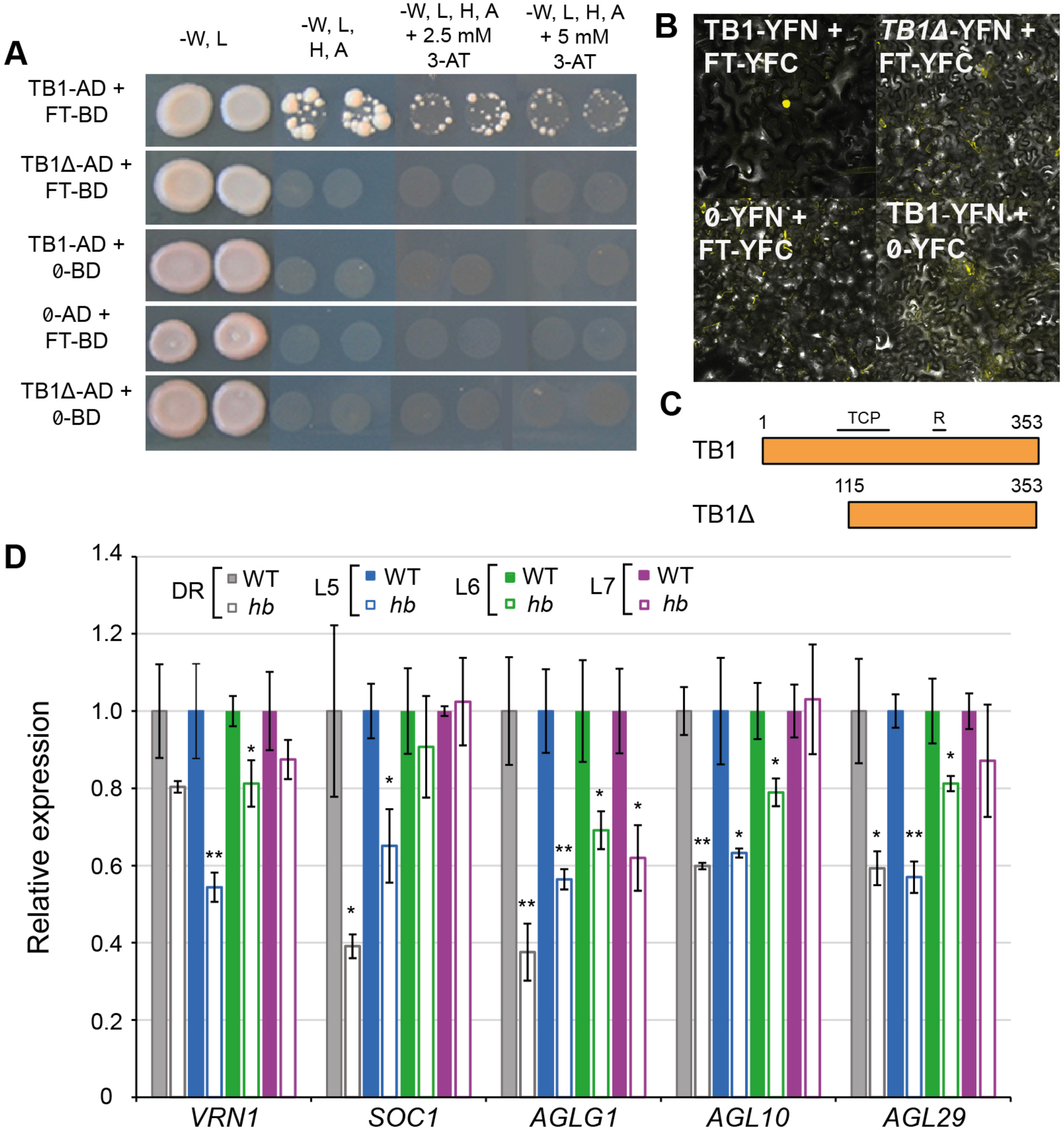

Figure 4: TB1 interacts with FLOWERING LOCUS T and modulates expression of meristem identity genes. A) Yeast two-hybrid (Y2H) assay between TB1 and FT, including control reactions with truncated TB-D1 (TB1Δ) and empty vectors (Ø), grown on varying selective media. **B**) Bimolecular fluorescence complementation (BiFC) assay for TB1 and FT, and control reactions including truncated TB-D1 (TB1Δ) and empty vectors (Ø). **C**) Schematic of full-length TB1 and truncated TB1 (TB1Δ) proteins used for Y2H and BiFC assays; TCP and R refer to domains of TB1 protein, numbers indicate amino acid positions. **D**) Expression of meristem identity genes in developing inflorescences of *hb* (white bars), relative to WT (solid bars), at double ridge (DR, grey), leaf 5 (L5, blue), leaf 6 (L6, green) and leaf 7 (L7, magenta) developmental stages. Data are mean ± s.e.m. of 4 biological replicates. *$p < 0.05$; **$p < 0.01$.

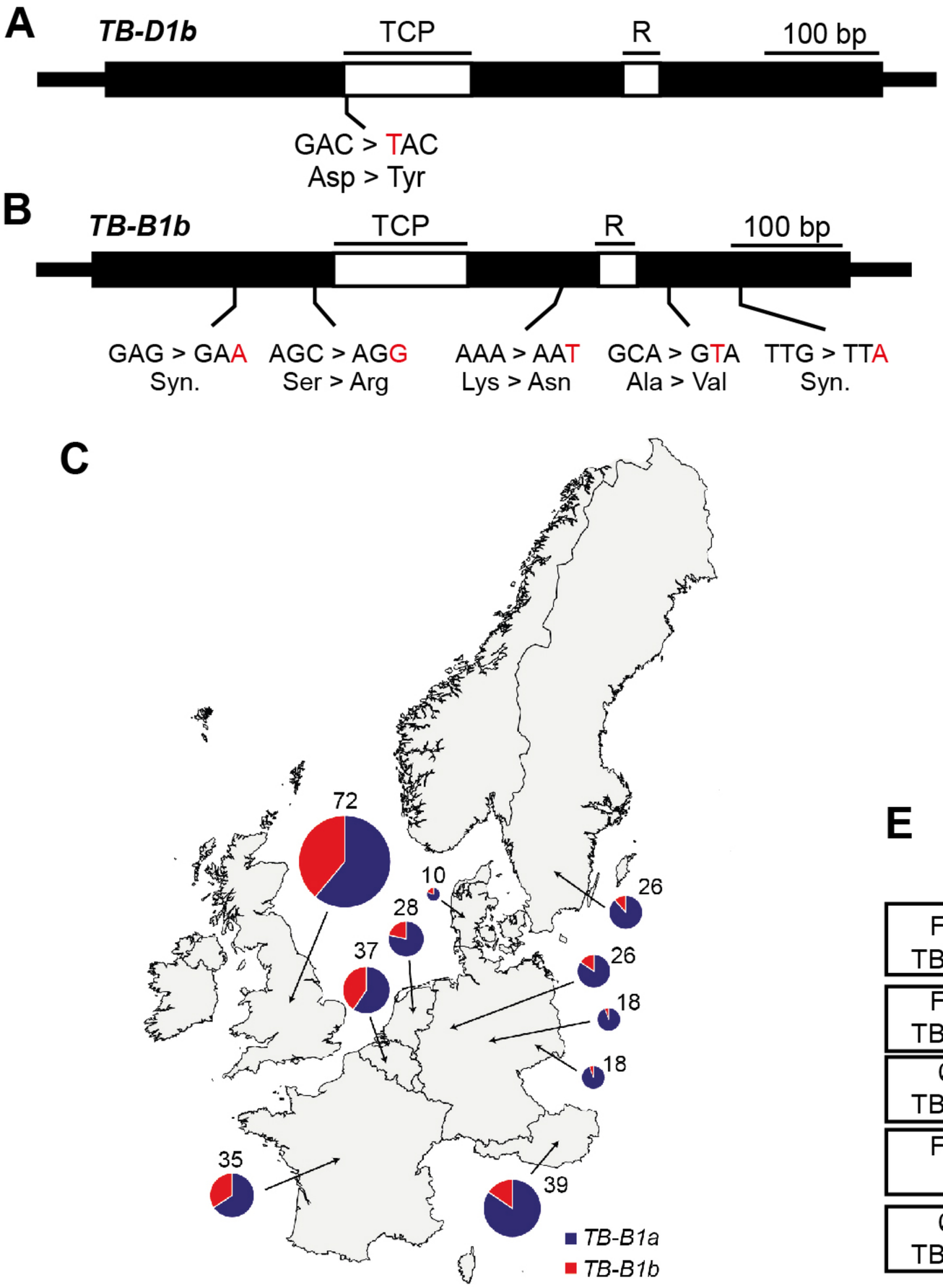

Figure 5: Allelic variation for *TB-B1* and *TB-D1* contributes to inflorescence architecture diversity in spring and winter wheat. A-B) Schematic diagrams of variant alleles for *TB-D1* (**A**, *TB-D1b*) from spring wheat and *TB-B1* (**B**, *TB-B1b*) from winter wheat, with positions of polymorphisms (indicated in red text) and molecular effect indicated (Syn., synonymous). TCP and R refer to genic regions that encode domains of the TB1 protein. **C**) Geographical distribution of *TB-B1a* (purple) and *TB-B1b* (red) alleles in European wheat cultivars of the GEDIFLUX collection. **D**) Genome-wide composite interval mapping scan displaying QTL that contribute to paired spikelet development from the UK winter wheat MAGIC population from the (2015 trial, including a highly significant QTL on chromosome 4B (indicated by yellow star). Red line indicates threshold of high significance ($p < 0.01$). **E**) Yeast two-hybrid (Y2H) assay between TB-B1 alleles (TB-B1a and TB-B1b) and FT, including control reactions with empty vectors (Ø), grown on varying selective media. A 10-fold serial dilution was performed for each interaction experiment.

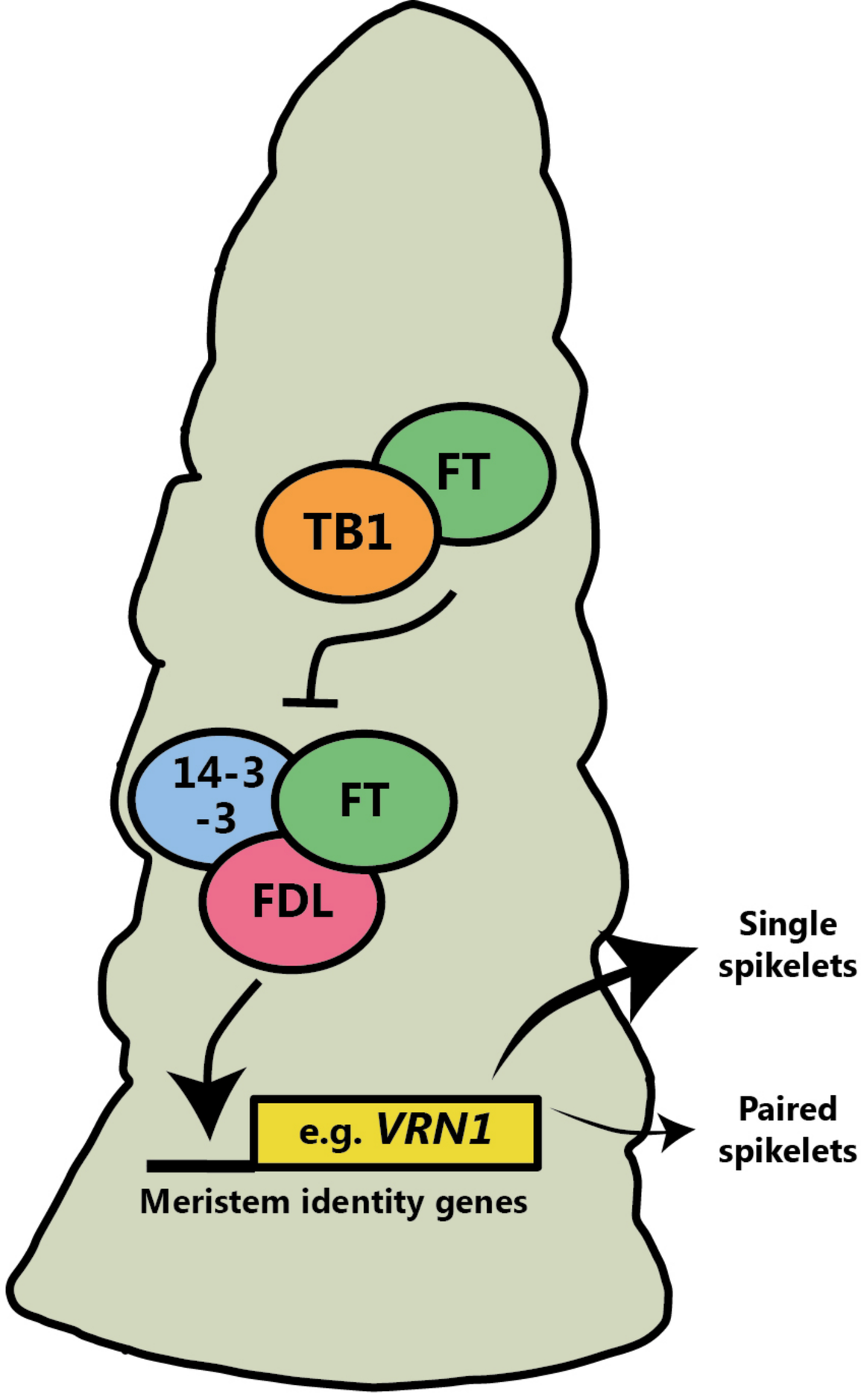

Figure 6: A model explaining the effect of increased dosage of TB1 on spikelet development in wheat. Increased levels of TB1 restrict the interaction of FT with other members of the floral activating complex (FDL and 14-3-3), which reduces expression of meristem identity genes (e.g. *VRN1*) and facilitates paired spikelet development. At standard levels of TB1, the floral activating complex promotes robust expression of meristem identity genes, and paired spikelet development is suppressed.

Parsed Citations

Abe M, Kobayashi Y, Yamamoto S, Daimon Y, Yamaguchi A, Ikeda Y, Ichinoki H, Notaguchi M, Goto K, Araki T. 2005. FD, a bZIP protein mediating signals from the floral pathway integrator FT at the shoot apex. Science 309: 1052-1056.
Pubmed: Author and Title
CrossRef: Author and Title
Google Scholar: Author Only Title Only Author and Title

Aguilar-Martinez JA, Poza-Carrion C, Cubas P. 2007. Arabidopsis BRANCHED1 acts as an integrator of branching signals within axillary buds. The Plant Cell 19: 458-472.
Pubmed: Author and Title
CrossRef: Author and Title
Google Scholar: Author Only Title Only Author and Title

Alonso-Peral MM, Oliver SN, Casao MC, Greenup AA, Trevaskis B. 2011. The promoter of the cereal VERNALIZATION1 gene is sufficient for transcriptional induction by prolonged cold. PLoS ONE 6: e29456.
Pubmed: Author and Title
CrossRef: Author and Title
Google Scholar: Author Only Title Only Author and Title

Altschul, S, Gish, W, Miller, W. 1990. Basic local alignment search tool. Journal of Molecular Biology 215, 403-410 (1990).
Pubmed: Author and Title
CrossRef: Author and Title
Google Scholar: Author Only Title Only Author and Title

Beales J, Turner A, Griffiths S, Snape JW, Laurie DA. 2007. A Pseudo-Response Regulator is misexpressed in the photoperiod insensitive Ppd-D1a mutant of wheat (Triticum aestivum L.). Theoretical and Applied Genetics 115: 721-733.
Pubmed: Author and Title
CrossRef: Author and Title
Google Scholar: Author Only Title Only Author and Title

Bedbrook, JR, Jones, J, O'Dell, M, Thompson, R, Flavell, RB. 1980. A molecular description of telomeric heterochromatin in Secale species. Cell 19, 545-560.
Pubmed: Author and Title
CrossRef: Author and Title
Google Scholar: Author Only Title Only Author and Title

Belda-Palazon B, Ruiz L, Marti E, Tarrage S, Tiburcio AF, Culianez F, Farras R, Carrasco P, Ferrando A. 2012. Aminopropyltransferases involved in polyamine biosynthesis localize preferentially in the nucleus of plant cells. PLoS ONE 7: e46907.
Pubmed: Author and Title
CrossRef: Author and Title
Google Scholar: Author Only Title Only Author and Title

Boden SA, Cavanagh C, Cullis BR, Ramm K, Greenwood J, Finnegan EJ, Ben Trevaskis, Swain SM. 2015. Ppd-1 is a key regulator of inflorescence architecture and paired spikelet development in wheat. Nature Plants 1:14016.
Pubmed: Author and Title
CrossRef: Author and Title
Google Scholar: Author Only Title Only Author and Title

Boden SA, Weiss D, Ross JJ, Davies NW, Trevaskis B, Chandler PM, Swain SM. 2014. EARLY FLOWERING3 regulates flowering in spring barley by mediating gibberellin production and FLOWERING LOCUS T expression. The Plant Cell 26: 1557-1569.
Pubmed: Author and Title
CrossRef: Author and Title
Google Scholar: Author Only Title Only Author and Title

Bolker BM, Brooks ME, Clark CJ, Geange SW, Poulsen JR, Stevens MHH, White J-SS. 2009. Generalized linear mixed models: a practical guide for ecology and evolution. Trends in Ecology and Evolution 24: 127-135.
Pubmed: Author and Title
CrossRef: Author and Title
Google Scholar: Author Only Title Only Author and Title

Bommert P, Nagasawa NS, Jackson D. 2013. Quantitative variation in maize kernel row number is controlled by the FASCIATED EAR2 locus. Nature Genetics 45: 334-337.
Pubmed: Author and Title
CrossRef: Author and Title
Google Scholar: Author Only Title Only Author and Title

Borrill P, Ramirez-Gonzalez R, Uauy C. 2016. expVIP: a customizable RNA-seq data analysis and visualization platform. Plant Physiology 170: 2172-2186.
Pubmed: Author and Title
CrossRef: Author and Title
Google Scholar: Author Only Title Only Author and Title

Clavijo BJ, Venturini L, Schudoma C, Accinelli GG, Kaithakottil G, Wright J, Borrill P, Kettleborough G, Heavens D, Chapman, H et al. 2017. An improved assembly and annotation of the allohexaploid wheat genome identifies complete families of agronomic genes and provides genomic evidence for chromosomal translocations. Genome Research: doi:10.1101/gr.217117.116.
Pubmed: Author and Title
CrossRef: Author and Title

Google Scholar: Author Only Title Only Author and Title

Consortium TU. 2016. UniProt: the universal protein knowledgebase. Nucleic Acids Research 45: D158-D169.
Pubmed: Author and Title
CrossRef: Author and Title
Google Scholar: Author Only Title Only Author and Title

Crop Committee Handbook. 2013. Crop Committee Handbook. Agriculture and Horticulture Development Board Cereals and Oilseeds.
Pubmed: Author and Title
CrossRef: Author and Title
Google Scholar: Author Only Title Only Author and Title

Debernardi JM, Lin H, Chuck G, Faris JD, Dubcovsky J. 2017. microRNA172 plays a crucial role in wheat spike morphogenesis and grain threshability. Development 144: 1966-1975.
Pubmed: Author and Title
CrossRef: Author and Title
Google Scholar: Author Only Title Only Author and Title

Dobrovolskaya O, Pont C, Sibout R, Martinek P, Badaeva E, Murat F, Chosson A, Watanabe N, Prat E, Gautier N, et al. 2014. FRIZZY PANICLE drives supernumerary spikelets in bread wheat (T. aestivum L.). Plant Physiology 167: 189-199.
Pubmed: Author and Title
CrossRef: Author and Title
Google Scholar: Author Only Title Only Author and Title

Doebley J, Stec A, Gustus C. 1995. teosinte branched1 and the origin of maize: Evidence for epistasis and the evolution of dominance. Genetics 141: 333-346.
Pubmed: Author and Title
CrossRef: Author and Title
Google Scholar: Author Only Title Only Author and Title

Doebley J, Stec A, Hubbard L. 1997. The evolution of apical dominance in maize. Nature 386: 485-488.
Pubmed: Author and Title
CrossRef: Author and Title
Google Scholar: Author Only Title Only Author and Title

Egea-Cortines M, Saedler H, Sommer H. 1999. Ternary complex formation between the MADS-box proteins SQUAMOSA, DEFICIENS and GLOBOSA is involved in the control of floral architecture in Antirrhinum majus. The EMBO Journal 18: 5370-5379.
Pubmed: Author and Title
CrossRef: Author and Title
Google Scholar: Author Only Title Only Author and Title

Fischer T, Byerlee D, Edmeades G. 2014. Crop yields and global food security. Australian Centre of International Agricultural Research.
Pubmed: Author and Title
CrossRef: Author and Title
Google Scholar: Author Only Title Only Author and Title

Gardner KA, Wittern LM, Mackay IJ. 2016. A highly recombined, high-density, eight-founder wheat MAGIC map reveals extensive segregation distortion and genomic locations of introgression segments. Plant Biotechnology Journal 14: 1406-1417.
Pubmed: Author and Title
CrossRef: Author and Title
Google Scholar: Author Only Title Only Author and Title

Gonzalez FG, Miralles DJ, Slafer GA. 2011. Wheat floret survival as related to pre-anthesis spike growth. Journal of Experimental Botany 62: 4889-4901.
Pubmed: Author and Title
CrossRef: Author and Title
Google Scholar: Author Only Title Only Author and Title

González-Navarro OE, Griffiths S, Molero G, Reynolds MP, Slafer GA. 2015. Dynamics of floret development determining differences in spike fertility in an elite population of wheat. Field Crops Research 172: 21-31.
Pubmed: Author and Title
CrossRef: Author and Title
Google Scholar: Author Only Title Only Author and Title

Greenwood JR, Finnegan EJ, Watanabe N, Trevaskis B, Swain SM. 2017. New alleles of the wheat domestication gene Q reveal multiple roles in growth and reproductive development. Development 144: 1959-1965.
Pubmed: Author and Title
CrossRef: Author and Title
Google Scholar: Author Only Title Only Author and Title

Guo Z, Schnurbusch T. 2015. Variation of floret fertility in hexaploid wheat revealed by tiller removal. Journal of Experimental Botany 66: 5945-5958.
Pubmed: Author and Title
CrossRef: Author and Title
Google Scholar: Author Only Title Only Author and Title

Hedden P. 2013. The genes of the Green Revolution. Trends in Genetics 19: 5-9.
Pubmed: Author and Title
CrossRef: Author and Title

Google Scholar: Author Only Title Only Author and Title

Houston K, McKim SM, Comadran J, Bonar N, Druka I, Uzrek N, Cirillo E, Guzy-Wrobelska J, Collins NC, Halpin C, et al. 2013. Variation in the interaction between alleles of HvAPETALA2 and microRNA172 determines the density of grains on the barley inflorescence. Proceedings of the National Academy of Sciences of USA 110: 16675-16680.
Pubmed: Author and Title
CrossRef: Author and Title
Google Scholar: Author Only Title Only Author and Title

Huang BE, George AW. 2011. R/mpMap: a computational platform for the genetic analysis of multiparent recombinant inbred lines. Biochemistry 27: 727-729.
Pubmed: Author and Title
CrossRef: Author and Title
Google Scholar: Author Only Title Only Author and Title

Huang BE, George AW, Forrest KL, Kilian A, Hayden MJ, Morell MK, Cavanagh CR. 2012. A multiparent advanced generation inter-cross population for genetic analysis in wheat. Plant Biotechnology Journal 10: 826-839.
Pubmed: Author and Title
CrossRef: Author and Title
Google Scholar: Author Only Title Only Author and Title

Hubbard L, McSteen P, Doebley J, Hake S. 2002. Expression patterns and mutant phenotype of teosinte branched1 correlate with growth suppression in maize and teosinte. Genetics 162: 1927-1935.
Pubmed: Author and Title
CrossRef: Author and Title
Google Scholar: Author Only Title Only Author and Title

Ishida Y, Tsunashima M, Hiei Y, Komari T. 2015. Wheat transformation. Wang K ed. Agrobacterium protocols: methods in molecular biology. Springer, 189-198.
Pubmed: Author and Title
CrossRef: Author and Title
Google Scholar: Author Only Title Only Author and Title

Jiao Y, Wang Y, Xue D, Wang J, Yan M, Liu G, Dong G, Zeng D, Lu Z, Zhu X, et al. 2010. Regulation of OsSPL14 by OsmiR156 defines ideal plant architecture in rice. Nature Genetics 42: 541-544.
Pubmed: Author and Title
CrossRef: Author and Title
Google Scholar: Author Only Title Only Author and Title

Kosugi S, Ohashi Y. 1997. PCFI and PCF2 specifically bind to cis elements in the rice proliferating cell nuclear antigen gene. The Plant Cell 9: 1607-1619.
Pubmed: Author and Title
CrossRef: Author and Title
Google Scholar: Author Only Title Only Author and Title

Kyozuka J, Tokunaga H, Yoshida A. 2014. Control of grass inflorescence form by the fine-tuning of meristem phase change. Current Opinion in Plant Biology 17: 110-115.
Pubmed: Author and Title
CrossRef: Author and Title
Google Scholar: Author Only Title Only Author and Title

Lemmon ZH, Park SJ, Jiang K, Van Eck J, Schatz MC, Lippman ZB. 2016. The evolution of inflorescence diversity in the nightshades and heterochrony during meristem maturation. Genome Research 26: 1676-1686.
Pubmed: Author and Title
CrossRef: Author and Title
Google Scholar: Author Only Title Only Author and Title

Lewis JM, Mackintosh CA, Shin S, Gilding E, Kravchenko S, Baldridge G, Zeyen R, Muehlbauer GJ. 2008. Overexpression of the maize Teosinte Branched1 gene in wheat suppresses tiller development. Plant Cell Reports 27: 1217-1225.
Pubmed: Author and Title
CrossRef: Author and Title
Google Scholar: Author Only Title Only Author and Title

Li C, Lin H, Dubcovsky J. 2015. Factorial combinations of protein interactions generate a multiplicity of florigen activation complexes in wheat and barley. The Plant Journal 84: 70-82.
Pubmed: Author and Title
CrossRef: Author and Title
Google Scholar: Author Only Title Only Author and Title

Luo D, Carpenter R, Vincent C, Copsey L, Coen E. 1996. Origin of floral asymmetry in Antirrhinum. Nature 383: 794-799.
Pubmed: Author and Title
CrossRef: Author and Title
Google Scholar: Author Only Title Only Author and Title

Mackay IJ, Bansept-Balser P, Barber T, Bentley AR, Cockram J, Gosman N, Greenland AJ, Horsnell R, Howells R, O'Sullivan D, et al. 2014. An eight-parent multiparent advanced generation inter-cross Population for winter-sown wheat: creation, properties, and validation. G3-Genes, Genomes, Genetics 4: 1603-1610.
Pubmed: Author and Title
CrossRef: Author and Title
Google Scholar: Author Only Title Only Author and Title

Meyer RS, Purugganan MD. 2013. Evolution of crop species: genetics of domestication and diversification. Nature Reviews Genetics 14: 840-852.
Pubmed: Author and Title
CrossRef: Author and Title
Google Scholar: Author Only Title Only Author and Title

Mieog JC, Howitt CA, Ral J-P. 2013. Fast-tracking development of homozygous transgenic cereal lines using a simple and highly flexible real-time PCR assay. BMC Plant Biology 13: 71.
Pubmed: Author and Title
CrossRef: Author and Title
Google Scholar: Author Only Title Only Author and Title

Milner SG, Maccaferri M, Huang BE, Mantovani P, Massi A, Frascaroli E, Tuberosa R, Salvi S. 2016. A multiparental cross population for mapping QTL for agronomic traits in durum wheat (Triticum turgidum ssp. durum). Plant Biotechnology Journal 14: 735-748.
Pubmed: Author and Title
CrossRef: Author and Title
Google Scholar: Author Only Title Only Author and Title

Miralles D, Richards RA, Slafer GA. 2000. Duration of the stem elongation period influences the number of fertile florets in wheat and barley. Australian Journal of Plant Physiology 27: 931-940.
Pubmed: Author and Title
CrossRef: Author and Title
Google Scholar: Author Only Title Only Author and Title

Miura K, Ikeda M, Matsubara A, Song X-J, Ito M, Asano K, Matsuoka M, Kitano H, Ashikari M. 2010. OsSPL14 promotes panicle branching and higher grain productivity in rice. Nature Genetics 42: 545-549.
Pubmed: Author and Title
CrossRef: Author and Title
Google Scholar: Author Only Title Only Author and Title

Niwa M, Daimon Y, Kurotani KI, Higo A, Pruneda-Paz JL, Breton G, Mitsuda N, Kay SA, Ohme-Takagi M, Endo M, et al. 2013. BRANCHED1 interacts with FLOWERING LOCUS T to repress the floral transition of the axillary meristems in Arabidopsis. The Plant Cell 25: 1228-1242.
Pubmed: Author and Title
CrossRef: Author and Title
Google Scholar: Author Only Title Only Author and Title

Park SJ, Jiang K, Schatz MC, Lippman ZB. 2012. Rate of meristem maturation determines inflroescence architecture in tomato. Proceedings of the National Academy of Sciences of USA 109: 639-644.
Pubmed: Author and Title
CrossRef: Author and Title
Google Scholar: Author Only Title Only Author and Title

Park SJ, Jiang K, Tal L, Yichie Y, Gar O, Zamir D, Eshed Y, Lippman ZB. 2014. Optimization of crop productivity in tomato using induced mutations in the florigen pathway. Nature Genetics 46: 1337-1342.
Pubmed: Author and Title
CrossRef: Author and Title
Google Scholar: Author Only Title Only Author and Title

Paterson, AH, Brubaker, CL, Wendel, JF 1993. A rapid method for extraction of cotton (Gossypium ssp.) genomic DNA suitable for RFLP and PCR analysis. Plant Molecular Biology Reporter 11: 122-127.
Pubmed: Author and Title
CrossRef: Author and Title
Google Scholar: Author Only Title Only Author and Title

Pearce S, Saville R, Vaughan SP, Chandler PM, Wilhelm EP, Sparks CA, Al-Kaff N, Korolev A, Boulton MI, Phillips AL, et al. 2011. Molecular characterization of Rht-1 dwarfing genes in hexaploid wheat. Plant Physiology 157: 1820-1831.
Pubmed: Author and Title
CrossRef: Author and Title
Google Scholar: Author Only Title Only Author and Title

Poursarebani N, Seidensticker T, Koppolu R, Trautewig C, Gawronski P, Bini F, Govind G, Rutten T, Sakuma S, Tagiri A, et al. 2015. The genetic basis of composite spike form in barley and 'Miracle-Wheat'. Genetics 201: 155-165.
Pubmed: Author and Title
CrossRef: Author and Title
Google Scholar: Author Only Title Only Author and Title

Ramirez-Gonzalez R, Segovia V, Bird N, Fenwick P, Holdgate S, Berry S, Jack P, Caccamo M, Uauy C. 2015. RNA-Seq bulked segregant analysis enables the identification of high-resolution genetic markers for breeding in hexaploid wheat. Plant Biotechnology Journal 13: 613-624.
Pubmed: Author and Title
CrossRef: Author and Title
Google Scholar: Author Only Title Only Author and Title

Ramsay L, Comadran J, Druka A, Marshall DF, Thomas WTB, Macaulay M, MacKenzie K, Simpson C, Fuller J, Bonar N, et al. 2011. INTERMEDIUM-C, a modifier of lateral spikelet fertility in barley, is an ortholog of the maize domestication gene TEOSINTE BRANCHED 1. Nature Genetics 43: 169-172.
Pubmed: Author and Title
CrossRef: Author and Title

Google Scholar: Author Only Title Only Author and Title

Rawson HM. 1970. Spikelet number, its control and relation to yield per ear in wheat. Australian Journal of Biological Science 23: 1-15.
Pubmed: Author and Title
CrossRef: Author and Title
Google Scholar: Author Only Title Only Author and Title

Rayburn, AL, Gill, BS. 1986. Isolation of a D-genome specific repeated DNA sequence from Aegilops squarrosa. Plant Mol. Biol. Rep. 4, 102-109.
Pubmed: Author and Title
CrossRef: Author and Title
Google Scholar: Author Only Title Only Author and Title

Reynolds M, Foulkes MJ, Slafer GA, Berry P, Parry MAJ, Snape JW, Angus WJ. 2009. Raising yield potential in wheat. Journal of Experimental Botany 60: 1899-1918.
Pubmed: Author and Title
CrossRef: Author and Title
Google Scholar: Author Only Title Only Author and Title

Richardson, T, Thistleton, J, Higgins, TJ, Howitt, C, Ayliffe, M. 2014. Efficient Agrobacterium transformation of elite wheat germplasm without selection. Plant Cell Tissue Organ Culture 119, 647- 659.
Pubmed: Author and Title
CrossRef: Author and Title
Google Scholar: Author Only Title Only Author and Title

Sainsbury F, Thuenemann EC, Lomonossoff GP. 2009. pEAQ: versatile expression vectors for easy and quick transient expression of heterologous proteins in plants. Plant Biotechnology Journal 7: 682-693.
Pubmed: Author and Title
CrossRef: Author and Title
Google Scholar: Author Only Title Only Author and Title

Schindelin J, Arganda-Carreras I, Frise E, Kaynig V, Longair M, Pietzsch T, Preibisch S, Rueden C, Saalfield S, Schmid B, et al. 2012. Fiji: an open-source platform for biological-image analysis. Nature Methods 9: 676-682.
Pubmed: Author and Title
CrossRef: Author and Title
Google Scholar: Author Only Title Only Author and Title

Sharman BC. 1944. Branched heads in wheat and wheat hybrids. Nature: 497-498.
Pubmed: Author and Title
CrossRef: Author and Title
Google Scholar: Author Only Title Only Author and Title

Sharman BC. 1967. Interpretation of the morphology of various naturally occurring abnormalities of the inflorescence of wheat (Triticum). Canadian Journal of Botany 45: 2073-2080.
Pubmed: Author and Title
CrossRef: Author and Title
Google Scholar: Author Only Title Only Author and Title

Shaw LM, Turner AS, Laurie DA. 2012. The impact of photoperiod insensitive Ppd-1a mutations on the photoperiod pathway across the three genomes of hexaploid wheat (Triticum aestivum). The Plant Journal 71: 71-84.
Pubmed: Author and Title
CrossRef: Author and Title
Google Scholar: Author Only Title Only Author and Title

Simons KJ, Fellers JP, Trick HN, Zhang Z, Tai Y-S, Gill BS, Faris JD. 2005. Molecular characterization of the major wheat domestication gene Q. Genetics 172: 547-555.
Pubmed: Author and Title
CrossRef: Author and Title
Google Scholar: Author Only Title Only Author and Title

Slafer GA. 2003. Genetic basis of yield as viewed from a crop physiologist's perspective. Annals of Applied Biology 142: 117-128.
Pubmed: Author and Title
CrossRef: Author and Title
Google Scholar: Author Only Title Only Author and Title

Soyk S, Lemmon ZH, Oved M, Fisher J, Liberatore KL, Park SJ, Goren A, Jiang K, Ramos A, van der Knaap E, et al. 2017. Bypassing negative epistasis on yield in tomato imposed by a domestication gene. Cell 169: 1142-1155.
Pubmed: Author and Title
CrossRef: Author and Title
Google Scholar: Author Only Title Only Author and Title

Studer A, Zhao Q, Ross-Ibarra J, Doebley J. 2011. Identification of a functional transposon insertion in the maize domestication gene. Nature Genetics 43: 1160-1163.
Pubmed: Author and Title
CrossRef: Author and Title
Google Scholar: Author Only Title Only Author and Title

Takeda T, Suwa Y, Suzuki M, Kitano H, Ueguchi-Tanaka M, Ashikari M, Matsuoka M, Ueguchi C. 2003. The OsTB1 gene negatively regulates lateral branching in rice. The Plant Journal: 513-520.
Pubmed: Author and Title

CrossRef: Author and Title
Google Scholar: Author Only Title Only Author and Title

Taoka K-I, Ohki I, Tsuji H, Furuita K, Hayashi K, Yanase T, Yamaguchi M, Nakashima C, Purwestri YA, Tamaki S, et al. 2011. 14-3-3 proteins act as intracellular receptors for rice Hd3a florigen. Nature 476: 332-335.
Pubmed: Author and Title
CrossRef: Author and Title
Google Scholar: Author Only Title Only Author and Title

Tatematsu K, Nakabayashi K, Kamiya Y, Nambara E. 2008. Transcription factor AtTCP14 regulates embryonic growth potential during seed germination in Arabidopsis thaliana. The Plant Journal 53: 42-52.
Pubmed: Author and Title
CrossRef: Author and Title
Google Scholar: Author Only Title Only Author and Title

Tenesa A, Haley CS. 2013. The heritability of human disease: estimation, uses and abuses. Nature Reviews Genetics 14: 139-149.
Pubmed: Author and Title
CrossRef: Author and Title
Google Scholar: Author Only Title Only Author and Title

Wang L, Sun S, Jin J, Fu D, Yang X, Weng X, Xu C, Li X, Xiao J, Zhang Q. 2015. Coordinated regulation of vegetative and reproductive branching in rice. Proceedings of the National Academy of Sciences of USA 112: 15504-15509.
Pubmed: Author and Title
CrossRef: Author and Title
Google Scholar: Author Only Title Only Author and Title

Wang S, Wong D, Forrest K, Allen A, Chao S, Huang BE, Maccaferri M, Salvi S, Milner SG, Cattivelli L, et al. 2014. Characterization of polyploid wheat genomic diversity using a high-density 90 000 single nucleotide polymorphism array. Plant Biotechnology Journal 12:787-796.
Pubmed: Author and Title
CrossRef: Author and Title
Google Scholar: Author Only Title Only Author and Title

Wigge PA, Kim MC, Jaeger KE, Busch W, Schmid M, Lohmann JU, Weigel D. 2005. Integration of spatial and temporal information during floral induction in Arabidopsis. Science 309: 1056-1059.
Pubmed: Author and Title
CrossRef: Author and Title
Google Scholar: Author Only Title Only Author and Title

Wu TD, Watanabe CK. 2005. GMAP: a genomic mapping and alignment program for mRNA and EST sequences. Biochemistry 21: 1859-1875.
Pubmed: Author and Title
CrossRef: Author and Title
Google Scholar: Author Only Title Only Author and Title

Yan L, Loukoianov A, Tranquilli G, Helguera M, Fahima T, Dubcovsky J. 2003. Positional cloning of the wheat vernalization gene VRN1. Proceedings of the National Academy of Sciences of USA100: 6263-6268.
Pubmed: Author and Title
CrossRef: Author and Title
Google Scholar: Author Only Title Only Author and Title

Yoshida A, Sasao M, Yasuno N, Takagi K, Daimon Y, Chen R, Yamazaki R, Tokunaga H, Kitaguchi Y, Sato Y, et al. 2012. TAWAWA1, a regulator of rice inflorescence architecture, functions through suppression of meristem phase transition. Proceedings of the National Academy of Sciences of USA 110: 767-772.
Pubmed: Author and Title
CrossRef: Author and Title
Google Scholar: Author Only Title Only Author and Title

Zhang D, Yuan Z. 2014. Molecular control of grass inflorescence development. Annual Review of Plant Biology 65: 553-578
Pubmed: Author and Title
CrossRef: Author and Title
Google Scholar: Author Only Title Only Author and Title

Zhang P, Li W, Fellers JP, Friebe B. 2004. BAC-FISH in wheat identifies chromosome landmarks consisting of different types of transposable elements. Chromosoma 112: 288-299.
Pubmed: Author and Title
CrossRef: Author and Title
Google Scholar: Author Only Title Only Author and Title

Zhu Z, Tan L, Fu Y, Liu F, Cai H, Xie D, Wu F, Wu J, Matsumoto T, Sun C. 2013. Genetic control of inflorescence architecture during rice domestication. Nature Communications 4: 2200.
Pubmed: Author and Title
CrossRef: Author and Title
Google Scholar: Author Only Title Only Author and Title

© 2017. Published by The Company of Biologists Ltd | Development (2017) 144, 1959-1965 doi:10.1242/dev.146407

RESEARCH REPORT

New alleles of the wheat domestication gene *Q* reveal multiple roles in growth and reproductive development

Julian R. Greenwood[1,2], E. Jean Finnegan[1], Nobuyoshi Watanabe[3], Ben Trevaskis[1] and Steve M. Swain[1,*]

ABSTRACT

The advantages of free threshing in wheat led to the selection of the domesticated *Q* allele, which is now present in almost all modern wheat varieties. *Q* and the pre-domestication allele, *q*, encode an AP2 transcription factor, with the domesticated allele conferring a free-threshing character and a subcompact (i.e. partially compact) inflorescence (spike). We demonstrate that mutations in the miR172 binding site of the *Q* gene are sufficient to increase transcript levels via a reduction in miRNA-dependent degradation, consistent with the conclusion that a single nucleotide polymorphism in the miRNA binding site of *Q* relative to *q* was essential in defining the modern *Q* allele. We describe novel gain- and loss-of-function alleles of *Q* and use these to define new roles for this gene in spike development. *Q* is required for the suppression of 'sham ramification', and increased Q expression can lead to the formation of ectopic florets and spikelets (specialized inflorescence branches that bear florets and grains), resulting in a deviation from the canonical spike and spikelet structures of domesticated wheat.

KEY WORDS: Wheat, Spike, Inflorescence, AP2, Domestication, microRNA

INTRODUCTION

The causal molecular mechanism for the domestication of *Q* is thought to be an amino acid change in the predicted Q protein (Simons et al., 2006) and/or a single nucleotide polymorphism (SNP) present in a presumed miRNA binding site of *Q* (Sormacheva et al., 2015; Chuck et al., 2007). Unlike the domesticated homeoallele *Q* (chromosome 5A) (Faris et al., 2003), the B and D homeoalleles of hexaploid bread wheat are thought to be a pseudogene and expressed at a low level, respectively (Zhang et al., 2011). Q is a member of the AP2 class of transcription factors, which are known to influence many traits associated with floral transition, including both flowering time and the definition of floral organs (Aukerman and Sakai, 2003; Chuck et al., 2007; Lauter et al., 2005; Lee and An, 2012; Lee et al., 2007; Brown and Bregitzer, 2011; Varkonyi-Gasic et al., 2012). Generally, gain-of-function mutations and overexpression of *AP2* genes result in delayed flowering (Mlotshwa et al., 2006; Aukerman and Sakai, 2003; Schmid et al., 2003; Jung et al., 2007) and additional florets in the *Tassleseed6* mutant of corn (Chuck et al., 2007). Loss-of-function mutations and reduced expression can cause early flowering and disruptions in floral patterning and determinacy (Chuck et al., 1998, 2008; Lee and An, 2012; Mlotshwa et al., 2006; Jung et al., 2007; Mathieu et al., 2009); these effects can be masked by redundant function of other *AP2* genes (Yant et al., 2010). *AP2* genes can be regulated by miR172, and mutations affecting the expression of miR172 or SNPs in either *miR172* or in its conserved target site in *AP2* genes can lead to misregulation, with the potential to increase or reduce regulatory targeting by the miRNA (Aukerman and Sakai, 2003; Chuck et al., 2007; Varkonyi-Gasic et al., 2012; Zhu et al., 2009).

[1]CSIRO Agriculture and Food, Black Mountain Science and Innovation Park, GPO Box 1700, Canberra, Australian Capital Territory 2601, Australia. [2]Research School of Biology, Australian National University, Canberra, Australian Capital Territory 2601, Australia. [3]College of Agriculture, Ibaraki University, 3-21-1 Chuo, Ami, Inashiki, Ibaraki 300-0393, Japan.

*Author for correspondence (steve.swain@csiro.au)

S.M.S., 0000-0002-6118-745X

Received 31 October 2016; Accepted 18 April 2017

RESULTS AND DISCUSSION

A dwarf, compact spike mutant was identified in an M_2 mutant population derived from the Australian wheat cultivar Sunstate (SS) and backcrossed to the progenitor line SS. The F_2 progeny of this cross could be separated into three distinct height classes, namely SS-like, intermediate (heterozygous) and short (homozygous mutant) (Fig. 1A,B), which were subsequently confirmed by genetic analysis (see below). Differences in height were substantial (Fig. 1B,C) and unambiguously separated plants into the three classes. Both heterozygous and homozygous mutant plants were characterized by a reduction in internode length relative to SS-like siblings, resulting in spike compaction and reduced overall height (Fig. 1C,D; Fig. S1). Mutant plants were also late flowering and possessed a small increase in rachis node number (nodes along the spike that potentially bear a fertile spikelet) (Fig. 1E,F).

The compact mutant resembled transgenic wheat lines with increased copy number and expression of *Q* (Simons et al., 2006; Förster et al., 2012, 2013). The mutant (hereafter called *Q′*) contained a novel single nucleotide change in the miRNA binding site of *Q* that causes an additional mismatch when aligned to the targeting miRNA Ta-miR172 (Fig. 2A; Fig. S2). No other sequence changes were observed in the coding region. Expression of *Q*, as measured by qPCR, was higher in developing inflorescences of *Q′* plants than in their SS-like siblings (Fig. 2B,C). Modified 5′ RACE detected multiple *Q* cleavage products in mRNA from SS-like plants, whereas only a single cleavage product was detected from *Q′* mRNA (Fig. 2D). The most abundant class of *Q* cleavage products matched the expected product from miRNA-directed cleavage between the tenth and eleventh nucleotides within the miRNA, whereas the single *Q′* cleavage product detected was shifted by a single base. Combined with our expression data, the reduced levels of cleavage product in *Q′* indicate that the induced mismatch to Ta-miR172 results in reduced targeted mRNA degradation, and ultimately higher Q protein abundance. Based on its partial genetic dominance and increased mRNA expression, *Q′* appears to be a gain-of-function allele relative to *Q*. We cannot exclude the possibility that the amino acid change (G to E) in the predicted Q protein resulting from the *Q′* SNP also contributes to the observed phenotypes. However, similar compact spike phenotypes have been

Development (2017) 144, 1959-1965 doi:10.1242/dev.146407

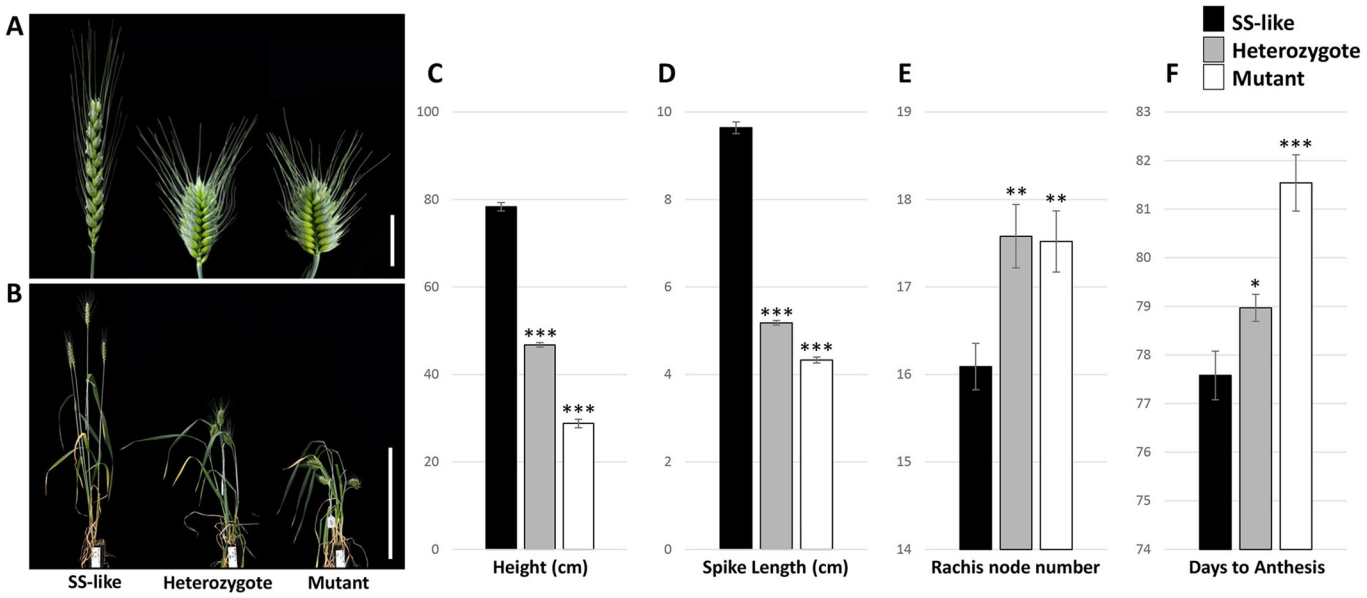

Fig. 1. Identification and characterization of a compact spike mutant. (A) Adult wheat inflorescence (spike) of the Sunstate (SS)-like sibling line, heterozygous line and homozygous mutant line. Scale bar: 3 cm. (B) SS-like, heterozygous and homozygous mutant plants at maturity. Scale bar: 30 cm. (C-F) Plant height (C), spike length (D), rachis node number (number of nodes along the spike, E) and days to anthesis (flowering time, F) of SS-like, heterozygous and compact spike mutant plants. Data are presented as mean±s.e.m. n=33 SS-like, n=35 heterozygous, n=22 mutant. *P<0.05, **P<0.01, ***P<0.001, compared with SS-like plants.

reported in transgenic plants containing an miR172 binding site mimic (MIM172) and reduced levels of miR172 (Debernardi et al., 2017), suggesting that reduced miR172 cleavage in *Q′* is sufficient to induce the observed phenotypes. For the barley paralog *HvAP2 (2H)*, both synonymous and non-synonymous mutations causing mismatches to miR172 result in compact spikes, further supporting that nucleotide mismatches without amino acid changes can affect this trait (Houston et al., 2013).

To establish that the *Q′* mutation was causal, we first confirmed complete genetic linkage between the *Q′* SNP and the reduced height/compact spike phenotypes (Fig. 3B). Second, we investigated additional alleles. Two allelic dwarf mutant lines with compact spikes, ANBW5C Dwarf (5CD) and ANBW5B Dwarf (5BD) (Fig. 3A), have previously been described and mapped to chromosome 5AL (which contains *Q*), although the genetic basis was not determined (Kosuge et al., 2012). Sequencing revealed that both mutant lines contained SNPs within the miRNA binding site of *Q*, with 5CD containing the exact same mutation as *Q′* and 5BD (*Q′-like*) featuring a unique SNP in the miRNA binding site of *Q* (Fig. 3C; Fig. S2). The similar phenotypes of the two independent mutants support the hypothesis that the causal effect of the *Q′* mutation is associated with a reduction in miR172 repression rather than with the change in the encoded amino acid. Consistent with impaired regulation by miR172, all compact spike mutants showed higher expression of *Q* than their sibling or parent lines in both developing inflorescence and elongating peduncle internode tissue (Fig. 3G,H).

To formally confirm that the *Q′* mutation was causal to the observed phenotypes, we performed a second round of mutagenesis in the *Q′* background. Two unique revertant alleles were isolated with SNPs in the first exon of the *Q′* gene: *Q′-Rev1*, a presumed complete loss-of-function revertant with an introduced stop codon; and *Q′-Rev2*, a partial revertant with an amino acid change immediately before the first predicted AP2 domain (Fig. 3C). Both 'revertants' retained the *Q* and *Q′* mutations, as expected. The *Q′* revertants completely (*Q′-Rev1*) or partially (*Q′-Rev2*) suppressed the phenotypic changes in *Q′* (see below), confirming that changes in *Q* are responsible for the *Q′* gain-of-function phenotypes.

The presence of independent gain- and loss-of-function *Q* alleles in a common background allows the function of *Q* to be analyzed with a precision not previously possible. In contrast to *Q′*, *Q′-Rev1* plants showed a reduction in rachis node number compared with SS-like plants, demonstrating an earlier (in terms of nodes) transition from inflorescence meristem to terminal spikelet meristem (Fig. 3F). Whereas plant height was increased in *Q′-Rev1* plants compared with SS-like (*Q*) plants, spike length did not differ significantly (Fig. 3D,E). Reduced rachis node number in *Q′-Rev1* compared with *Q* meant that the average internode length between each spikelet was greater, resulting in reduced spikelet density, also known as a lax spike. Compared with SS-like and *Q′*, the lax spikes of *Q′-Rev1* were difficult to hand thresh (Fig. S3), consistent with observations of plants containing pre-domestication *q*, or 5A deletions that lack domesticated *Q* (Faris et al., 2003; Simons et al., 2006; Förster et al., 2012), and with *Q* playing an important role in wheat domestication. Partial reversion of the *Q′* mutant phenotype in *Q′-Rev2* was characterized by an increase in height and spike length relative to *Q′*, although not to the extent of SS-like plants (Fig. 3A).

Given that *AP2* genes in other species have diverse roles in spikelet and floret development, we examined whether increased Q activity resulted in additional, previously undescribed changes in reproductive development. The two independent *Q′* mutants and *Q′-like* all exhibited several alterations in spikelet and floret development, although we focused on detailed analysis of the original *Q′* allele in the SS background. *Q′* plants produced fully formed floret-containing spikelets usually by the second rachis node from the base of the spike, whereas *Q* and *Q′-Rev1* plants typically produced three or four rudimentary spikelets at the basal rachis nodes before producing fertile floret-bearing spikelets, as often occurs for modern wheat varieties (Fig. 4D; Fig. S4). Thus, increased *Q* activity can promote basal spikelet fertility as well as increase total rachis node number (Fig. 3F). A role for *Q′* in delaying conversion of the inflorescence to spikelet meristem is consistent

Development (2017) 144, 1959-1965 doi:10.1242/dev.146407

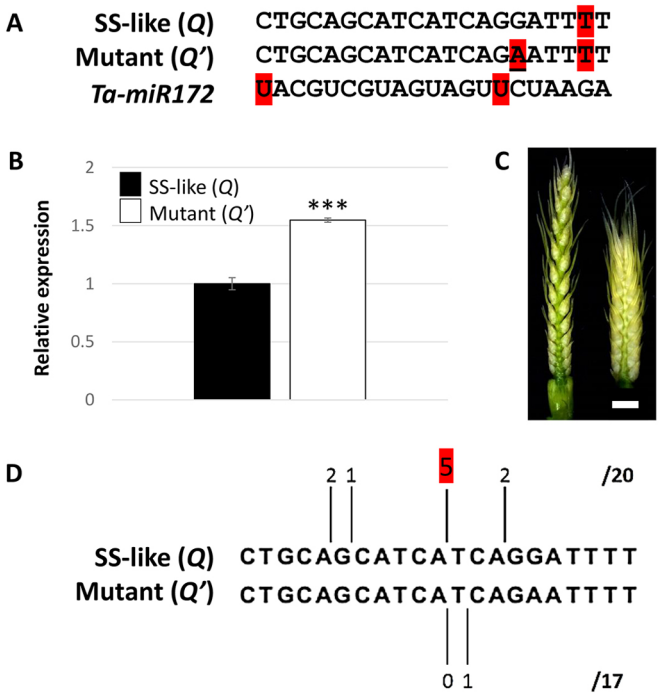

Fig. 2. The compact spike mutant *Q*′ contains a novel SNP in the miRNA binding site that leads to changes in transcriptional regulation. (A) Sequence alignment showing the miRNA binding site sequence of SS-like with the domesticated Q allele and the mutant (*Q*′), and the complementary wheat Ta-miR172 sequence. The miRNA mismatch underlying the domestication *Q* allele (C to T) is indicated by the 'T' highlighted in red, and is present in both *Q* and *Q*′. The 'U's highlighted in red in the miR172 sequence represent mismatches with all known *Q* sequences. The *Q*′ mutation is highlighted in red and underlined. (B) Expression of *Q* in SS-like and mutant inflorescence tissue harvested at the beginning of internode elongation (~10 mm inflorescences at terminal spikelet stage). Data are presented as mean±s.e.m. of four biological replicates. ***P<0.001. (C) Developing inflorescence of SS-like (left) and mutant (right) plants at the early internode elongation stage when the compaction phenotype first becomes apparent. Scale bar: 2 mm. (D) Cleavage products as determined by sequencing of 5′ RACE products using RNA pooled from the biological samples used for the expression analysis in B. The number of clones sequenced and their detected cleavage site location are presented (expected cleavage site of *Q* is marked in red). The total number of clones presented (20 for SS-like and 17 for *Q*′) is from sequenced clones which contained *Q* transcript.

with the recently proposed role of miR172 and *AP2* genes in regulating panicle development in rice (Wang et al., 2015).

Wheat spikelets comprise two basal glumes (always sterile) followed by an indeterminate number of florets (Fig. 4A). *Q*′ plants deviated from this fundamental pattern, with spikelets often possessing floret structures in place of glumes (Fig. 4B,C; Fig. S5). In the basal and apical portion of the spike, glumes were often replaced either by rudimentary florets with only a lemma and palea, or – with increasing frequency towards the terminal spikelet – complete fertile florets (Fig. 4B,C). Florets occupying typical positions in *Q*′ formed normally. SEM analysis revealed floret organs forming early in spikelet development adaxial to glume-lemma organs in *Q*′ (Fig. S5), with no additional lemma-like organ visible. These ectopic florets contributed to an increase in visible florets per spikelet along the spike of *Q*′ plants (Fig. 4D). Spikelets in the central portion of *Q*′ spikes were less likely to form florets (partial or complete) in place of glumes (Fig. 4C). In *Q*′ plants there was a tendency for the glume-like structures of the spikelet to be elongated and produce lemma-like awns, with awn length increasing along the spike from the base to the terminal spikelet (Figs S6 and S7) independently of whether floret structures were visible. Similar phenotypes were observed in MIM172 plants with increased *Q* expression (Debernardi et al., 2017). The simplest interpretation of these *Q*′ phenotypes is a replacement of glumes with partially or fully developed florets, including awned lemmas. This in turn suggests that increased Q activity promotes ectopic floret formation during spikelet development and, remarkably, that it can alter one of the defining features of the grasses, namely two sterile glumes at the base of each spikelet.

Another characteristic of wheat spikes is that a single spikelet is usually present at each rachis node. However, in some genetic backgrounds or under appropriate environmental conditions, two spikelets can form at a single node to generate a 'paired spikelet', which might be the equivalent of a 'spikelet pair' in plants such as corn (Boden et al., 2015 and references therein). Although absent in *Q* and *Q*′*-Rev1* plants, *Q*′ spikes contained paired spikelets, with their frequency peaking around the central rachis nodes of the spike (Figs S8 and S9).

While increased Q activity has multiple effects on spike, spikelet and floret development, the loss-of-function *Q*′*-Rev1* allele also reveals that *Q* possesses broader, previously unidentified roles (see also Debernardi et al., 2017). Unlike *Q* and *Q*′, *Q*′*-Rev1* plants intermittently produced spikelets with elongated rachilla internodes and many florets (also known as 'sham ramification', reminiscent of the *shr1*/*exg* locus on 5A (Amagai et al., 2014, 2015) (Fig. 4D,E). This trait was more severe in tillers (data not shown) than in the main spike, but the 'extra' florets in these spikelets did not produce grains. The sham ramification trait has been mapped to chromosome 5AL, in a similar position to *Q*, and has been shown to be repressed by the presence of the D genome in some backgrounds (Alieva and Aminov, 2013; Amagai et al., 2014). In the absence of a D genome, sham ramification and extra florets were observed in tetraploid wheat lines with loss-of-function alleles of *Q* and in lines overexpressing miR172 (Debernardi et al., 2017). Debernardi et al. (2017) also report extra sterile glumes in place of florets associated with *Q* loss-of-function, although we did not observe these traits in our *Q*′*-Rev1* line. Our observations suggest that Q activity must be tightly regulated, as both increases (ectopic florets in place of glumes) and decreases (sham ramification) in expression can lead to increases in floret number, similar to reports in maize *AP2* mutants (Chuck et al., 2007, 2008).

Many of the inflorescence architecture defects of *Q*′ are confined to, or more severe in, certain regions of the spike. Most notably, spike compaction (Fig. S10), replacement of glumes with florets and increased awn length all become more severe in nodes closer to the terminal spikelet (Fig. 4; Figs S6 and S7). *Q* expression exhibited temporal and spatial variation during spike development (Fig. S11), with *Q*′ typically more highly expressed than *Q*, and a somewhat reciprocal relationship between *Q* and miR172 expression, consistent with the results of Debernardi et al. (2017). Increased expression of *Q* in the peduncle internode and severe reduction in the size of this internode suggest that targeted degradation of *Q* by miR172 is broadly required to ensure correct elongation of internodes (stem, rachis and rachilla) in the wheat plant, demonstrating that Q plays an important role throughout wheat reproductive development.

In summary, using mutagenesis and a candidate gene approach we have generated a series of gain- and loss-of-function *Q* alleles that have allowed us to identify previously unknown aspects of *Q* gene function in wheat reproductive development. The presumed miRNA mismatches in the gain-of-function mutants we have isolated confirm that the common miRNA regulation of *AP2* genes

Development (2017) 144, 1959-1965 doi:10.1242/dev.146407

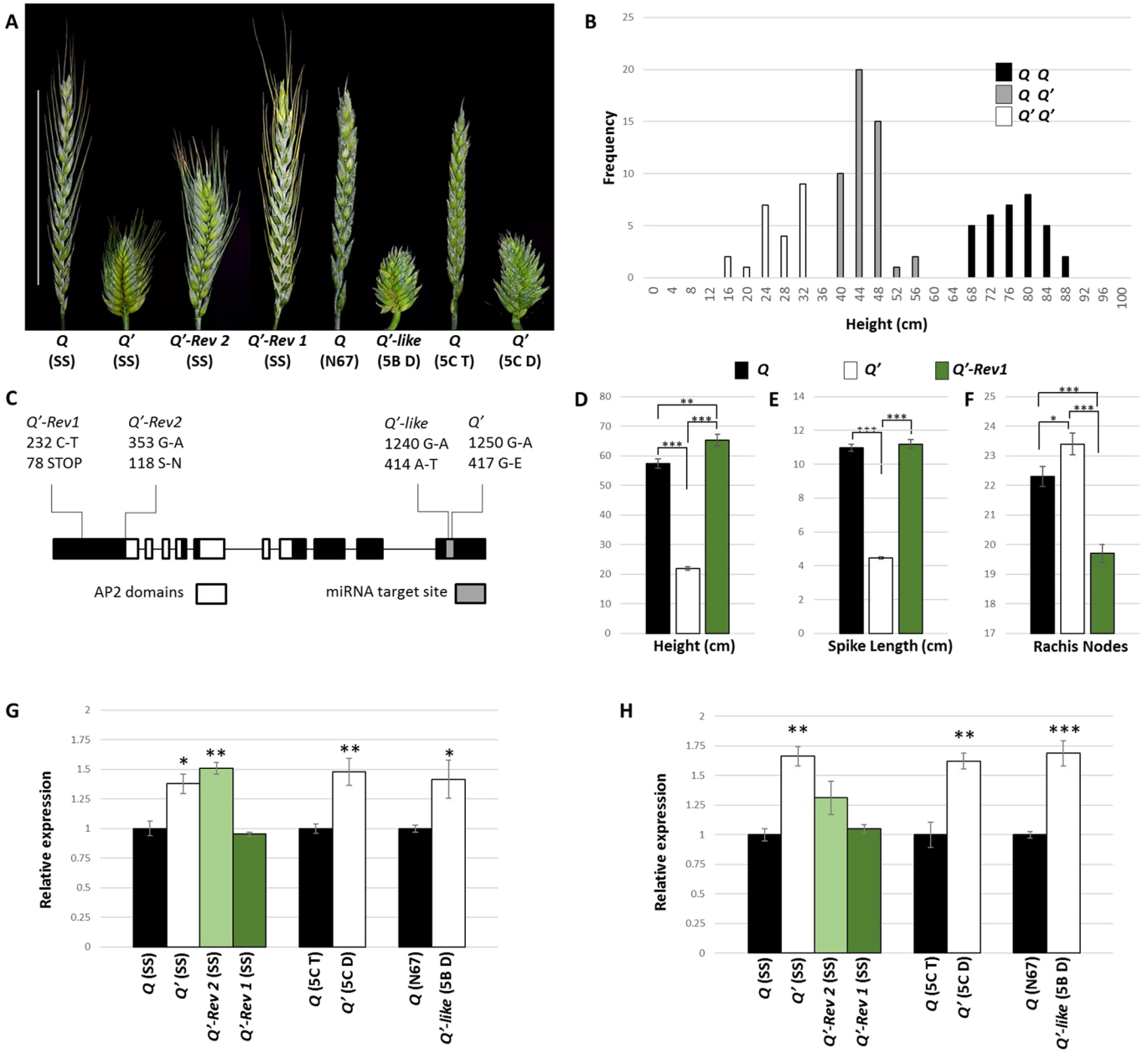

Fig. 3. Co-segregation analysis, loss-of-function mutants derived from *Q*′ and additional *Q* miRNA mutants confirm that the novel SNP is causal for *Q*′ phenotypes. (A) Adult wheat inflorescences of SS-like sibling (*Q*), *Q*′ and secondary induced mutants *Q*′*-Rev2* and *Q*′*-Rev1* in the SS background, as well as Novosibirskaya 67 (N67) and *Q*′*-like* mutant ANBW5B Dwarf (5BD) in the N67 background, and sibling lines of ANBW5C Tall (5CT) and ANBW5C Dwarf (5CD, *Q*′). Scale bar: 10 cm. (B) Co-segregation of *Q* and *Q*′ in the SS background showing the frequency of plants grown from heterozygous parents that fell within specific height ranges (bins covering 4 cm). Bars are shaded according to the genotype of plants within those height ranges as determined by cleaved amplified polymorphic sequence (CAPS) marker analysis. Plants segregated in agreement with a 1:2:1 ratio as determined by a chi-squared test (P=0.281, n=104 progeny). (C) *Q* gene schematic showing exons (black boxes), introns (thin lines), miRNA target site and AP2 domains. The location of *Q*′ and *Q*′*-like* mutations and derived revertant mutations in *Q*′ are shown, including nucleotide changes and predicted translational changes. (D-F) Plant height (D), spike length (E) and rachis node number (F) of *Q*, *Q*′and *Q*′*-Rev1* plants. Data are presented as mean±s.e.m. n=10. (G,H) Relative expression of *Q* transcript in compact mutant lines normalized to their sibling or parent line in developing inflorescences (~10 mm inflorescences at terminal spikelet stage) (G) and in elongating peduncle internode tissue (H). Data are presented as mean±s.e.m. of three biological replicates. *P<0.05, **P<0.01, ***P<0.001.

also extends to wheat and that correct regulation of *Q* expression is required for normal formation of the wheat spike and spikelets.

MATERIALS AND METHODS

Plant materials and mutagenesis

The spring habit, bread wheat cultivar Sunstate (SS) was mutagenized using sodium azide as described by Chandler and Harding (2013). SS contains the domesticated *Q* allele. The same mutagenesis was performed on *Q*′ grain when generating revertant alleles. Further information regarding additional *Q* alleles, threshing and growth conditions is provided in the supplementary Materials and Methods.

Expression analysis by qRT-PCR

Developing inflorescence tissue was harvested for qRT-PCR at terminal spikelet stage. Five developing inflorescences were harvested per biological replicate. Peduncle internode tissue was harvested when the peduncle

Development (2017) 144, 1959-1965 doi:10.1242/dev.146407

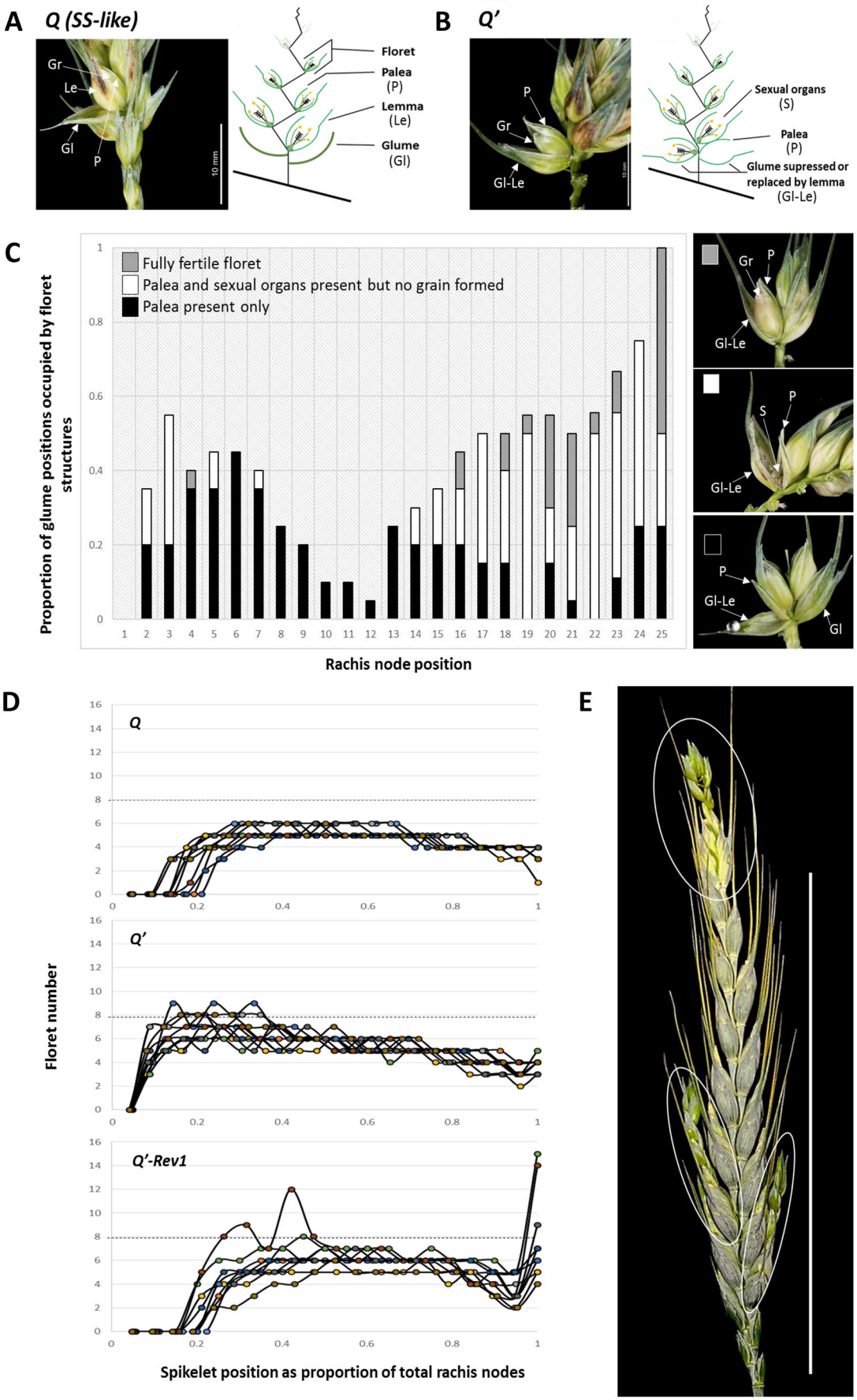

Fig. 4. See next page for legend.

Development (2017) 144, 1959-1965 doi:10.1242/dev.146407

Fig. 4. Detailed phenotyping of *Q*, *Q′* and *Q′-Rev1* plants reveals inflorescence architecture defects. (A) SS-like (Q) spikelet image and schematic showing typical wheat spikelet structure in which no ectopic florets form. (B) *Q′* spikelet, by contrast, shows a severe ectopic floret phenotype in which complete florets replace glumes. Scale bars: 10 mm in A,B. (C) *Q′* plants exhibit complete ectopic florets or floret-like structures in place of glumes, most frequently in the base and apical portions of the spike. Data are presented as the proportion of ectopic florets at each rachis node position across ten plants, where the total number of possible glumes is 2 per rachis node per plant. P, palea; Le, lemma; Gl, glume; Gr, grain; Gl-Le, glume-lemma; S, sexual organs. (D) Floret numbers of sequential spikelets from the base (left) to top (right) of spikes, where total spike length is set at 1 for Q, *Q′* and *Q′-Rev1* plants. Data are presented for each of ten individuals per genotype. Plot points mark individual spikelets (terminal spikelet at distance =1), with colors indicating separate spikes scored. Dotted line is for ease of comparison between genotypes. (E) *Q′-Rev1* spike illustrating elongated spikelets (sham ramification) containing many florets (circled). Scale bar: 10 cm.

internode of lines containing the *Q* domestication allele were 10 mm in length. A single peduncle internode was harvested for each biological replicate. Details of sample preparation and the qPCR protocol, including primers, are provided in the supplementary Materials and Methods and Table S1.

Modified 5′ RACE

For 5′ RACE, mRNA was purified from the same inflorescence RNA samples as used for the initial qRT-PCR analysis of *Q* in SS-like and *Q′* plants (Fig. 2). A GeneRacer Kit (Invitrogen) was used, except the de-capping protocol was not carried out, and the adapter was ligated directly to mRNA. Amplification of cleaved and ligated *Q* transcript was performed using gene-specific and GeneRacer adapter-specific primers (Table S1). Amplicon of the expected size was ligated into pGEM®-T Easy (Promega) before transformation, selection and sequencing of individual clones to determine cleavage location and frequency. See the supplementary Materials and Methods for more details.

Scanning electron microscopy (SEM)

Developing inflorescence samples were prepared for SEM with a Zeiss Evo LS15 scanning electron microscope as described in the supplementary Materials and Methods.

Sequence information

The miR172 sequence shown in this study is that of Ta-miR172a obtained from Yao et al. (2007). Although other isoforms have been reported and might contribute to regulation of *Q*, Ta-miR172a was used as a reference sequence for alignment purposes. *Q* sequence is available through GenBank accession AY702956.1.

Statistical analysis

Two-tailed Student's *t*-test was employed to compare means. Sample sizes (*n*) and *P*-values are given in figure legends.

Acknowledgements

We thank the ANU and CSIRO OCE PhD scheme for support to Julian Greenwood, Prof. John Evans for advice and supervision, Bjorg Sherman and Kerrie Ramm for technical help with mutant populations, and Carl Davies for photography.

Competing interests

The authors declare no competing or financial interests.

Author contributions

Conceptualization: J.R.G., E.J.F., B.T., S.M.S.; Methodology: J.R.G., E.J.F., B.T., S.M.S.; Validation: J.R.G., E.J.F.; Formal analysis: J.R.G., E.J.F.; Investigation: J.R.G., E.J.F.; Resources: J.R.G., N.W., B.T., S.M.S.; Writing - original draft: J.R.G., E.J.F., B.T., S.M.S.; Writing - review & editing: J.R.G., E.J.F., S.M.S.; Visualization: J.R.G.; Supervision: B.T., S.M.S.; Project administration: B.T., S.M.S.; Funding acquisition: S.M.S.

Funding

This work was supported by an Australian National University (ANU) University Research Scholarship and a Commonwealth Scientific and Industrial Research Organisation (CSIRO) OCE PhD Top-up Scholarship.

Supplementary information

Supplementary information available online at
http://dev.biologists.org/lookup/doi/10.1242/dev.146407.supplemental

References

Alieva, A. J. and Aminov, N. K. (2013). Influence of D genome of wheat on expression of novel type spike branching in hybrid populations of 171ACS line. *Russ. J. Genet.* **49**, 1119-1126.

Amagai, Y., Aliyeva, A. J., Aminov, N. K., Martinek, P., Watanabe, N. and Kuboyama, T. (2014). Microsatellite mapping of the genes for sham ramification and extra glume in spikelets of tetraploid wheat. *Genet. Resour. Crop Evol.* **61**, 491-498.

Amagai, Y., Aliyeva, A. J., Aminov, N. K., Martinek, P., Watanabe, N. and Kuboyama, T. (2015). Microsatellite mapping of the gene for sham ramification in spikelets derived from a hexaploid wheat (Triticum spp.) accession 171ACS. *Genet. Resour. Crop Evol.* **62**, 1079-1084.

Aukerman, M. J. and Sakai, H. (2003). Regulation of flowering time and floral organ identity by a microRNA and its APETALA2-like target genes. *Plant Cell* **15**, 2730-2741.

Boden, S. A., Cavanagh, C., Cullis, B. R., Ramm, K., Greenwood, J., Jean Finnegan, E., Trevaskis, B. and Swain, S. M. (2015). Ppd-1 is a key regulator of inflorescence architecture and paired spikelet development in wheat. *Nat. Plants* **1**, 14016.

Brown, R. H. and Bregitzer, P. (2011). A Ds insertional mutant of a barley miR172 gene results in indeterminate spikelet development. *Crop Sci.* **51**, 1664.

Chandler, P. M. and Harding, C. A. (2013). 'Overgrowth' mutants in barley and wheat: new alleles and phenotypes of the 'Green Revolution' Della gene. *J. Exp. Bot.* **64**, 1603-1613.

Chuck, G., Meeley, R. B. and Hake, S. (1998). The control of maize spikelet meristem fate by the APETALA2-like gene indeterminate spikelet1. *Genes Dev.* **12**, 1145-1154.

Chuck, G., Meeley, R., Irish, E., Sakai, H. and Hake, S. (2007). The maize tasselseed4 microRNA controls sex determination and meristem cell fate by targeting Tasselseed6/indeterminate spikelet1. *Nat. Genet.* **39**, 1517-1521.

Chuck, G., Meeley, R. and Hake, S. (2008). Floral meristem initiation and meristem cell fate are regulated by the maize AP2 genes ids1 and sid1. *Development* **135**, 3013-3019.

Debernardi, J. M., Lin, H., Chuck, G., Faris, J. D. and Dubcovsky, J. (2017). microRNA172 plays a crucial role in wheat spike morphogenesis and grain threshability. *Development* **144**, 1966-1975.

Faris, J. D., Fellers, J. P., Brooks, S. A. and Gill, B. S. (2003). A bacterial artificial chromosome contig spanning the major domestication locus Q in wheat and identification of a candidate gene. *Genetics* **164**, 311-321.

Förster, S., Schumann, E., Eberhard Weber, W. and Pillen, K. (2012). Discrimination of alleles and copy numbers at the Q locus in hexaploid wheat using quantitative pyrosequencing. *Euphytica* **186**, 207-218.

Förster, S., Schumann, E., Baumann, M., Weber, W. E. and Pillen, K. (2013). Copy number variation of chromosome 5A and its association with Q gene expression, morphological aberrations, and agronomic performance of winter wheat cultivars. *Theor. Appl. Genet.* **126**, 3049-3063.

Houston, K., McKim, S. M., Comadran, J., Bonar, N., Druka, I., Uzrek, N., Cirillo, E., Guzy-Wrobelska, J., Collins, N. C., Halpin, C. et al. (2013). Variation in the interaction between alleles of HvAPETALA2 and microRNA172 determines the density of grains on the barley inflorescence. *Proc. Natl. Acad. Sci. USA* **110**, 16675-16680.

Jung, J.-H., Seo, Y.-H., Seo, P. J., Reyes, J. L., Yun, J., Chua, N.-H. and Park, C.-M. (2007). The GIGANTEA-regulated microRNA172 mediates photoperiodic flowering independent of CONSTANS in Arabidopsis. *Plant Cell* **19**, 2736-2748.

Kosuge, K., Watanabe, N., Melnik, V. M., Laikova, L. I. and Goncharov, N. P. (2012). New sources of compact spike morphology determined by the genes on chromosome 5A in hexaploid wheat. *Genet. Resour. Crop Evol.* **59**, 1115-1124.

Lauter, N., Kampani, A., Carlson, S., Goebel, M. and Moose, S. P. (2005). microRNA172 down-regulates glossy15 to promote vegetative phase change in maize. *Proc. Natl. Acad. Sci. USA* **102**, 9412-9417.

Lee, D.-Y. and An, G. (2012). Two AP2 family genes, supernumerary bract (SNB) and Osindeterminate spikelet 1 (OsIDS1), synergistically control inflorescence architecture and floral meristem establishment in rice. *Plant J.* **69**, 445-461.

Lee, D.-Y., Lee, J., Moon, S., Park, S. Y. and An, G. (2007). The rice heterochronic gene SUPERNUMERARY BRACT regulates the transition from spikelet meristem to floral meristem. *Plant J.* **49**, 64-78.

Mathieu, J., Yant, L. J., Mürdter, F., Küttner, F. and Schmid, M. (2009). Repression of flowering by the miR172 target SMZ. *PLoS Biol.* **7**, e1000148.

Mlotshwa, S., Yang, Z., Kim, Y. and Chen, X. (2006). Floral patterning defects induced by Arabidopsis APETALA2 and microRNA172 expression in Nicotiana benthamiana. *Plant Mol. Biol.* **61**, 781-793.

Schmid, M., Uhlenhaut, N. H., Godard, F., Demar, M., Bressan, R., Weigel, D. and Lohmann, J. U. (2003). Dissection of floral induction pathways using global expression analysis. *Development* **130**, 6001-6012.

Development (2017) 144, 1959-1965 doi:10.1242/dev.146407

Simons, K. J., Fellers, J. P., Trick, H. N., Zhang, Z., Tai, Y.-S., Gill, B. S. and Faris, J. D. (2006). Molecular characterization of the major wheat domestication gene Q. *Genetics* **172**, 547-555.

Sormacheva, I., Golovnina, K., Vavilova, V., Kosuge, K., Watanabe, N., Blinov, A. and Goncharov, N. P. (2015). Q gene variability in wheat species with different spike morphology. *Genet. Resour. Crop Evol.* **62**, 837-852.

Varkonyi-Gasic, E., Lough, R. H., Moss, S. M. A., Wu, R. and Hellens, R. P. (2012). Kiwifruit floral gene APETALA2 is alternatively spliced and accumulates in aberrant indeterminate flowers in the absence of miR172. *Plant Mol. Biol.* **78**, 417-429.

Wang, L., Sun, S., Jin, J., Fu, D., Yang, X., Weng, X., Xu, C., Li, X., Xiao, J. and Zhang, Q. (2015). Coordinated regulation of vegetative and reproductive branching in rice. *Proc. Natl. Acad. Sci. USA* **112**, 15504-15509.

Yant, L., Mathieu, J., Dinh, T. T., Ott, F., Lanz, C., Wollmann, H., Chen, X. and Schmid, M. (2010). Orchestration of the floral transition and floral development in Arabidopsis by the bifunctional transcription factor APETALA2. *Plant Cell* **22**, 2156-2170.

Yao, Y., Guo, G., Ni, Z., Sunkar, R., Du, J., Zhu, J.-K. and Sun, Q. (2007). Cloning and characterization of microRNAs from wheat (Triticum aestivum L.). *Genome Biol.* **8**, R96.

Zhang, Z., Belcram, H., Gornicki, P., Charles, M., Just, J., Huneau, C., Magdelenat, G., Couloux, A., Samain, S., Gill, B. S. et al. (2011). Duplication and partitioning in evolution and function of homoeologous Q loci governing domestication characters in polyploid wheat. *Proc. Natl. Acad. Sci. USA* **108**, 18737-18742.

Zhu, Q.-H., Upadhyaya, N. M., Gubler, F. and Helliwell, C. A. (2009). Over-expression of miR172 causes loss of spikelet determinacy and floral organ abnormalities in rice (Oryza sativa). *BMC Plant Biol.* **9**, 149.

Supplementary Materials and Methods

Plant material, threshing and growth conditions

Threshing was performed by hand and by the same person to gauge the threshability of mutant wheat lines. In reference to the loss-of-function mutant *Q'-Rev1* threshing required the identification of individual grain for removal by splitting apart florets and spikelets whereas in *Q'* and SS-like spikes, grain could easily be separated by rolling the spike back and forth between clapped palms.

The compact mutant near isogenic lines ANBW5B (5B D in Fig 3) and ANBW5C (5C D in Figure 3) were isolated and mapped by (Kosuge et al., 2011). The lines were established by backcrossing the mutants Cp-M808 (ANBW5B) and MCK 2617 (ANBW5C) with Novosibirskaya 67 (N67) for six generations. N67 contains the typical domesticated *Q* allele. The line 5C T included in Figure 3 represents an N67-like segregant from a line heterozygous for the ANBW5C mutation after backcrossing, however by this round of backcrossing N67 and N67-like segregants are effectively genetically identical.

Screening of mutant lines and phenotyping for co-segregation analysis was performed in glasshouse conditions with temperature controlled to ~22°C (Day) and ~16°C (Night) over Spring and Summer. All other phenotyping and tissue extraction for RNA was from plants grown in cabinets (Conviron PGC20) under 16h light (Measured at 420µM m^{-1} s^{-1} 50cm below light source) (22°C) and 8h dark (16°C).

Modified 5' RACE

mRNA was purified from the same inflorescence RNA samples used for the initial qRT-PCR analysis of *Q* in SS-like and *Q'* plants (Fig 2). A Gene-racer kit (Invitrogen) was used for 5'-RACE, except the de-capping protocol was not carried out, and the adapter was ligated directly to mRNA. Amplification of cleaved and ligated *Q* transcript was performed using gene specific and Gene-racer specific primers. Secondary nested PCR was performed to ensure amplification of gene specific products. Amplification products were gel purified and ligated into pGEM®-T easy before being transformed into *E.coli* XL-Blue cells and selected on ampicillin plates containing 100 µL of 100mM IPTG and 20 µL of 50 mg/ml X-Gal. Individual colonies were selected and grown overnight in LB with 50 µg/ml ampicillin and purified using Qiagen mini-preps. In total, 96 colonies were selected for sequencing of *Q'* (n=48) and SS-like (n=48) amplification product. Only sequenced clones containing correct *Q* transcript sequence were included with the proportion of cleavage within the miR172-binding site presented. Gene specific primer sequences are listed in Supplementary Table 1.

qRT-PCR

All tissue was ground to fine powder in 1.5ml snap lock tubes containing two ball bearings using a mixermill. RNA extraction and DNASE treatment was performed using the Maxwell® RSC Plant RNA Kit and Maxwell® RSC Instrument following the advised protocol. cDNA synthesis was performed using Maxima H-minus reverse transcriptase from invitrogen with oligo dT to prime mRNA using 5µg total RNA. cDNA was diluted 30 fold and 5µl of diluted cDNA was used in each qPCR reaction. qPCR was performed using SYBR Green on a Roche LightCycler®480II using RP15 as an endogenous control. Primers are shown in Supplementary Table S1.

Routine testing of cDNA samples was performed by serial dilution and calculation of R^2 from the standard curve. Analysis was performed using Roche LightCycler®480II and associated software. For all cDNA samples presented, 5 log serial dilutions were performed and R^2 values ≥0.982 were determined before qPCR analysis. Primer efficiency was calculated from the exponential phase of amplification in each reaction sample in each qRT-PCR run. qRT-PCR Primer pairs used in this study routinely achieved amplification efficiencies ≥90%.

Scanning Electron Microscopy (SEM)

Developing inflorescence samples for SEM were prepared by immediate transfer to 100% ethanol after harvest. Ethanol was replaced twice daily until samples appeared completely white (2-3 days). Sample preparation adapted from (Talbot and White, 2013). Samples were then put through a critical point drying process in a tousimis autosamdri®-815 critical point drying device with purge timer set to 4. After critical point drying, samples were mounted on specimen stubs using adhesive carbon discs. Samples were imaged with a Zeiss Evo LS15 scanning electron microscope using backscattered electron detector (Gain= High), at 20KV and extended pressure setting (10pa).

Supplementary Table S1. Primers used in this study

Primer Name	Purpose	Sequence	
pJG31	*Q* Full genomic sequence	GATGGTGCTGGATCTCAATGTGG	
PJG33	*Q* Full genomic sequence	CAACAATGGCGGACTGCTG	
pJG14	*Q* genomic sequence spanning miRNA-Binding site	TCACTGCTGGTGCTGGTGC	
PJG18	*Q* genomic sequence spanning miRNA-Binding site	AAGTAGAACCGGTGGTGGTCC	
pJG38	Sequencing *Q*	CTACGAGGAGGATTTGAAGCAG	
pJG39	Sequencing *Q*	ACACGACACTCGATTGCAGAC	
pJG5	Sequencing *Q*	AATGAGGGTACTACTACAATCGGTC	
pJG2	Sequencing *Q*	CTACCCGAACGTACAGGTATCA	
pJG13	Sequencing *Q*	GGTGCAGGAGAGGCCCAT	
pJG29	*Q* specific 5' Race	GGAAGTAGAACCGGTGGTGGTCC	
pJG30	*Q* specific 5' Race Nested	GTGGTGGTCCGGGTACGGC	
Q qPCR F	*Q* qPCR	CCCTGAATCGTCAACCACAATG	(Simons et al., 2006)
Q qPCR R	*Q* qPCR	CCGTGCCATGTTGATGCA	(Simons et al., 2006)
TaRP15 F	Control gene qPCR	GCACACGTGCTTTGCAGATAAG	(Shaw et al., 2012)
TaRP15 R	Control gene qPCR	GCCCTCAAGCTCAACCATAACT	(Shaw et al., 2012)

miR172 Reverse transcription, expression, control primers associated methods used in this study can be found in companion paper Debernardi et al., 2017.

Supplementary Figures

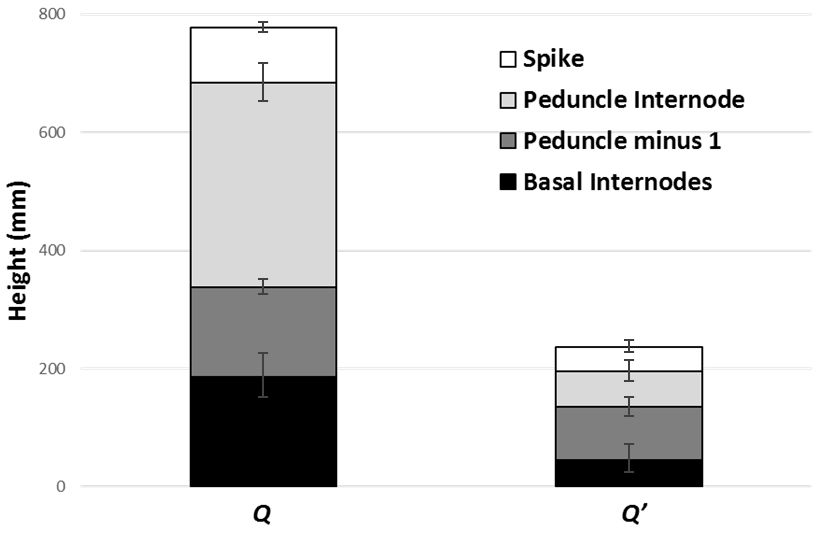

Supplementary Figure 1 Internode elongation phenotype of *Q'*. Total height of *Q'* mutant and its sibling line containing the normal *Q* domestication allele with total height being shown as stacked histogram of average spike, peduncle internode, peduncle minus 1 and remaining basal internode lengths. n= 12 plants. The number of basal peduncle internodes varied between two and three visible internodes amongst measured plants. The length of peduncle and peduncle internode were measured individually as differences in the length of these internodes, as well as the spike, accounted for most of the height reduction in *Q'* plants.

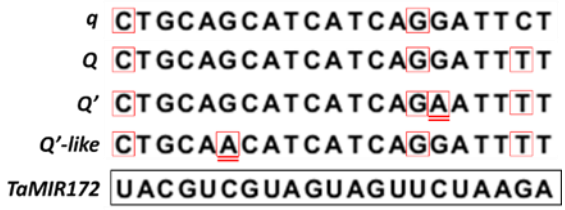

Supplementary Figure 2 miRNA-binding site alignments of pre-domesticated *q*, domesticated *Q*, gain-of-function alleles *Q' and Q'-like*. miRNA-binding site alignments and complementary *miRNA172* with mismatches shown in red and induced mismatches shown by red double underline.

Supplementary Figure 3 The loss-of-function *Q'-Rev1* is difficult to thresh A mechanical thresh test was performed by applying downward pressure to whole spikes with a hand threshing tool before sliding the tool horizontally. SS-like plants containing the domestication allele *Q* had spikes that were easy to thresh and *Q'* plants had spikes that were very easy to thresh with all grain separating from the head leaving an intact rachis. In contrast, *Q'-Rev1* plants had spikes that were firm and required more pressure to thresh with some grain not separating from the spikelets. In addition, the rachis of *Q'-Rev1* spikes had a greater tendency to break into individual nodes/spikelets. In each image the threshed rachis and intact spikelets have been arranged on the left hand side of the image. In *Q* and *Q'* plants, no grain remained bound in spikelets unlike *Q'-Rev1*.

Supplementary Figure 4 The *Q'* mutant reduces the number of basal rudimentary (sterile) spikelets and produces fertile spikelets at basal rachis nodes that are unfilled in *Q* and the loss-of-function mutant *Q'-Rev1*. A, Basal portion of *Q, Q'* and *Q'-Rev1* spikes. Rachis nodes with rudimentary spikelets (those lacking developed florets) are marked *. Scale bar= 1cm. **B,** The average number of infertile spikelets (those that produced no grain) and the number of infertile spikelets which appeared to be rudimentary (without florets) in the basal portion of the main spike of *Q, Q'* and *Q'-Rev1* plants. n= 10. ** $P < 0.01$

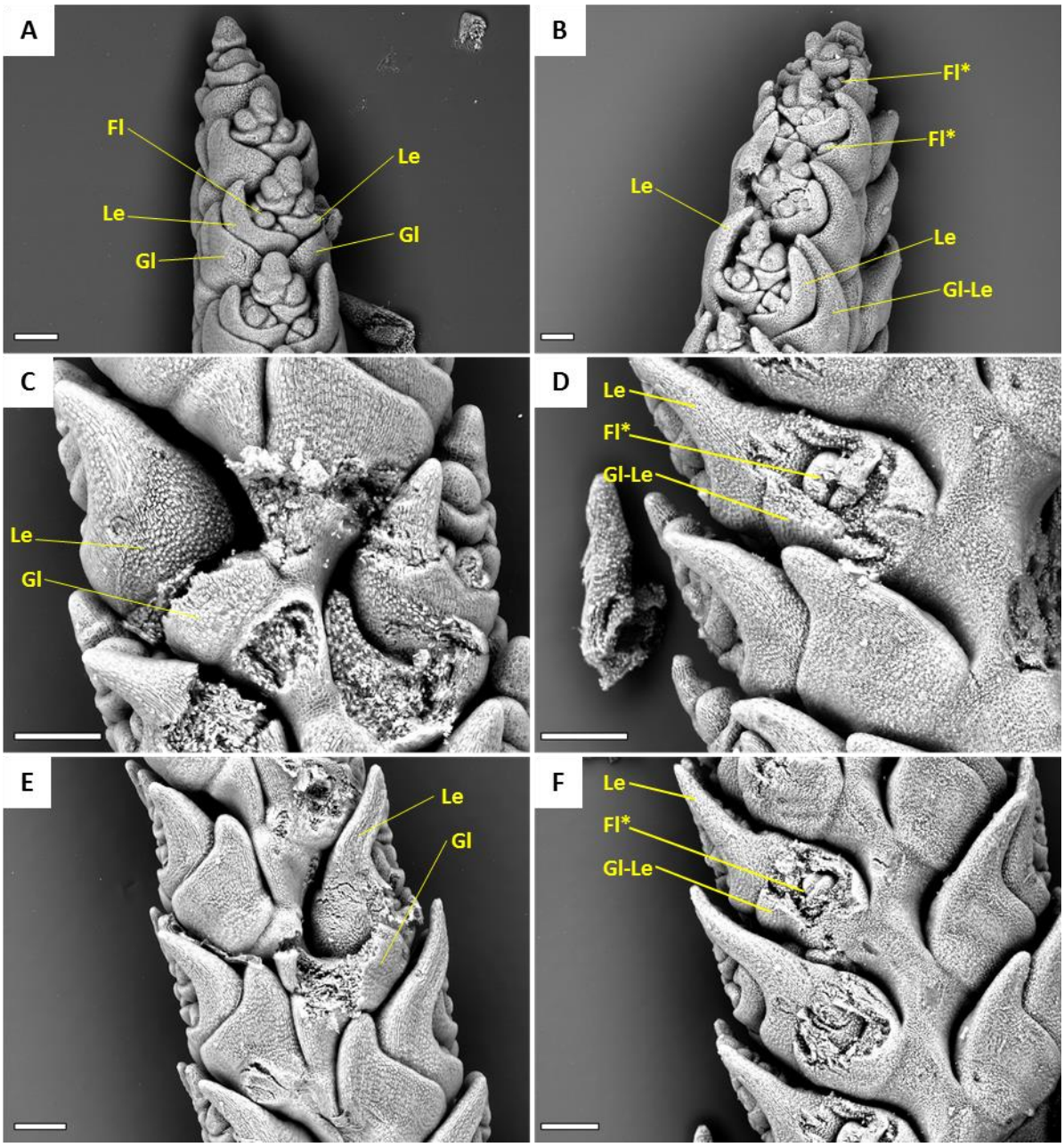

Supplementary Figure 5 Ectopic florets are produced in *Q'* spikelets. SEMs of *SS-like* (Left: **A, C, E**) and *Q'* (Right: **B, D, F**) spikes. Outer-most bracts have been removed from selected spikelets in **C, D, E, F** to reveal structures beneath. In the case of *Q'* ectopic florets (Fl*) are visible beneath the outermost bracts of apical **B,** and dissected **D, F,** spikelets, while the outer-most bracts (glumes) of *SS-like* plants **A, C, E** feature typical sterile glumes. Scale bars= 200µm

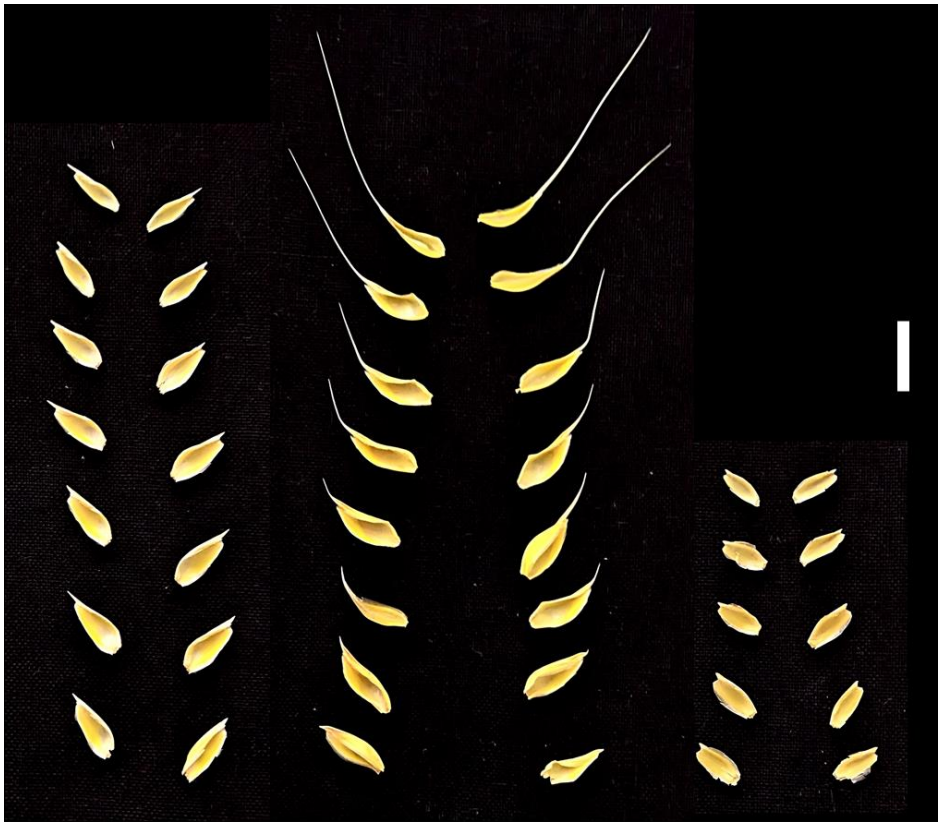

Q ***Q'*** ***Q'-Rev1***

Supplementary Figure 6 Glumes of *Q'* mutant appear lemma-like with awns present in increasing length toward the apical portion of the spike. Glumes of *Q*, *Q'* and *Q'-Rev1* plants removed from one side of asingle spike and placed in order to reflect their position on an intact and upright spike. Note that glumes of *Q'*, or the outermost positions on spikelets which should be occupied by glumes, are only simmilar to the glumes of *Q* when comparing basal spikelets. Scale bar= 1cm

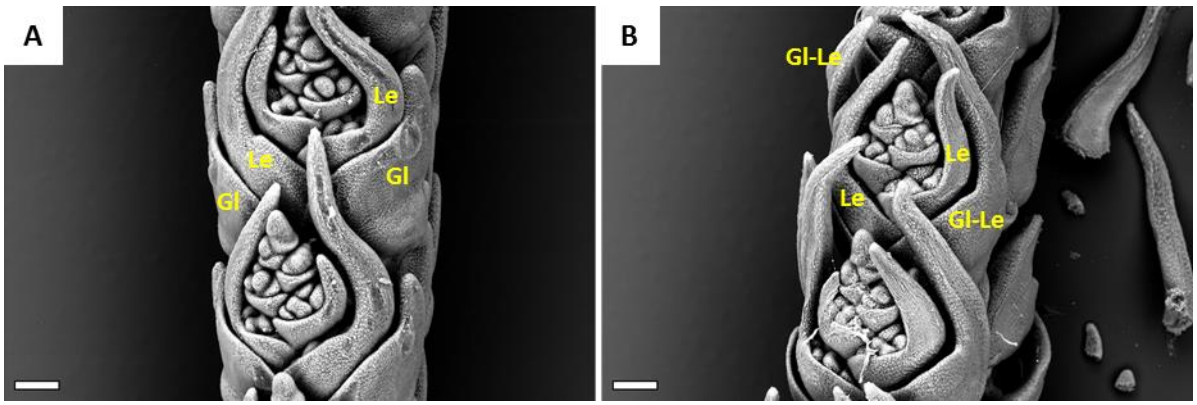

Supplementary Figure 7 Outer most bracts of *Q'* spikelets exhibit elongation of tips as in lemmas. SEMs of spikes shown are at comparable stages of inflorescence development when the tips of lemmas (awns) are beginning to elongate in both *SS*-like (*Q*) and *Q'* plants. The outermost bracts of *Q'* spikelets **B,** feature elongating tips much like a lemma at this stage whereas the outermost bracts of *Q* spikelets **A,** do not elongate and maintain short tips until maturity. See also **S Fig 5.** Gl= glume, Le= Lemma and Gl-Le= Glume-Lemma**.** Scale bars= 200µm

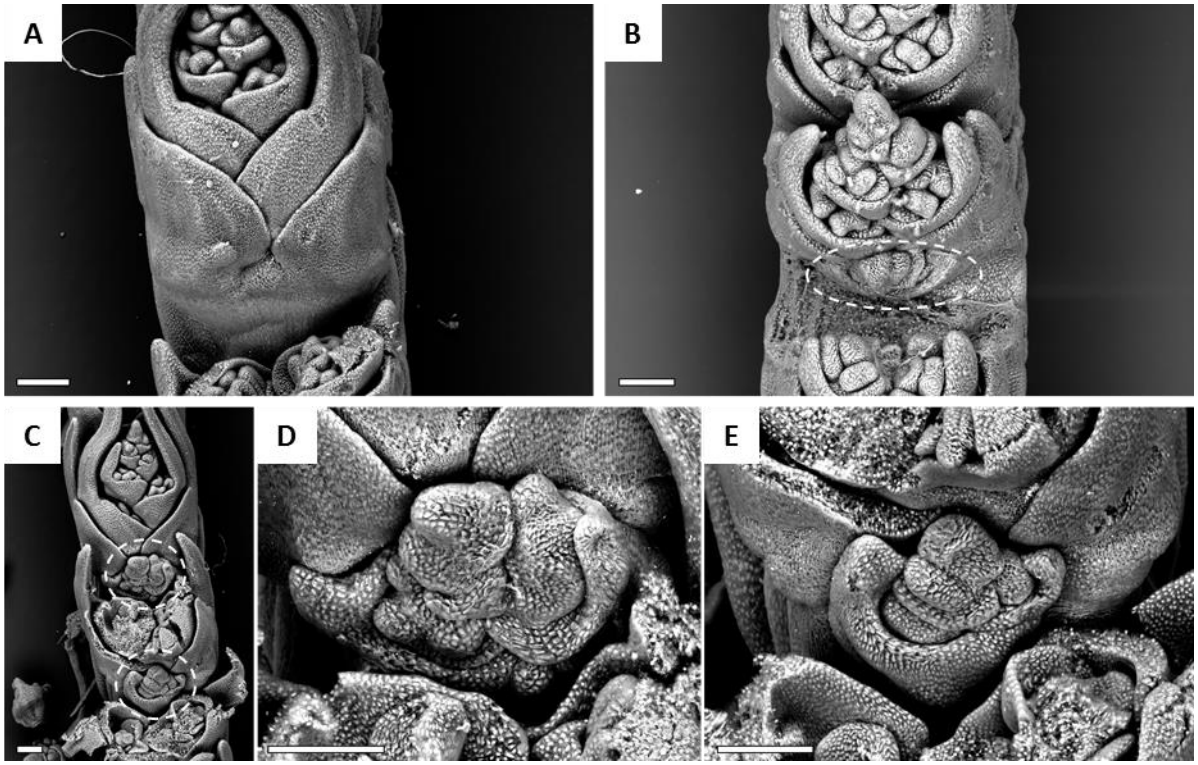

Supplementary Figure 8 Pairs of spikelets form at the central rachis nodes of *Q'* spikes. SEMs of dissected *SS-like* (*Q*) **A,** and *Q'* spikes **B, C, D, E.** to reveal the base of selected spikelets where spikelet pairs form, the spikelet beneath has been removed. The base of the *SS-like* spikelet shown in **A,** represents a typical single spikelet formation. The base of *Q'* spikelets in **B** and **D** show the formation of additional, or paired spikelet at the base of other spikelets. Scale bars= 200µm

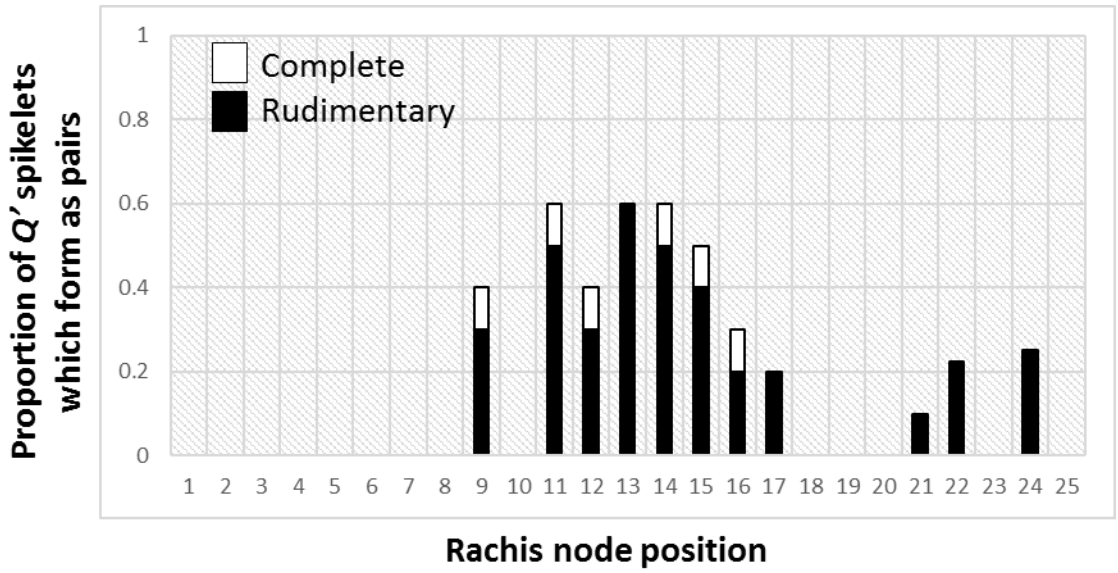

Supplementary Figure 9 Proportion of paired spikelets in *Q'* plants forming at each rachis node. Paired spikelets at specific rachis node positions in *Q'* plants are shown as proportion of all spikelets scored at that rachis node position in main spikes of *Q'* plants. n= 10. Complete paired spikelets contained at least one macroscopic floret.

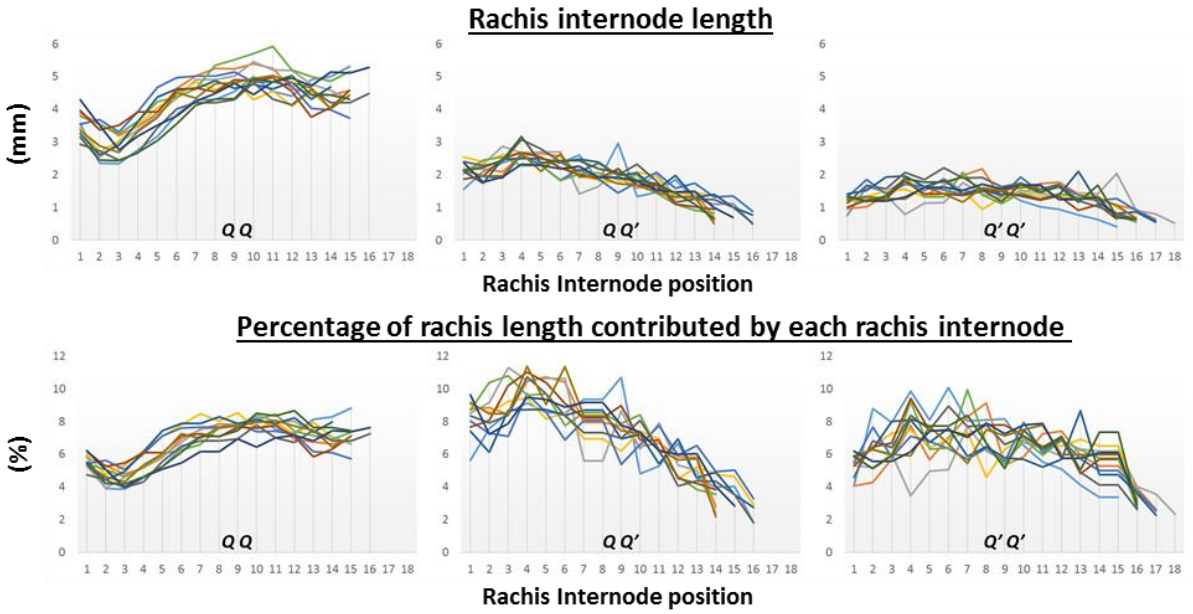

Supplementary Figure 10 Rachis internode elongation is reduced in plants containing the *Q'* with the most severe reduction in internode length occurring at the top of the spike. Rachis internode length profiles of SS-like (*Q Q*), heterozygous (*Q Q'*) and homozygous (*Q' Q'*) mutants where 1 equals the most basal rachis internode of the main spike. n= 12. As rachis internode number varies between individuals, each individual has been plotted and represented by a different color.

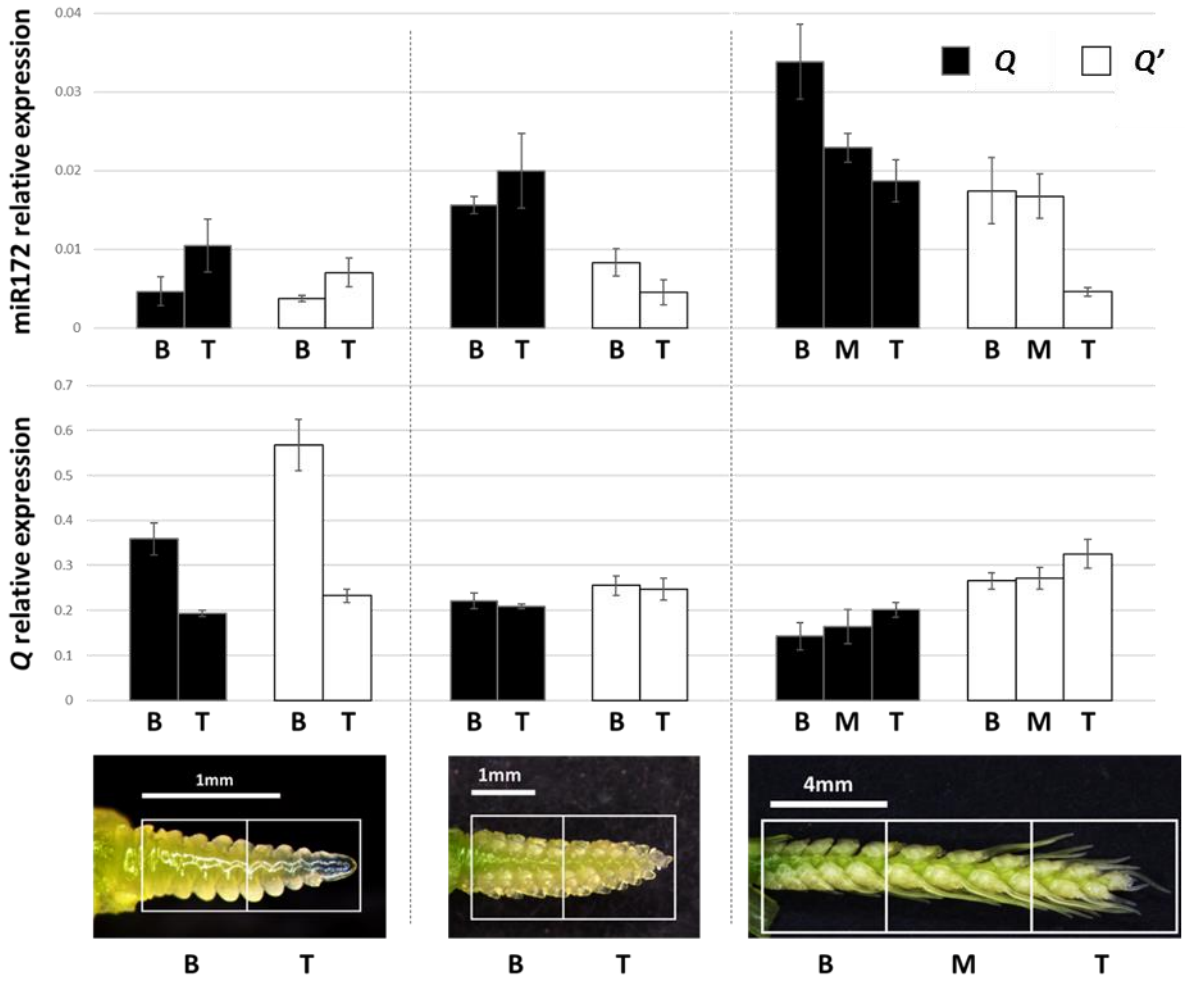

Supplementary Figure 11 Spatial and temporal expression of *Q* and miR172. Images along the bottom of this figure correspond to the developmental stage at which spike sections were harvested. Expression analysis is shown relative to control genes for both *Q* and miR172. Data are presented as mean ± s.e.m of 4 biological replicates in each section, at each timepoint.

Supplementary References

Kosuge, K., Watanabe, N., Melnik, V. M., Laikova, L. I. & Goncharov, N. P. 2011. New sources of compact spike morphology determined by the genes on chromosome 5A in hexaploid wheat. *Genetic Resources and Crop Evolution,* **59,** 1115-1124.

Shaw, L. M., Turner, A. S. & Laurie, D. A. 2012. The impact of photoperiod insensitive Ppd-1a mutations on the photoperiod pathway across the three genomes of hexaploid wheat (Triticum aestivum). *Plant Journal,* **71,** 71-84.

Simons, K. J., Fellers, J. P., Trick, H. N., Zhang, Z., Tai, Y. S., Gill, B. S. & Faris, J. D. 2006. Molecular characterization of the major wheat domestication gene Q. *Genetics,* **172,** 547-555.

Talbot, M. J. & White, R. G. 2013. Methanol fixation of plant tissue for Scanning Electron Microscopy improves preservation of tissue morphology and dimensions. *Plant Methods,* **9,** 36.